8-2012

Characterization of Chemosensing in the Alphaproteobacterium *Azospirillum brasilense*

Matthew Hamilton Russell
University of Tennessee - Knoxville, mhrussel@utk.edu

To the Graduate Council:

I am submitting herewith a dissertation written by Matthew Hamilton Russell entitled "Characterization of Chemosensing in the Alphaproteobacterium *Azospirillum brasilense* ." I have examined the final electronic copy of this dissertation for form and content and recommend that it be accepted in partial fulfillment of the requirements for the degree of Doctor of Philosophy, with a major in Biochemistry and Cellular and Molecular Biology.

Gladys M. Alexandre, Major Professor

We have read this dissertation and recommend its acceptance:

Dan Roberts, Andreas Nebenfuehr, Erik Zinser

Accepted for the Council:

Carolyn R. Hodges

Vice Provost and Dean of the Graduate School

(Original signatures are on file with official student records.)

Characterization of the chemosensory abilities of the alphaproteobacterium *Azospirillum brasilense*

A Dissertation Presented for the
Doctor of Philosophy
Degree
The University of Tennessee, Knoxville

Matthew Hamilton Russell
August 2012

Dedication

This body of work is dedicated to my loving, patient wife. Without her patience and support I would not have been able to pursue and complete this endeavor. She serves as an example in life and work for me to follow and I thank her for all she does. I also dedicate this work to our daughter who reminds me daily why all of this is worth it. Thank you both. I love you.

Acknowledgements

I would like to thank Dr. Gladys Alexandre for ALL of her patience and help as I have pursued my dream. Without her passion and guidance to help me become a good scientist, I would have not have become the person I am. All my career endeavors will be a consequence of her passion to answer the basic questions or how biology works. I thank you. I would also like to thank my committee for helpful advice and the opportunity to pursue this Ph.D. degree. I would like to thank Dr. Dan Roberts and Dr. John Koontz for the inspiration to turn my curiosity of how cells work into a career path. I would also like to thank all current and previous lab members for making daily lab life interesting and enjoyable (usually).

Abstract

Motile bacteria must navigate their environment in constant search of nutrients to sustain life. Thus they have evolved precise and adaptable sensory systems to achieve this goal, making the navigation system of the model bacterium Escherichia coli the best characterized signal transduction pathway in Biology. However, many bacteria have evolved more sophisticated arsenals for sensing and responding to their environment including chemoreceptors to identify novel attractants in the microenvironment. The diazotrophic alphaproteobacterium *Azospirillum brasilense* inhabits the soil and colonizes the roots of cereals like rice, corn, and wheat. Like most proteobacterial, *A. brasilense* encodes multiple chemotaxis-like pathways, 4, of which only Che1 has been characterized in detail. Also, of the approximately 50 chemoreceptors encoded within the genome, only the function of AerC and Tlp1 have been determine and their role in energy taxis, the dominant behavior of *A. brasilense*. In this dissertation, I will describe the characterization of another chemoreceptor, Tlp2, with a sensing domain of unknown function and the role it plays in *A. brasilense* behavior. I will also describe my work in expanding knowledge of the chemotaxis-like pathway of Che1. Also, the role of Tlp1 in root colonization, chemotaxis, and aerotaxis, the ability to navigate oxygen gradients, has been published. My work will detail the role of the C-terminal PilZ domain, a domain shown to bind the ubiquitous bacterial second messenger cyclic-di-GMP. I will characterize the necessity of c-di-GMP binding to Tlp1 for cells to maintain the ability to remain sensitive to temporal changes in aeration. I will also discuss the novel role c-di-GMP plays in modulating the cell's ability to remain motile and remain sensitive to addition changes in oxygen availability.

Table of Contents

Table of Contents, continued

Table of Contents, continued

List of Tables

List of Figures

List of Figures, continued

List of Figures, continued

List of Figures, continued

Chapter 1

Introduction

Chemotaxis

Chemotaxis is the net movement of a motile organism towards chemical attractants and away from repellants. The study of motile bacteria began with the popularization and convenience of Anton van Leeuwenhoek's small light microscope. In the 1880's, the observations of the plant physiology pioneer Wilhem Pfeffer began in earnest the study of chemotaxis with his descriptions that certain organic and inorganic compounds attracted some bacteria at exceptionally low concentrations [1]. It wasn't until 80 years later when the curiosity of Julius Adler expanded the knowledge of the field with the publication, "Chemotaxis in Bacteria" in Science in 1966 using *Escherichia coli* as his model organism [2]. Since that time, the chemotaxis pathway of *E. coli* has become the best characterized signaling system in biology. The study of chemotaxis of various motile bacterial species shows certain common themes. One is that flagellar rotation propels the cells in an aqueous environment with random switches or stops in rotation allowing reorientation of the cell in a new swimming direction. Second, the "random walk" of swimming bacteria is biased. As cells near attractants, the rate of switching decreases due to more favorable conditions. Conversely, as cells near repellants, the rate of switching increases as they search for a better niche. Many environmental cues have been shown to elicit a response in the bacterial swimming bias including pH, temperature, gravity, light, oxygen, and numerous sources of carbon and nitrogen [3-9]. Another theme conserved across Bacteria and Archaea is the cellular machinery necessary for chemotaxis which localizes at one or both cell poles [10]. The ultimate goal of sensing multiple environmental and cellular signals is to allow the cell to navigate to the most favorable niche [11]. Consistent with this hypothesis, bacteria with dynamic metabolic

strategies (nitrogen fixation, photosynthesis, anaerobiosis, etc.), due to the changing conditions within the niche they occupy (e.g. soil or aquatic), have larger repertoires of chemoreceptor genes [12].

Model organisms for chemotaxis: *Escherichia coli* and *Bacillus subtilis*

***Escherichia coli*.** The *E. coli* genome encodes one chemotaxis operon consisting of the necessary molecular components for the signaling pathway [13, 14] (Figure 1.1). CheA is an auto-phosphorylating histidine kinase that associates with the C-terminal domain of the methyl-accepting chemotaxis proteins (MCPs) via the adapter protein CheW [15, 16]. The MCPs, or chemoreceptors, in *E. coli* are membrane bound proteins that detect extracellular concentrations of attractants and repellants in the cell's microenvironment as it swims [17]. Binding and dissociation of these ligands initiate the signal across the membrane to CheA which autophosphorylates at a conserved histidine residue [18]. The phosphate group is transferred to one of two cognate response regulators, CheY and the methyl esterase CheB [19]. CheY-P diffuses through the cell and binds the flagellar switch protein FliM, reversing the direction of flagella rotation from counter clockwise to clockwise [20-22]. The signal output through CheY-P is terminated by phosphatase activity of CheZ [23-25]. As part of the chemotaxis- specific adaptation system, phosphorylated CheB removes methyl groups from specific glutamyl residues of MCPs which are added by the constitutively active methyltransferase CheR [13, 26, 27]. This chemical modification of chemotaxis receptors by differential methylation allow them to maintain greater sensitivity over a large ligand concentration range [28].

Escherichia coli encodes five individual chemoreceptors; the two abundant receptors, Tar and Tsr, along with Trg, Tap, and Aer. Tar allows cells to respond chemotactically to aspartate and

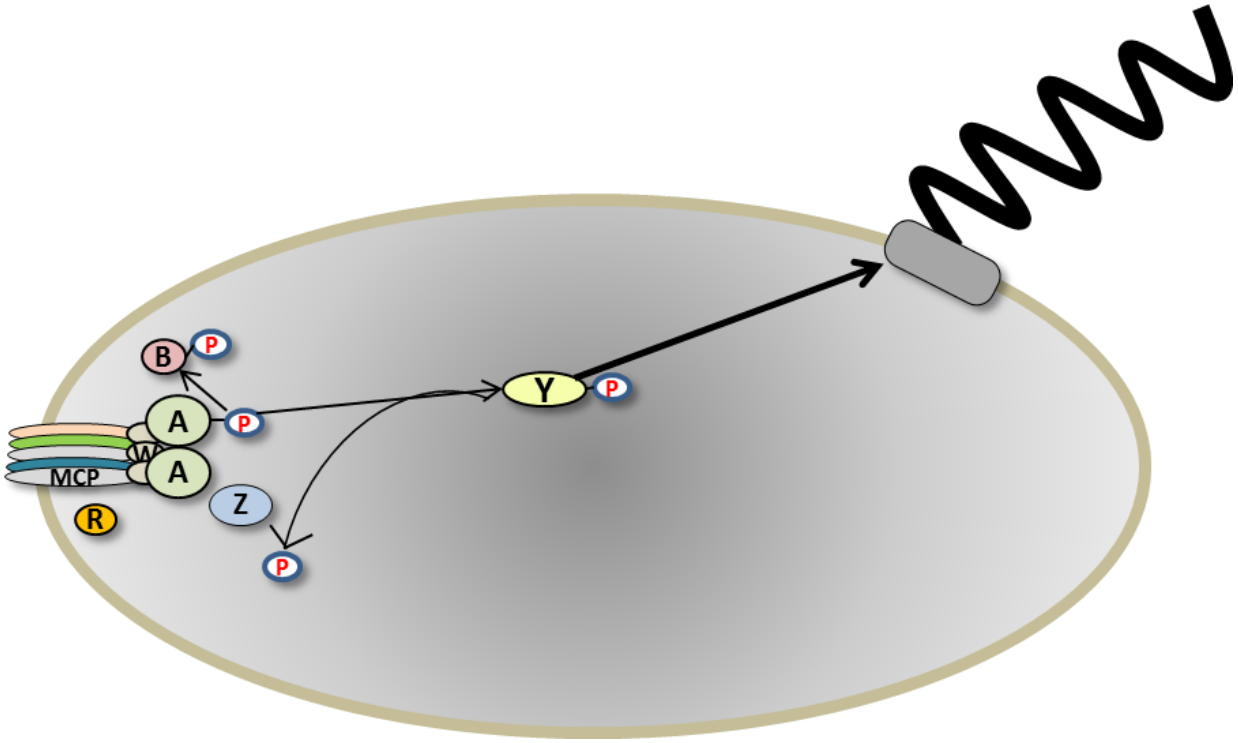

Figure 1.1: Chemotaxis pathway of the model organism *Escherichia coli*. Upon repellant binding or attractant dissociation, MCPs activate histidine kinase CheA via the adapter protein CheW. CheA undergoes autophosphorylation and phospho-transfer to the cognate response regulator CheY. Phosphorylated CheY diffuses through the cells, binds the flagellar switch complex protein FliM, and causes a change in flagellar rotation. To reset CheY and respond to additional stimuli, CheY-P is dephosphorylated by the phosphatase CheZ. The methyltransferase CheR constitutively adds methyl groups to conserved glutamate residues of receptors to modulate CheA activity. Another response regulator, CheB, is phosphorylated by CheA (at a slower rate than CheY) activating methylesterase activity to restore CheR substrates through demethylation.

maltose (when the sugar is bound to the periplasmic maltose binding protein, MBP) [29, 30], with relatively high affinity for aspartate at 3 μM in *E. coli* [31]. Several solved structures for the ligand binding periplasmic domain are available for different bacteria including *E. coli* and *Salmonella typhimurium* (*S. typhimurium*). The other abundant receptor is Tsr which binds serine directly [32] as well as participates in energy and aero-taxis with the more recently discovered Aer [33]. Unlike the other four MCPs, Aer does not contain transmembrane domains and thus monitors the cytoplasm via the FAD-containing PAS domain [33, 34]. The chemoreceptor Trg recognizes ribose and galactose while Tap is specific for dipeptides. Recent research uncovered a novel role for Tap in response to the pyrimidines thymine and uracil [35]. Another general positive and negative chemotactic response for phenol is associated with Tar and Tsr, respectively [36]. Recent work has also shown Tsr to be the chemoreceptor responsible for chemotaxis to the quorum sensing molecule AI-2 [37].

***Bacillus subtilis*.** The chemotaxis pathways of *B. subtilis* have become the best studied among Gram positive bacteria. Upon binding of a chemical attractant, CheA becomes phosphorylated and phosphorylates CheY, which is opposite to the situation in *E. coli*, where CheY-P is produced in response to an increase in repellent concentrations [38, 39] (Figure 1.2). Another major difference with chemotaxis in *E. coli* lies within the adaptation system. In *E. coli*, methylation ultimately decreases CheA activity [40] while the methylation pattern of McpB, for example, in *B. subtilis* determines how the cell adapts: E637 methylation leads to adaptation to the presence of attractant while methylated E630 (but not E637) leads to adaptation to removal of attractant [41]. Adaptation in *B. subtilis* depends on CheB and CheR as well as proteins not encoded within *E. coli*; CheD, CheC and CheV. CheD is a receptor deamidase converting conserved glutamine residues to glutamate thus creating new methylation sites for CheR [42-44]. CheC is a protein phosphatase localizing to receptor clusters as well as the flagellar switch complex [45] . At the

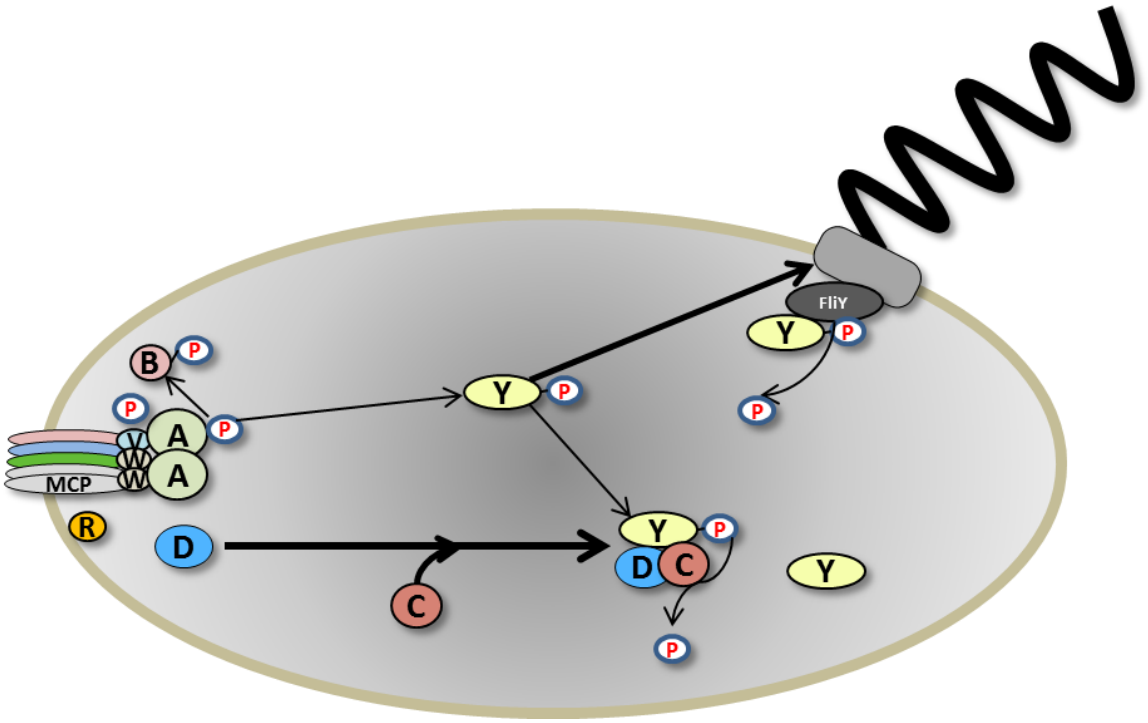

Figure 1.2: Chemotaxis pathway of the Gram-positive model organism *Bacillus subtilis*. When attractant binds, MCPs transmit the signal to CheA through the adapter proteins CheW and CheV (necessary for adaptation to asparagine). Autophosphorylation of CheA results in phospho-transfer to CheY. Che-P diffuses through the cell binding to the flagellar switch complex causing a change in flagellar rotation. The genome of *B. subtilis* contains no CheZ homologs. Therefore, hydrolysis of the phosphate group occurs at the switch complex by the phosphatase FliY. For adaptation, methylation/demethylation occurs via CheR and phosphorylated CheB, respectively. In addition, the deamidase CheD converts conserved glutamine residues of receptors to glutamate, increasing the available substrates for CheR. The poor phosphatase CheC effects adaptation by targeting CheD away from chemoreceptor clusters, forming a complex with CheY-P.

receptor complexes, CheC interacts with CheD, thus decreasing the number of available CheR substrate sites by lowering the rate of deamidation [42]. CheV is a response regulator, CheW fusion protein [46] modulating adaptation to the chemoattractant asparagine [46]. B. subtilis does not encode a CheZ homolog, leading to different modes of dephosphorylation of CheY-P, rather, using CheC-CheD and FliY to return CheY to its prestimulus state [47]. The dephosphorylation of CheY-P occurs predominantly at the flagellar switch via FliY [48]. FliY is found predominantly in Gram-positive bacteria (and some Spirochetes) and is a homolog of CheC [47]. In fact, the primary function of CheC is modulating adaptation through its interactions with CheD, rather than as a CheY-P phosphatase [42-44]. As attractant binds to the chemoreceptors, an increase in CheY-P leads to an increase in CheC-CheY-P complexes which become alternative interaction partners for CheD, luring the deamidase away from the receptor complex thus lowering CheA activity.

Diversity in bacterial chemotaxis

Like other model systems in Biology, *E. coli* does not reflect the chemotactic variation and complexity of all characterized Bacteria and Archaea. The alphaproteobacterium *Rhodobacter sphaeroides* is another well understood chemotaxis model system; however, it is an example of a more complex model. First, unlike *E. coli*, the genome of *R. sphaeroides* encodes multiple chemotaxis pathways [7, 49]. It also has two flagellar systems, Fla1 and Fla2, controlled by separate chemotaxis pathways [50, 51]. Fla1 is a unidirectional flagellar system with frequency and duration of stops regulated by two distinct chemotaxis systems, the membrane localized CheOp2 and cytoplasmic CheOp3 [52, 53]. The membrane-bound chemoreceptors associated with CheOp2 presumably sense periplasmic concentrations of attractants while the soluble chemoreceptors of CheOp3 sense the intracellular metabolic state. The *che*Op1 encoded proteins

regulate the Fla2 system [54]. However, this flagellar system is not expressed under normal laboratory conditions.

Another departure from the *E. coli* model is the predominance of a strategy known as energy taxis in which cell motility depends upon cell metabolism and not necessarily on concentrations of attractants. The cytoplasmic cluster of chemoreceptors and their associated Che proteins are predicted to sense the intracellular energy state and regulate $CheA_3$ phosphorylation [55]. Interestingly, through the use of mathematical modeling and experimental verification, it was recently showed that *R. sphaeroides* uses a phosphorelay system to link the membrane and cytoplasmic receptor clusters [56]. Activation of $CheA_3$ leads to phosphorylation of $CheY_6$ or $CheB_2$. Phospho-$CheB_2$ can then phosphorylate $CheA_2$, part of the membrane cluster complex, which itself can then transfer a phosphate one of its cognate response regulators. This phosphorelay between CheA3 and cheA2, involving CheB2, allows for cytoplasmic $CheA_3$ to indirectly modulate the phosphorylation of non-cognate regulators, and thus affecting the motility pattern. This strategy has been proposed to be advantageous under conditions where attractant concentrations are high ($CheA_2$ activity is low) but intracellular metabolic conditions are becoming less favorable (increased $CheA_3$ activity) and a change in direction is needed [55].

The genome of the deltaproteobacterium *Myxococcus xanthus* encodes 8 *che* operons, the most of any sequenced genome [57]. *M. xanthus* also has two distinct motility systems; adventurous (A) and social (S) motility [58, 59]. S motility, motility of groups of cells, is necessary for aggregation into fruiting bodies while A motility is required for movement of individual cells using Type IV pili (TFP) [60]. The most studied pathway was discovered screening mutants deficient in aggregating to form fruiting bodies when nutrients were limiting [61]. Closer analysis determined the mutations targeted the *frz* (“frizzy”) operon controlling cell reversals and sequence analysis revealed the gene products were homologous to *che* genes of enteric bacteria

[62, 63]. The MCP homolog FrzCD has no predicted transmembrane domain and fluorescent protein fusions to FrzCD showed cytoplasmic clusters localized in a helical pattern along the length of the cell [64]. The FrzCD clusters were dynamic in size and number, and interestingly sensitive to cell-cell contacts; appearance of localization at the site of contact [64].

Another characterized *che* system in *M. xanthus* is the Dif (*d*efective *i*n *f*ruiting) pathway, which was discovered after screening fruiting body-null mutants [65]. Some of these mutants were found to be lacking the ability to produce exopolysaccharides (EPS) (CheA, CheW, MCP homologs) [66] while others overproduced EPS (CheY and CheC homologs) [67] suggesting this pathway does not follow the canonical phosphorelay of two component systems (CheA to CheY). Studies have shown an epistatic link between the Dif system and TFP in EPS regulation [68]. The authors have proposed pili are the sensor stimulating Dif-regulation of EPS [68]. Besides EPS regulation, the Dif system controls reversal frequency of starved cells which respond chemotactically to some phosphatidylethanolamines (PEs), a chemoattractant for the DifA chemoreceptor [69]. A link between the Dif and Frz systems were observed in response to PE. *M. xanthus* suppresses reversal frequency when on PE agar via the Dif system then adapt and return to a prestimulus frequency in about an hour [70]. However, *frz* mutants were unable to return to prestimulus reversal frequency indicating the two systems interact to control motility. The Che3 system is involved in gene regulation during the vegetative to fruiting body transition with no direct role in motility [71]. Che4 functions in regulating S motility [72]. The function of the other chemotaxis systems has not yet been elucidated [73].

Pseudomonas aeruginosa is another well studied organism for chemotaxis and chemotaxis-like systems. The *P. aeruginosa* PAO1 genome encodes four che-like signaling pathways as well as 26 chemoreceptors [74] with 6 receptors expressed in stationary phase [75]. One operon regulates pilus-mediated surface motility [76]. Another system, the Wsp system, is involved in c-di-GMP

regulated biofilm formation [77, 78]. The Wsp system is homologous to chemotaxis in *E. coli* with few modifications. The signal output of *E. coli* chemotaxis, phosphorylated CheY (a single domain protein), leads to a switch in flagella rotation while in *P. aeruginosa*, the signal output promotes production of c-di-GMP via WspR [78]. WspR is a two-domain protein possessing a REC domain (CheY-like) homolog fused to a diguanylate cyclase domain and when WspR is activated by phosphorylation, it is responsible for conversion of 2 GTP to c-di-GMP, thereby contributing to an elevated concentration of intracellular c-di-GMP [79, 80]. C-di-GMP has been characterized as a second messenger signaling molecule in bacteria [81-83]. One effect of an increase in cellular c-di-GMP concentrations is the transcription of genes necessary for biofilm formation [78]. One mechanism by which this occurs has been determined in *P. aeruginosa*. The transcription factor FleQ, a repressor of biofilm synthesis operons, was shown to directly bind c-di-GMP and activate transcription [84].

Using fluorescent protein fusions to Che and Che2 proteins, the Harwood laboratory determined Che is the major regulator of flagellar motility while Che2 is upregulated in stationary phase [85]. Interestingly, McpA-CFP, a receptor fused to cyan fluorescent protein which is expressed during stationary phase appeared to colocalize with CheA-YFP when cells entered stationary phase [85]. This suggested chemotaxis clusters reorganize over the life of the cell with at least some chemoreceptors being introduced into the complex. However, a colocalization study with CheA-CFP and the stationary phase expressed CheY2-YFP suggested the two chemosensory systems do not colocalize or "inter-mix".

Rhodospirillum centenum is one of the most similar microorganisms to *A. brasilense* with respect to construction of its three *che* operons [86]. *R. centenum* is a purple nonsulfur photosynthetic bacterium, predominantly aquatic, and capable of nitrogen fixation [87]. It also has all three *che* operons characterized. *che*$_1$, homologous to Che1 from *A. brasilense*, is the chemotaxis pathway

similar to the model from *E. coli* [88, 89]. *che*$_2$ is a chemotaxis-like pathway regulating flagella biosynthesis [90]. Mutants of *che*$_2$ are defective in swarming and swimming motility due to perturbations in lateral and polar flagella [90]. *che*$_3$ was shown to regulate cell differentiation into dessication-resistant cyst cells with deletions in *cheY*$_3$, *cheB*$_3$, *cheS*$_3$, and *che*$_3$ resulting in constitutive cyst development [91]. The remainder of deletion mutants, *cheW*$_{3a}$, *cheW*$_{3b}$, *cheA*$_3$, *cheR*$_3$, and *mcp*$_3$, are unable to efficiently form cyst cells on nutrient-deprived media [91].

Chemoreceptor architecture and function

The genomes of motile bacteria encode many chemotaxis proteins absent in *E. coli*. The most variable component of chemotaxis systems is the chemoreceptor repertoire in both number per genome and specificity. Prototypical chemoreceptors contain several domains; a sensing domain, two transmembrane domains, a HAMP domain, and a methyl-accepting (MA) domain (Figure 1.3A). The most conserved region is the MA domain. It consists of two methylation helices where the adaptation proteins interact and a highly conserved region at the hinge necessary for interaction with CheW and CheA. The methylation helices contain conserved glutamate (or glutamine) residues available for modification via a variety of adaptation proteins. These modifications alter CheA activity and ultimately lead to a greater sensitivity over a dynamic attractant concentration range and a molecular memory [94]. The highly conserved region contains the residues necessary for interaction with CheW and CheA [95]. The structure of each component of the ternary complex has been solved separately, but the interactions between them that govern regulation of kinase activity are still poorly understood. The sequence conservation of this region also allows identification of new representatives of this protein family in newly sequenced bacterial genomes (Figure 1.3B).

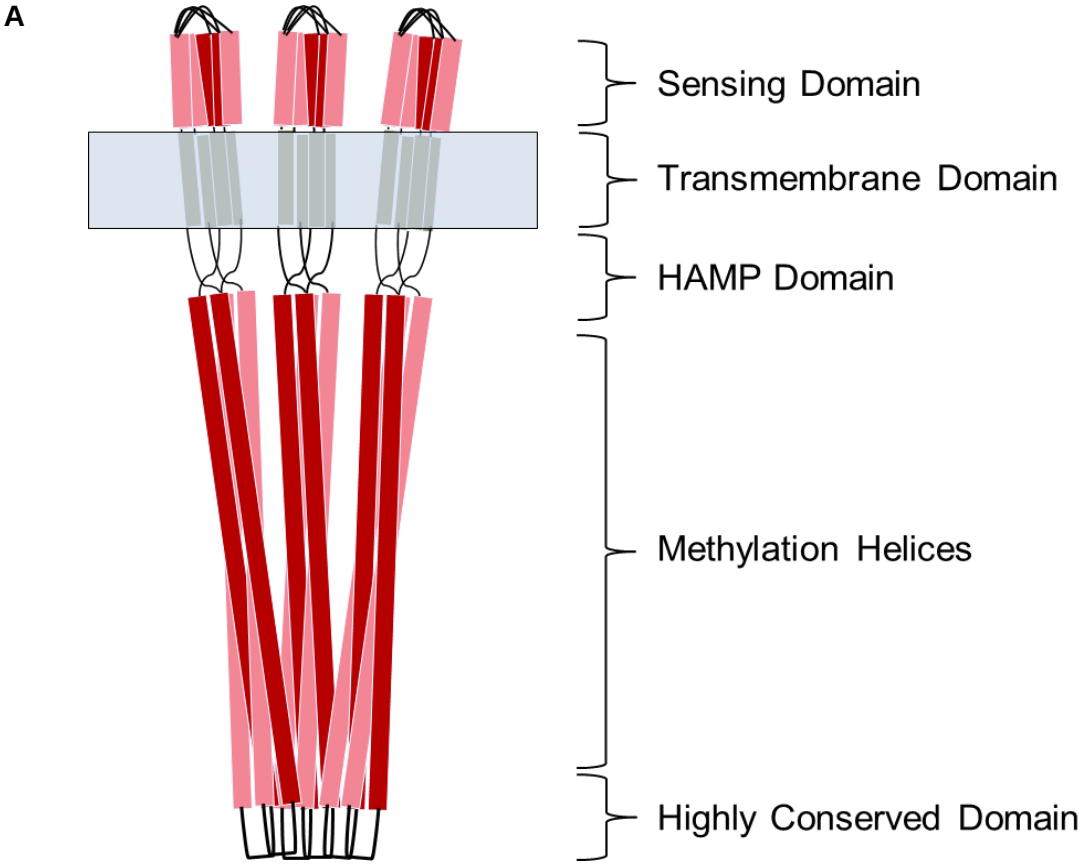

Figure 1.3: Chemoreceptor domain organization and distinguishing sequence. A, Prototypical chemoreceptors form homodimers with two long methylation helices as coiled coils. B, Sequence Logo [92] generated from 100 homologs of the Tlp1 chemoreceptor from *A. brasilense* [93]. Sequence conservation within the Highly Conserved Domain makes annotation possible from newly sequenced genomes for putative receptor proteins.

Another cytoplasmic domain common to chemoreceptors is the HAMP domain named for the proteins it is found in; **h**istidine kinases, **a**denylate cyclases, **M**CPs, **p**hosphatases. Despite the large amount of experimental data for this domain, the structure is poorly understood, with the exception of a solution structure from an archaeal HAMP protein (Af1503) [96], as well as how this domain converts the periplasmic signal into a cytoplasmic signal. The most variable domain and least characterized is the sensing, or ligand binding, domain. This domain serves as the input module which interacts with specificity to attractants or repellants. As of January 2012, the MiST2 database contained 21,722 annotated receptor genes from sequenced bacterial and archaeal genomes [97]. However, over 80 percent of bacterial receptor sequences have no identifiable sensing domain suggesting these characterized protein domains are not detectable by available algorithms or represent sensory domains with unknown function [12, 98]. Due to gene duplication leading to overlap of function and the number of potential ligands (sugars, organic acids, etc.), the characterization of individual chemoreceptors within an organism is not trivial.

The positioning of chemotaxis protein clusters is also not random within cells. Using fluorescent protein fusions and immunogold labeling electron micrographs, chemoreceptors were shown to localize to the polar region within bacteria [99-102]. In fact, polar localization of chemotaxis clusters is conserved across Eubacteria and Archaea [10]. Receptors colocalize with other chemotaxis proteins creating a macromolecular protein signaling complex.

Role of the signaling complex for sensitivity and amplification.

Data suggest chemoreceptors form homodimers that associate with two other homodimers to form a “trimer of dimers”, with CheA and the adapter CheW interacting at the membrane-distal tip of trimer of receptor dimers, forming functional signaling complexes[103, 104]. Having signaling teams clustered together is thought to increase cooperativity and sensitivity to small net

changes in ligand occupancy of receptors [28]. Using GFP fusions in *E. coli*, newly transcribed receptors were shown to be first inserted into the lateral membrane in a Sec pathway-dependent manner and later were observed at the cell poles [105]. Even though localization of chemotaxis clusters is observed in the polar region, smaller lateral clusters are also observed using fluorescent protein fusions [106]. These nascent-periodic clusters are thought to become polar clusters after several rounds of cell division.

Thousands of copies of chemotaxis proteins are localized in the receptor clusters. This sub-localization allows for all necessary components to colocalize to maximize efficiency; CheW and CheA co-localize by associating with receptors, CheY and CheB co-localize via interaction with CheA, and in *E. coli* and closely related bacteria, CheR co-localizes to signaling complexes via interactions with a conserved pentapeptide found on the C-terminus of abundant receptors [107, 108]. Many studies have shown these signaling clusters to be highly cooperative [28, 109] and a functional CheB is necessary for sensitivity [110]. Electron microscopy cryotomography has revealed that receptor arrays are arranged in a hexagonal lattice in all bacterial species where they have been analyzed, suggesting that this is a universal architectures of chemotaxis signaling complexes [111-113]. The stoichiometry of CheA, CheW, and receptors can vary somewhat (1:1:6, 1:2:6 [113], 1:4:6 [114], 1:3:6-9 [115]) suggesting protein-protein interactions are dynamic. Evidence for this was provided using disulfide linking, crystallographic, and fluorescence studies [116-118]. Attractant binding to chemoreceptors, aspartate for example, can alter cluster stability leading to a decrease in CheA activity [117]. Inactive CheA leads to an increase in receptor methylation via CheR; predicted to stabilize the receptor packing and to increase the probability of CheA autophosphorylation activity [118].

Another property of some chemoreceptors is the ability to respond to temperature changes. However, this response is not mediated through the sensing domain. Tar, the aspartate receptor

from *E. coli*, has involvement in thermotaxis [119-121]. In fact, thermotaxis is described for all 5 *E. coli* receptors [122-125]. Site-directed mutagenesis has suggested the transmembrane region, HAMP domain, and CheR methylation sites are responsible for this ability [119-121]. For instance, in presence of aspartate, methylation of any of the four sites can change the temperature dependent swim bias of a cell [120].

Studies have investigated the presence, function, and localization of cytoplasmic chemotaxis clusters in other bacteria including *Myxococcus xanthus* [64], *Pseudomonas aeruginosa* [126], and *Sinorhizobium meliloti* [102, 127]. Many observed soluble chemoreceptors localize to the membrane and are predicted to interact with the membrane associated chemotaxis machinery [126, 127].

Chemoreceptor diversity

The number of receptor genes per genome also varies from 1 (*Mezorhizobium loti*) to 93 (putative, *Pseudomonas syringae pv. oryzae str. 1_6*) with no correlation between number of chemoreceptor genes and genome size [12]. Lifestyle and environment of a bacterium, however, show strong correlation with the number of chemoreceptor its genome encodes. A recent study by Lacal and colleagues (2011) noted that bacteria with several metabolic strategies (diazotrophic, photosynthetic, etc.) or found in diverse environmental niches have larger receptor repertoires than commensal or metabolically limited organisms. They also organized receptors into classes based upon topology. The most dominant class is Class I, comprised of Ia and Ib, which contain two or one transmembrane domains, respectively, and a periplasmic ligand binding region [12]. Class II also contains transmembrane domains. Class IIa has a cytoplasmic ligand binding region and IIb lacks any putative sensing domain and contains one to eight transmembrane domains. Class III is comprised of the cytoplasmic chemoreceptors, IIIa contain a sensing domain and IIIb

do not. According to analysis from this study, the relative abundance of Class I, II, and III are 74%, 13%, and 13%, respectively.

Another important study by Alexander and Zhulin analyzed the cytoplasmic signaling domains of 2,125 annotated chemoreceptors [128]. A multiple sequence alignment of the receptors detected symmetric insertions or deletions, referred to as indels within the sequences. The indels were 7-amino acid segments called heptads. The study also clearly defined the regions of the methylation helices and signaling domains and described a third domain called the flexible bundle which the authors predicted would allow for signal transmission to the signaling domain. This study also led to the classification of chemoreceptors based upon the length of their cytoplasmic domain measured in heptads. The 5 receptors of the model organism *E. coli* are all 36H meaning the cytoplasmic domain consists of 36 heptads while the 10 receptors of *B. subtilis* are 44H (44 heptads) [128].

As stated earlier, the sensing domain of chemoreceptors is highly variable with almost 9 out of 10 having no known sequence conservation to annotated, functional domains [12]. However, a majority of chemoreceptors in which the sensing domain is annotated contain a PAS domain, a ubiquitous protein domain named after the 3 proteins Per, Arnt, Smt [129, 130]. The PAS domain is common within energy taxis transducers. The Aer receptor from *E. coli* is the most studied energy taxis receptor containing a PAS domain [33]. The Aer PAS domain binds the cofactor FAD [131], an important redox molecule within the cell. PAS containing receptors have been classified using a comparative genomics approach into three classes based upon sequence conservation [132]. Class I and II non-covalently bind FAD, however, class I is membrane-bound and class II cytoplasmic. Class III contains PAS-containing receptors that may or may not bind FAD. PAS domains are known to bind several cofactors including heme-b [133], heme-c [134, 135], FMN [136], dicarboxylates [137, 138], and divalent cations [139, 140]. Many bacteria

capable of energy taxis contain Aer-like receptors [11, 141-143] including the alpha-proteobacterium *Azospirillum brasilense*.

Azospirillum chemotaxis systems from a genome perspective

Azospirillum brasilense is a motile diazotrophic soil bacterium commonly associated with the roots of various cereals including corn, wheat, and rice [144]. The recently published genome of strain Sp245 has four chemotaxis-like operons [86] as well as 53 putative chemoreceptors. The genus *Azospirillum* is very diverse and it is closely related to several species of bacteria that are found in aquatic environments, including *Rhodospirillum* [86]. The major motility chemotaxis operon of *Rhodospirillum centenum* is present in *A. brasilense* but Che1 only plays a minor role in the regulation of chemotaxis in *A. brasilense* [145]. The other two operons of *R. centenum* which have been studied experimentally in this species are homologous to *A. brasilense* Che2 and Che3 controlling flagellar biosynthesis and cyst development, respectively [90, 91]. Che4 is thought to be the result of horizontal gene transfer in a common ancestor to all sequenced *Azospirilla* and is not found in closely related *R. centenum* (Figure 1.4). The genome also encodes numerous chemotaxis genes products that are not found within operons including CheD (2), CheB (3), CheR (2), and CheZ (4) [86]. The genes encoding the chemoreceptors were annotated based upon the high conservation within the methyl-accepting domain. However, assigning function or ligand specificity is much more arduous. Che1 does not encode receptors, but Che2 and Che3 have one each. Che4 encodes two receptors, one of which is transcriptionally coupled to the methyltransferase CheR. The presence of chemoreceptor genes within chemotaxis-like operons suggests their importance for the function of that pathway. However, the cellular function of these three operons is unknown as is the specificity of the operon-encoded receptors.

***Azospirillum* sensing, locomotor behavior and chemoreceptors**

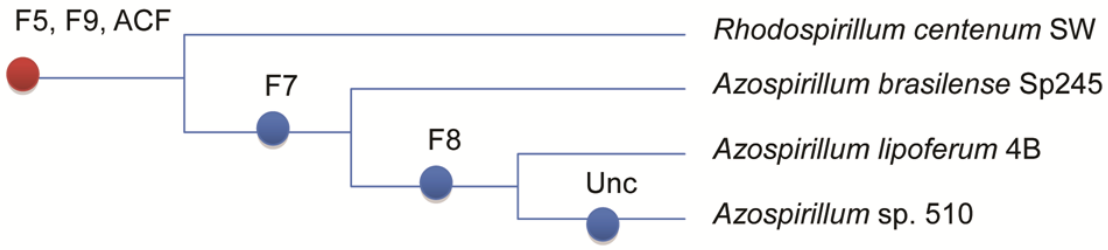

Figure 1.4: Phylogenetic analysis representing horizontal chemotaxis operon transfers among sequenced *Azospirilla* and closely related *Rhodospirillum centenum*. Reprinted from [86]. Operon classifications are detailed in [146].

To date, the characterization of *A. brasilense* chemotaxis systems has led to assigned function to one *che* operon, Che1 [145], and two chemoreceptors, Tlp1 and AerC [93, 132]. Unlike most chemotaxis systems, Che1 controls the swimming speed but not the swimming reversal frequency and thus has only a limited role in chemotaxis [Chapter 3; Bible, Russell, and Alexandre, in press]. Che1 also appears to affect the ability of cells to change their cell surface properties as well as cell size at division [145]. AerC is a soluble receptor containing two PAS domains and it was shown to non-covalently bind the redox cofactor FAD [132]. The location of *aerC* on the genome, within a nitrogen fixation cluster, suggested its role under nitrogen-limiting conditions. This was confirmed using a promoter report fusion and antibodies specific to this protein. The predominant role of AerC is energy taxis, under conditions of nitrogen fixation.

The ability to bind FAD by PAS-containing chemoreceptors allows cells to monitor reduction potential and the redox status of their metabolism, and thus to potentially respond by changing their swimming bias to avoid microenvironments that would reduce intracellular energy production. For example, *E. coli* uses the serine receptor Tsr and Aer (aerotaxis receptor) to monitor the energy state of the cell [33, 131, 147]. Tsr was shown to monitor proton motive force while Aer monitors reduction potential via an FAD cofactor found in its PAS domain, similar to AerC [147]. A proton motive force is critical for ATP production and active transport in aerobic bacteria [148], therefore, the ability to respond tactically to insults to this parameter would be essential. Tsr has been proposed to sense the proton motive force but the detailed mechanism is yet to be elucidated [147]

Tlp1 (transducer-like protein 1) was found to have a conserved sensing domain of unknown function that is also found among chemoreceptors and histidine kinases of various bacteria. Through mutagenesis, Tlp1 was described as an energy taxis transducer involved in chemotaxis to oxidizable substrates, aerotaxis, and redox taxis [93]. Because it lacks any redox motif or any

known element for energy sensing, Tlp1 was proposed to perhaps sense the proton motive force, similar to Tsr [93]. Tlp1 also contains an extreme C-terminal amino acid sequence beyond the conserved signaling domain that is common to all receptors. Two years after the characterization of Tlp1, a landmark paper entitled, **PilZ domain is part of the bacterial c-di-GMP binding protein**, by Amikam and Galperin, annotated this sequence as a PilZ domain [149]. The PilZ domain was predicted and subsequently verified as a binding partner for the bacterial second messenger molecule cyclic-di-GMP (c-di-GMP) [82, 150]. C-di-GMP is a relative newcomer in second messenger research; only discovered by the Benziman laboratory in the 1980's by studying regulation of cellulose synthesis [151, 152]. Now, c-di-GMP is known as a ubiquitous second messenger implicated in many bacterial processes including pathogenesis [153-155], biofilm formation [156-158], exopolysaccharide (EPS) production [81, 159], motility [160, 161], cell differentiation [162, 163], and others [156, 164, 165]. Synthesis of c-di-GMP occurs via the diguanylate cyclase domain [79, 80], referred to as the GGDEF domain due to active site residues, and degraded by phosphodiesterase activity of the EAL domain [166, 167] and/or HD-GYP domain [168]. Enzyme activity is regulated by several mechanisms including product inhibition [169, 170] and numerous sensing domains like PAS [171-173], GAF [174], and REC [175, 176].

To date, the PilZ domain is the only specific protein binding partner for c-di-GMP. Cyclic nucleotide binding (cNMP) domains have evolved to link intracellular levels of c-di-GMP to transcription regulation [165, 177] and c-di-GMP specific riboswitches have also been identified [178, 179]. Unlike binding to transcription factors or translation regulators, the output effect of c-di-GMP binding to the PilZ domain remains elusive because the downstream protein-protein interactions have not been identified. A search of the Microbial Signal Transduction 2 database (MiST2) [97] reveals a large number of annotated PilZ domain proteins from sequenced bacterial

genomes are single domain proteins (2049 out of 3998, ~51%) and only a very small subset, 42, are coupled to chemoreceptors. The PilZ-containing Tlp1 from *A. brasilense* offers an opportunity to investigate a direct role of the second messenger c-di-GMP in modulation of energy taxis and motility.

Concluding Remarks

The purpose of my work was to i) investigate the function of a novel chemoreceptor mutant derivative of *A. brasilense* Sp7 [180] and ii) elucidate the PilZ domain function of Tlp1 and its role in motility. Chapter 2 will detail the work characterizing the function and ligand specificity of the *A. brasilense* chemoreceptor, Tlp2. Chapter 3 will detail the work linking cell-to-cell contacts (clumping) associated with *A. brasilense* with the sensory output of Che1 through control of swimming speed [Bible, Russell, and Alexandre, in press]. Chapter 4 will detail cyclic-di-GMP effects on Tlp1 sensing and sensitivity with regards to aerotaxis. Finally, in Chapter 5, I will discuss work detailing possible crosstalk between Che1 and other chemotaxis pathways as revealed through changes in transient clumping of various relevant mutants and complementation strategies.

List of References

1. Pfeffer, W., Locomotorische Richtungsbewegungen Durch Chemische Reize. *Unters. Bot. Inst. Tübingen*, 1884. 1: p. 363.
2. Adler, J., Chemotaxis in Bacteria. *Science*, 1966. 153(3737): p. 708-&.
3. Croxen, M.A., et al., The *Helicobacter Pylori* Chemotaxis Receptor TlpB (Hp0103) Is Required for Ph Taxis and for Colonization of the Gastric Mucosa. *Journal of Bacteriology*, 2006. 188(7): p. 2656-65.
4. Repaske, D.R. and J. Adler, Change in Intracellular Ph of *Escherichia Coli* Mediates the Chemotactic Response to Certain Attractants and Repellents. *J Bacteriol*, 1981. 145(3): p. 1196-208.
5. Lewus, P. and R.M. Ford, Temperature-Sensitive Motility of *Sulfolobus Acidocaldarius* Influences Population Distribution in Extreme Environments. *Journal of Bacteriology*, 1999. 181(13): p. 4020-5.
6. Wenter, R., et al., Ultrastructure, Tactic Behaviour and Potential for Sulfate Reduction of a Novel Multicellular Magnetotactic Prokaryote from North Sea Sediments. *Environmental Microbiology*, 2009. 11(6): p. 1493-505.
7. Hamblin, P.A., et al., Evidence for Two Chemosensory Pathways in *Rhodobacter Sphaeroides*. *Molecular Microbiology*, 1997. 26(5): p. 1083-96.
8. Frankel, R.B., et al., Magneto-Aerotaxis in Marine Coccoid Bacteria. *Biophysical Journal*, 1997. 73(2): p. 994-1000.
9. Jiang, Z.Y. and C.E. Bauer, Component of the *Rhodospirillum Centenum* Photosensory Apparatus with Structural and Functional Similarity to Methyl-Accepting Chemotaxis Protein Chemoreceptors. *Journal of Bacteriology*, 2001. 183(1): p. 171-7.

10. Gestwicki, J.E., et al., Evolutionary Conservation of Methyl-Accepting Chemotaxis Protein Location in Bacteria and Archaea. *Journal of Bacteriology*, 2000. 182(22): p. 6499-502.

11. Alexandre, G., S. Greer-Phillips, and I.B. Zhulin, Ecological Role of Energy Taxis in Microorganisms. *Fems Microbiology Reviews*, 2004. 28(1): p. 113-26.

12. Lacal, J., et al., Sensing of Environmental Signals: Classification of Chemoreceptors According to the Size of Their Ligand Binding Regions. *Environmental Microbiology*, 2010. 12(11): p. 2873-84.

13. Parkinson, J.S., Complementation Analysis and Deletion Mapping of *Escherichia Coli* Mutants Defective in Chemotaxis. *J Bacteriol*, 1978. 135(1): p. 45-53.

14. Silverman, M. and M. Simon, Operon Controlling Motility and Chemotaxis in *Escherichia Coli*. *Nature*, 1976. 264(5586): p. 577-80.

15. Borkovich, K.A., et al., Transmembrane Signal Transduction in Bacterial Chemotaxis Involves Ligand-Dependent Activation of Phosphate Group Transfer. *Proceedings of the National Academy of Sciences of the United States of America*, 1989. 86(4): p. 1208-12.

16. Liu, J.D. and J.S. Parkinson, Role of Chew Protein in Coupling Membrane-Receptors to the Intracellular Signaling System of Bacterial Chemotaxis. *Proceedings of the National Academy of Sciences of the United States of America*, 1989. 86(22): p. 8703-7.

17. Adler, J., Chemoreceptors in Bacteria. *Science*, 1969. 166(913): p. 1588-97.

18. Bilwes, A.M., et al., Structure of Chea, a Signal-Transducing Histidine Kinase. *Cell*, 1999. 96(1): p. 131-41.

19. Lukat, G.S., et al., Phosphorylation of Bacterial Response Regulator Proteins by Low-Molecular-Weight Phospho-Donors. *Proceedings of the National Academy of Sciences of the United States of America*, 1992. 89(2): p. 718-22.

20. Barak, R. and M. Eisenbach, Correlation between Phosphorylation of the Chemotaxis Protein Chey and Its Activity at the Flagellar Motor. *Biochemistry*, 1992. 31(6): p. 1821-6.

21. Bourret, R.B., J.F. Hess, and M.I. Simon, Conserved Aspartate Residues and Phosphorylation in Signal Transduction by the Chemotaxis Protein Chey. *Proceedings of the National Academy of Sciences of the United States of America*, 1990. 87(1): p. 41-5.

22. Li, J.Y., et al., The Response Regulators CheB and CheY Exhibit Competitive-Binding to the Kinase Chea. *Biochemistry*, 1995. 34(45): p. 14626-36.

23. Hao, S.F., et al., Structural Basis for the Localization of the Chemotaxis Phosphatase CheZ by CheA(S). *Journal of Bacteriology*, 2009. 191(18): p. 5842-4.

24. HUANG, C. and R. STEWART, Chez Mutants with Enhanced Ability to Dephosphorylate CheY, the Response Regulator in Bacterial Chemotaxis. *Biochimica Et Biophysica Acta*, 1993. 1202(2): p. 297-304.

25. KUO, S. and D. KOSHLAND, Roles of *cheY* and *cheZ* Gene-Products in Controlling Flagellar Rotation in Bacterial Chemotaxis of *Escherichia coli*. *Journal of Bacteriology*, 1987. 169(3): p. 1307-14.

26. Kleene, S.J., M.L. Toews, and J. Adler, Isolation of Glutamic-Acid Methyl-Ester from an *Escherichia Coli* Membrane-Protein Involved in Chemotaxis. *Journal of Biological Chemistry*, 1977. 252(10): p. 3214-8.

27. Kirsch, M.L., et al., Chemotactic Methylesterase Promotes Adaptation to High-Concentrations of Attractant in *Bacillus Subtilis*. *Journal of Biological Chemistry*, 1993. 268(25): p. 18610-6.

28. Sourjik, V. and H.C. Berg, Functional Interactions between Receptors in Bacterial Chemotaxis. *Nature*, 2004. 428(6981): p. 437-41.

29. Slocum, M.K. and J.S. Parkinson, Genetics of Methyl-Accepting Chemotaxis Proteins in *Escherichia coli* - Organization of the Tar Region. *Journal of Bacteriology*, 1983. 155(2): p. 565-77.

30. Richarme, G., Interaction of the Maltose-Binding Protein with Membrane-Vesicles of *Escherichia coli*. *Journal of Bacteriology*, 1982. 149(2): p. 662-7.

31. Bjorkman, A.M., et al., Mutations That Affect Ligand Binding to the *Escherichia coli* Aspartate Receptor - Implications for Transmembrane Signaling. *Journal of Biological Chemistry*, 2001. 276(4): p. 2808-15.

32. Ames, P. and J.S. Parkinson, Constitutively Signaling Fragments of Tsr, the *Escherichia coli* Serine Chemoreceptor. *Journal of Bacteriology*, 1994. 176(20): p. 6340-8.

33. Rebbapragada, A., et al., The Aer Protein and the Serine Chemoreceptor Tsr Independently Sense Intracellular Energy Levels and Transduce Oxygen, Redox, and Energy Signals for *Escherichia coli* Behavior. *Proceedings of the National Academy of Sciences of the United States of America*, 1997. 94(20): p. 10541-6.

34. Bibikov, S.I., et al., Domain Organization and Flavin Adenine Dinucleotide-Binding Determinants in the Aerotaxis Signal Transducer Aer of *Escherichia coli*. *Proceedings of the National Academy of Sciences of the United States of America*, 2000. 97(11): p. 5830-5.

35. Liu, X. and R.E. Parales, Chemotaxis of *Escherichia coli* to Pyrimidines: A New Role for the Signal Transducer Tap. *J Bacteriol*, 2008. 190(3): p. 972-9.

36. Pham, H.T. and J.S. Parkinson, Phenol Sensing by *Escherichia coli* Chemoreceptors: A Nonclassical Mechanism. *Journal of Bacteriology*, 2011. 193(23): p. 6597-604.

37. Hegde, M., et al., Chemotaxis to the Quorum-Sensing Signal Ai-2 Requires the Tsr Chemoreceptor and the Periplasmic LsrB AI-2-Binding Protein. *J Bacteriol*, 2011. 193(3): p. 768-73.

38. Gegner, J.A., et al., Assembly of an Mcp Receptor, CheW, and Kinase CheA Complex in the Bacterial Chemotaxis Signal Transduction Pathway. *Cell*, 1992. 70(6): p. 975-82.

39. Schuster, S.C., et al., Assembly and Function of a Quaternary Signal-Transduction Complex Monitored by Surface-Plasmon Resonance. *Nature*, 1993. 365(6444): p. 343-7.

40. Anand, G.S. and A.M. Stock, Kinetic Basis for the Stimulatory Effect of Phosphorylation on the Methylesterase Activity of CheB. *Biochemistry*, 2002. 41(21): p. 6752-60.

41. Zimmer, M.A., et al., Selective Methylation Changes on the *Bacillus subtilis* Chemotaxis Receptor McpB Promote Adaptation. *Journal of Biological Chemistry*, 2000. 275(32): p. 24264-72.

42. Rosario, M.M. and G.W. Ordal, CheCand CheD Interact to Regulate Methylation of *Bacillus subtilis* Methyl-Accepting Chemotaxis Proteins. *Molecular Microbiology*, 1996. 21(3): p. 511-8.

43. Rosario, M.M., et al., Chemotactic Methylation and Behavior in *Bacillus subtilis*: Role of Two Unique Proteins, CheC and CheD. *Biochemistry*, 1995. 34(11): p. 3823-31.

44. Kristich, C.J. and G.W. Ordal, *Bacillus subtilis* CheD Is a Chemoreceptor Modification Enzyme Required for Chemotaxis. *Journal of Biological Chemistry*, 2002. 277(28): p. 25356-62.

45. Kirby, J.R., et al., CheC Is Related to the Family of Flagellar Switch Proteins and Acts Independently from Ched to Control Chemotaxis in *Bacillus subtilis*. *Molecular Microbiology*, 2001. 42(3): p. 573-85.

46. Karatan, E., et al., Phosphorylation of the Response Regulator CheV Is Required for Adaptation to Attractants During *Bacillus subtilis* Chemotaxis. *Journal of Biological Chemistry*, 2001. 276(47): p. 43618-26.

47. Szurmant, H., T.J. Muff, and G.W. Ordal, *Bacillus subtilis* CheC and FliY Are Members of a Novel Class of CheY-P-Hydrolyzing Proteins in the Chemotactic Signal Transduction Cascade. *Journal of Biological Chemistry*, 2004. 279(21): p. 21787-92.

48. Szurmant, H., et al., *Bacillus subtilis* Hydrolyzes CheY-P at the Location of Its Action, the Flagellar Switch. *Journal of Biological Chemistry*, 2003. 278(49): p. 48611-6.

49. Romagnoli, S. and J.P. Armitage, Roles of Chemosensory Pathways in Transient Changes in Swimming Speed of *Rhodobacter sphaeroides* Induced by Changes in Photosynthetic Electron Transport. *Journal of Bacteriology*, 1999. 181(1): p. 34-9.

50. Porter, S.L., et al., The Third Chemotaxis Locus of *Rhodobacter sphaeroides* Is Essential for Chemotaxis. *Molecular Microbiology*, 2002. 46(4): p. 1081-94.

51. Shah, D.S.H., et al., Fine Tuning Bacterial Chemotaxis: Analysis of *Rhodobacter sphaeroides* Behaviour under Aerobic and Anaerobic Conditions by Mutation of the Major Chemotaxis Operons and *cheY* Genes. *Embo Journal*, 2000. 19(17): p. 4601-13.

52. Martin, A.C., G.H. Wadhams, and J.P. Armitage, The Roles of the Multiple CheW and CheA Homologues in Chemotaxis and in Chemoreceptor Localization in *Rhodobacter sphaeroides*. *Molecular Microbiology*, 2001. 40(6): p. 1261-72.

53. Wadhams, G.H., et al., Requirements for Chemotaxis Protein Localization in *Rhodobacter sphaeroides*. *Molecular Microbiology*, 2005. 58(3): p. 895-902.

54. del Campo, A.M., et al., Chemotactic Control of the Two Flagellar Systems of *Rhodobacter sphaeroides* Is Mediated by Different Sets of CheY and FliM Proteins. *J Bacteriol*, 2007. 189(22): p. 8397-401.

55. Porter, S.L., et al., A Bifunctional Kinase-Phosphatase in Bacterial Chemotaxis. *Proc Natl Acad Sci U S A*, 2008. 105(47): p. 18531-6.

56. Tindall, M.J., et al., Modeling Chemotaxis Reveals the Role of Reversed Phosphotransfer and a Bi-Functional Kinase-Phosphatase. *Plos Computational Biology*, 2010. 6(8).

57. Goldman, B.S., et al., Evolution of Sensory Complexity Recorded in a Myxobacterial Genome. *Proc Natl Acad Sci U S A*, 2006. 103(41): p. 15200-5.

58. Hodgkin, J. and D. Kaiser, Genetics of Gliding Motility in *Myxococcus xanthus* (Myxobacterales): Two Gene Systems Control Movement. *Molecular and General Genetics MGG*, 1979. 171(2): p. 177-91.

59. Hodgkin, J. and D. Kaiser, Genetics of Gliding Motility in *Myxococcus xanthus* (Myxobacterales): Genes Controlling Movement of Single Cells. *Molecular and General Genetics MGG*, 1979. 171(2): p. 167-76.

60. Wall, D. and D. Kaiser, Type IV Pili and Cell Motility. *Molecular Microbiology*, 1999. 32(1): p. 1-10.

61. Zusman, D.R., "Frizzy" Mutants: A New Class of Aggregation-Defective Developmental Mutants of *Myxococcus xanthus*. *J Bacteriol*, 1982. 150(3): p. 1430-7.

62. McBride, M.J., R.A. Weinberg, and D.R. Zusman, "Frizzy" Aggregation Genes of the Gliding Bacterium *Myxococcus xanthus* Show Sequence Similarities to the Chemotaxis Genes of Enteric Bacteria. *Proc Natl Acad Sci U S A*, 1989. 86(2): p. 424-8.

63. Blackhart, B.D. and D.R. Zusman, "Frizzy" Genes of *Myxococcus xanthus* Are Involved in Control of Frequency of Reversal of Gliding Motility. *Proc Natl Acad Sci U S A*, 1985. 82(24): p. 8767-70.

64. Mauriello, E.M., et al., Localization of a Bacterial Cytoplasmic Receptor Is Dynamic and Changes with Cell-Cell Contacts. *Proc Natl Acad Sci U S A*, 2009. 106(12): p. 4852-7.

65. Yang, Z., et al., A New Set of Chemotaxis Homologues Is Essential for *Myxococcus xanthus* Social Motility. *Molecular Microbiology*, 1998. 30(5): p. 1123-30.

66. Yang, Z., et al., *Myxococcus xanthus dif* Genes Are Required for Biogenesis of Cell Surface Fibrils Essential for Social Gliding Motility. *J Bacteriol*, 2000. 182(20): p. 5793-8.

67. Black, W.P. and Z.M. Yang, *Myxococcus xanthus* Chemotaxis Homologs DifD and DifG Negatively Regulate Fibril Polysaccharide Production. *Journal of Bacteriology*, 2004. 186(4): p. 1001-8.

68. Black, W.P., et al., Isolation and Characterization of a Suppressor Mutation That Restores *Myxococcus xanthus* Exopolysaccharide Production. *Microbiology-Sgm*, 2009. 155: p. 3599-610.

69. Bonner, P.J. and L.J. Shimkets, Phospholipid Directed Motility of Surface-Motile Bacteria. *Molecular Microbiology*, 2006. 61(5): p. 1101-9.

70. Kearns, D.B. and L.J. Shimkets, Chemotaxis in a Gliding Bacterium. *Proceedings of the National Academy of Sciences of the United States of America*, 1998. 95(20): p. 11957-62.

71. Kirby, J.R. and D.R. Zusman, Chemosensory Regulation of Developmental Gene Expression in *Myxococcus xanthus*. *Proceedings of the National Academy of Sciences of the United States of America*, 2003. 100(4): p. 2008-13.

72. Vlamakis, H.C., J.R. Kirby, and D.R. Zusman, The Che4 Pathway of *Myxococcus xanthus* Regulates Type IV Pilus-Mediated Motility. *Molecular Microbiology*, 2004. 52(6): p. 1799-811.

73. Zusman, D.R., et al., Chemosensory Pathways, Motility and Development in *Myxococcus xanthus*. *Nature Reviews Microbiology*, 2007. 5(11): p. 862-72.

74. Stover, C.K., et al., Complete Genome Sequence of *Pseudomonas aeruginosa* Pao1, an Opportunistic Pathogen. *Nature*, 2000. 406(6799): p. 959-64.

75. Schuster, M., et al., The *Pseudomonas aeruginosa* RpoS Regulon and Its Relationship to Quorum Sensing. *Molecular Microbiology*, 2004. 51(4): p. 973-85.

76. Darzins, A., Characterization of a *Pseudomonas aeruginosa* Gene-Cluster Involved in Pilus Biosynthesis and Twitching Motility - Sequence Similarity to the Chemotaxis Proteins of Enterics and the Gliding Bacterium *Myxococcus xanthus*. *Molecular Microbiology*, 1994. 11(1): p. 137-53.

77. D'Argenio, D.A., et al., Autolysis and Autoaggregation in *Pseudomonas aeruginosa* Colony Morphology Mutants. *J Bacteriol*, 2002. 184(23): p. 6481-9.

78. Hickman, J.W., D.F. Tifrea, and C.S. Harwood, A Chemosensory System That Regulates Biofilm Formation through Modulation of Cyclic Diguanylate Levels. *Proceedings of the National Academy of Sciences of the United States of America*, 2005. 102(40): p. 14422-7.

79. Ausmees, N., et al., Genetic Data Indicate That Proteins Containing the GGDEF Domain Possess Diguanylate Cyclase Activity. *Fems Microbiology Letters*, 2001. 204(1): p. 163-7.

80. Tal, R., et al., Three *cdg* Operons Control Cellular Turnover of Cyclic Di-Gmp in *Acetobacter xylinum*: Genetic Organization and Occurrence of Conserved Domains in Isoenzymes. *Journal of Bacteriology*, 1998. 180(17): p. 4416-25.

81. Merighi, M., et al., The Second Messenger Bis-(3'-5')-Cyclic-GMP and Its Pilz Domain-Containing Receptor Alg44 Are Required for Alginate Biosynthesis in *Pseudomonas aeruginosa*. *Molecular Microbiology*, 2007. 65(4): p. 876-95.

82. Ryjenkov, D.A., et al., The Pilz Domain Is a Receptor for the Second Messenger c-di-GMP - the PilZ Domain Protein YcgR Controls Motility in Enterobacteria. *Journal of Biological Chemistry*, 2006. 281(41): p. 30310-4.

83. Romling, U., M. Gomelsky, and M.Y. Galperin, C-di-GMP: The Dawning of a Novel Bacterial Signalling System. *Molecular Microbiology*, 2005. 57(3): p. 629-39.

84. Hickman, J.W. and C.S. Harwood, Identification of FleQ from *Pseudomonas aeruginosa* as a c-di-GMP-Responsive Transcription Factor. *Molecular Microbiology*, 2008. 69(2): p. 376-89.

85. Guvener, Z.T., D.F. Tifrea, and C.S. Harwood, Two Different *Pseudomonas aeruginosa* Chemosensory Signal Transduction Complexes Localize to Cell Poles and Form and Remould in Stationary Phase. *Molecular Microbiology*, 2006. 61(1): p. 106-18.

86. Wisniewski-Dyé, F., et al., *Azospirillum* Genomes Reveal Transition of Bacteria from Aquatic to Terrestrial Environments. *Plos Genetics*, 2011. 7(12): p. e1002430.

87. Yildiz, F.H., H. Gest, and C.E. Bauer, Attenuated Effect of Oxygen on Photopigment Synthesis in *Rhodospirillum centenum*. *J Bacteriol*, 1991. 173(17): p. 5502-6.

88. Jiang, Z.Y., H. Gest, and C.E. Bauer, Chemosensory and Photosensory Perception in Purple Photosynthetic Bacteria Utilize Common Signal Transduction Components. *J Bacteriol*, 1997. 179(18): p. 5720-7.

89. Jiang, Z.Y. and C.E. Bauer, Analysis of a Chemotaxis Operon from *Rhodospirillum centenum*. *J Bacteriol*, 1997. 179(18): p. 5712-9.

90. Berleman, J.E. and C.E. Bauer, A Che-Like Signal Transduction Cascade Involved in Controlling Flagella Biosynthesis in *Rhodospirillum centenum*. *Molecular Microbiology*, 2005. 55(5): p. 1390-402.

91. Berleman, J.E. and C.E. Bauer, Involvement of a Che-Like Signal Transduction Cascade in Regulating Cyst Cell Development in *Rhodospirillum centenum*. *Molecular Microbiology*, 2005. 56(6): p. 1457-66.

92. Crooks, G.E., et al., Weblogo: A Sequence Logo Generator. *Genome Research*, 2004. 14(6): p. 1188-90.

93. Greer-Phillips, S.E., B.B. Stephens, and G. Alexandre, An Energy Taxis Transducer Promotes Root Colonization by *Azospirillum brasilense*. *Journal of Bacteriology*, 2004. 186(19): p. 6595-604.

94. Hazelbauer, G.L., J.J. Falke, and J.S. Parkinson, Bacterial Chemoreceptors: High-Performance Signaling in Networked Arrays. *Trends in Biochemical Sciences*, 2008. 33(1): p. 9-19.

95. Vu, A., et al., The Receptor-CheW Binding Interface in Bacterial Chemotaxis. *Journal of Molecular Biology*, 2011.

96. Hulko, M., et al., The HAMP Domain Structure Implies Helix Rotation in Transmembrane Signaling. *Cell*, 2006. 126(5): p. 929-40.

97. Ulrich, L.E. and I.B. Zhulin, The MiST2 Database: A Comprehensive Genomics Resource on Microbial Signal Transduction. *Nucleic Acids Research*, 2010. 38(Database issue): p. D401-7.

98. Wuichet, K., R.P. Alexander, and I.B. Zhulin, Comparative Genomic and Protein Sequence Analyses of a Complex System Controlling Bacterial Chemotaxis. *Methods Enzymol*, 2007. 422: p. 1-31.

99. Sourjik, V. and H.C. Berg, Localization of Components of the Chemotaxis Machinery of *Escherichia coli* Using Fluorescent Protein Fusions. *Molecular Microbiology*, 2000. 37(4): p. 740-51.

100. Maddock, J.R. and L. Shapiro, Polar Location of the Chemoreceptor Complex in the *Escherichia coli* Cell. *Science*, 1993. 259(5102): p. 1717-23.

101. Wadhams, G.H., A.C. Martin, and J.P. Armitage, Identification and Localization of a Methyl-Accepting Chemotaxis Protein in *Rhodobacter sphaeroides*. *Molecular Microbiology*, 2000. 36(6): p. 1222-33.

102. Meier, V.M., P. Muschler, and B.E. Scharf, Functional Analysis of Nine Putative Chemoreceptor Proteins in *Sinorhizobium meliloti*. *Journal of Bacteriology*, 2007. 189(5): p. 1816-26.

103. Studdert, C.A. and J.S. Parkinson, Crosslinking Snapshots of Bacterial Chemoreceptor Squads. *Proceedings of the National Academy of Sciences of the United States of America*, 2004. 101(7): p. 2117-22.

104. Studdert, C.A. and J.S. Parkinson, Insights into the Organization and Dynamics of Bacterial Chemoreceptor Clusters through in vivo Crosslinking Studies. *Proceedings of the National Academy of Sciences of the United States of America*, 2005. 102(43): p. 15623-8.

105. Shiomi, D., et al., Helical Distribution of the Bacterial Chemoreceptor Via Colocalization with the Sec Protein Translocation Machinery. *Molecular Microbiology*, 2006. 60(4): p. 894-906.

106. Thiem, S., D. Kentner, and V. Sourjik, Positioning of Chemosensory Clusters in *E. coli* and Its Relation to Cell Division. *Embo Journal*, 2007. 26(6): p. 1615-23.

107. Wu, J., et al., The Receptor Binding Site for the Methyltransferase of Bacterial Chemotaxis Is Distinct from the Sites of Methylation. *Biochemistry*, 1996. 35(15): p. 4984-93.

108. Li, M. and G.L. Hazelbauer, Adaptational Assistance in Clusters of Bacterial Chemoreceptors. *Molecular Microbiology*, 2005. 56(6): p. 1617-26.

109. Lai, R.Z., et al., Cooperative Signaling among Bacterial Chemoreceptors. *Biochemistry*, 2005. 44(43): p. 14298-307.

110. Sourjik, V. and H.C. Berg, Receptor Sensitivity in Bacterial Chemotaxis. *Proceedings of the National Academy of Sciences of the United States of America*, 2002. 99(1): p. 123-7.

111. Briegel, A., et al., Location and Architecture of the *Caulobacter crescentus* Chemoreceptor Array. *Molecular Microbiology*, 2008. 69(1): p. 30-41.

112. Khursigara, C.M., X.W. Wu, and S. Subramaniam, Chemoreceptors in *Caulobacter crescentus*: Trimers of Receptor Dimers in a Partially Ordered Hexagonally Packed Array. *Journal of Bacteriology*, 2008. 190(20): p. 6805-10.

113. Briegel, A., et al., Bacterial Chemoreceptor Arrays Are Hexagonally Packed Trimers of Receptor Dimers Networked by Rings of Kinase and Coupling Proteins. *Proc Natl Acad Sci U S A*, 2012. 109(10): p. 3766-71.

114. Levit, M.N., T.W. Grebe, and J.B. Stock, Organization of the Receptor-Kinase Signaling Array That Regulates *Escherichia coli* Chemotaxis. *Journal of Biological Chemistry*, 2002. 277(39): p. 36748-54.

115. Erbse, A.H. and J.J. Falke, The Core Signaling Proteins of Bacterial Chemotaxis Assemble to Form an Ultrastable Complex. *Biochemistry*, 2009. 48(29): p. 6975-87.

116. Borrok, M.J., E.M. Kolonko, and L.L. Kiessling, Chemical Probes of Bacterial Signal Transduction Reveal That Repellents Stabilize and Attractants Destabilize the Chemoreceptor Array. *Acs Chemical Biology*, 2008. 3(2): p. 101-9.

117. Homma, M., et al., Attractant Binding Alters Arrangement of Chemoreceptor Dimers within Its Cluster at a Cell Pole. *Proceedings of the National Academy of Sciences of the United States of America*, 2004. 101(10): p. 3462-7.

118. Kim, S.H., W.R. Wang, and K.K. Kim, Dynamic and Clustering Model of Bacterial Chemotaxis Receptors: Structural Basis for Signaling and High Sensitivity. *Proceedings of the National Academy of Sciences of the United States of America*, 2002. 99(18): p. 11611-5.

119. Nara, T., et al., Modulation of the Thermosensing Profile of the *Escherichia coli* Aspartate Receptor Tar by Covalent Modification of Its Methyl-Accepting Sites. *Journal of Biological Chemistry*, 1996. 271(30): p. 17932-6.

120. Nishiyama, S., et al., Conversion of a Bacterial Warm Sensor to a Cold Sensor by Methylation of a Single Residue in the Presence of an Attractant. *Molecular Microbiology*, 1999. 32(2): p. 357-65.

121. Nishiyama, S.I., et al., Thermosensing Properties of Mutant Aspartate Chemoreceptors with Methyl-Accepting Sites Replaced Singly or Multiply by Alanine. *Journal of Bacteriology*, 1997. 179(21): p. 6573-80.

122. Nara, T., L. Lee, and Y. Imae, Thermosensing Ability of Trg and Tap Chemoreceptors in *Escherichia coli*. *Journal of Bacteriology*, 1991. 173(3): p. 1120-4.

123. Salman, H. and A. Libchaber, A Concentration-Dependent Switch in the Bacterial Response to Temperature. *Nature Cell Biology*, 2007. 9(9): p. 1098-U78.

124. Paster, E. and W.S. Ryu, The Thermal Impulse Response of *Escherichial coli*. *Proceedings of the National Academy of Sciences of the United States of America*, 2008. 105(14): p. 5373-7.

125. Nishiyama, S., et al., Thermosensing Function of the *Escherichia coli* Redox Sensor Aer. *Journal of Bacteriology*, 2010. 192(6): p. 1740-3.

126. Bardy, S.L. and J.R. Maddock, Polar Localization of a Soluble Methyl-Accepting Protein of *Pseudomonas aeruginosa*. *Journal of Bacteriology*, 2005. 187(22): p. 7840-4.

127. Meier, V.M. and B.E. Scharf, Cellular Localization of Predicted Transmembrane and Soluble Chemoreceptors in *Sinorhizobium meliloti*. *J Bacteriol*, 2009. 191(18): p. 5724-33.

128. Alexander, R.P. and I.B. Zhulin, Evolutionary Genomics Reveals Conserved Structural Determinants of Signaling and Adaptation in Microbial Chemoreceptors. *Proceedings of the National Academy of Sciences of the United States of America*, 2007. 104(8): p. 2885-90.

129. Nambu, J.R., et al., The Drosophila Single-Minded Gene Encodes a Helix-Loop-Helix Protein That Acts as a Master Regulator of Cns Midline Development. *Cell*, 1991. 67(6): p. 1157-67.

130. Hoffman, E.C., et al., Cloning of a Factor Required for Activity of the Ah (Dioxin) Receptor. *Science*, 1991. 252(5008): p. 954-8.

131. Bibikov, S.I., et al., A Signal Transducer for Aerotaxis in *Escherichia coli*. *Journal of Bacteriology*, 1997. 179(12): p. 4075-9.

132. Xie, Z.H., et al., Pas Domain Containing Chemoreceptor Couples Dynamic Changes in Metabolism with Chemotaxis. *Proceedings of the National Academy of Sciences of the United States of America*, 2010. 107(5): p. 2235-40.

133. Delgado-Nixon, V.M., G. Gonzalez, and M.A. Gilles-Gonzalez, Dos, a Heme-Binding Pas Protein from *Escherichia coli*, Is a Direct Oxygen Sensor. *Biochemistry*, 2000. 39(10): p. 2685-91.

134. Yoshioka, S., et al., Biophysical Properties of a C-Type Heme in Chemotaxis Signal Transducer Protein DcrA. *Biochemistry*, 2005. 44(46): p. 15406-13.

135. Londer, Y.Y., et al., Characterization of a C-Type Heme-Containing Pas Sensor Domain from *Geobacter sulfurreducens* Representing a Novel Family of Periplasmic Sensors in *Geobacteraceae* and Other Bacteria. *Fems Microbiology Letters*, 2006. 258(2): p. 173-81.

136. Avila-Perez, M., K.J. Hellingwerf, and R. Kort, Blue Light Activates the Sigmab-Dependent Stress Response of *Bacillus subtilis* Via YtvA. *J Bacteriol*, 2006. 188(17): p. 6411-4.

137. Zhou, Y.F., et al., C4-Dicarboxylates Sensing Mechanism Revealed by the Crystal Structures of DctB Sensor Domain. *Journal of Molecular Biology*, 2008. 383(1): p. 49-61.

138. Cheung, J. and W.A. Hendrickson, Crystal Structures of C4-Dicarboxylate Ligand Complexes with Sensor Domains of Histidine Kinases DcuS and DctB. *Journal of Biological Chemistry*, 2008. 283(44): p. 30256-65.

139. Cheung, J., et al., Crystal Structure of a Functional Dimer of the PhoQ Sensor Domain. *Journal of Biological Chemistry*, 2008. 283(20): p. 13762-70.

140. Cho, U.S., et al., Metal Bridges between the PhoQ Sensor Domain and the Membrane Regulate Transmembrane Signaling. *Journal of Molecular Biology*, 2006. 356(5): p. 1193-206.

141. Schweinitzer, T. and C. Josenhans, Bacterial Energy Taxis: A Global Strategy? *Archives of Microbiology*, 2010. 192(7): p. 507-20.

142. Taylor, B.L., I.B. Zhulin, and M.S. Johnson, Aerotaxis and Other Energy-Sensing Behavior in Bacteria. *Annual Review of Microbiology*, 1999. 53: p. 103-28.

143. Henry, J.T. and S. Crosson, Ligand-Binding Pas Domains in a Genomic, Cellular, and Structural Context. *Annual Review of Microbiology, Vol 64, 2010*, 2011. 65: p. 261-86.

144. Steenhoudt, O. and J. Vanderleyden, *Azospirillum*, a Free-Living Nitrogen-Fixing Bacterium Closely Associated with Grasses: Genetic, Biochemical and Ecological Aspects. *Fems Microbiology Reviews*, 2000. 24(4): p. 487-506.

145. Bible, A.N., et al., Function of a Chemotaxis-Like Signal Transduction Pathway in Modulating Motility, Cell Clumping, and Cell Length in the Alphaproteobacterium *Azospirillum brasilense*. *J Bacteriol*, 2008. 190(19): p. 6365-75.

146. Wuichet, K. and I.B. Zhulin, Origins and Diversification of a Complex Signal Transduction System in Prokaryotes. *Science Signaling*, 2010. 3(128): p. ra50.

147. Edwards, J.C., M.S. Johnson, and B.L. Taylor, Differentiation between Electron Transport Sensing and Proton Motive Force Sensing by the Aer and Tsr Receptors for Aerotaxis. *Molecular Microbiology*, 2006. 62(3): p. 823-37.

148. Harold, F.M. and P.C. Maloney, Energy Transduction by Ions Currents, in *Escherichia coli and Salmonella: Cellular and Molecular Biology*, F.C. Neidhardt, Editor 1996, American Society for Microbiology Press: Washington D.C. p. 283-306.

149. Amikam, D. and M.Y. Galperin, PilZ Domain Is Part of the Bacterial c-di-Gmp Binding Protein. *Bioinformatics*, 2006. 22(1): p. 3-6.

150. Pratt, J.T., et al., PilZ Domain Proteins Bind Cyclic Diguanylate and Regulate Diverse Processes in *Vibrio cholerae*. *Journal of Biological Chemistry*, 2007. 282(17): p. 12860-70.

151. Ross, P., et al., Regulation of Cellulose Synthesis in *Acetobacter xylinum* by Cyclic Diguanylic Acid. *Nature*, 1987. 325(6101): p. 279-81.

152. Ross, P., et al., Control of Cellulose Synthesis in *Acetobacter xylinum* - a Unique Guanyl Oligonucleotide Is the Immediate Activator of the Cellulose Synthase. *Carbohydrate Research*, 1986. 149(1): p. 101-17.

153. Tischler, A.D. and A. Camilli, Cyclic Diguanylate (c-di-Gmp) Regulates *Vibrio cholerae* Biofilm Formation. *Molecular Microbiology*, 2004. 53(3): p. 857-69.

154. Tischler, A.D. and A. Camilli, Cyclic Diguanylate Regulates *Vibrio cholerae* Virulence Gene Expression. *Infection and Immunity*, 2005. 73(9): p. 5873-82.

155. Yi, X.A., et al., Genetic Analysis of Two Phosphodiesterases Reveals Cyclic Diguanylate Regulation of Virulence Factors in *Dickeya dadantii*. *Molecular Microbiology*, 2010. 77(3): p. 787-800.

156. Ueda, A. and T.K. Wood, Connecting Quorum Sensing, c-di-GMP, Pel Polysaccharide, and Biofilm Formation in *Pseudomonas aeruginosa* through Tyrosine Phosphatase Tpba (Pa3885). *Plos Pathogens*, 2009. 5(6).

157. Wilksch, J.J., et al., MrkH, a Novel c-di-GMP-Dependent Transcriptional Activator, Controls *Klebsiella pneumoniae* Biofilm Formation by Regulating Type 3 Fimbriae Expression. *Plos Pathogens*, 2011. 7(8).

158. Sun, Y.C., et al., Differential Control of *Yersinia pestis* Biofilm Formation in vitro and in the Flea Vector by Two c-di-GMP Diguanylate Cyclases. *Plos One*, 2011. 6(4).

159. Guo, Y.Z. and D.A. Rowe-Magnus, Identification of a c-di-GMP-Regulated Polysaccharide Locus Governing Stress Resistance and Biofilm and Rugose Colony Formation in *Vibrio vulnificus*. *Infection and Immunity*, 2010. 78(3): p. 1390-402.

160. Martinez-Wilson, H.F., et al., The *Vibrio cholerae* Hybrid Sensor Kinase VieS Contributes to Motility and Biofilm Regulation by Altering the Cyclic Diguanylate Level. *Journal of Bacteriology*, 2008. 190(19): p. 6439-47.

161. Paul, K., et al., The c-di-GMP Binding Protein YcgR Controls Flagellar Motor Direction and Speed to Affect Chemotaxis by a "Backstop Brake" Mechanism. *Mol Cell*, 2010. 38(1): p. 128-39.

162. Christen, M., et al., Asymmetrical Distribution of the Second Messenger c-di-GMP Upon Bacterial Cell Division. *Science*, 2010. 328(5983): p. 1295-7.

163. Aldridge, P., et al., Role of the GGDEF Regulator PleD in Polar Development of *Caulobacter crescentus*. *Molecular Microbiology*, 2003. 47(6): p. 1695-708.

164. Kozlova, E.V., et al., Quorum Sensing and c-di-GMP-Dependent Alterations in Gene Transcripts and Virulence-Associated Phenotypes in a Clinical Isolate of *Aeromonas hydrophila*. *Microbial Pathogenesis*, 2011. 50(5): p. 213-23.

165. Chin, K.H., et al., The cAMP Receptor-Like Protein Clp Is a Novel c-di-GMP Receptor Linking Cell-Cell Signaling to Virulence Gene Expression in *Xanthomonas campestris*. *Journal of Molecular Biology*, 2010. 396(3): p. 646-62.

166. Schmidt, A.J., D.A. Ryjenkov, and M. Gomelsky, The Ubiquitous Protein Domain EAL Is a Cyclic Diguanylate-Specific Phosphodiesterase: Enzymatically Active and Inactive EAL Domains. *Journal of Bacteriology*, 2005. 187(14): p. 4774-81.

167. Tamayo, R., A.D. Tischler, and A. Camilli, The EAL Domain Protein VieA Is a Cyclic Diguanylate Phosphodiesterase. *Journal of Biological Chemistry*, 2005. 280(39): p. 33324-30.

168. Ryan, R.P., et al., Cell-Cell Signaling in *Xanthomonas campestris* Involves an Hd-GYP Domain Protein That Functions in Cyclic di-GMP Turnover. *Proceedings of the National Academy of Sciences of the United States of America*, 2006. 103(17): p. 6712-7.

169. Wassmann, P., et al., Structure of BeF3- -Modified Response Regulator PleD: Implications for Diguanylate Cyclase Activation, Catalysis, and Feedback Inhibition. *Structure*, 2007. 15(8): p. 915-27.

170. Yang, C.Y., et al., The Structure and Inhibition of a GGDEF Diguanylate Cyclase Complexed with (c-di-GMP)(2) at the Active Site. *Acta Crystallographica Section D-Biological Crystallography*, 2011. 67: p. 997-1008.

171. Carreno-Lopez, R., et al., Characterization of *chsa*, a New Gene Controlling the Chemotactic Response in *Azospirillum brasilense* Sp7. *Archives of Microbiology*, 2009. 191(6): p. 501-7.

172. Huang, B., C.B. Whitchurch, and J.S. Mattick, FimX, a Multidomain Protein Connecting Environmental Signals to Twitching Motility in *Pseudomonas aeruginosa*. *J Bacteriol*, 2003. 185(24): p. 7068-76.

173. Qi, Y., et al., A Flavin Cofactor-Binding PAS Domain Regulates c-di-GMP Synthesis in AxDGC2 from *Acetobacter xylinum*. *Biochemistry*, 2009. 48(43): p. 10275-85.

174. Marmont, L.S., et al., Expression, Purification, Crystallization and Preliminary X-Ray Analysis of *Pseudomonas aeruginosa* PelD. *Acta Crystallogr Sect F Struct Biol Cryst Commun*, 2012. 68(Pt 2): p. 181-4.

175. Paul, R., et al., Activation of the Diguanylate Cyclase PleD by Phosphorylation-Mediated Dimerization. *Journal of Biological Chemistry*, 2007. 282(40): p. 29170-7.

176. Kazmierczak, B.I., M.B. Lebron, and T.S. Murray, Analysis of FimX, a Phosphodiesterase That Governs Twitching Motility in *Pseudomonas aeruginosa*. *Molecular Microbiology*, 2006. 60(4): p. 1026-43.

177. Krasteva, P.V., et al., *Vibrio cholerae* VpsT Regulates Matrix Production and Motility by Directly Sensing Cyclic di-GMP. *Science*, 2010. 327(5967): p. 866-8.

178. Sudarsan, N., et al., Riboswitches in Eubacteria Sense the Second Messenger Cyclic di-GMP. *Science*, 2008. 321(5887): p. 411-3.

179. Lee, E.R., et al., An Allosteric Self-Splicing Ribozyme Triggered by a Bacterial Second Messenger. *Science*, 2010. 329(5993): p. 845-8.

180. Stephens, B.B., Chemosensory Responses in *Azospirillum brasilense*, in *Biology Dissertations* 2006, Georgia State University: Atlanta, GA.

Chapter 2

A chemotaxis-receptor for nitrogen sensing in *Azospirillum brasilense*

The following work is in preparation for publication by Matthew Russell, Eric Farrell, and Gladys Alexandre

Author Contributions

Eric Farrell's work is presented in Figures 2.2B and C, 2.6, and 2.8. The remainder of data are result of my work. Gladys Alexandre wrote a majority of the manuscript, and I wrote the remainder.

Abstract

The chemotaxis sensory repertoire of most microorganisms and the environmental cues motile organisms may respond to via dedicated chemotaxis receptors is vastly uncharacterized. The *Azospirillum brasilense* chemotaxis receptor Tlp2 encodes for a periplasmic domain of unknown function. We demonstrate that Tlp2 is constitutively expressed and significantly overexpressed under conditions of low oxygen tension or nitrogen limitation and it is part of the cell's NtrC regulon. The pattern of P*tlp2* regulation correlated with the subcellular localization of a Tlp2-YFP fusion. A set of behavioral assays and mutants lacking Tlp2 or possessing variant alleles in which conserved residues were mutated, we demonstrate that Tlp2 senses both nitrate and ammonium at two distinct sites within the sensory domain. Further biochemical characterization using intrinsic tyrosine fluorescence supports specificity of the Tlp2 sensory domain for inorganic nitrogenous compounds including nitrate and ammonium with a K_d in the low-to-submicromolar range. The pattern of expression suggests a function for Tlp2 when the preferred nitrogen source, ammonium is limiting, an assumption supporting by demonstrating a function for Tlp2 under conditions of nitrogen limitation.

Introduction

Microorganisms are constantly monitoring their surroundings and responding to prevalent conditions that most likely affect their growth and survival. Two-component signal transduction systems are major molecular components that mediate the responses of microorganisms to changes in the environment and they are ubiquitously found in the genomes of both Bacteria and Archaea [1-3]. The signal transduction pathway that controls the bacterial chemotaxis response is also widespread in completely sequenced microbial genomes, probably reflecting the ecological (and thus evolutionary) benefit which it provides motile organisms [4-6].

In chemotaxis, chemoeffectors are detected by receptors that relay this information to cytoplasmic chemotaxis proteins by modulating their phosphorylation status. These signal transduction events ultimately control the probability of changes in the rotational direction of flagellar motors and thus the swimming pattern (i.e. chemotaxis) [7-11]. In most bacterial species studied in this respect, chemotaxis receptors are organized as discrete clusters of interacting trimers of dimers, a molecular organization that contributes to the high sensitivity and the dynamic range of the chemotaxis response [12-16]. Prototypical chemotaxis receptors contain a cytoplasmic conserved C-terminal signaling domain which forms ternary complexes with cytoplasmic chemotaxis proteins [17-20] and a N-terminal sensory domain of variable sequences which may be periplasmic (greatest majority of available sequences) or cytoplasmic [21, 22]. The sensory specificity of bacterial chemotaxis receptors has been established only for a relatively small number of these receptors. Physiochemical parameters such as electron donors and electron acceptors, pH or temperature as well as chemicals that serve as nutrient sources are potential cues detected by chemotaxis receptors [22]. Comparative genomics analyses of completely sequenced genomes indicate that most motile and chemotactic bacteria possess a large number of putative chemotaxis receptors that have N-terminal sensory domains of unknown specificity [21].

Therefore most environmental cues that trigger behavioral responses and modulate the adaptation of motile bacteria to their surroundings remain to be determined.

Azospirillum brasilense are soil alphaproteobacteria that have a versatile oxidative metabolism and are capable of diazotrophy under conditions of low oxygen tension. These bacteria are motile and capable of aerotaxis (directed movement in oxygen gradients) as well as chemotaxis in gradients of various organic substrates [23, 24]. Chemotactic and aerotactic behaviours contribute to the ability of *A.brasilense* to colonize the rhizosphere of wheat as well as to their ability to locate optimal conditions for nitrogen fixation [23, 25-27]. The *A. brasilense* genome sequence indicates the presence of four putative chemotaxis-like signal transduction pathways and 48 chemotaxis receptors [28]. One chemotaxis-like pathway, named Che1, has been implicated in chemotaxis [26] as well as other cellular behaviours including cell-to-cell clumping and flocculation [29, 30]. The function of two chemotaxis receptors, Tlp1 and AerC, that mediate chemotaxis to some organic compounds (Tlp1) and contribute to aerotaxis (Tlp1 and AerC) have also been characterized [23, 25]. The present study reports the characterization of a third *A. brasilense* chemoreceptor, named Tlp2 (transducer-like protein 2) which has a prototypical topology and a conserved periplasmic N-terminal domain of unknown function. We demonstrate that Tlp2 is constitutively expressed and significantly overexpressed under conditions of low oxygen tension or nitrogen limitation and it is part of the cell's NtrC regulon. A set of behavioral assays and mutants lacking Tlp2 or possessing variant alleles in which conserved residues were mutated, we demonstrate that Tlp2 senses both nitrate and ammonium at two distinct sites within the sensory domain. Amino acids or other salts were not shown to be sensed by Tlp2. The Tlp2 pattern of expression and its sensory specificity suggest that this receptor allows cells to actively seek source of nitrogenous compounds when this nutrient becomes limiting and cells have initiated the energy demanding nitrogen fixation.

Experimental Procedures

Bacteria strains, Medium, Growth conditions

The strains and plasmids used in this study are listed in Table 1. *Azospirillum brasilense* strains were grown in TY medium (10g tryptone $^{-l}$, 5g yeast extract $^{-l}$) or minimal MMAB medium [31] at 28°C with shaking, supplemented with appropriate antibiotics. When the MMAB medium lacking a combined nitrogen source was used, cells were grown at 28°C without shaking to allow for nitrogen fixation under low oxygen tension conditions [32]. *E. coli* B834 (DE3) was grown in 2xYT medium (Yeast Extract 16g $^{-l}$, Tryptone 10g $^{-l}$, NaCl 5g $^{-l}$) at 37°C with vigorous shaking. The antibiotics were used at the following final concentrations: Kanamycin (50mg/ml for 30mg/ml for *A. brasilense*), Tetracycline 10mg/ml, Ampicillin 100mg/ml, and Chloramphenicol (17mg/ml for *A. brasilense*).

Soft agar assay and other behavioral assays

The soft agar assay was performed as previously described (Alexandre et al., 2000) with minor modifications. The MMAB semi-soft agar medium (solidified with 0.3% (w/v) agar) [24] was supplemented with carbon or nitrogen sources at a final concentration of 5 mM or 10 mM. The cultures used for inoculation of the MMAB soft agar plates were grown in liquid MMAB medium aerobically with shaking supplemented with nitrate as a nitrogen source at a final concentration of 10mM overnight at 28°C or under anaerobic (BD GasPak EZ system) conditions. Where indicated cultures were grown in MMAB without combined nitrogen approximately 48 hours before the assay. The optical density of the cultures was standardized and 5 µl was inoculated into MMAB semi-solid medium (solidified with 0.3% (w/v) agar) with varying nitrogen and carbon sources as indicated. Plates were incubated 48 or 72 hours at 28°C in either aerobic or anaerobic conditions, respectively. Assay of chemotaxis was measured by ring

diameters relative to wild type as previously described (Alexandre et al., 2000). At least 3 independent repetitions were used.

Spatial aerotaxis assays was performed in a perfused chamber as previously described (Alexandre et al., 2000). For the aerotaxis assay, actively growing cultures (early Log phase) are washed with 0.8% (w/v) sterile potassium chloride three times and resuspended in Chemotaxis buffer (10mM potassium phosphate, pH 7.0, and 0.1mM EDTA) supplemented with 10mM malate (as the electron donor) to an $O.D._{600}$ of 1.0. Over 95% of cells are motile within the cell suspension prepared. Typical aerotactic band formation occurs within 2 minutes in the wild type strain.

Mutagenesis of tlp2 and complementation

PCR was used to construct an insertion-deletion mutant of *tlp2*. A 606-bp region upstream of the tlp2 open reading frame and spanning into the first 154bp of the *tlp2* coding region was amplified using the primer set Tlp2up-F1 and Tlp2up-R1 (see Table S1 for sequences), The PCR product was cloned into pCR2.1-TOPO (Invitrogen, Carlsbad, CA) , yielding pBS6. The pBS6 construct was verified by sequencing and the DNA fragment containing the partial *tlp2* region and upstream DNA were digested with *Kpn*I and *Not*I and ligated with the pCM184 vector [33] digested with the same enzymes, yielding pBS7. A 533 bp region downstream of *tlp2* was PCR amplified with the primers Tlp2down-F1 and Tlp2down-R1 and cloned into pCR2.1 (Invitrogen) yielding pBS8. The pBS7 and pBS8 vectors were transformed into *E. coli* SCS110. The pBS8 vector was digested with *Apa*I and *Sac*I and ligated into pBS7 digested with the same enzymes resulting in pBS9 with the upstream and downstream regions of *tlp2* flanking a kanamycin resistance cassette which replaced a 784 bp coding region of *tlp2* (Table 1). The Δ*tlp2::kan* region was amplified with primers Tlp2up-F1 and Tlp2down-R1, cloned into pCR2.1-TOPO, and excised with *Eco*RI digestion after verification by sequencing, and ligated into the suicide vector

pSUP202 [34], yielding pBS10 (Table 1). The pBS10 plasmid was transferred into *A. brasilense* using triparental mating with the helper plasmid pRK2013 [35] using standard procedures for *A. brasilense* (Hauwaerts *et al*., 2002). Double homologous recombinants were selected for on MMAB medium supplemented with kanamycin (30µg/ml) and tetracycline (10µg/ml). Proper deletion and allelic replacement of *tlp2* in one such *A. brasilense* mutant strain was verified using PCR and southern blotting and it was named AB401 (Table 2.1) and further characterized.

For functional complementation, the *tlp2* open reading frame plus 487 bp upstream of the start codon were PCR-amplified with Tlp2-Hind-F2 and Tlp2-Xho-R2 primers, incorporating *Hind*III and *Xho*I restriction sites (underlined), respectively. The PCR product was cloned into pCR2.1-TOPO resulting in pTOPO-Tlp2 (Table 1). The *Hind*III/*Xho*I fragment was ligated into the pRK415 vector [36] digested with the same enzymes, yielding pRKTlp2 (Table 1). pRKTlp2 was introduced into *A. brasilense* AB401 by triparental mating using pRK2013 as a helper (Hauwaerts *et al*., 2002).

For site-directed mutagenesis of Tlp2, reactions were carried out in 2x Go Taq Colorless Master Mix (Promega), and used pUC*tlp2* as the template DNA. Additives used included bovine serum albumin (BSA) obtained from New England Biolababs, and dimethylsulfoxide (DMSO) obtained from Acros Organics. Gel Extractions were performed using the QIAquick Gel Extraction Kit (Qiagen). To obtain these mutants an overlap extension protocol was used in combination with a BSA PCR step plus touchdown method. Polymerase Chain Reactions were carried out in a Mastercycler ep from Eppendorf, in 500 µl thin-walled PCR tubes. Two initial reactions were set up for each desired mutant with one containing the Tlp2-Forward primer and a reverse mutagenic primer (Tlp2SDM1-2-R, Tlp2SDM2-2-R, and Tlp2SDM3-2-R), and the other reaction containing the Tlp2 Reverse primer and a forward mutagenic primer. For the BSA step plus "Touchdown"

Table 2.1: Bacteria strains and plasmids used in this study

Bacteria/Plasmid	Relevant Characteristics	Reference
E. coli		
S17.1	*thi endA recA hsdR with RP4-2Tc::Mu-Km::Tn7* integrated in chromosome	Simon et al. 1983
BL21 Star (DE3)	F $^-$ ompT hsdS B (r B - m B -) gal dcm rne131 (DE3)	Invitrogen
Top10	F $^-$ mcrA Δ(mrr-hsdRMS-mcrBC) φ80lacZΔM15 ΔlacX74 nupG recA1 araD139 Δ(ara-leu)7697 galE15 galK16 rpsL(Str^R) endA1 λ$^-$	Invitrogen
Azospirillum brasilense		
Sp7	Wild Type	ATCC 29145
AB401	Δ*tlp2::kan* mutant derivative of Sp7; Km^r	This work
Plasmids		
pUC19	Ap^r, General cloning vector	Yanish-Perron et al. 1985
pCR2.1-TOPO	3.9 kb vector for PCR cloning; Km^r	Invitrogen
pSUP202	mobilizable plasmid, suicide vector for *A. brasilense*; Tc^r Km^r Ap^r	Simon et al. 1983
pCM184	allelic exchange vector and source of *kan* cassette; Tc^r Ap^r Km^r	Marx et al. 2002
pBS6	pCR2.1-TOPO with a 606bp upstream region of *tlp2; Km^r*	Stephens 2006
pBS7	pCM184 with *Kpn*I/*Not*I fragment of pBS6	Stephens 2006
pBS8	pCR2.1-TOPO with a 533 bp downstream region of *tlp2; Km^r*	Stephens 2006
pBS9	pBS7 with *Apa*I/*Sac*I fragment of pBS8 yielding a *Δtlp2*::*kan* construct	Stephens 2006
pBS10	pSUP202 with *EcoR*I fragment of pCR2.1-TOPO with Δtlp2::*kan* construct; Tc^r Km^r Ap^r	Stephens 2006
pRK2013	helper plasmid with *tra* genes; Km^r	Figurski and Helinski 1979
pRK415	Tc^r *mob*$^+$ *lacZ*	Keen et al. 1988
pTOPO-Tlp2	pCR2.1-TOPO with 2269 bp fragment of *tlp2* promoter and gene; Km^r	This study
pRKTlp2	pRK415 with *Hind*III/*Xho*I fragment of pTOPO-Tlp2; Tc^r	This study
pRH005	Gateway vector with RK2oriV, lac promoter, yfp; Km^r Cm^r	Hallez et al. 2007
pRHTlp2	pRH005 with 2269 bp fragment containing *tlp2* promoter and gene	This study

Ap^r, ampicillin resistance; Km^r, kanamycin resistance; Tc^r, tetracycline resistance; Cm^r, chloramphenicol resistance

PCR, the cycling parameters consisted of an initial denaturation step of 95°C for 5 minutes followed by a three step cycle comprised of a denaturation step of 95°C and annealing step for 1 minute in which the temperature was initially set 10°C above the predicted annealing temperature and decreased one degree per cycle, and an extension time of 72°C for 1 minute per kilobase of target gene. Another three step cycle followed this one in which there was an initial denaturation step of 95°C for 1 minute, an annealing step of 45 seconds, and an extension step of 72°C for 1 minute per kilobase of target gene. The initial cycling step was repeated for fifteen cycles and the second cycling step was repeated for 20 cycles. The final cycling step was followed by a final extension time of 72°C for 10 minutes and was cooled down to 4°C. Reactions were supplemented with BSA at intermediate steps followed the same cycling parameters as listed above, except that the cycle was manually paused after every five steps to allow BSA addition. The reactions resulting reactions were then run on and extracted from an agarose gel. After extraction, DNA concentration was determined on an Eppendorf Biophotometer. The second reaction involved each of the extracted DNA templates combined in a 1:1 ratio. The cycling parameters here were the same as the parameters for the initial reactions. The resulting reaction was then extracted from an agarose gel and ligated into puc19. After the presence of the desired mutation was verified by sequencing, the tlp2 fragments were then cloned into pRK415 and subsequently mated into *Azospirillum brasilense* SP7 following a triparental mating protocol.

Tlp2 promoter expression and beta-glucuronidase (GUS) assay

The vector pTOPO-Tlp2 (Table 1) was digested with *Eco*RI and the *tlp2* fragment was purified by gel extraction (Qiagen, Valencia, CA). A *Hind*III and *Pst*I digestion of the purified DNA was performed to isolate a 565 base pair fragment including 487 base pairs upstream of the start codon for *tlp2*. The 565 base pair fragment was gel extracted and ligated into pFUS1 [37] digested with *Hind*III and *Pst*I, yielding pFUSTlp2 (Table 1). After verification of correct

orientation and sequence by sequencing, the pFUSTlp2 construct was introduced into *A. brasilense* Sp7 through triparental mating using pRK2013 as a helper, as previously described (Hauwaerts *et al*., 2002).

To quantitate promoter expression, the Sp7(pFUSTlp2) strain was grown overnight from a single colony in TY medium supplemented with tetracycline at 28°C then re-inoculated into various media (see Results section) for *tlp2::gusA* expression analysis and incubated overnight if incubated with shaking (high oxygen tension cultures) or for 48 hours if incubated without shaking (low oxygen tension cultures). Tlp2 promoter activity was determined using the beta-glucuronidase assay [38], from 1 to 5 ml of pelleted culture, essentially as described previously (Miller *et al*., 2007). The fluorescence of 4-methyl umbelliferone (MU) was measured by excitation at 365nm and emission at 455nm. The fluorescence at time zero was subtracted from all other measurements. Amounts of MU present were interpolated from a standard calibration of MU in stop buffer from a range of 50nM to 1µM MU. Promoter activity was measured in pmol MU/min/mg protein

Tlp2 protein localization

A 2269 bp fragment of *tlp2* including the putative (487 bp) promoter region was amplified by PCR using the following primers: Tlp2GateFor and Tlp2GateRev. The PCR fragment obtained was gel purified and recombined *in vitro* into pDONR 221 (Invitrogen) using BP Clonase® II (Invitrogen) per the manufacturer's instructions yielding pDONR-Tlp2. A positive clone was then recombined into the Gateway-compatible, C-terminal YFP fusion broad host range vector, pRH005 [39] using LR Clonase® II (Invitrogen), according to the manufacturer's instructions. Positive clones were selected on LB medium with chloramphenicol 34µg/ml and kanamycin 50µg/ml, verified by sequencing, and one of them was named pRHTlp2 (Table 1) and used in

subsequent studies. The pRHTlp2 vector was transformed into *E. coli* S17.1 [34] and introduced into *A. brasilense* AB401 and other strains where noted by biparental mating and selection on MMAB lacking combined nitrogen (to select for diazotrophic *A. brasilense* cells) containing chloramphenicol and kanamycin. An empty pRH005 vector was also introduced into similar backgrounds as a negative control. The functionality of the Tlp2-YFP fusion was verified by complementing the mutant strain phenotype (AB401) in the soft agar plate assay. Expression level of Tlp2-YFP produced from this vector was verified by Western blot using anti-GFP (cross-reacts with YFP, gift from R. Goodchild, The University of Tennessee, Knoxville).

Expression and purification of a soluble periplasmic domain of Tlp2

The coding sequence for amino acids 41-193 (the putative ligand-binding domain) of Tlp2 was amplified by PCR with primers SUMO-Tlp2N-For and SUMO-Tlp2N-Rev, and the product obtained was then cloned into pET-SUMO (Invitrogen). Correct insertion and in-frame orientation in the pET-SUMO vector was verified by DNA sequencing and one of the resulting vectors was named pSuTlp2N. For expression of recombinant protein, pSuTlp2N was transformed into *E. coli* B834 (DE3) (Novagen, Darmstadt, Germany) and incubated overnight in 2xYT medium containing kanamycin. Next day, fresh 2xYT with antibiotic is inoculated with overnight culture and incubated at 37°C shaking until $O.D._{600}$ reached 0.6. IPTG is added to a final concentration of 1mM and cultures are incubated overnight at 30°C. Cells are collected by centrifugation for 10 minutes at 8,000 x g. The cells were resuspended in lysis buffer (50mM Tris-HCl, pH 8.0, 0.5M NaCl, 30mM Imidazole, 1mM PMSF, and glycerol 5% (v/v)) and homogenized by passing 3 times through a Thermo Electron Corp. French Press Cell Disrupter (Waltham, Mass.) at 25,000 psi. The cell lysate is cleared by centrifugation at 16,500 x g for 45 minutes. SUMO-$Tlp2^{LBD}$ is purified by immobilized metal affinity chromatography (IMAC),

batch binding 15-30 minutes with Ni-NTA agarose (Qiagen, Valencia, CA) and loaded on a Kontes Flex-Column Economy column (Vineland, NJ). The column is washed extensively with wash buffer (25mM Tris-HCl, pH 8.0, 1M NaCl, 40mM Imidazole) and protein is eluted with elution buffer (25mM Tris-HCl, pH 7.8, 250mM NaCl, 250mM Imidazole). The eluted protein is concentrated by ultrafiltration and dialyzed against 10mM Tris-HCl, pH 8.0 and 150mM NaCl. Cleavage of the N-terminal SUMO tag was performed per the manufacturer's protocol (Life Sensors, Malvern, PA) using SUMO protease. Native $Tlp2^{LBD}$ was checked for purity on an overloaded SDS-PAGE and any detectable contaminating protein was removed by ultrafiltration. Purity was then re-assessed until homogeneity was obtained and protein concentration was measured using the Bradford assay [40].

Ligand binding using intrinsic tyrosine fluorescence

Ligand binding was determined using tyrosine fluorescence on a Perkin-Elmer LS-50B fluorescence spectrometer (Waltham, Mass.) with excitation wavelength of 280nm and monitoring emission spectra from 295nm to 350nm using FL WinLab software (Perkin-Elmer, Waltham, MA). The $Tlp2^{LBD}$ protein concentration used was 10 µM as determined by protein quantitation using the Bradford Assay [40] and fluorescence intensity measurements were collected by titrating in the analyte tested in 100 nM increments until 1µM final concentration was achieved and then in 1 µM increments until no further change in fluorescence intensity was observed. To determine an apparent K_d, the decreases in fluorescence maxima were plotted against the analyte concentration. The data were analyzed with Prism 5.0 software (GraphPad, Inc.) to calculate apparent K_d with standard deviations. As a negative control, buffer alone was titrated into protein solution in 1µl increments with no decrease in fluorescence intensity observed. Fluorescence spectra were not affected by buffer pH changes from pH 7.4 to pH 8.0.

Western blots

For Western blot analyses, proteins separated on SDS-PAGE gels were transferred to nitrocellulose (Whatman) membranes using a Trans-Blot® SD Semi-Dry Transfer Cell (BioRad, Hercules, CA). Western blots were carried out essentially as described previously [25]. For detection of Sumo-Tlp2N and Tlsr chimera, HRP-conjugated Mouse Anti-6xHis (BD Pharmingen) antibodies were used at a 1:4000 dilution and detected by SuperSignal® West Dura Extended Duration Substrate (Pierce, Rockford, IL). For detection of Tlp2-YFP, proteins were probed with rabbit anti-GFP sera at a 1:2000 dilution overnight.

Flocculation assay

Cells are grown overnight at 28°C shaking in TY medium to an $O.D._{}^{600}$ 1.1-1.3. The O.D. is standardized to 1.0 and 200µl is inoculated into 5ml MMAB supplied with 0.5mM sodium nitrate and 8mM fructose as the nitrogen and carbon sources, respectively. The cultures are incubated 48 hours at 28°C with shaking. After 48 hours, cultures are placed on benchtop for 30 min to settle flocculated cells. The fraction of flocculated cells was determined as previously described (Bible et al., 2008) as

$$\frac{O.D._{final}^{600} - O.D._{initial}^{600}}{O.D._{final}^{600}}$$

Data were expressed as flocculation relative to wild type (taken as 1) because absolute flocculation percentage values are dependent upon the O.D. of the pre-culture.

Preparation of wheat seedlings and plant root colonization assay

Sterilization of wheat seedlings (*Triticum aestivum* cv. Jagger) provided by R. L. Bowden (U.S. Department of Agriculture-Agricultural Research Service, Manhattan, Kans.) and plant root colonization assay were performed as previously described [23].

Protein sequence and phylogenetic analysis

A similarity search against the non-redundant database was performed using the PSI-BLAST program [41] with residues 42-193 of Tlp2 as the query. Domain architecture was analyzed using SMART program [42] and a multiple sequence alignment was constructed using ClustalX2 [43, 44] with residues 65-166. A maximum likelihood tree was constructed from the multiple sequence alignment using PhyML 3.0 [45] and viewed using NJplot [46].

Results

Identification of Tlp2 and phylogenetic distribution

The sequence corresponding to *tlp2* was originally identified from an *Azospirillum brasilense* Sp7 genomic library using Southern blot analysis with a 1 kb nucleotide probe derived from the C-terminal sequence of a known MCP from *A. brasilense*, Tlp1 [23], and later identified in the genome sequence of *A. brasilense* [28]. The open reading frame for *tlp2* lies within a region of the genome devoid of other putative chemotaxis proteins with 321 base-pairs and 236 base-pairs of the nearest upstream (probable Ni-Fe Hydrogenase) and downstream (putative protein of unknown function) genes, respectively. *tlp2* is predicted to encode for a chemotaxis receptor of prototypical topology, i.e., a N-terminal periplasmic putative sensory domain (152 amino acids) flanked by two transmembrane helices and a large cytoplasmic conserved domain with homology to signaling domain of other chemotaxis receptors [47]. A PSI-BLAST search of the non-redundant database [41] using the periplasmic sensing domain of Tlp2 as a

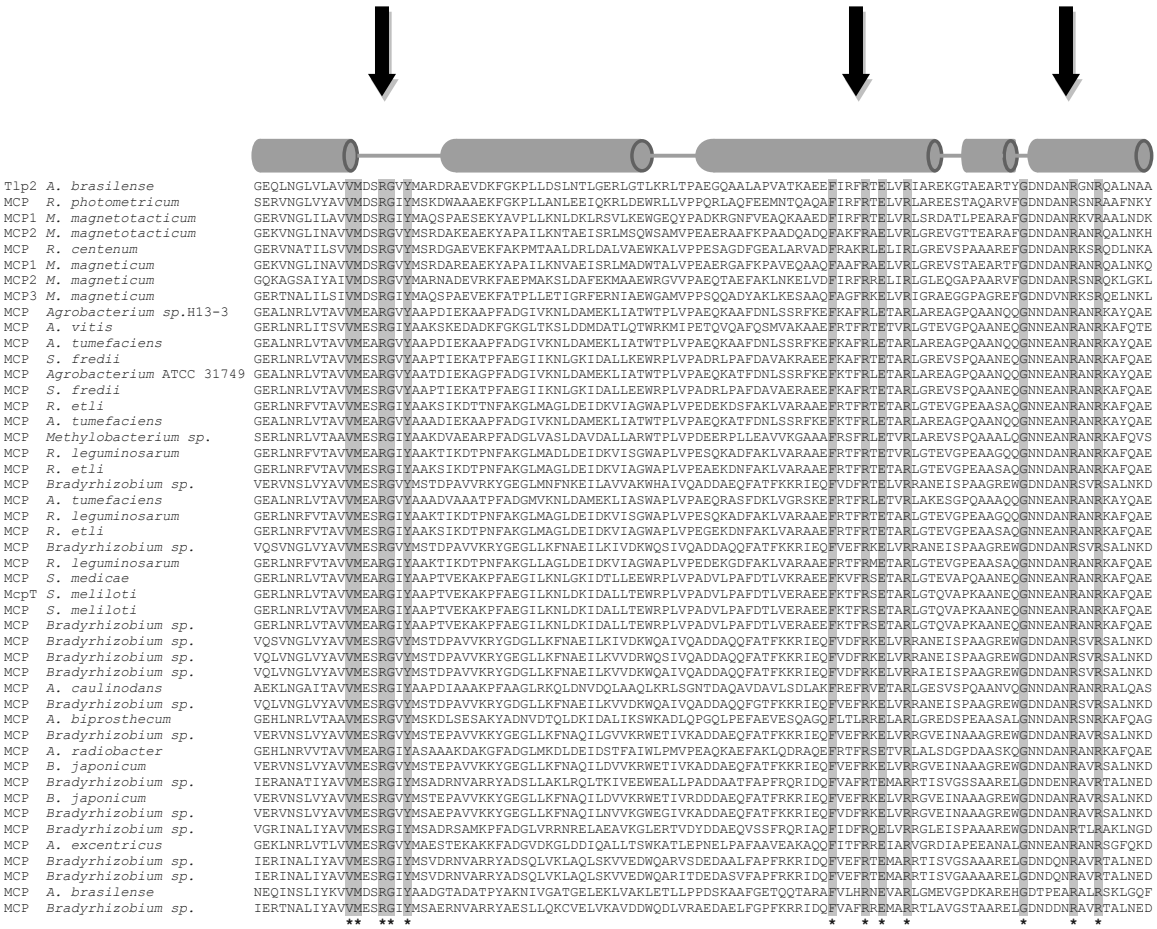

Figure 2.1: Multiple sequence alignment of the sensing domain of Tlp2 and its homologs from *Rhodospirillaceae* and *Rhizobiaceae*. Strictly conserved residues are shaded in gray with the predicted secondary structure of the polypeptide illustrated above the alignment. Cylindrical objects are predicted alpha helices while straight lines are predicted random coil regions. Conserved arginine residues mutated to alanine are indicated by black arrows.

query indicated that this putative sensory domain is conserved but its function is unknown (Figure 2.1) and present in other chemotaxis-like receptor sequences from the genomes of closely related alphaproteobacteria belonging to the *Rhodospirillaceae* and the *Rhizobiaceae.* The *A. brasilense* genome shares homology with both *Rhodospirillaceae* and *Rhizobiaceae* but over 50% of the *A. brasilense* genome has been transferred horizontally from the *Rhizobiaceae* [28]. The closest homologs of Tlp2 are found in the *Rhodospirillaceae*, suggesting that it was present in the ancestral organism that gave rise to the genus *Azospirillum.* The bacterial species that harbor these homologs correspond to isolates that dwell in soils and sediments, suggesting a function for this sensory domain in these habitats (Figure 2.1B). A multiple sequence alignment of the sensing domain of Tlp2 and its homologs using ClustalX [44] shows 3 regions of strictly conserved residues (12 total) (Figure 2.1) suggesting their importance in structure or function with conserved arginine residues present in each region; 1 arginine in region 1 (Arg76) and 2 each in region 2 (Arg139 and Arg144) and region 3 (Arg159 and Arg162).

Expression of tlp2 is maximal in presence of nitrate and/or under low aeration conditions

The putative sensory specificity of Tlp2 as a chemotaxis transducer is unknown but previous work has suggested that the pattern of expression of at least some chemoreceptors parallel their function in *A. brasilense* [48]. Furthermore, analysis of the DNA sequence upstream of Tlp2 indicated the presence of conserved motifs for binding of RpoN (Sigma 54) and NtrC (data not shown). NtrC regulates Sigma 54-dependent promoters under conditions of nitrogen limitation (absence of fixed nitrogen) and low oxygen concentrations, suggesting that expression of Tlp2 may be regulated by the availability of ammonium and oxygen [49]. Therefore, we tested the activity of the putative *tlp2* promoter (P*tlp2*) by using a translational fusion to the promoterless

gusA gene, in the broad-host range pFUS1 vector [37] under diverse growth conditions. The expression of the P*tlp2* was also tested in *A. brasilense* Sp7 mutant derivatives 7148 (*ntrC::Tn5* [50]) and FAJ301 (Δ*rpoN* [51]). The activity of the P*tlp2* was found to be higher in early stationary phase under all conditions tested (data not shown). The Tlp2 promoter expression was the lowest when cells grew the fastest, including in rich medium (TY) or in presence of the preferred substrate for growth (malate or pyruvate) under high aeration conditions in wild type Sp7 (Figure 2.2A). On the other hand, in Sp7, expression of P*tlp2* was the highest under nitrogen fixation conditions and under anaerobic growth with nitrate as the electron acceptor (Figure 2.2A). Expression was also high in minimal medium supplemented with nitrate, the non-preferred combined nitrogen with high aeration, consistent with its putative regulation by RpoN and NtrC. Similarly, growth under low aeration conditions was sufficient to induce promoter activity, regardless of the presence (no nitrogen) or the nature of the fixed nitrogen (ammonium or nitrate) (Figure 2.2A). In agreement with a role for RpoN and NtrC in regulating the expression of Tlp2, the activity of P*tlp2* was significantly reduced when analyzed in strain 7148 (*ntrC*::Tn5) or FAJ301 (Δ*rpoN*) (Figure 2.2B). Furthermore, addition of ammonium to the medium did not affect P*tlp2* activity in the absence of functional NtrC. Taken together, these results indicate that *tlp2* expression is significantly increased under conditions of nitrogen fixation or when the preferred nitrogen source is absent (presence of nitrate instead of ammonium), suggesting a significant functional role for this receptor under these conditions.

A

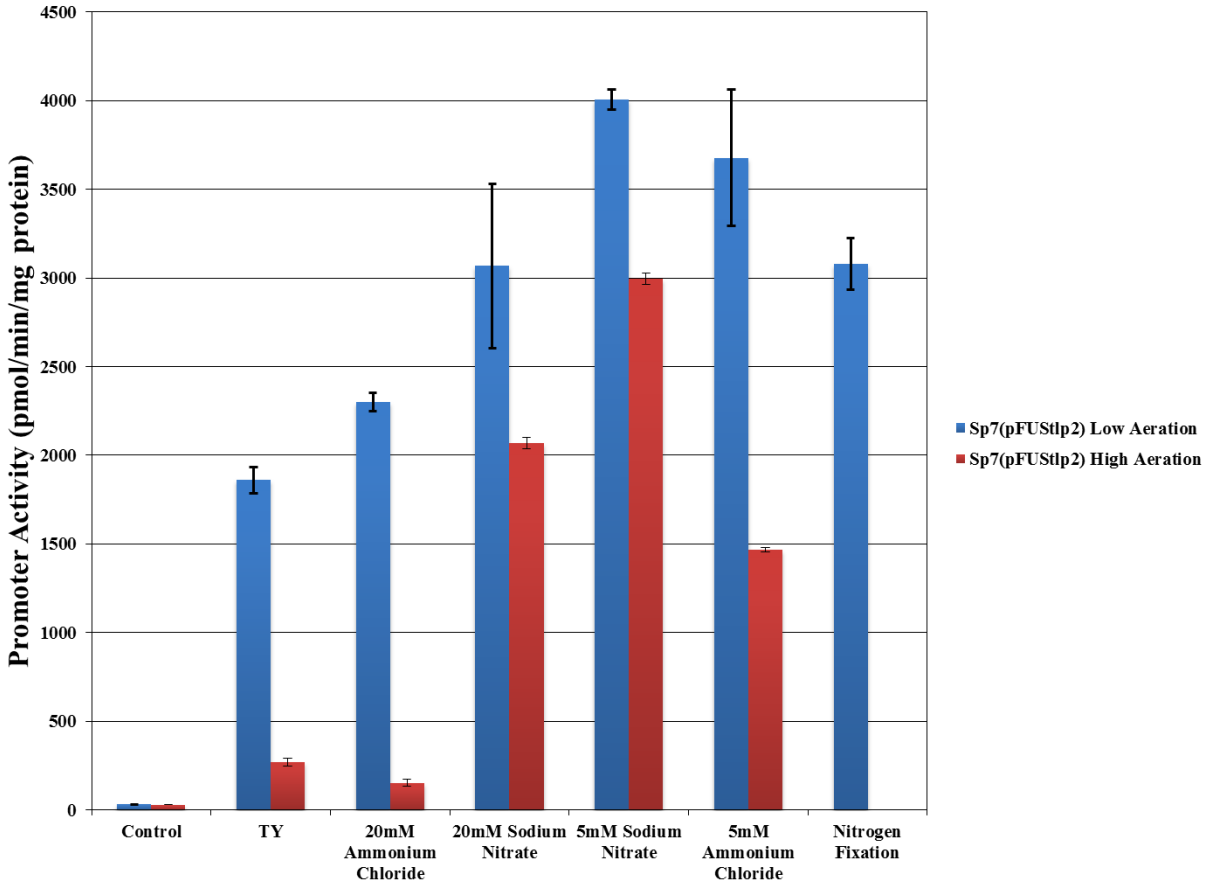

Figure 2.2: Tlp2 promoter expression measured by the β-glucuronidase assay. A, promoter activity of Tlp2 in wild type *A. brasilense* Sp7 under various growth conditions in low (blue bar) and high (red bar) aeration. B, Tlp2 promoter activity under low aeration of Sp7 and its mutant derivatives *ntrC*::Tn5 and *ΔrpoN* supplied with 5mM (red bar) or 20mM (green bar) ammonium chloride. C, Tlp2 promoter activity under high aeration in the same strains with ammonium chloride 5mM or 20mM.

B

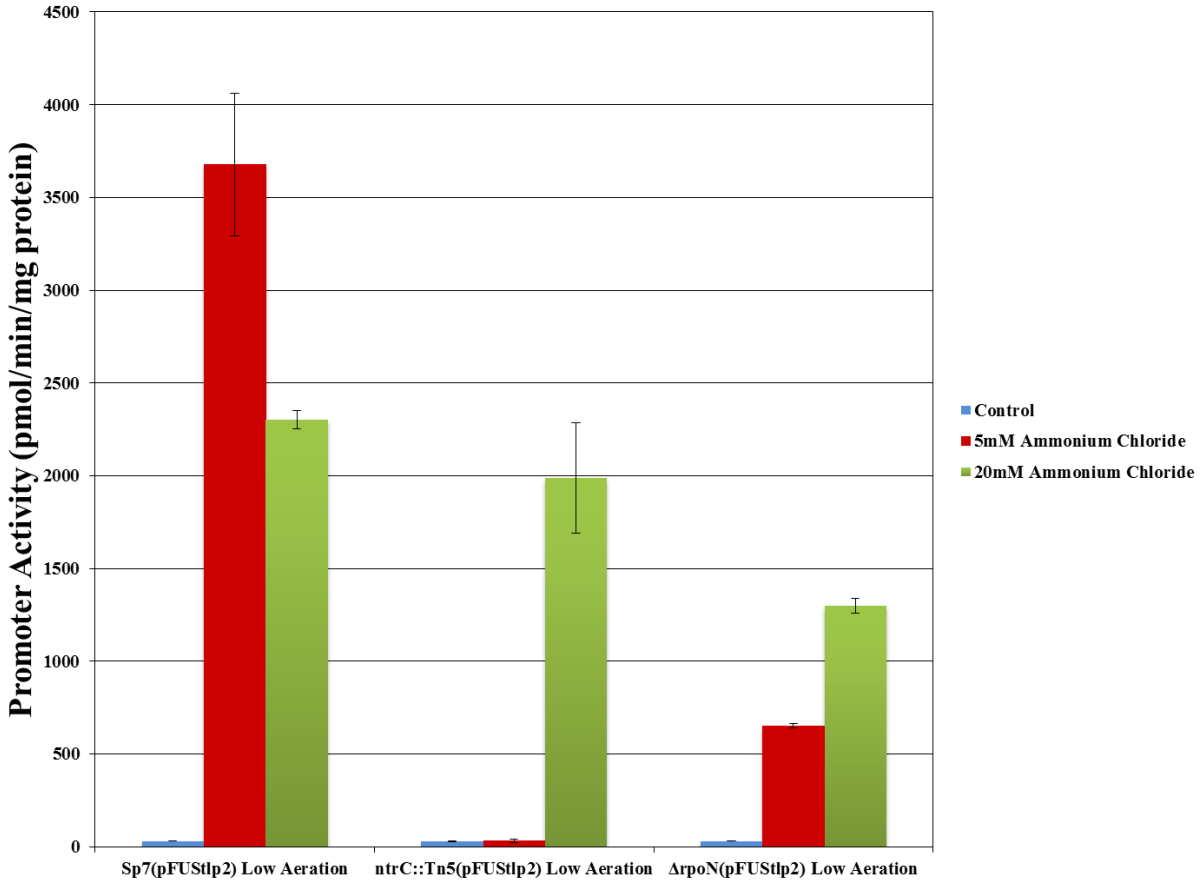

Figure 2.2, continued

C

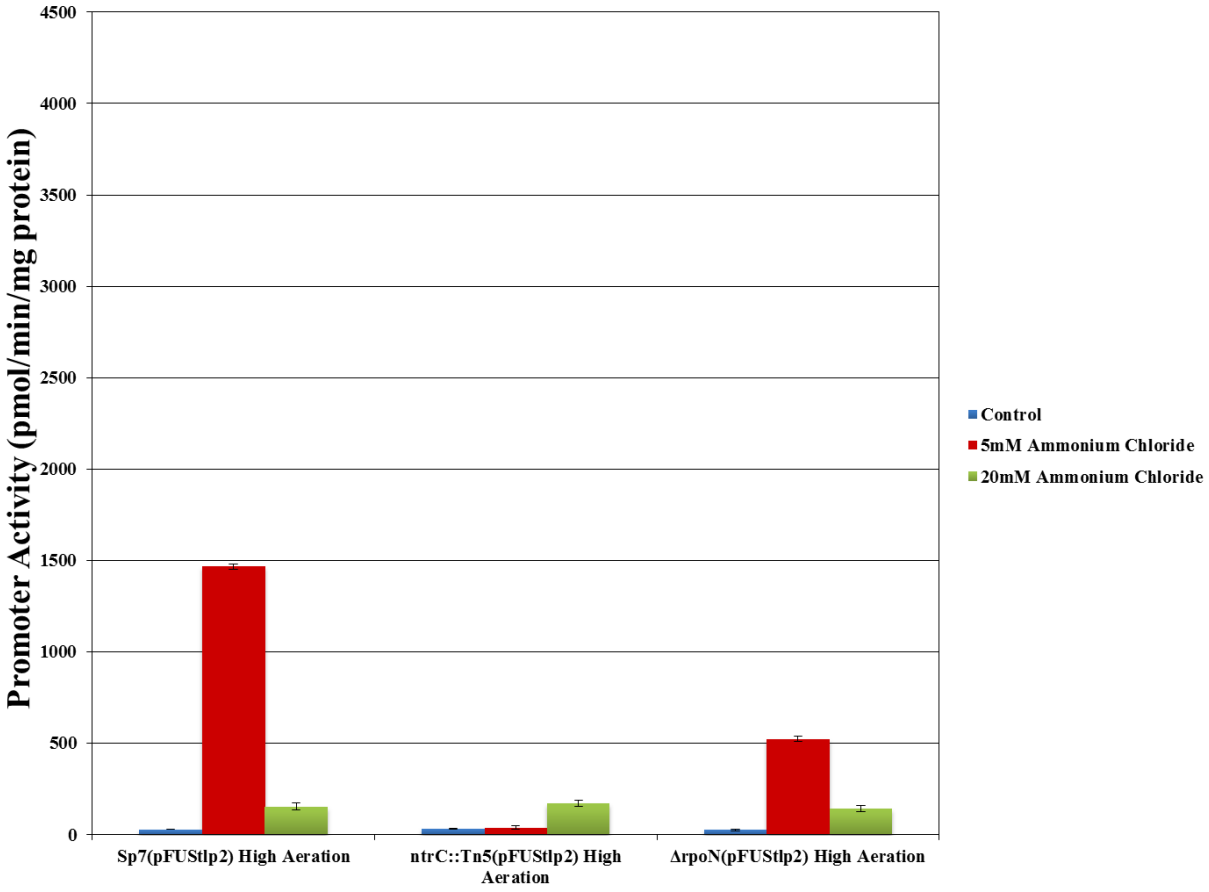

Figure 2.2, continued

Tlp2-YFP subcellular localization depends on growth conditions

The subcellular localization of a Tlp2-YFP fusion, expressed from the native *tlp2* promoter on a low copy plasmid in wild type and mutant strains backgrounds under conditions of high Tlp2 (nitrate /malate) and low Tlp2 expression (malate/ammonium or TY), was analyzed next using fluorescence microscopy. Tlp2-YFP restored chemotaxis of the AB401 strain (Δ*tlp2*::Km) in an anaerobic soft agar assay with nitrate and malate as the sole nitrogen and carbon sources, respectively, indicating that the Tlp2-YFP fusion is functional (data not shown). Bright fluorescent foci could be seen when cells were grown with nitrate, where *tlp2* expression (and thus Tlp2-YFP localization) is expected to be high, but not with ammonium were only background fluorescence could be detected (Figure 2.3A). The fluorescent foci were predominantly polar or subpolar with occasional lateral localization also observed. Expression of Tlp2-YFP could be detected by Western blot when cells were grown with nitrate but not when cells were grown with ammonium (Figure 2.3B), suggesting that the observation of polar fluorescent foci correlate with the relative expression of Tlp2-YFP. Expression and localization of Tlp2-YFP thus appear to correlate and suggest that a functional role for Tlp2 may be best revealed under conditions when the protein is most abundant. This prompted us to analyze the contribution of Tlp2 to chemotaxis and cellular behaviors that depend on nitrogen

Figure 2.3: Tlp2-YFP cellular localization under different growth conditions. A, representative pictures of localization of Tlp2-YFP grown anaerobically (top panel), aerobically with high aeration with nitrate (middle panel), and high aeration with ammonium (bottom panel). White arrows show representative fluorescent foci. B, Western blot detection of Tlp2-YFP in cells grown under high aeration with ammonium (lane 1) or nitrate (lane 2). Black arrow shows expected molecular weight of Tlp2-YFP.

A

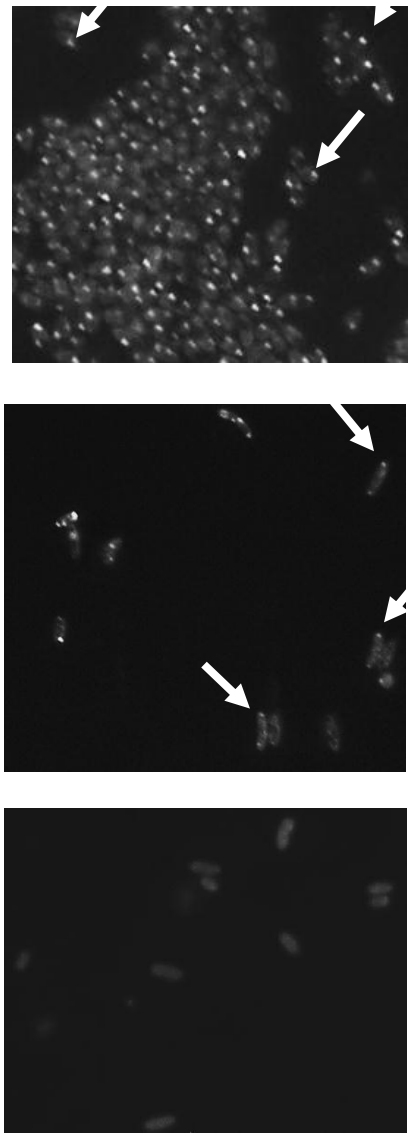

B

1 **2**

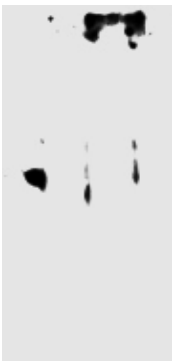

metabolism. In order to gain insight into the sensory function of Tlp2, a mutant strain carrying an in-frame deletion of most of the *A. brasilense tlp2* open reading frame (Table 2.1) was constructed (strain AB401). In addition, we constructed a low-copy plasmid containing a wild type *tlp2* gene to express *tlp2 in trans* from its own promoter. Also, of the 12 strictly conserved residues found in the sensory domain of Tlp2, 5 are arginine residues (Figure 2.1). Therefore, we also constructed 3 variant alleles of *tlp2* lacking one of these three conserved arginines (1 from each region): Arg76, Arg139, and Arg159.

Tlp2 in A. brasilense chemotaxis and behavior

Aerotaxis is a strong behavior in the microaerophilic bacterium *A. brasilense*. Therefore, we first tested the motility behavior of strain AB401 in a spatial aerotaxis assay but no difference could be detected between the wild type and the mutant strain (Figure 2.4), indicating no major function for Tlp2 in aerotaxis under these conditions. We then tested chemotaxis in gradients of different concentrations of strong attractants using the soft-agar plate assay. The chemotactic ring sizes between wild type Sp7(pRK415), AB401(pRK415), and AB401(pRKTlp2), were found to vary significantly but did not appear to correlate with the concentration or the type of carbon source used (Figure 2.5A). This suggested the effects of the carbon sources on chemotaxis abilities under these conditions were indirectly related to the chemotactic ring sizes formed by the strains tested. Given the profiles of expression of P*tlp2* (see above), we next tested whether the changes in the chemotactic behavior could be affected by the nitrogen source added to the soft agar plate, rather than the carbon source. To test this hypothesis, we varied the concentration of the nitrogen source available for growth in the soft agar plate assay in presence of different carbon sources. Regardless of the carbon source used, a correlation between chemotaxis ring sizes and the concentration of the nitrogen source available for growth in soft agar plate assay could be

observed when sodium nitrate was present as the sole nitrogen source (Figure 2.5B). Such correlation was not apparent when ammonium was present in the medium. The defect in chemotaxis to nitrate could be restored by expressing the wild type *tlp2* from a low copy plasmid. These observations strongly suggested that Tlp2 senses gradients of nitrate when tested in the soft agar plat assay. In addition, a faint outer ring observed around wild type cells inoculated in soft agar plates containing sodium nitrate and malate as a carbon source, was absent in the mutant strain but could be restored by expressing a wild type Tlp2 receptor from a low copy plasmid (data not shown). To confirm this function, we analyzed chemotaxis in gradients of sodium nitrate in soft agar plates incubated anaerobically. Under anaerobic conditions, *A. brasilense* can use nitrate as a terminal electron acceptor and we hypothesize that lack of *tlp2* should result in impaired ability to navigate in soft agar plates containing sodium nitrate as the sole electron acceptor and nitrogen source. When cells were inoculated in soft agar plates with sodium nitrate and either malate, pyruvate, or succinate as the carbon source and incubated under anaerobic conditions, the mutant strain lacking Tlp2 (AB401(pRK415)) was incapable of chemotaxis (growth but no ring detected), but chemotaxis ability (as seen by chemotactic ring formation) was restored in (AB401(pRKTlp2) by functional complementation (Figure 2.5C). Given that no growth differences under these conditions were found when comparing these strains, these data

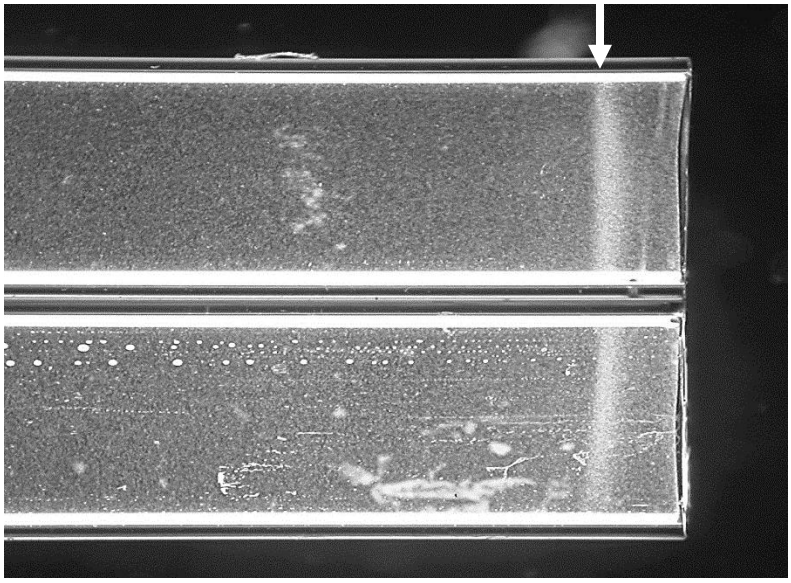

Figure 2.4: Spatial aerotaxis of *A. brasilense* Sp7 and its *Δtlp2* mutant derivative. Motile Sp7 (top) and *Δtlp2* (bottom) were resuspended in a flat capillary where an aerotactic band of motile cells forms some distance from the air/liquid interface (meniscus) which is optimum for intracellular energy production. Arrow indicates position of aerotactic band.

A

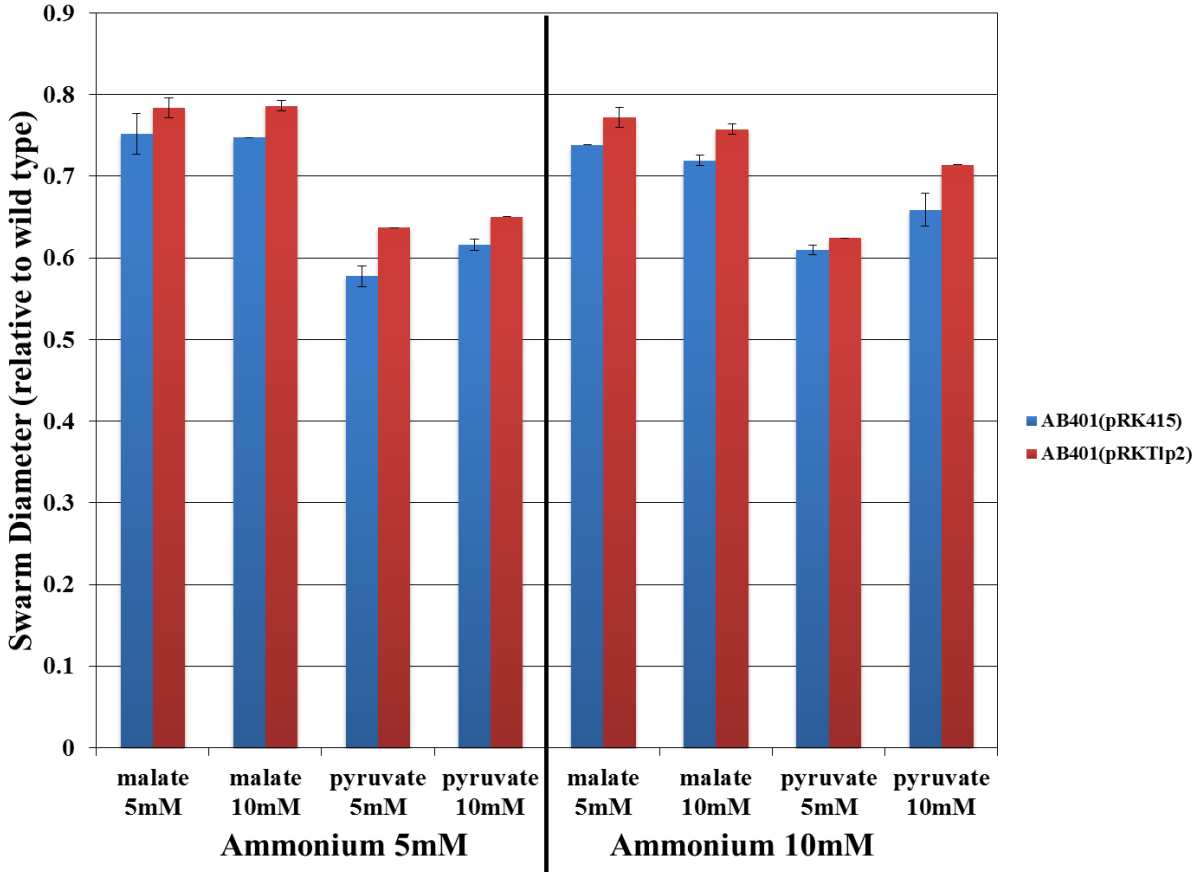

Figure 2.5: Assay for chemotaxis defects and complementation of *Δtlp2* by the soft agar assay. A, Soft agar assay assessing chemotaxis for the organic acids malate and pyruvate at 5mM and 10mM supplemented with 5mM or 10mM ammonium chloride. B, Soft agar assay assessing chemotaxis for the organic acids malate and pyruvate at 5mM and 10mM supplemented with 5mM or 10mM sodium nitrate. C, Measure of chemotaxis during anaerobiosis with 10mM nitrate (sodium or potassium salt) for *Δtlp2*(pRK415) and *Δtlp2*(pRKTlp2).

B

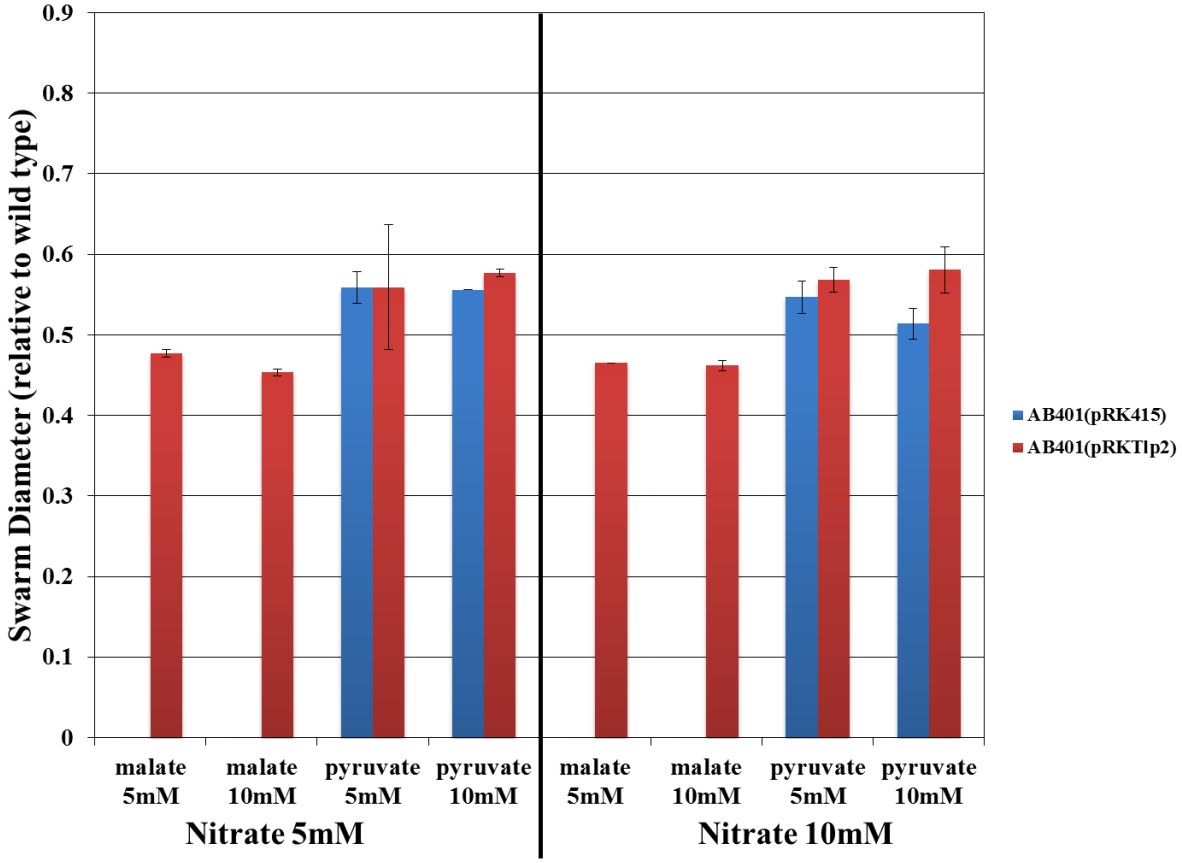

Figure 2.5, continued

C

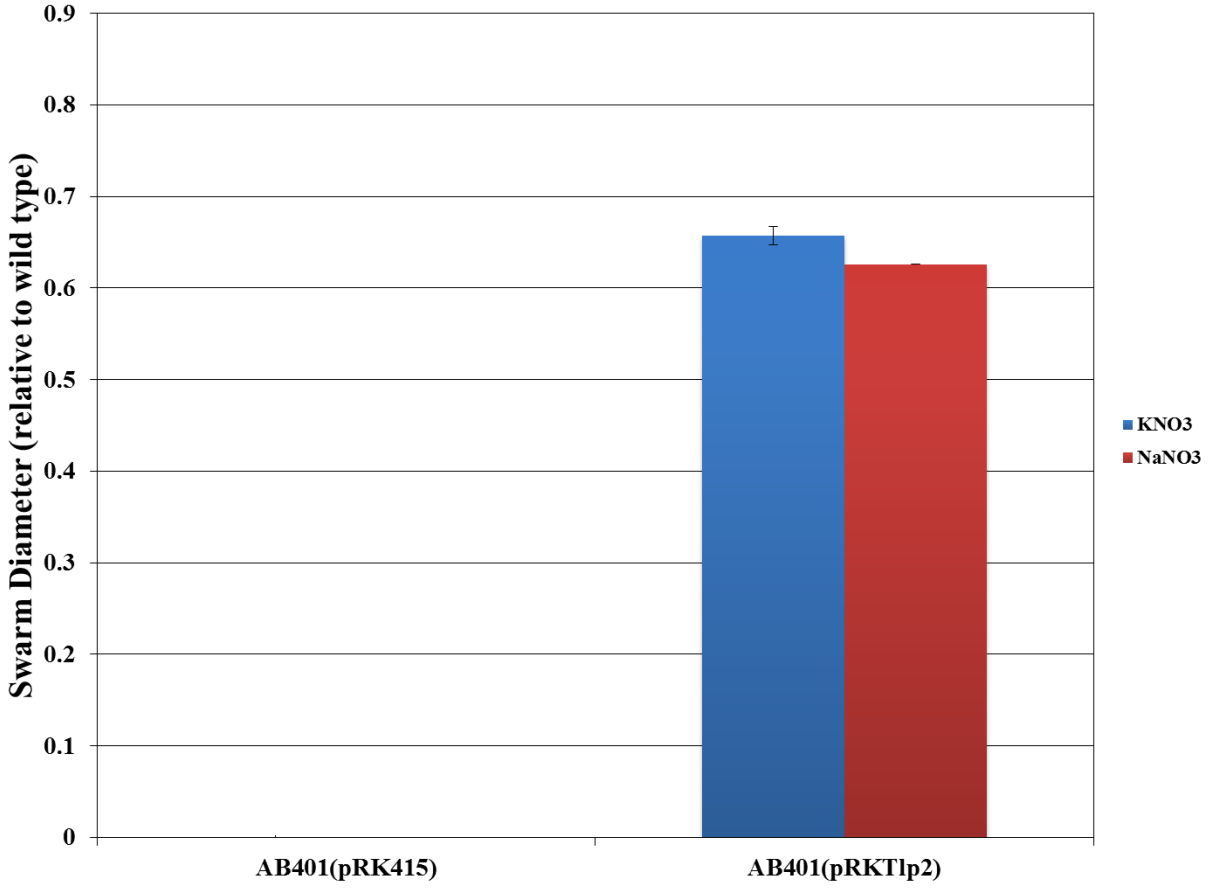

Figure 2.5, continued

suggest that Tlp2 mediates tactic responses to sodium nitrate. To verify chemotaxis was towards nitrate and not the sodium salt, a similar ring was observed with potassium nitrate (Figure 2.5C). Of the 12 strictly conserved residues found in the sensory domain of Tlp2, 5 are arginine residues and 3 are strictly conserved. Thus, we also constructed 3 variant alleles of Tlp2 lacking one of the three highly conserved residues within the sensory domain: Arg76 ($Tlp2^{R76A}$), Arg139 ($Tlp2^{R139A}$), and Arg159 ($Tlp2^{R159A}$) and first tested their effect on chemotaxis toward malate with either nitrate or ammonium also added in the soft agar plate assay (Figure 2.6). As expected from previous results, the Δ*tlp2* mutant did not have any defect in chemotaxis when ammonium was present in the plates and none of the Tlp2 variants tested affected this response (Figure 2.6). In contrast, the Δ*tlp2* mutant had a significant defect in chemotaxis when nitrate was present as the nitrogen source in the plate (Figure 2.6) and this defect could be rescued by expressing Tlp2 *in trans* or partially by $Tlp2^{R76A}$, but not $Tlp2^{R139A}$ or $Tlp2^{R159A}$ (differences were not statistically significant at the $P < 0.05$ level). These effects were pronounced when the assay was repeated under anaerobic conditions with none of the Tlp2 variants being able to restore chemotaxis to nitrate to the Δ*tlp2* mutant, in contrast to the wild type Tlp2. Furthermore, of the three Tlp2 variants, $Tlp2^{R159A}$ was the most dramatically affected in the ability to support taxis toward nitrate under these conditions. These results provide further support to the notion that Tlp2 senses nitrate with conserved arginine residues R76, R139 and R159 being implicated in this function.

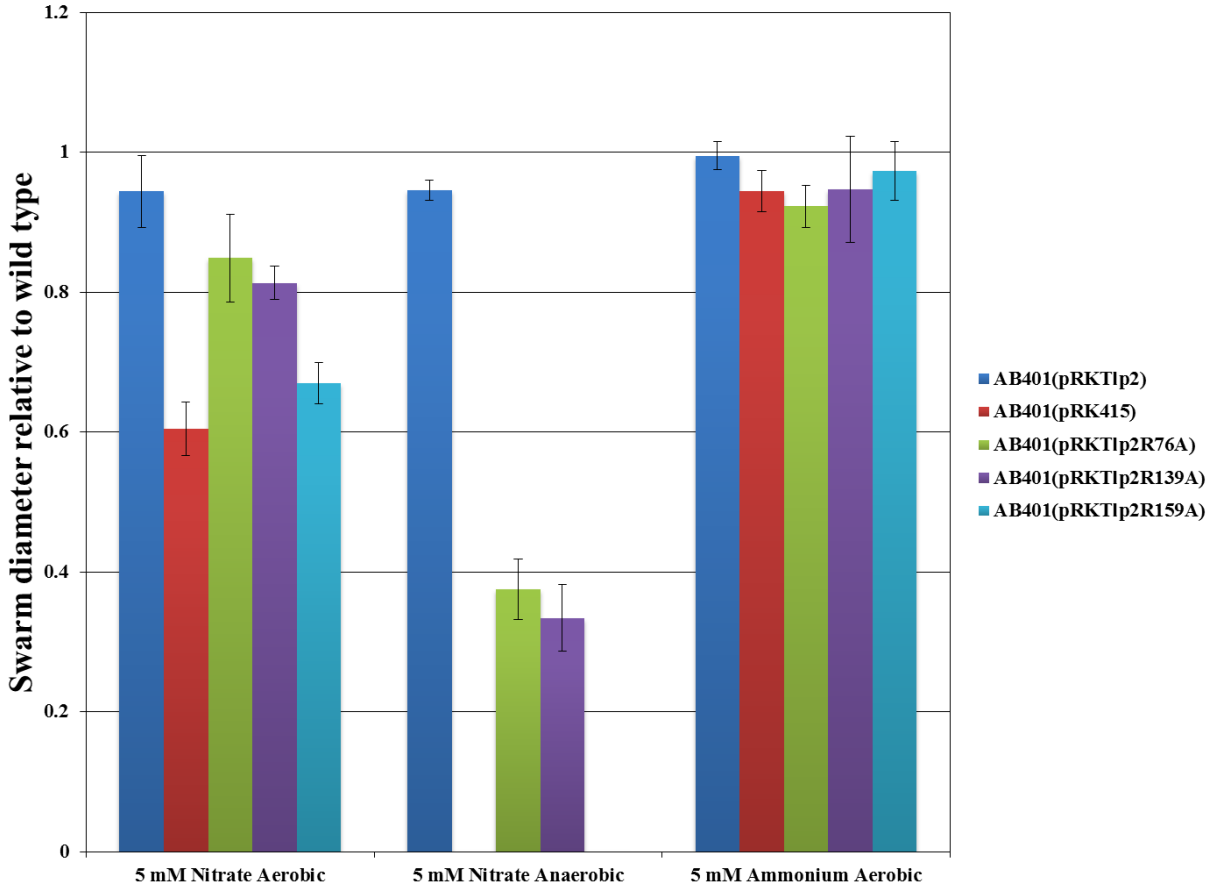

Figure 2.6: Measure of chemotaxis defects using the soft agar assay for *Δtlp2*(pRK415) and site-directed mutants. Soft agar to assay chemotaxis with 5mM nitrate incubated aerobically or anaerobically as the terminal electron acceptor and nitrogen source or aerobically with 5mM ammonium. Faint outer ring was present for AB401(pRK415) in aerobically incubated plates supplemented with nitrate when precultures were grown to late growth phase ($O.D._{600}$ > 1.3).

Intrinsic fluorescence study of the soluble periplasmic sensing domain of Tlp2

We next used intrinsic tyrosine fluorescence in order to characterize the specificity and affinity biochemically of the sensory domain of Tlp2. The periplasmic sensory domain of Tlp2 contains two tyrosine residues (but no tryptophan), one of which (Tyr79) is strictly conserved in all homologs (Figure 2.1). This suggested an essential functional and/or structural role for this residue making it a suitable candidate for measuring potential changes in intrinsic tyrosine fluorescence upon ligand binding. The putative N-terminal periplasmic ligand binding domain of Tlp2 ($Tlp2^{LBD}$) was thus recombinantly expressed and purified as a native soluble protein as described in the methods section. CD spectra analysis of $Tlp2^{LBD}$ indicated that the secondary structure was predominantly alpha-helical (Figure 2.7A). Since nitrate, and to a lesser extent ammonium, were potential $Tlp2^{LBD}$ ligands suggested by the soft agar assay, both were tested for *in vitro* binding to $Tlp2^{LBD}$ by changes in intrinsic tyrosine fluorescence. In addition to nitrate and ammonium, other nitrogenous compounds were also tested (urea, nitrite, and ammonium nitrate) as well as the nitrate analog chlorate, phosphate salts, sodium chloride and the amino acids, alanine and glutamate. Sequential addition of potential $Tlp2^{LBD}$ ligand triggered a decrease in the fluorescence maxima until saturation was observed (Figure 2.7B). Amongst the ligands tested, binding was found for the inorganic nitrogenous compounds urea, nitrite, ammonium nitrate, nitrate, and ammonium (Figure 2.7C). The apparent binding affinities were in the sub-micromolar range. The analyte chlorate which is structurally similar to nitrate also had a relatively high affinity (7.5µM) for $Tlp2^{LBD}$, suggesting a *de facto* binding site for nitrate/chlorate. The amino acids tested (alanine and

A

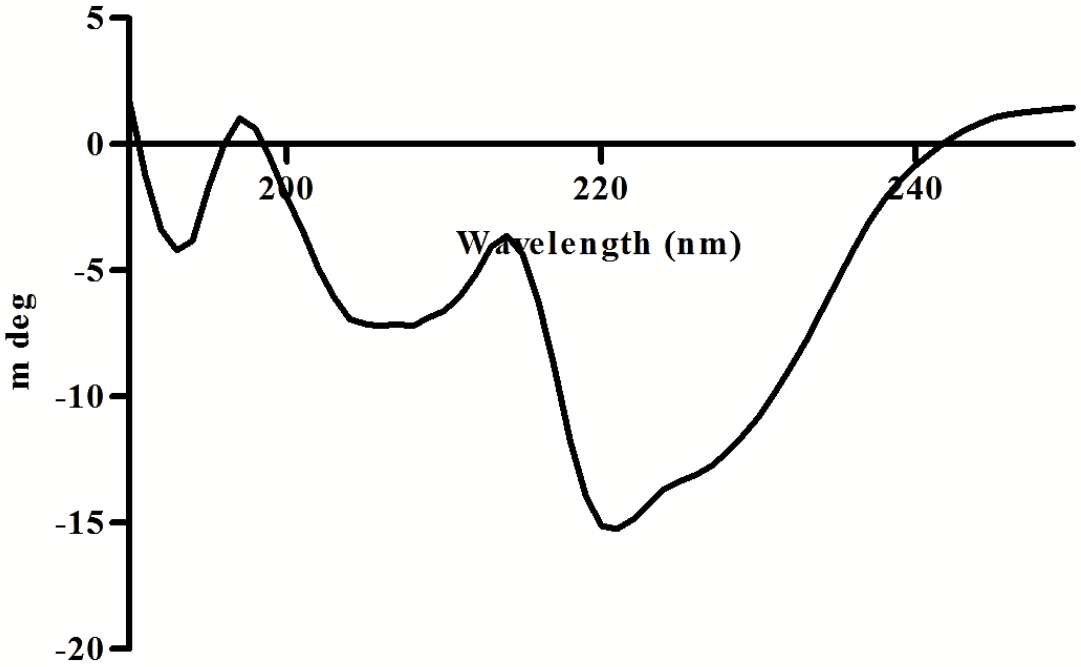

Figure 2.7: Analysis of the Tlp2^{LBD} recombinant protein and intrinsic tyrosine fluorescence analysis upon ligand binding. A, Circular dichroism spectrum of recombinant Tlp2^{LBD} illustrating secondary structure. B, Decrease in intrinsic tyrosine fluorescence at the characteristic Tyr emission wavelength (305nm; excitation wavelength of 280nm) upon serial addition of nitrate until saturation is reached. C, Plot of change in tyrosine fluorescence maxima versus total concentration of analytes added to cell. Non-linear regression using GraphPad (Prism) to calculate apparent $K_{1/2}$ values listed next to corresponding color of analyte. D, Reversibility of nitrate binding to Tlp2^{LBD}. Nitrate was serially added to protein until saturation, dialyzed overnight against 4L of protein buffer with the same sample tested for nitrate binding again.

B

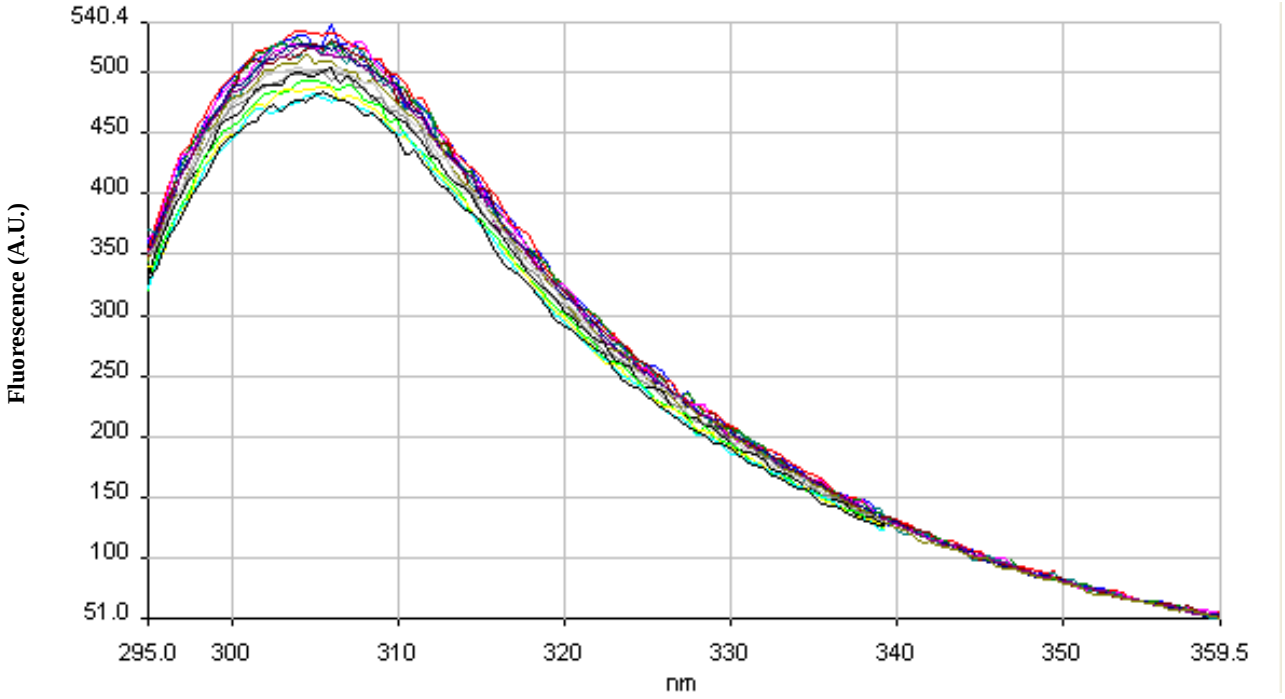

C

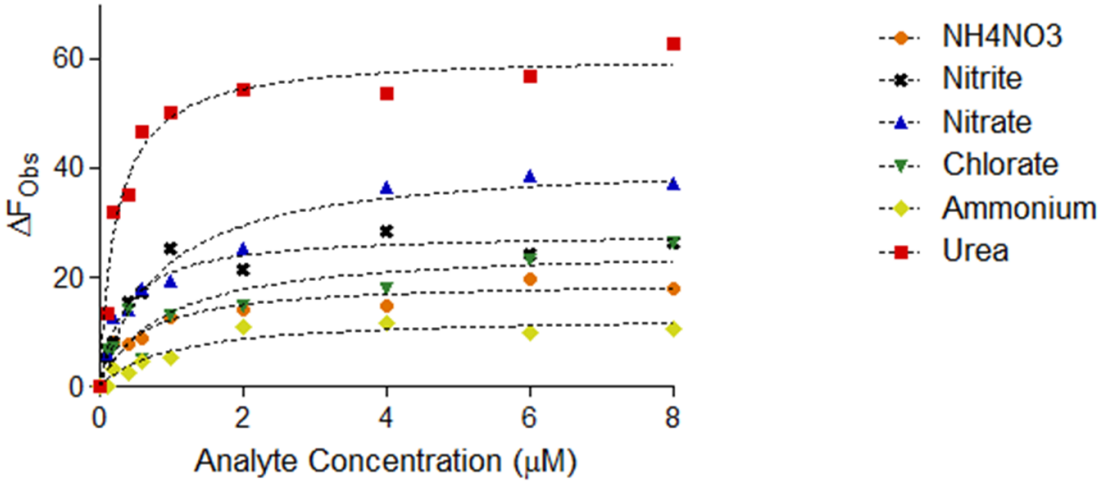

Figure 2.7, continued

D

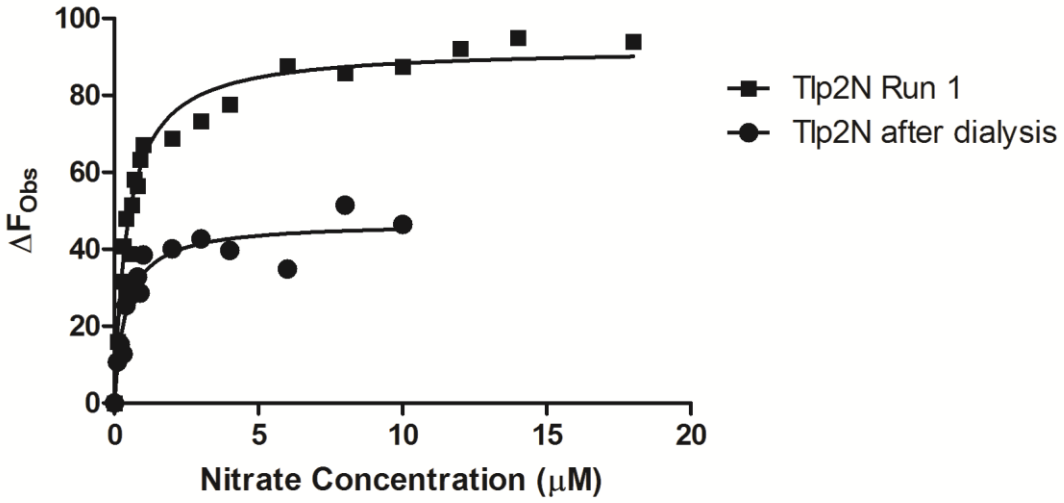

Figure 2.7, continued

glutamate) showed no binding to $Tlp2^{LBD}$ (data not shown). Sodium chloride and sodium phosphate were also tested as controls and were not found to bind to $Tlp2^{LBD}$ in this assay (data not shown). To test reversibility of nitrate binding, nitrate-saturated $Tlp2^{LBD}$ was dialyzed overnight and assayed again for nitrate binding. Upon re-addition of nitrate, saturation was reached with a similar apparent $K_{1/2}$ (Figure 2.7D).

Flocculation, a behavior dependent on nitrogen metabolism is affected by Tlp2

In *A brasilense*, chemotaxis signal transduction proteins, including chemotaxis receptors, have been previously shown to have defects in non-chemotactic phenotypes, such as flocculation [25, 29, 52]. The contribution of Tlp2 to flocculation was thus tested (Figure 2.8). Given that flocculation depends on nitrogen metabolism and is induced upon growth under high aeration and low nitrogen concentrations (high carbon to nitrogen ratio), we tested next the role of Tlp2 in this behavior. Analysis of expression of P*tlp2* indicated that *tlp2* was expressed under conditions of flocculation (Figure 2.8A). The AB401 strain was found to display a significant increase in total flocculation compared to wild type under flocculating conditions (Figure 2.8B) (see *Experimental Procedures*). The enhanced flocculation phenotype of strain AB401 could be complemented to lower than wild type levels by expressing a functional Tlp2 *in trans* from a low copy vector (Figure 2.8B) suggesting that the enhanced flocculation phenotype of strain AB401 is directly caused by lack of functional sensing and/or signaling by Tlp2 . Given the likely sensory function of Tlp2 in gradients of nitrate, we tested whether flocculation could also be sensitive to changes in nitrate concentrations. When the amount of nitrate was varied in cultures of the wild type, we found that the wild type strain flocculated more in presence of 0.5mM nitrate and gradually less (value/figure) when nitrate increased to 1 or 2.5 mM (Figure 2.8B). The

A

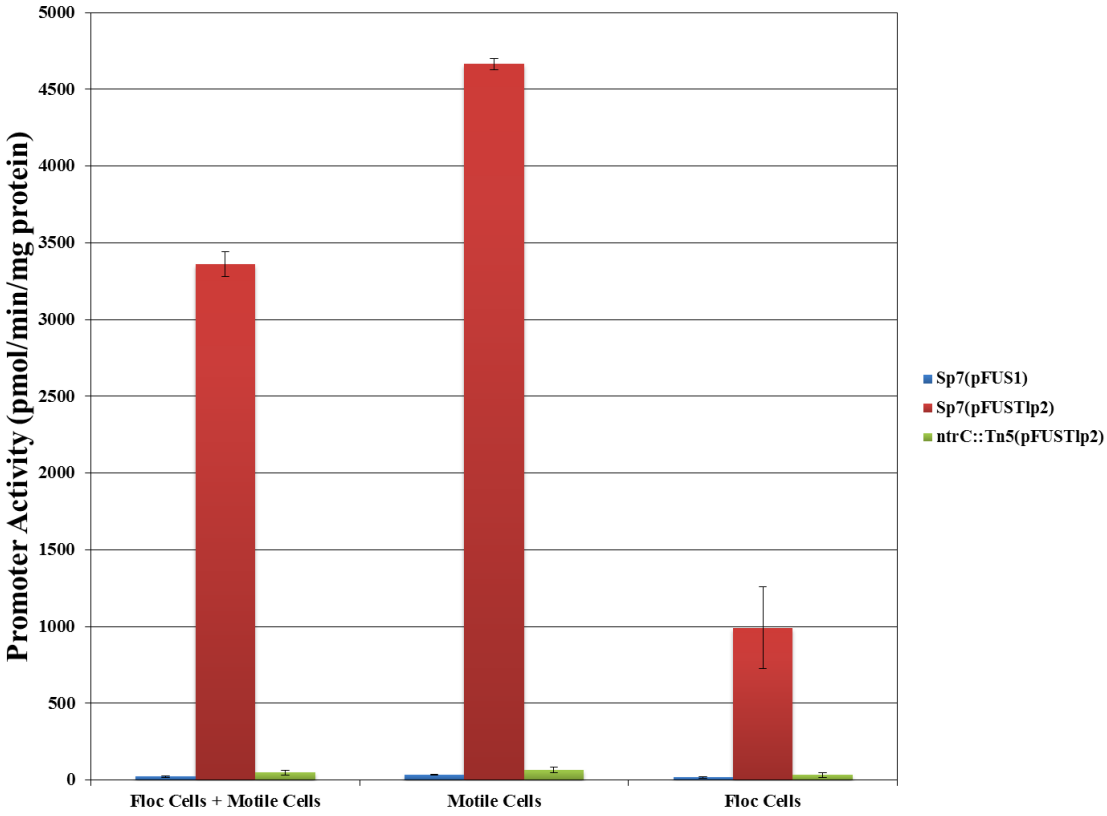

Figure 2.8: Tlp2 promoter activity during flocculation and amount of flocculation after 21 hours incubation. A, Tlp2 promoter activity of Tlp2 in *A. brasilense* Sp7 and *ntrC*::Tn5 mutant during flocculation. Beta-glucuronidase activity was assay for the entire sample (Floc Cells + Motile Cells), cells not yet non-motile and flocculated (Motile Cells), and cells flocculating (Floc Cells). B, Flocculation of *Δtlp2*(pRK) and *Δtlp2* harboring wild type Tlp2 or the site-directed mutants in floc media supplemented with indicated concentrations of nitrate after 21 hours. C, Flocculation of *Δtlp2*(pRK) and *Δtlp2* harboring wild type Tlp2 or the site-directed mutants in floc media supplemented with indicated concentrations of ammonium. Same dose-dependent decrease in flocculation at 21 hours and 48 hours.

B

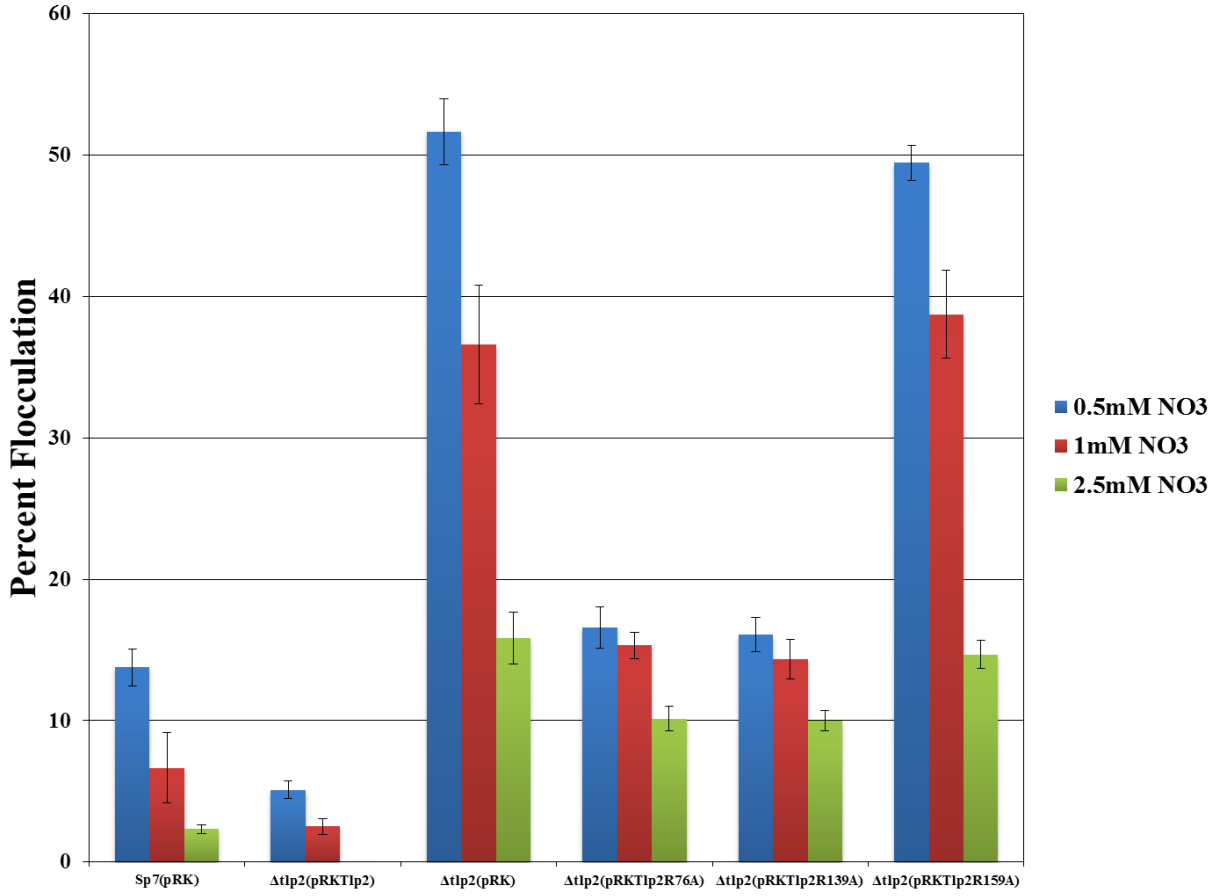

Figure 2.8, continued

C

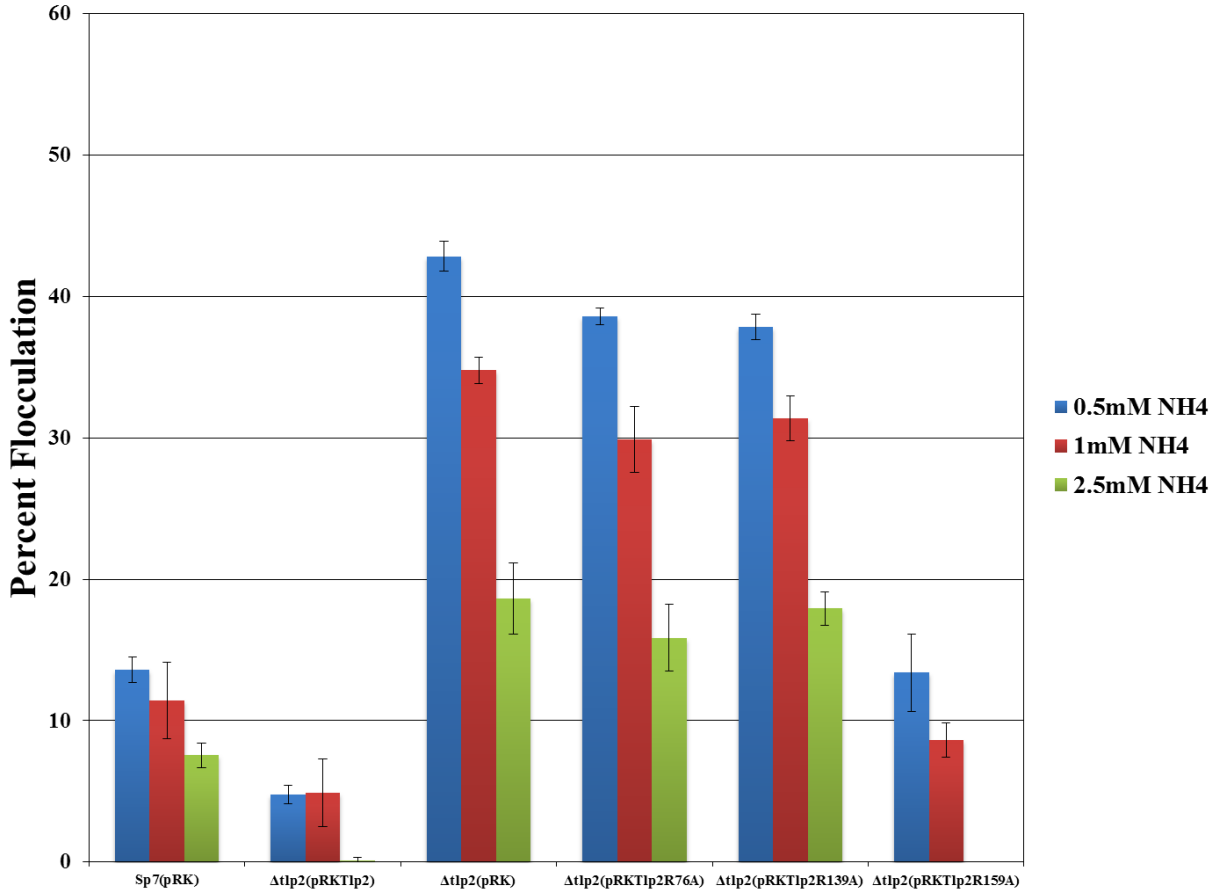

Figure 2.8, continued

Δ*tlp2* mutant strain flocculated more than the wild type strain and, similarly, increasing concentration of nitrate from 0.5mM, to 1mM or 2.5 mM gradually decreased the amount of flocculation. The difference in flocculation between the wild type strain and the AB401 strain was abolished when wild type Tlp2 was expressed in the Δ*tlp2* mutant strain background from a low copy plasmid (Figure 2.8B). Expression of $Tlp2^{R139A}$ did not rescue the flocculation phenotype of the Δ*tlp2* mutant and a strain expressing $Tlp2^{R139A}$ behaved similar to the Δ*tlp2* mutant strain expressing an empty vector control (Figure 2.8B). In contrast, expressing $Tlp2^{R76A}$ or $Tlp2^{R159A}$ restored the flocculation defect of the mutant and strains expressing these variant proteins behaved as the wild type strain. These results suggest that R139 is essential for Tlp2 function in nitrate sensing during flocculation, while R76 and R159 are dispensable.

Given the fluorescence data that suggested that the sensory domain of Tlp2 might also bind ammonium, we also tested the effect of varying ammonium concentration on the ability of the wild type strain and the *Δtlp2* to flocculate using a similar experimental strategy, i.e., varied the ammonium chloride concentrations (0.5mM, 1 mM, and 2.5mM) added to the flocculation basal medium. Similar to the effect of nitrate, the wild type strain flocculated significantly more at lower concentrations of ammonium in the medium and increasing the concentration of ammonium gradually caused a decrease in flocculation (Figure 2.8C). The Δ*tlp2* mutant strain flocculated significantly more compared to the wild type strain, regardless of the concentration of ammonium present in the medium and this behavior was also sensitive to the concentration of ammonium present: flocculation was greater at lower ammonium concentrations (Figure 2.8C). Expressing the wild type Tlp2 or $Tlp2^{R139A}$ rescued the flocculation phenotype of the *Δtlp2* mutant (Figure 2.8C). In contrast, strains *Δtlp2*(pRKTlp2^{R76A}) and *Δtlp2*(pRKTlp2^{R159A}) behaved as the *Δtlp2*(pRK) mutant strain, regardless of the concentration of ammonium present. These data

suggest that under conditions of the flocculation assay, Tlp2 contributes to sensing ammonium and the residues R76 and R159 are essential for this ability, while R139 is dispensable.

Plant colonization

In order to determine if Tlp2 has a role in *A. brasilense* wheat root colonization (similar to Tlp1 [23]), the ability of the mutant strain lacking a functional Tlp2 receptor (AB401) was compared with that of the wild type strain, in single and co-inoculation (competition at a 1:1 ratio of wild type to mutant strain) experiments. In both experimental conditions, cells were initially inoculated to sterile wheat roots at a final concentration of about 10^7 cells, but no statistical differences were detected in the amount of cells recovered from the roots colonized by the wild type or the mutant strain (in single inoculation, Sp7 population levels were: 8.35 $\pm$1.57 x 10^7 cells/g root and AB401 populations levels were 1.42 $\pm$-0.63 x 10^7 cells/g of roots; p-value 0.111) (In competition experiments, Sp7 population levels were: 4.36 $\pm$ 1.86 x 10^7 cells/g root and AB401 populations levels were 2.06 $\pm$-0.85 x 10^7 cells/g of roots; p-value 0.594), suggesting that sensing by Tlp2 has no significant contribution to root colonization *per se* or the competitive ability of *A. brasilense* to colonize sterile wheat roots under the conditions of the assay.

Discussion

At the time of preparation of this chapter, 21,722 MCPs have been annotated among genomes in the MiST2 database [53]. However, very few have been characterized and their specificity studied biochemically. The chemotaxis sensory repertoire of most microorganisms and the environmental cues motile organisms may respond to thus remain to be established. Data obtained in the present study argue that the Tlp2 chemoreceptor of *A. brasilense*, which has

homologs in soil or sediment-dwelling motile alphaproteobacteria, is expressed in an NtrC-dependent manner in *A. brasilense*. NtrC is a transcriptional regulator shown to be involved in nitrate utilization as a nitrogen source in *A. brasilense* [54, 55]. Consistent with being part of the NtrC regulon, Tlp2 was expressed the most under conditions of low aeration and in the absence of nitrogen or with nitrate, instead of high concentration of ammonium, as the nitrogen source. Interestingly, the pattern of a Tlp2-YFP localization at the cell poles is similar to the localization pattern of other chemoreceptors in Bacteria and Archaea [14, 56] and it also paralleled the pattern of expression, suggesting that Tlp2 contributes most to chemotaxis signaling clusters under these conditions of high expression. Indeed, our data show that Tlp2 contributed to chemotaxis toward nitrate. Thus the contribution of Tlp2 to the chemotaxis behavior of cells correlated with its expression and localization pattern, suggesting that Tlp2 participation in the sensory ability of cells varies in response to growth conditions. A similar observation was made when analyzing the subcellular localization of the energy taxis receptor AerC in *A. brasilense* [14, 25]. Remolding of chemoreceptor clusters under different growth conditions has also been shown in other bacteria [57, 58] but how these changes may affect chemotaxis has not. In *A. brasilense* chemotaxis, variations in the expression level of particular chemoreceptors (Tlp2 or AerC) with growth conditions may represent a strategy to effectively couple chemosensing with metabolism.

Here, we show that Tlp2 sensory specificity is toward nitrate with conserved arginine residues (R76, R139 and R159) within the N-terminal sensory domains being critical for this function. The sensory specificity of Tlp2 was further supported by demonstrating that the purified ligand binding domain of Tlp2 bound nitrate reversibly and with high affinity (~ 450 nM), *in vitro*. The analyte chlorate which is structurally similar to nitrate and used to mimic nitrate [59] also had a relatively high affinity (7.5μM) for $Tlp2^{LBD}$, suggesting the existence of a binding site for nitrate/chlorate within the sensory domain of Tlp2. Interestingly, $Tlp2^{LBD}$ also tightly bound the

positively charged analyte ammonium and the neutral compound urea. Despite these *in vitro* results, we failed to identify any chemotaxis defect of cells lacking functional Tlp2 toward ammonium or urea. On the other hand, we detected an effect of low ammonium concentrations, similar to that of nitrate, on the ability of cells to flocculate, under conditions of high aerations. Flocculation depends first on the ability of cells to clump with the extent of clumping being correlated with changes dependent upon motility and chemotaxis [29, Bible, Russell, and Alexandre accepted]. Thus, Tlp2 contribution to flocculation could be expected through an effect on the extent of clumping, prior to flocculation, similar to other chemotaxis mutants characterized in this respect [Bible, Russell, and Alexandre accepted]. High aeration conditions are detrimental to the microaerophilic metabolism of *A. brasilense* [49]. Under flocculation conditions, nitrogen sources are also limiting but cells are unlikely to be able to initially fix nitrogen unless they are completely flocculated to limit the inhibitory effect of oxygen diffusion inside cells that would express the nitrogenase enzyme. Thus flocculation conditions represent conditions of metabolic stress to these cells, an assumption in agreement with other findings [60]. While Tlp2 is expressed under flocculation conditions, the metabolism of the cells is likely to be different from that of cells experiencing a gradient in a soft agar plate assay where cells could navigate the gradient at preferred lower oxygen concentrations within the plate. Taken together these data suggest that while Tlp2 senses nitrate under apparently all growth conditions, it is also able to sense ammonium, but only under certain growth conditions.

How could these distinct cues be sensed by the same sensory domain? One possibility for $Tlp2^{LBD}$ having specificity for multiple ligands, would be for these ligands to bind at different sites within the binding site(s) or with some ligand binding to periplasmic proteins that themselves interact with Tlp2. The difference in charge between nitrate and ammonium suggests these bind at different sites within the periplasmic sensory domain. Several chemotaxis receptors

were shown to detect ligands via periplasmic proteins in addition to sensing ligands directly [61-63]. The effect of expressing Tlp2 variants in which conserved arginine residues are mutated and analyzed in the flocculation assay provides some support to this assumption. Indeed, while Arg139 was essential for the cells to respond to low nitrate concentrations in the flocculation assay, it was dispensable for sensing ammonium. In contrast, Arg76 and Arg159 were dispensable for nitrate sensing but important for ammonium sensing in this assay. Both Arg76 and Arg159 are located 3 residues down from negatively charged aspartate, suggesting potential salt bridge interactions. In support of this hypothesis, recent literature describes MCP specificity for multiple ligands with *Pseudomonas putida* McpS recognizing 6 different TCA intermediates and butyrate [64]. However, the ligand binding region of McpS is considerably larger [64] and belonging to another size cluster (251 aa vs. 154 aa for Tlp2) [65]. The binding curves of nitrate and ammonium display different levels of saturation ($\Delta F_{Obs} = 10$ for ammonium and $\Delta F_{Obs} = 30$ for nitrate). It is conceivable that different binding sites would have different net changes in the tyrosine fluorescence observed. Testing ammonium nitrate binding had an intermediate level of saturation ($\Delta F_{Obs} \approx 20$) suggesting a net change in fluorescence upon both ions binding. The measured affinity of $Tlp2^{LBD}$ for nitrate, and ammonium as well as the apparent reversibility of the binding event is consistent with the characteristic binding of ligands to chemoreceptors and the ligand binding affinity falls within the range of that reported for other characterized chemoreceptors, i.e. between 1-50μM [19, 66, 67]. Given that the conditions of growth appears to affect the ability of cells to sense ammonium, it is likely that sensing of nitrate and/or ammonium under flocculation conditions may depend on other proteins that would be expressed specifically under these conditions. The fact that the Tlp2 variants also seem to have somewhat different effects on the ability of cells to sense nitrate under conditions of the soft agar assay and the flocculation assay lends further support to this hypothesis.

There are few reported nitrate or nitrogenous compound sensors described in the literature and the one that has been best characterized is the ligand binding domain of NarX, which is a sensor histidine kinase that regulates *Escherichia coli* gene expression in response to nitrate [68]. The ligand binding domain of Tlp2 is larger than that of NarX (152 residues versus 114 in NarX) and does not appear to share any homology with NarX. Furthermore, the binding affinity of NarX for nitrate is 35μM which is weaker compared to the apparent binding affinity of Tlp2 for nitrate. These observations are consistent with independent evolution of these sensory domains.

Coupling chemosensing and metabolism is an effective strategy to allow cells to remain responsive and competitive under changing environmental and metabolic growth conditions. The expression pattern of Tlp2 is consistent with its function in sensing nitrogen sources.Tlp2 is expressed when cells do not have any available preferred nitrogen source in high concentration and Tlp2 might afford cells the ability to seek nitrogen nutrients under these conditions. *A. brasilense* is a diazoptroph but nitrogen fixation is energetically costly and it is likely that cells will induce the nitrogenase, only when no other nitrogen source suitable for growth could be detected and used by the cells. The data presented here demonstrate that a chemotaxis receptor, Tlp2 contributes to sensing of nitrate under all growth conditions and suggest that its sensory contribution to the cells' behavior vary with the growth conditions, revealing an additional level of diversity and flexibility of the chemosensing machinery.

Acknowledgments:

The authors thank Rose Goodchild (University of Tennessee, Knoxville) for the gift of the anti-GFP antibody. The authors also wish to thank Amber Bible for comments on the manuscript as well as the following past members of the laboratory: Bonnie Stephens, Star Loar (for making initial mutant construction), Andrew Stafford (for analysis of Tlp2-YFP localization by

fluorescent microscopy), and Joseph Gooch (for plant colonization assays). This work was supported by a NSF CAREER award (MCB-0622277) and MCB-0919819 to G.A.

List of REFERENCES

1. Koretke, K.K., et al., *Evolution of two-component signal transduction.* Molecular Biology and Evolution, 2000. **17**(12): p. 1956-1970.

2. Wuichet, K., B.J. Cantwell, and I.B. Zhulin, *Evolution and phyletic distribution of two-component signal transduction systems.* Current Opinion in Microbiology, 2010. **13**(2): p. 219-25.

3. Hoch, J.A., *Two-component and phosphorelay signal transduction.* Current Opinion in Microbiology, 2000. **3**(2): p. 165-170.

4. Belas, R., I.B. Zhulin, and Z. Yang, *Bacterial signaling and motility: sure bets.* J Bacteriol, 2008. **190**(6): p. 1849-56.

5. Mitchell, J.G. and K. Kogure, *Bacterial motility: links to the environment and a driving force for microbial physics.* Fems Microbiology Ecology, 2006. **55**(1): p. 3-16.

6. Overmann, J., *Chemotaxis and behavioral physiology of not-yet-cultivated microbes*, in *Environmental Microbiology*2005. p. 133-+.

7. DiLuzio, W.R., et al., *Escherichia coli swim on the right-hand side.* Nature, 2005. **435**(7046): p. 1271-1274.

8. Berg, H.C., *Motile behavior of bacteria.* Physics Today, 2000. **53**(1): p. 24-29.

9. Bren, A. and M. Eisenbach, *Changing the direction of flagellar rotation in bacteria by modulating the ratio between the rotational states of the switch protein FliM.* Journal of Molecular Biology, 2001. **312**(4): p. 699-709.

10. Szurmant, L. and G.W. Ordal, *Diversity in chemotaxis mechanisms among the bacteria and archaea.* Microbiology and Molecular Biology Reviews, 2004. **68**(2): p. 301-+.

11. Wadhams, G.H. and J.P. Armitage, *Making sense of it all: Bacterial chemotaxis.* Nature Reviews Molecular Cell Biology, 2004. **5**(12): p. 1024-1037.

12. Ames, P., et al., *Collaborative signaling by mixed chemoreceptor teams in Escherichia coli.* Proceedings of the National Academy of Sciences of the United States of America, 2002. **99**(10): p. 7060-7065.

13. Briegel, A., et al., *Universal architecture of bacterial chemoreceptor arrays.* Proceedings of the National Academy of Sciences of the United States of America, 2009. **106**(40): p. 17181-17186.

14. Gestwicki, J.E., et al., *Evolutionary conservation of methyl-accepting chemotaxis protein location in Bacteria and Archaea.* Journal of Bacteriology, 2000. **182**(22): p. 6499-6502.

15. Studdert, C.A. and J.S. Parkinson, *Crosslinking snapshots of bacterial chemoreceptor squads.* Proceedings of the National Academy of Sciences of the United States of America, 2004. **101**(7): p. 2117-2122.

16. Hazelbauer, G.L., J.J. Falke, and J.S. Parkinson, *Bacterial chemoreceptors: high-performance signaling in networked arrays.* Trends in Biochemical Sciences, 2008. **33**(1): p. 9-19.

17. Hazelbauer, G.L. and W.C. Lai, *Bacterial chemoreceptors: providing enhanced features to two-component signaling.* Current Opinion in Microbiology, 2010. **13**(2): p. 124-132.

18. Long, D.G. and R.M. Weis, *OLIGOMERIZATION OF THE CYTOPLASMIC FRAGMENT FROM THE ASPARTATE RECEPTOR OF ESCHERICHIA-COLI.* Biochemistry, 1992. **31**(41): p. 9904-9911.

19. Milligan, D.L. and D.E. Koshland, *Purification and characterization of the periplasmic domain of the aspartate chemoreceptor.* Journal of Biological Chemistry, 1993. **268**(27): p. 19991-19997.

20. Zhulin, I.B., *The superfamily of chemotaxis transducers: from physiology to genomics and back.* Adv Microb Physiol, 2001. **45**: p. 157-98.

21. Lacal, J., et al., *Sensing of environmental signals: classification of chemoreceptors according to the size of their ligand binding regions.* Environmental Microbiology, 2010. **12**(11): p. 2873-2884.

22. Alexandre, G., *Coupling metabolism and chemotaxis-dependent behaviours by energy taxis receptors.* Microbiology-Sgm, 2010. **156**: p. 2283-2293.

23. Greer-Phillips, S.E., B.B. Stephens, and G. Alexandre, *An energy taxis transducer promotes root colonization by Azospirillum brasilense.* Journal of Bacteriology, 2004. **186**(19): p. 6595-6604.

24. Alexandre, G., S.E. Greer, and I.B. Zhulin, *Energy taxis is the dominant behavior in Azospirillum brasilense.* J Bacteriol, 2000. **182**(21): p. 6042-8.

25. Xie, Z., et al., *PAS domain containing chemoreceptor couples dynamic changes in metabolism with chemotaxis.* Proc Natl Acad Sci U S A, 2010. **107**(5): p. 2235-40.

26. Hauwaerts, D., et al., *A major chemotaxis gene cluster in Azospirillum brasilense and relationships between chemotaxis operons in alpha-proteobacteria.* FEMS Microbiol Lett, 2002. **208**(1): p. 61-7.

27. vandeBroek, A., V. Keijers, and J. Vanderleyden, *Effect of oxygen on the free-living nitrogen fixation activity and expression of the Azospirillum brasilense NifH gene in various plant-associated diazotrophs.* Symbiosis, 1996. **21**(1): p. 25-40.

28. Wisniewski-Dye, F., et al., *Azospirillum genomes reveal transition of bacteria from aquatic to terrestrial environments.* PLoS Genet, 2011. **7**(12): p. e1002430.

29. Bible, A.N., et al., *Function of a chemotaxis-like signal transduction pathway in modulating motility, cell clumping, and cell length in the alphaproteobacterium Azospirillum brasilense.* Journal of Bacteriology, 2008. **190**(19): p. 6365-6375.

30. Edwards, A.N., et al., *Characterization of cell surface and extracellular matrix remodeling of Azospirillum brasilense chemotaxis-like 1 signal transduction pathway mutants by atomic force microscopy.* Fems Microbiology Letters, 2011. **314**(2): p. 131-9.

31. Vanstockem, M., et al., *TRANSPOSON MUTAGENESIS OF AZOSPIRILLUM-BRASILENSE AND AZOSPIRILLUM-LIPOFERUM - PHYSICAL ANALYSIS OF TN5 AND TN5-MOB INSERTION MUTANTS.* Applied and Environmental Microbiology, 1987. **53**(2): p. 410-415.

32. Zhulin, I.B., et al., *Oxygen taxis and proton motive force in Azospirillum brasilense.* J Bacteriol, 1996. **178**(17): p. 5199-204.

33. Marx, C.J. and M.E. Lidstrom, *Broad-host-range cre-lox system for antibiotic marker recycling in Gram-negative bacteria.* Biotechniques, 2002. **33**(5): p. 1062-1067.

34. Simon, R., U. Priefer, and A. Puhler, *A Broad Host Range Mobilization System for Invivo Genetic-Engineering - Transposon Mutagenesis in Gram-Negative Bacteria.* Bio-Technology, 1983. **1**(9): p. 784-791.

35. Figurski, D.H. and D.R. Helinski, *Replication of an origin-containing derivative of plasmid RK2 dependent on a plasmid function provided in trans.* Proc Natl Acad Sci U S A, 1979. **76**(4): p. 1648-52.

36. Keen, N.T., et al., *Improved Broad-Host-Range Plasmids for DNA Cloning in Gram-Negative Bacteria.* Gene, 1988. **70**(1): p. 191-197.

37. Reeve, W.G., et al., *Constructs for insertional mutagenesis, transcriptional signal localization and gene regulation studies in root nodule and other bacteria.* Microbiology-Uk, 1999. **145**: p. 1307-1316.

38. Jefferson, R.A., T.A. Kavanagh, and M.W. Bevan, *GUS fusions: beta-glucuronidase as a sensitive and versatile gene fusion marker in higher plants.* EMBO J, 1987. **6**(13): p. 3901-7.

39. Hallez, R., et al., *Gateway-based destination vectors for functional analyses of bacterial ORFeomes: Application to the min system in Brucella abortus.* Applied and Environmental Microbiology, 2007. **73**(4): p. 1375-1379.

40. Bradford, M.M., *Rapid and Sensitive Method for Quantitation of Microgram Quantities of Protein Utilizing Principle of Protein-Dye Binding.* Analytical Biochemistry, 1976. **72**(1-2): p. 248-254.

41. Altschul, S.F., et al., *Gapped BLAST and PSI-BLAST: a new generation of protein database search programs.* Nucleic Acids Res, 1997. **25**(17): p. 3389-402.

42. Letunic, I., et al., *SMART 5: domains in the context of genomes and networks.* Nucleic Acids Res, 2006. **34**(Database issue): p. D257-60.

43. Thompson, J.D., et al., *The CLUSTAL_X windows interface: flexible strategies for multiple sequence alignment aided by quality analysis tools.* Nucleic Acids Res, 1997. **25**(24): p. 4876-82.

44. Larkin, M.A., et al., *Clustal W and Clustal X version 2.0.* Bioinformatics, 2007. **23**(21): p. 2947-8.

45. Guindon, S. and O. Gascuel, *A simple, fast, and accurate algorithm to estimate large phylogenies by maximum likelihood.* Syst Biol, 2003. **52**(5): p. 696-704.

46. Perrière, G. and M. Gouy, *WWW-query: An on-line retrieval system for biological sequence banks.* Biochimie, 1996. **78**(5): p. 364-369.

47. Alexander, R.P. and I.B. Zhulin, *Evolutionary genomics reveals conserved structural determinants of signaling and adaptation in microbial chemoreceptors.* Proc Natl Acad Sci U S A, 2007. **104**(8): p. 2885-90.

48. Xie, Z.H., et al., *PAS domain containing chemoreceptor couples dynamic changes in metabolism with chemotaxis.* Proceedings of the National Academy of Sciences of the United States of America, 2010. **107**(5): p. 2235-2240.

49. Zhang, Y., et al., *Regulation of nitrogen fixation in Azospirillum brasilense.* FEMS Microbiol Lett, 1997. **152**(2): p. 195-204.

50. Liang, Y.Y., F. Arsene, and C. Elmerich, *Characterization of the ntrBC genes of Azospirillum brasilense Sp7: their involvement in the regulation of nitrogenase synthesis and activity.* Mol Gen Genet, 1993. **240**(2): p. 188-96.

51. Milcamps, A., et al., *The Azospirillum brasilense rpoN gene is involved in nitrogen fixation, nitrate assimilation, ammonium uptake, and flagellar biosynthesis.* Can J Microbiol, 1996. **42**(5): p. 467-78.

52. Stephens, B.B., *Chemosensory Responses in Azospirillum brasilense*, 2006, Georgia State University: Atlanta.

53. Ulrich, L.E. and I.B. Zhulin, *The MiST2 database: a comprehensive genomics resource on microbial signal transduction.* Nucleic Acids Research, 2010. **38**: p. D401-D407.

54. Huergo, L.F., et al., *Regulation of glnB gene promoter expression in Azospirillum brasilense by the NtrC protein.* FEMS Microbiol Lett, 2003. **223**(1): p. 33-40.

55. Van Dommelen, A., et al., *(Methyl)ammonium transport in the nitrogen-fixing bacterium Azospirillum brasilense.* J Bacteriol, 1998. **180**(10): p. 2652-9.

56. Briegel, A., et al., *Universal architecture of bacterial chemoreceptor arrays.* Proc Natl Acad Sci U S A, 2009. **106**(40): p. 17181-6.

57. Guvener, Z.T., D.F. Tifrea, and C.S. Harwood, *Two different Pseudomonas aeruginosa chemosensory signal transduction complexes localize to cell poles and form and remould in stationary phase.* Mol Microbiol, 2006. **61**(1): p. 106-18.

58. Wadhams, G.H., et al., *Requirements for chemotaxis protein localization in Rhodobacter sphaeroides.* Mol Microbiol, 2005. **58**(3): p. 895-902.

59. Stewart, V. and C.H. Macgregor, *Nitrate Reductase in Escherichia-Coli K-12 - Involvement of Chlc, Chle, and Chlg Loci.* Journal of Bacteriology, 1982. **151**(2): p. 788-799.

60. Wasim, M., et al., *Alkyl hydroperoxide reductase has a role in oxidative stress resistance and in modulating changes in cell-surface properties in Azospirillum brasilense Sp245.* Microbiology, 2009. **155**(Pt 4): p. 1192-202.

61. Bjorkman, A.J., et al., *Probing Protein-Protein Interactions - the Ribose-Binding Protein in Bacterial Transport and Chemotaxis.* Journal of Biological Chemistry, 1994. **269**(48): p. 30206-30211.

62. Gardina, P.J., et al., *Maltose-binding protein interacts simultaneously and asymmetrically with both subunits of the Tar chemoreceptor.* Molecular Microbiology, 1997. **23**(6): p. 1181-1191.

63. Shilton, B.H., et al., *Conformational changes of three periplasmic receptors for bacterial chemotaxis and transport: The maltose-, glucose/galactose- and ribose-binding proteins.* Journal of Molecular Biology, 1996. **264**(2): p. 350-363.

64. Lacal, J., et al., *Physiologically relevant divalent cations modulate citrate recognition by the McpS chemoreceptor.* J Mol Recognit, 2011. **24**(2): p. 378-85.

65. Lacal, J., et al., *Sensing of environmental signals: classification of chemoreceptors according to the size of their ligand binding regions.* Environmental Microbiology, 2010. **12**(11): p. 2873-2884.

66. Danielson, M.A., et al., *Attractant-Induced and Disulfide-Induced Conformational-Changes in the Ligand-Binding Domain of the Chemotaxis Aspartate Receptor - a F-19 Nmr-Study*. Biochemistry, 1994. **33**(20): p. 6100-6109.

67. Hartley-Tassell, L.E., et al., *Identification and characterization of the aspartate chemosensory receptor of Campylobacter jejuni*. Molecular Microbiology, 2010. **75**(3): p. 710-730.

68. Cavicchioli, R., et al., *The NarX and NarQ sensor-transmitter proteins of Escherichia coli each require two conserved histidines for nitrate-dependent signal transduction to NarL*. J Bacteriol, 1995. **177**(9): p. 2416-24.

Chapter 3

The *Azospirillum brasilense* Che1 chemotaxis pathway controls the swimming velocity which affects transient cell-to-cell clumping

The following chapter is a manuscript recently accepted for publication in the Journal of Bacteriology by Amber Bible, Matthew H. Russell and Gladys Alexandre

Author Contributions

GA designed and led the experimental project. AB and MH conducted molecular genetics experiments (mutant construction and complementation), microscopy experiments, and behavioral assays, including aerotaxis and analyzed the data. GA designed the experiments, analyzed the data and wrote the paper.

Abstract

The Che1 chemotaxis-like pathway of *Azospirillum brasilense* contributes to chemotaxis and aerotaxis, and it has also been found to contribute to regulating changes in cell surface adhesive properties that affect the propensity of cells to clump and to flocculate. The exact contribution of Che1 to the control of chemotaxis and flocculation in *A. brasilense* remains poorly understood. Here, we show that Che1 affects reversible cell-to-cell clumping, a cellular behavior in which motile cells transiently interact by adhering to one another at their non-flagellated pole before swimming apart. Clumping precedes and is required for flocculation and both processes appear independently regulated. The phenotypes of an *ΔaerC* receptor mutant and of mutant strains lacking *cheA1*, *cheY1*, *cheB1*, *cheR1* (alone or in combination) or deleted for che1 show that Che1 directly mediates changes in the flagellar swimming velocity and that this behavior directly modulates the transient nature of clumping. Our results also suggest that additional receptor(s) and signaling pathway(s) are implicated in mediating other Che1-independent changes in clumping identified in the present study. Transient clumping precedes the transition to stable

clump formation, which involves the production of specific extracellular polysaccharide (EPS); however, production of these clumping-specific EPS is not directly controlled by Che1 activity. Che1-dependent clumping may antagonize motility and prevent chemotaxis, thereby maintaining cells in a metabolically favorable niche.

Introduction

The ability of bacteria to sense and adapt to changes within their environment is an essential survival strategy. At the molecular level, signal transduction pathways couple sensing of environmental changes with adaptive responses which includes modulation of gene expression, enzyme activities or protein-protein interactions [1].

Chemotaxis in *Escherichia coli* is considered the best studied signal transduction pathway. The *E. coli* chemotaxis signal transduction pathway functions to control the probability of changes in the flagellar motility pattern in response to physicochemical cues detected by dedicated chemotaxis receptors. These receptors form ternary signaling complexes with cytoplasmic chemotaxis proteins that include a histidine kinase, CheA, and an adaptor protein, CheW. Following repellent signal reception, CheA becomes autophosphorylated at a conserved histidine residue and phosphorylates its cognate response regulator, CheY. Phosphorylated CheY controls the probability of changes in the direction of flagellar rotation. The signaling activity of chemoreceptors is modulated by antagonistic activities of the methyltransferase CheR and the methylesterase CheB, thus allowing sensory adaptation. CheR constitutively adds methyl groups to specific glutamate residues in the C-terminal signaling region of receptors, while CheB esterase activity depends on phosphorylated CheA. CheA is thus the central regulator of the chemotaxis response as it links the forward excitation pathway that triggers the CheY-dependent signaling output with the feedback adaptive loop dependent on CheB activity [1, 2]. This prototypical chemotaxis signal transduction pathway is conserved in closely and distantly related bacterial species [3]. Emerging evidence from the analysis of completely sequenced genomes indicates that most bacterial species possess more than one chemotaxis signal transduction pathway [4, 5]. Additional chemotaxis-like signal transduction pathways (also named

chemosensory signal transduction pathways) have been shown to be implicated in the regulation of non-motility behaviors [6].

Azospirillum brasilense is an alphaproteobacterium and diazotrophic motile microorganism found in soil and rhizosphere habitats. *A. brasilense* have an oxidative metabolism that is optimum under microaerophilic conditions, with maximum energy generated at about 0.4% dissolved oxygen [7]. Motile cells actively seek low oxygen concentrations for optimum metabolism by aerotaxis as well as by monitoring changes in the metabolic status via energy taxis [8, 9]. Energy taxis is mediated by dedicated energy sensing receptors that allow *A. brasilense* to locate environments that are optimum for growth [7, 9, 10]. Monitoring fluctuations in intracellular energy levels is the preeminent mode of sensing in *A. brasilense* [9], suggesting that in this organism, adaptive cellular behaviors such as aerotaxis, are tightly coupled with metabolism.

The *A. brasilense* Che1 chemotaxis signal transduction pathway comprises homologs of CheA, CheW, CheY, CheB and CheR that mediate energy taxis responses. Despite similarity to prototypical chemotaxis pathways, the *A. brasilense* Che1 pathway has been shown to be functionally divergent in that it appears to regulate taxis behaviors, as well as other cellular functions, including cell-to-cell clumping and flocculation [11]. Experimental evidence indicates that *che1* pathway mutants display changes in cell surface adhesive properties, likely in the structure and/or composition of EPS, that ultimately modulate the ability of cells to clump and to flocculate [11-15]. Furthermore, the contribution of Che1 to the control of motility-dependent taxis responses seems to be more complex than those in other bacterial species, perhaps involving additional chemotaxis signal transduction pathways and/or auxiliary chemotaxis proteins [14, 16, 17]. The Che1 pathway was also shown to indirectly affect changes in the swimming direction of cells, and thus the motility bias [16, 17]. Prior biochemical and genetic evidence have suggested that CheB1 and CheR1 from the Che1 pathway participate in signaling cross-talk with other

chemotaxis pathway(s) by altering the methylation status of chemoreceptors [14]. In support of this possibility, the genome of *A. brasilense* encodes for three chemotaxis-like signal transduction pathways, in addition to Che1, as well as several ancillary chemotaxis proteins [17]. The functions of these chemotaxis-like pathways and proteins have not been determined.

In *A. brasilense*, flocculation results from the differentiation of motile, rod-shaped cells into aggregates of non-motile, spherical cells that are encased in a dense fibrillar polysaccharide material (flocs) visible to the naked eye [18]. Flocculated cells are not dormant, but are highly resistant to various environmental insults [18]. To date, the only known regulator affecting this differentiation process is an orphan transcriptional regulator, named FlcA, for which no cognate sensor kinase has been identified [19-21]. Che1 signaling output might mediate changes in EPS production by directly affecting transcription of putative EPS biosynthetic genes. However, evidence for this hypothesis or in support of a genetic link between Che1 effects on taxis responses and on cell surface adhesive properties is lacking. In addition, the link between Che1 function and flocculation (and FlcA) remains uninvestigated.

In this study, we clarify the role of Che1 in flocculation. By characterizing a set of *che1* mutant strains and an energy taxis receptor mutant, we provide evidence that Che1 modulates reversible cell-to-cell interactions between motile cells, that we call "clumping". We also show that Che1 does not directly regulate changes in EPS production. Interestingly, we found that the mechanism by which Che1 affects clumping behavior is by modulating the swimming velocity of cells. The role for Che1 in modulating transient cell-to-cell clumping via direct regulation of the swimming velocity provides insight into how this chemotaxis pathway may function to coordinate taxis behaviors with reversible cell-to-cell interactions in clumping.

Experimental Procedures

Bacterial Strains and Growth Conditions

The strains and plasmids are described (Table 3.1). Cells were grown at 28ºC with shaking in rich TY (1 liter contains 10 grams Tryptone and 5 grams Yeast extract) media or MMAB (minimal media) [22]. In order to induce clumping behavior and flocculation, 100 µl of an overnight culture of cells grown in TY media (OD_{600nm} = 1) was used to inoculate 5 ml of flocculation media (MMAB containing 0.5 mM Sodium Nitrate as sole nitrogen source and 8 mM Fructose as sole carbon source) and then grown with shaking at 28ºC. For the time course of clumping and flocculation, cells were inoculated into flocculation media and grown with high aeration and vigorous shaking (225 rpm). Aliquots of cultures were observed microscopically at the time of inoculation, 3 hours post-inoculation (hpi), 6 hpi, 9 hpi, 14 hpi, and 24-30 hpi (time at which wild type cells are flocculated). The times (along with standard deviations) indicated in Table 2 were determined from multiple independent experiments (n = 5). Cells were visualized using a Nikon Eclipse E200 phase-contrast microscope at a final magnification of 400X and photographs were taken of at least three different fields-of-view per sample per time point during this time course using a Nikon Coolpix P5000 camera. Digital videos were captured using a Sony Hyper HAD high resolution black and white camera at 400X (final) magnification and

Table 3.1: Strains and plasmids used in this study

Strain or plasmid	Genotype, relevant characteristics	Reference or Source
Plasmids		
pBBR1MCS3	Cloning vector (Tc)	16
pRK415	Cloning vector (Tc)	14
pBBR-*cheA1*	pBBR1MCS3 containing *cheA1*	4
pBBR-$cheA1_{H252Q}$	pBBR1MCS3 containing $cheA1_{H252Q}$	this work
pBBR-*cheB1*	pBBR1MCS3 containing *cheB1*	this work
pBBR-$cheB1_{D78N}$	pBBR1MCS3 containing $cheB1_{D78N}$	this work
pRK-*cheY1*	pRK415 containing *cheY1*	4
pRK-$cheY1_{D52N}$	pRK415 containing $cheY1_{D52N}$	this work
Strains		
Escherichia coli		
TOP10	General cloning strain	Invitrogen
S17-1	*thi endA recA hsdR* with RP4-2Tc::Mu-Km::Tn7 integrated in chromosome	26
Azospirillum brasilense		
Sp7	Parental strain, “wild type”	ATCC29145
AB101	Δ(*cheA1*)::*gusA-Km* (Km)	4
GA3	Δ(*cheB1*)::*gusA-Km* (Km)	29
BS109	Δ(*cheR1*)::*Gm* (Gm)	29
BS104	Δ(*cheB1cheR1*)::*Km* (Km)	29
AB102	Δ(*cheY1*)::*Km* (Km)	4
AB103	Δ(*cheA1-cheR1*)::*Cm* (Cm), also named Δ*che1*	4
AB301	Δ*aerC*::*Km* (Km)	37
AB302	Δ(*cheA1-cheR1*) Δ(*aerC*)::*Km* (Cm, Km), also named Δ*che1* Δ*aerC*	this work
Sp72002	*flcA*::Tn5 (Km)	22
AB104	Δ(*cheA1-cheR1*), *flcA*::Tn5 (Cm, Km)	this work
Wild type(pRK415)	Wild type strain (Sp7) containing pRK415 (Tc)	4
Wild type(pBBR)	Wild type strain (Sp7) containing pBBR1MCS3 (Tc)	4
AB10 (pBBR)	AB101 containing pBBR1MCS3 (Tc)	4
AB101(pBBR-*cheA1*)	AB101 containing pBBR-*cheA1* (Tc)	4
AB101(pBBR-$cheA1_{H252Q}$)	AB101 containing pBBR-$cheA1_{H252Q}$ (Tc)	this work
GA3 (pBBR)	GA3 containing pBBR	this work
GA3 (pBBR-*cheB1*)	GA3 containing pBBR-*cheB1*	this work
GA3 (pBBR-$cheB1_{D78N}$)	GA3 containing pBBR-$cheB1_{D78N}$	this work
AB102 (pRK415)	AB102 containing pRK415	4
AB102 (pRK-*cheY1*)	AB102 containing pRK-*cheY1*	4
AB102 (pRK-$cheY1_{D52N}$)	AB102 containing pRK-$cheY1_{D52N}$	this work

Antibiotic resistance abbreviations: Tc (tetracycline), Km (kanamycin), Gm (gentamycin), Cm (chloramphenicol)

cover slips were added to enhance clarity. Timing of clumping and flocculation, as well as the accompanying behavioral and morphological changes observed were highly reproducible.

Construction of (Δche1-flcA::Tn5) (AB104) mutant and of a ΔaerCΔche1 (AB302) mutant

The Δ*che1-flcA* double mutant strain was generated using the previously described pKGmobGARCm construct, previously used to generate Δ*che1* [16]. A biparental mating with the *flcA*::Tn5 (Sp72002) mutant strain as a recipient was performed as previously described [14] to construct the double mutant. Candidate Δ*che1-flcA* (AB104) mutants were verified using PCR. The same technique was used to introduce a *che1* mutation in the previously constructed Δ*aerC* (AB301) mutant background [23] and generate the □*aerC*□*che1* strain AB302.

Complementation and site-specific mutations of Che1 genes

Generation of constructs for complementation of Δ*cheA1* (AB101) was performed previously [16]. The site-specific mutant, $cheA1_{H252Q}$, was generated previously (unpublished data) using the QuikChangeII Site-directed Mutagenesis Kit (Stratagene). The following primers were used to generate $cheA1_{H252Q}$: forward primer, 5'-CATCTTCCGTCTGGTGCAGACCATCAAGGG CACC-3' and reverse primer, 5'-GGTGCCCTTGATGGTCTGCACCAGACGGAAGATG-3' [underlined letter refers to the specific base which was mutated to change CAC (codon for histidine) to CAG (codon for glutamine)]. The $cheA1_{H252Q}$ was then cloned into pProEx-HTA (yielding pIZ105). In order to generate pBBR-$cheA1_{H252Q}$ expressed from its own promoter in the pBBR-MCS3 vector , the promoter region of the *che1* operon, found upstream of *cheA1*, was first amplify from pBBR-*cheA1* (4) using cheA1promXho-F (5'-CCGCTCGAGCAGCGCGATGAACTGGTT-3' with the XhoI restriction site underlined) and cheA1HQup-R (5'-AAGCTTACGGACCAGTTCCAC-3' with the HindIII restriction site

underlined). Next, primers cheA1HQdown-F (5'-AAGCTTCTGGAGCAGAATCCC-3' with the HindIII restriction site underlined) and cheA1fullXba-R (5'-GCTCTAGATCATGCGGCACCTTTCTGC-3' with the XbaI restriction site underlined) were used to amplify $cheA1_{H252Q}$ from pIZ105. Each PCR fragment was icloned into the pCR2.1 TOPO vector and sequenced prior to cloning into pBBR-MCS3 [24]. These fragments were inserted into the pBBR-MCS3 vector using the following digestions: cheA1HQup (XhoI and HindIII), cheA1 HQ down (HindIII and XbaI), pBBR-MCS3 (XhoI and XbaI). The final product fuses the upstream region of cheA1 containing the putative promoter with $cheA1_{H252Q}$ in pBBR-MCS3. The final construct was introduced into wild type *A. brasilense* Sp7 and Δ*cheA1* (AB101) strain using biparental mating as described previously [14].

Constructs for complementation of Δ*cheY1* (AB102) were also generated previously [11]. The site-specific mutant, $cheY1_{D52N}$, was generated by amplifying $cheY1_{D52N}$ from pIZ103 [25], using the primers used to amplify *cheY1* for complementation (4), and sub-cloning into the pCR2.1 TOPO vector. Upon verification by sequencing, $cheY1_{D52N}$ was isolated from this vector using restriction digestion with HindIII and EcoRI, and ligated into pRK415 digested with the same enzymes (14). The newly constructed pRK-$cheY1_{D52N}$ was introduced into the wild type Sp7 strain and the Δ*cheY1* mutant strain by biparental mating as described previously [14].

Complementation of the Δ*cheB1* mutant was performed by amplifying the *cheB1* gene from genomic DNA using the primers cheB1R1forward (5'-CCCAAGCTTTA**AGGAGA**GGCCCGTATGTCCGATGGTTTCGGCAGAC-3' with the HindIII site underlined and the ribosome binding site in bold) (4) and cheB1reverse (5'-GGGCTCGAGTCATGCTGCCCTCGATGCGAAC -3' with the XbaI site underlined). The amplified *cheB1* gene was sub-cloned into pCR2.1 TOPO and verified by sequencing. The *cheB1* gene was isolated by digestion with HindIII and XhoI, and ligated into pBBR-MCS3 digetsed

with the same enzymes [24]. The newly constructed pBBR-*cheB1* was introduced into the wild type Sp7 strain and Δ*cheB1* (GA3) strain by biparental mating.

The site-specific mutant, $cheB1_{D78N}$, was generated using the QuikChangeII Site-directed Mutagenesis Kit (Stratagene) according to the manufacturer's instructions using mutagenic primers CheBDN-F (5'-GACGTCATCGTTCTCAACATCGAGATGCCGGTG-3') and CheBDN-R (5'-CACCGGCATCTCGATGTTGAGAACGATGACGTC-3') (underlined letter refers to the specific base which was mutated to change GAC (codon for aspartic acid) to AAC (codon for asparagine)) using *cheB1* subcloned into pCR 2.1 TOPO as a template using cheB1R1forward and cheB1reverse (see above). The fragment generated ($cheB1_{D78N}$) was cloned into pCR2.1 TOPO and the presence of the correct mutation was verified by sequencing of the entire open reading frame in both directions. In order to generate pBBR-$cheB1_{D78N}$, HindIII and XhoI were used to isolate $cheB1_{D78N}$ before cloning it into pBBR-MCS3 [24] digested with the same enzymes. pBBR-$cheB1_{D78N}$, was introduced into wild type *A. brasilense* Sp7and Δ*cheB1* (GA3) using biparental mating as described previously [14].

Gas perfusion chamber assay for clumping and image analysis

A 10 µl drop of cells grown under high aeration in MMAB supplemented with 0.1% (w/v) NH_4Cl and 0.5% (w/v) sodium pyruvate to late log phase ($O.D._{600}$ ~ 0.7), first washed before being re-suspended in MMAB supplied with 10 mM pyruvate, was placed in a gas perfusion chamber in which the humidified gas flowing above the drop can be controlled [26]. First, compressed air (21% oxygen) is allowed to flow over the cell suspension until cells are equilibrated (usually 5 minutes) before recording of the cells' behavior begins. After one minute, a valve is switched to provide pure nitrogen to the atmosphere of the cell suspension (air removal). The cells remain motile under these conditions. After a period of 6 minutes, the nitrogen gas flowing into the

chamber is switched back to air (air addition) and recording is stopped after 3 minutes (10 minutes recorded total). Each experiment was performed at least 3 times on independent samples and the behavior of the cells was highly reproducible.

The fraction of clumps in the cell suspension was determined as the number of clumps (rather than cells within clumps) relative to free-swimming cells. These ratios were measured using digital movies and the Cell Counter plug-in from ImageJ (http://rsbweb.nih.gov/ij/). Briefly, the number of clumps were identified as transient cell-to-cell contacts between motile cells in suspension, and counted manually for a given video frame or image. A minimum of 2 video frames were analyzed for each time point and each video frame comprised at least 100 cells in the field of view. Clumping in videos was verified by analyzing the motion of cells in the field of view just prior to and after the frame because the motion analysis software could not always accurately distinguish between clumps and free-swimming cells. The number of free-swimming cells was also counted for a single field-of-view in the same video frame in order to determine the ratio of clumping cells to free-swimming cells. These measurements were repeated for at least two different fields-of-view per sample and per time point for each of the samples analyzed. The data shown are the average of these calculations. In the temporal assay in the gas perfusion chamber, the fractions of clumps were measured at given time points during the assay before and after air removal or addition. The determined ratios were then plotted over time using Microsoft Excel (Microsoft). The average swimming velocity of cells was determined on the same video files and frames described above, using computerized motion analysis (CellTrak 1.3, Santa Rosa, CA).

Extracellular complementation of clumping with extracted EPS

Extracellular polysaccharides (EPS) were extracted from 2-liter cultures of *A. brasilense* that were grown until clumping was observed. Samples of extracted EPS were used to treat 2 ml of wild type cells suspension grown under flocculation permissive conditions (but prior to clump formation), gently pelleted by centrifugation (2,500 x g for 2 minutes) and washed twice with 0.8% (w/v) sterile KCl in order to "remove" any EPS already present on the surface. We used this strategy because preliminary control experiments had shown that EPS present on the cell surface may mask the ability of exogenously added EPS to induce clumping. The cells were then re-suspended in 100 μl of flocculation medium (described above, under *Bacterial strains and growth conditions*) with 100 μl of extracted EPS (at a final concentration of 15 μg/ml), followed by 1-2 hours incubation at room temperature with shaking. A control was incubated with water alone. Treated cells were then visualized using light microscopy. Photographs and digital videos were of cells treated with extracted EPS (or water, as a control). The fraction of clumps was determined using both photographs and digital videos and manually counting the number of clumps (counting clumps rather than cells within clumps) relative to the total number of free-swimming cells in each field-of-view, with at least 3 distinct fields of view being analyzed per treatment and with counting a total of at least 100 cells per sample. The fold-increase in the clumping fraction was calculated relative to the control treated with water, which was taken as a reference and given the value of 1.00.

To test the effect of proteinase K treatment on the propensity of extracted EPS to mediate clumping, wild type *A. brasilense* cells were grown under flocculation conditions and collected at the onset of clumping. The cells were then concentrated by centrifugation at 2,500 x g for 2 minutes to a final volume of 100 μl. The control samples remained untreated. Test samples were treated using the following: 1) 100 μl of untreated wild type EPS and 2) 100 μl of Proteinase K-treated EPS. The EPS fraction was analyzed on a SDS-PAGE gel to verify the absence of protein

after treatment with proteinase K. Cells were incubated for approximately 3-4 hours at room temperature with shaking before visualization using light microscopy. The motility or viability of cells did not appear affected by these treatments.

Western Blotting

In order to verify expression of CheA1 and CheY1 in the complementation constructs, we grew overnight cultures for each strain, then collected and lysed the cells. For samples from CheA1 complementation constructs, 250 ml of actively growing cultures were collected and cells were lysed using sonication in a lysis buffer containing 50 mM KH_2PO_4, 2 mM $MgCl_2$, and 1 mM PMSF (phenylmethanesulfonylfluoride, a serine protease inhibitor). The lysate was then centrifuged for 5 minutes at 20,000 x g at 4°C and the supernatant was removed for analysis by SDS-PAGE. Protein concentrations were measured for each sample using the Bradford Assay [27] and each sample was adjusted to the same protein concentration. Next, a fresh solution of n-dodecyl-β-D-maltoside was added to each sample to a final concentration of 0.5% (w/v). Each sample was then boiled and analyzed using a 6% SDS-PAGE gel and an α-CheA1 antibody (against CheA1 from *A. brasilense*) at a 1:4,000 dilution with the HRP-tagged α-rabbit secondary antibody at a 1:10,000 dilution. For samples from CheY1 complementation constructs, 20 milliliters of an actively growing culture of cells were collected and lysed using sonication in phosphate-buffered saline (PBS). Each lysate was then centrifuged for 5 minutes at 20,000 x g at 4°C and the supernatant was removed for analysis by SDS-PAGE. Protein concentrations were measured for each sample using the Bradford Assay [27] and each sample was adjusted to the same protein concentration. Each sample was then boiled and analyzed using a 12% SDS-PAGE gel and an α-CheY1 antibody (against CheY1 from *A. brasilense*) at a 1:2,000 dilution and an HRP-tagged α-guinea pig secondary antibody at a 1:10,000 dilution. Analysis of CheB1

expression from the complementation constructs was not assessed due to the unavailability of an antibody against CheB1.

Results

Che1 affects clumping but not flocculation.

We have shown previously that mutants carrying deletions in *cheA1*, *cheB1*, *cheY1* and *che1* flocculate more than wild type cells [16]. We also found that a double mutant lacking both *cheB1* and *cheR1* flocculated very little, if at all [16]. These data suggested that the Che1 pathway directly regulates flocculation. To gain further insight into how the Che1 pathway regulates the amount of flocculation, we observed the behaviors of each strain during this process. Cells were inoculated into flocculation medium (low nitrogen and high aeration, see Materials and Methods) and the behaviors of the cells were analyzed at different times post inoculation (Figure 3.1). We found that the strains carrying mutations within *che1* not only differed in the amount of flocculation, but also in the timing at which they form flocs. In comparison to the wild type strain, the Δ*cheA1* mutant flocculated after 17 hours of growth in the flocculation medium, as opposed to 24-30 hours in the wild type (Figure 3.1). The Δ*cheB1* mutant flocculated the earliest, at 11 hours post-inoculation. The *ΔcheY1* mutant strain had an intermediate phenotype compared to what was observed for the Δ*cheA1* and the Δ*cheB1* mutant strain, in that it flocculated 14 hours post-inoculation. Deletion of the *che1* operon resulted in a strain (Δ*che1*) that flocculated slightly earlier than the wild type, at 19 hours. Consistent with previous

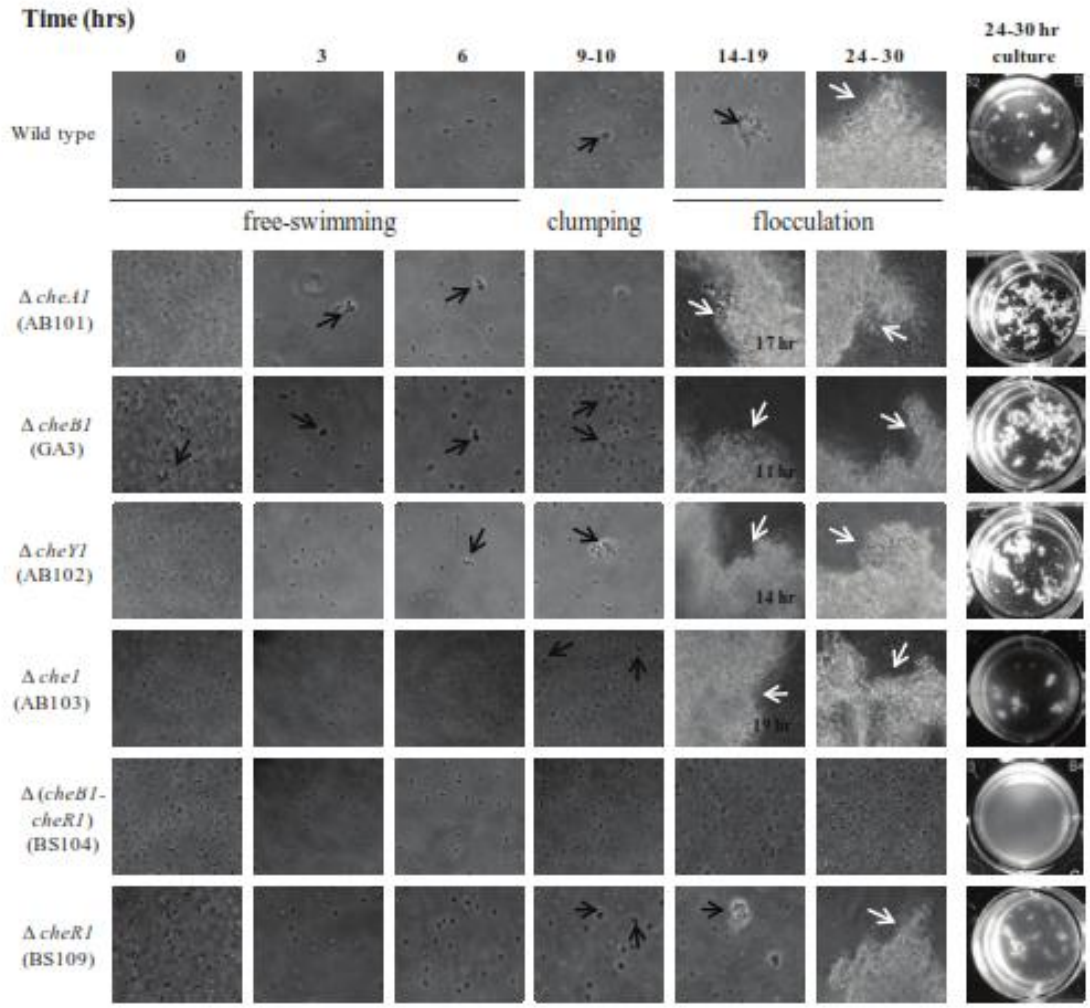

Figure 3.1: Time course of clumping and flocculation behaviors in wild type and *che1* mutant strains of *Azospirillum brasilense*. Cells grown under flocculation permissive conditions were analyzed by light microscopy and photographed at the indicated times post-inoculation into the flocculation medium. Black arrows indicate cells within clumps and white arrows indicate flocs. Times labeled in the 14 - 19 hour time frame indicate the time at which the strain formed visible flocs. (Right) Photographs of cultures at 24 - 30 hours post-inoculation are shown to illustrate flocculation (as seen as large aggregates) of the culture, if applicable. Data shown in this figure represent at least 5 independent experiments.

data [16], the Δ*cheB1cheR1* mutant did not flocculate [16]. Finally, the Δ*cheR1* mutant resembled the wild type, flocculating after 24-30 hours. Therefore, the *che1* mutant strains that flocculate more than the wild type, initiate flocculation earlier relative to the wild type strain.

Interestingly, when cells were grown under these conditions of flocculation, we observed that there was not only a difference in the amount and timing of flocculation between the strains, but there was also a difference in the amount and timing of clumping behavior. Free-swimming, wild type cells formed small, transient and highly dynamic "clumps" of two to five cells after approximately nine hours of incubation into the flocculation medium. These clumps consisted of cells that attached briefly (about 1 sec) at the cell poles before swimming apart. *A. brasilense* is motile by a single polar flagellum and cells in clumps appeared to adhere to one another at their non-flagellated pole: when clumping, the cells were seen rotating around the contact point between cells and the cell-to-cell contact did not hinder polar flagellum rotation. Approximately two to three hours later, the number of clumps in the culture increased. The nature of these clumps were different, too, in that clumps consisted of more motile cells (about 8-10cells per clump), and these clumps appeared more stable (most cells did not leave the clumps when observed over a period of 10minutes) in that some of the cells remained within the clumps without swimming away, while others were adherent only transiently (Figure 3.1). Starting around 15 hours post-inoculation, most cells appeared irreversibly attached to one another in larger clumps, and at about 18-19 hours post inoculation, larger aggregates comprised of non-motile, round-shaped cells ("mini-floc") were observed. Cells within "mini-flocs" appeared more refractile, suggesting that these cells contained intracellular polyhydroxybutyrate (PHB) granules (Figure 3.1), an assumption confirmed by Nile red staining (Data not shown). Over the next several hours, the mini-flocs continued to grow larger by aggregation until the culture consisted primarily of large flocs (24-30 hours post-inoculation) (Figure 3.1).

Table 3.2. Time course of clumping and flocculation in wild type and mutant derivatives of *A. brasilense*.

Strain	Initiation of transient clumping [a] (in hours[b])	Transition to stable clumping [c] (in hours[b])	Time to flocculation (in hours[b])
Sp7	9 ± 1	11 ± 1	24 ± 3
Δ*cheA1* (AB101)	2 ± 1	3 ± 2	17 ± 1
Δ*cheB1* (GA3)	2 ± 1	3 ± 2	11 ± 1
Δ*cheY1* (AB102)	6 ± 2	9 ± 1	14 ± 1
Δ*che1* (AB103)	9 ± 1	11 ± 1	19 ± 2
Δ*cheR1* (BS109)	9 ± 1	11 ± 1	24 ± 3
Δ(*cheB1cheR1*)(BS104)	no clumping	no clumping	no flocculation
flcA::Tn5 (Sp72002)	9 ± 1	11 ± 1	no flocculation
Δ*che1 flcA::Tn5* (AB104)	9 ± 1	13 ± 1	no flocculation
Δ*aerC* (AB301)	2 ± 1	3 ± 2	14 ± 1
Δ*aerC*Δ*che1* (AB302)	9 ± 1	11 ± 1	19 ± 2

Values represent the time (along with the standard deviation) in hours post-inoculation into flocculation media (n = 5).

[a] Time at which transient cell-to-cell clumping is first detected. The fraction of transient clumps increases over time.

[b] Time shown represents the hours post-inoculation into flocculation medium.

[c] Time at which stable cell-to-cell clumping is first detected. The fraction of stable clumps increases over time.

In comparison to the wild type, we observed that the Δ*cheA1* mutant began to form small, stable clumps after approximately three hours, much earlier than the wild type strain (Table 3.2). The *ΔcheB1* mutant showed clumping behavior resembling that of Δ*cheA1*. The Δ*cheY1* mutant formed clumps six hours post-inoculation, which was earlier than the wild type, but later than the Δ*cheA1* mutant. Clumps formed by the Δ*cheY1* mutant also appeared more transient initially than those produced by the Δ*cheA1* and Δ*cheB1* mutants. Clumping behavior was not observed in the Δ*cheB1cheR1* mutant, while the Δ*cheR1* mutant resembled the wild type. Differences in the timing of clumping behavior suggested that effects of Che1 on floccculation instead reflect an effect of Che1 on clumping.

Formation of clumps and flocs earlier than the wild type could explain why some Che1 mutants were shown previously to flocculate more than the wild type [16]. However, the Δ*che1* mutant does not form clumps earlier than wild type and flocculates only slightly earlier, making it difficult to explain why this mutant would flocculate more than the wild type. In order to gain insight into the mechanism by which the Δ*che1* mutant flocculates more than the wild type, we analyzed the amount of clumps (expressed as the fraction of clumps within the cell suspension) formed at different times post inoculation into the flocculation medium. First, we compared the fraction of clumps in strains grown under flocculation-conducive conditions for 9-10 hours, the timing at which wild type cells and Δ*che1* mutant cells begin to form clumps. We found that strains which produced clumps earlier than the wild type also had a larger proportion of clumps, suggesting that clumps accumulate over time under these conditions. On the other hand, the wild type and Δ*che1* mutant formed comparable amount of clumps at this time point (9-10 hours). However, at a later time point (17-18 hours post inoculation), the Δ*che1* mutant strain had approximately twice as many clumps as the wild type cells, an observation that support the

hypothesis that greater clumping correlates with greater flocculation. Taken together, these data indicate that the *che1* mutant strains that flocculate more than the wild type strain do so because they are able to form clumps at greater rates relative to the wild type strain.

The data thus show that (i) clumping precedes flocculation, (ii) the extent of clumping correlates with the extent of flocculation, (iii) mutations affecting Che1 function correlate with increased clumping, and (iv) a mutation that prevents clumping also prevents flocculation. These results suggest that Che1 affects flocculation indirectly, perhaps by modulating the ability of cells to clump. To test this hypothesis, the behavior of a *flcA* mutant strain which is null for flocculation [20] was analyzed in this assay (Table 3.2). The *flcA* mutant behaved like the wild type strain for clumping; but, in contrast to the wild type, it did not flocculate. A mutant strain carrying both *flcA* and *che1* mutations (Δ*flcA-che1*) behaved similar to the Δ*che1* mutant cells for the timing to clumping, but like the *flcA* mutant, it did not flocculate (Table 3.2). FlcA is thus required for flocculation, but not clumping, and Che1 affects clumping independently of FlcA.

Stable but not reversible (transient) clumping involves changes in the extracellular EPS matrix.

The time course analysis of clumping and flocculation revealed that clumping was initially a dynamic and reversible process. Over time, clumps became more stable with motile cells losing the ability to leave clumps in order to return to a free-swimming behavior. Formation of these stable clumps could be a result of changes in EPS or in the production of specific "adhesins". A role for EPS in mediating clumping and flocculation in *A. brasilense* has been previously suggested [15, 16], prompting us to test this hypothesis. The EPS were extracted at about 10 hours post inoculation into the flocculation medium which corresponds to the time where wild

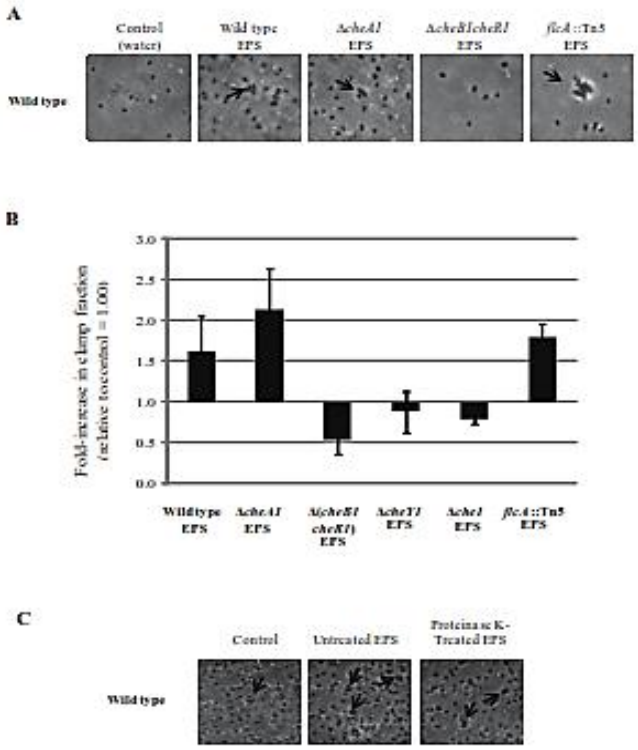

Figure 3.2: Effects of extracted exopolysaccharides (EPS) on clumping in *Azospirillum brasilense*. (A) Representative light microscopy photographs of wild type cells treated with EPS extracted from the strains indicated at the top. Arrows indicate clumping cells. (B) Fold increase in clumping upon treatment of wild type cells with EPS extracted from different strains. The fold-increase in the clumping fraction upon treatment with the extracted EPS as compared to the control treatment (water), taken as a value of 1. (C) Effect of proteinase K on the ability of extracted EPS to induce clumping. A suspension of wild type *A. brasilense* cells were prepared as in (A) and then treated as indicated. Arrows indicate clumping cells. Data shown in this figure represent at least three independent experiments.

type cells have transitioned to formation of more stable clumps (Table 3.2). Under these conditions, cultures of the wild type, the Δ*cheA1* and the *flcA::*Tn5 mutant strains displayed a significant proportion of stable clumps (Table 3.2). In contrast, cultures of the Δ*che1* and Δ*cheY1* mutant strains were mostly comprised of cells displaying a transient clumping behavior (Table 3.2). As expected, clumping was not observed in cultures of the Δ*cheB1cheR1* mutant. Extracted EPS samples were then added exogenously at similar concentrations to a suspension of wild type cells grown under flocculation permissive conditions. EPS extracted from the wild type, Δ*cheA1* and *flcA*::Tn5 strains were able to induce stable clumping behavior *per se* (and not flocculation) in wild type cells under these conditions, i.e., motile cells adhering to each other by their non-flagellated poles were observed in the EPS-treated samples but not in the control (Figure 3.2A). Conversely, treatment of cells with EPS extracted from the Δ*cheB1cheR1* strain, which does not exhibit any clumping behavior, was not able to induce clumping, and in fact appeared to promote free-swimming (Figure 3.2A and 3.2B). Noticeably, the exogenous addition of EPS extracted from the Δ*cheY1* and the Δ*che1* mutants failed to induce significant clumping under similar conditions (Figure 3.2B). Exogenous application of EPS extracted from some, but not all, strains carrying mutations affecting Che1 function is thus sufficient to trigger the formation of stable clumps. EPS samples which were the most potent for inducing stable clumping behavior were extracted from strains that produced the most stable clumps at the time of EPS extraction: the wild type strain, the Δ*cheA1* and the *flcA*::Tn5 mutant strains. Strains that clumped only transiently at the time of EPS extraction (Δ*cheY1* and Δ*che1*) produced EPS that did not trigger stable clumping. Therefore, it is likely that EPS production contributes to stabilizing clumping. However, mutations within different *che1* genes appear to yield strains producing EPS of variable potency for inducting stable clumping, indicating some variation in the nature of the EPS produced by these strains. This observation supports the hypothesis of an indirect role for Che1 in

modulating "clumping-specific" EPS production. To rule out any other indirect effects of the extracted EPS, the contribution of proteins potentially present within the extracted EPS was tested by examining the effect of proteinase K treatment of EPS on induction of clumping in this assay. Treatment of EPS with proteinase K did not affect the propensity of the EPS to induce clumping, suggesting that EPS but not any other protein within the extracted EPS, modulates increased clumping (Figure 3.2C). These results thus confirm that EPS produced by cells capable of forming stable clumps are potent inducers of clumping. Since different *che1* mutant strains produce EPS with different abilities to promote stable clumping, it follows that clumping-specific EPS production is most likely not directly regulated by Che1. Together with the observation that Che1 affects the timing to clumping in the flocculation assay, these results suggest that Che1 may function to modulate the transient nature of clumping which precedes the formation of stable clumps.

Clumping is modulated by temporal changes in aeration.

Changes in aeration conditions are likely to modulate clumping because clumping is observed when cultures of *A. brasilense* are grown under conditions of high aeration [11]. Therefore, we modified a gas perfusion chamber assay, typically used for aerotaxis, to directly measure temporal changes in clumping in order to further characterize the transient and reversible clumping behavior. In this assay, the gas atmosphere flowing above a suspension of cells can be controlled allowing one to analyze the behavioral responses of cells challenged with changes in the aeration conditions. In order to use the gas perfusion chamber assay to analyze clumping, we also grew all strains under high aeration conditions and to higher cell densities (late exponential phase) (see *Experimental Procedures*). Under these growth conditions, all strains clumped in a pattern similar to that detected in the flocculation assay, i.e., the Δ*cheA1*, Δ*cheY1*, Δ*che1*,

Δ*cheB1*, as well as the Δ*cheR1* mutant strains had more clumps relative to the wild type while the Δ*cheB1cheR1* mutant did not clump (Figure 3.1). When a suspension of wild type cells was analyzed in this assay, cells responded to a switching in the aeration (air removal) with a decrease in the overall amount of clumping (reduction by half relative to pre-stimulus levels; Figure 3.3) followed by an adaptation period where the fraction of clumps detected in the suspension returned to pre-stimulus levels. We observed that the fraction of clumps decreased transiently upon air removal because clumped cells briefly returned to free-swimming behavior, before adapting to the ambient aeration conditions and returning to clumps (Figure 3.3). Similarly, when air was returned to the atmosphere of the cell (air addition), cells displayed a similar response characterized by a similar decrease in clumping by half concomitant with the clumped cells becoming free-swimming for a short period before the clumps re-formed to return to pre-stimulus levels (Figure 3.3).

The Δ*cheR1* mutant resembled wild type cells the most (Figure 3.3). The Δ*cheR1* mutant differed from the wild type in that after the initial decrease in the clumping fraction (upon both air removal and air addition), cells were slower to return to pre-stimulus clumping levels. Where wild type cells would begin to re-form clumps after 30-40 seconds, the Δ*cheR1* mutant would take approximately 60 seconds to resume clumping behavior. The Δ*cheB1cheR1* mutant did not show any clumping behavior, regardless of the removal or addition of air (Figure 3.3). The clumping behavior of the Δ*cheA1* mutant differed in two key ways from that of the wild type strain which responded to both air addition and air removal with an initial decrease in clumping behavior (prior to adaptation where clumps are re-formed), in this assay. First, Δ*cheA1* responded to both air removal and air addition, but it did not adapt to the imposed aeration

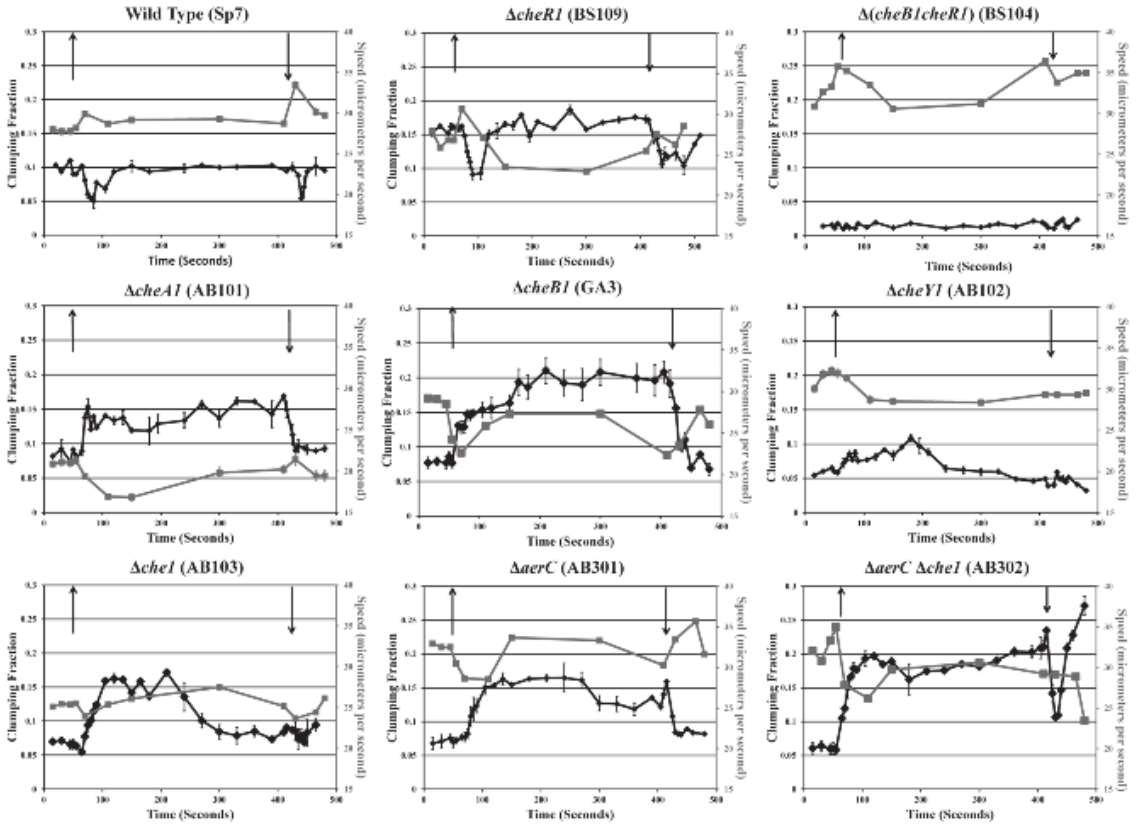

Figure 3.3: Clumping behavior of *A. brasilense* and the *che1* mutant strains in the gas perfusion chamber assay. The gas atmosphere of a suspension of cells placed in a gas perfusion chamber is changed from air to nitrogen gas (air removal) and back to air (air addition). Changes in the fraction of clumps (black line and axis) and the average velocity of free-swimming cells (gray line and axis) within the cell suspension were determined at regular time intervals (x-axis, in seconds), upon air removal (up arrow) and after air addition (down arrow) for the strains indicated. Time is in seconds with the entire experiment representing about 10 minutes. The fraction of clumps and the swimming velocity within the cell suspensions were determined from digital movies analyzed as described in Experimental Procedures.

conditions since clumping did not return to pre-stimulus levels upon air removal or air addition (Figure 3.3). Secondly, rather than experiencing a decrease in the number of clumps upon air removal, clumping levels in suspension of this mutant nearly doubled under these conditions. Upon air addition to the Δ*cheA1* cell suspension, the number of clumps decreased by half. Similar to Δ*cheA1*, the Δ*cheB1* mutant also responded to both air removal and air addition, but no adaptation to the changes in aeration conditions was observed. The number of clumps in the suspension of the Δ*cheB1* also doubled upon air removal and decreased upon air addition by the same amount, as in Δ*cheA1*.

In response to air addition, clumping also nearly doubled in suspension of the Δ*cheY1* which contrasted with the wild type response to similar changes in aeration conditions. In fact, the observed increase in clumping seen in the Δ*cheY1* upon air removal is similar to that observed in the Δ*cheA1* and Δ*cheB1* mutants; however, clumping in the Δ*cheY1* mutant slowly adapted to the new aeration conditions and decreased back to pre-stimulus levels (Figure 3.3). No further change in clumping was detected when air was returned to the atmosphere of Δ*cheY1* (air addition). The Δ*che1* mutant increased clumping by more than 2-fold, which is slightly higher than that observed in the other mutants; however, like Δ*cheY1*, clumping in response to air removal slowly adapted and it returned to pre-stimulus levels (Figure 3.3). Similar to Δ*cheY1*, the Δ*che1* mutant did not respond to air addition and no change in clumping was detected.

Collectively, we show that changes in transient clumping take place as a result of changes in aeration conditions. These results also indicate that Che1 functions to reduce clumping when cells experience a decrease in aeration (air removal), but its contribution to clumping under conditions of increased aeration (air addition) is not straightforward.

Clumping is not correlated with changes in reversal frequency.

Changes in the clumping pattern of wild type cells detected in the gas perfusion chamber assay were reminiscent of changes in the swimming pattern of cells in a temporal assay for chemotaxis or aerotaxis, suggesting a functional link between clumping and motility. First, we analyzed the swimming motility bias of cells that have experienced changes in clumping upon changes in aeration conditions in the gas perfusion chamber assay described above. Under these conditions, the wild type strain was found to display a nearly 3-fold decrease in the swimming reversal frequency (number of reversals in the swimming direction per second and per cell) upon air removal or addition to the atmosphere of the cells (Figure 3.4). While most of the che1 mutant strains responded to changes in aeration conditions by modulating the swimming motility bias under these conditions, no correlation between changes in clumping and changes in the reversal frequency of cells upon air removal or air addition could be established when analyzed in this assay (Figure 3.4). The most striking illustration of this fact is that no change in the swimming bias of the Δ*cheR1* mutant strain could be detected upon air removal or addition, yet its clumping behavior most resembled that of the wild type strain, albeit with longer transient free-swimming responses (Figure 3.3) (Figure 3.4).

Clumping and swimming velocity correlate.

While there was no detectable correlation between clumping behavior and changes in the motility bias, changes in swimming velocity appeared to correlate with changes in clumping detected upon air removal. For example, wild type cells showed a significant increase in swimming velocity by approximately 3 μm/sec upon air removal, which correlated with a transient decrease in the fraction of clumping cells by about half (Figure 3.3). When the swimming velocity of wild

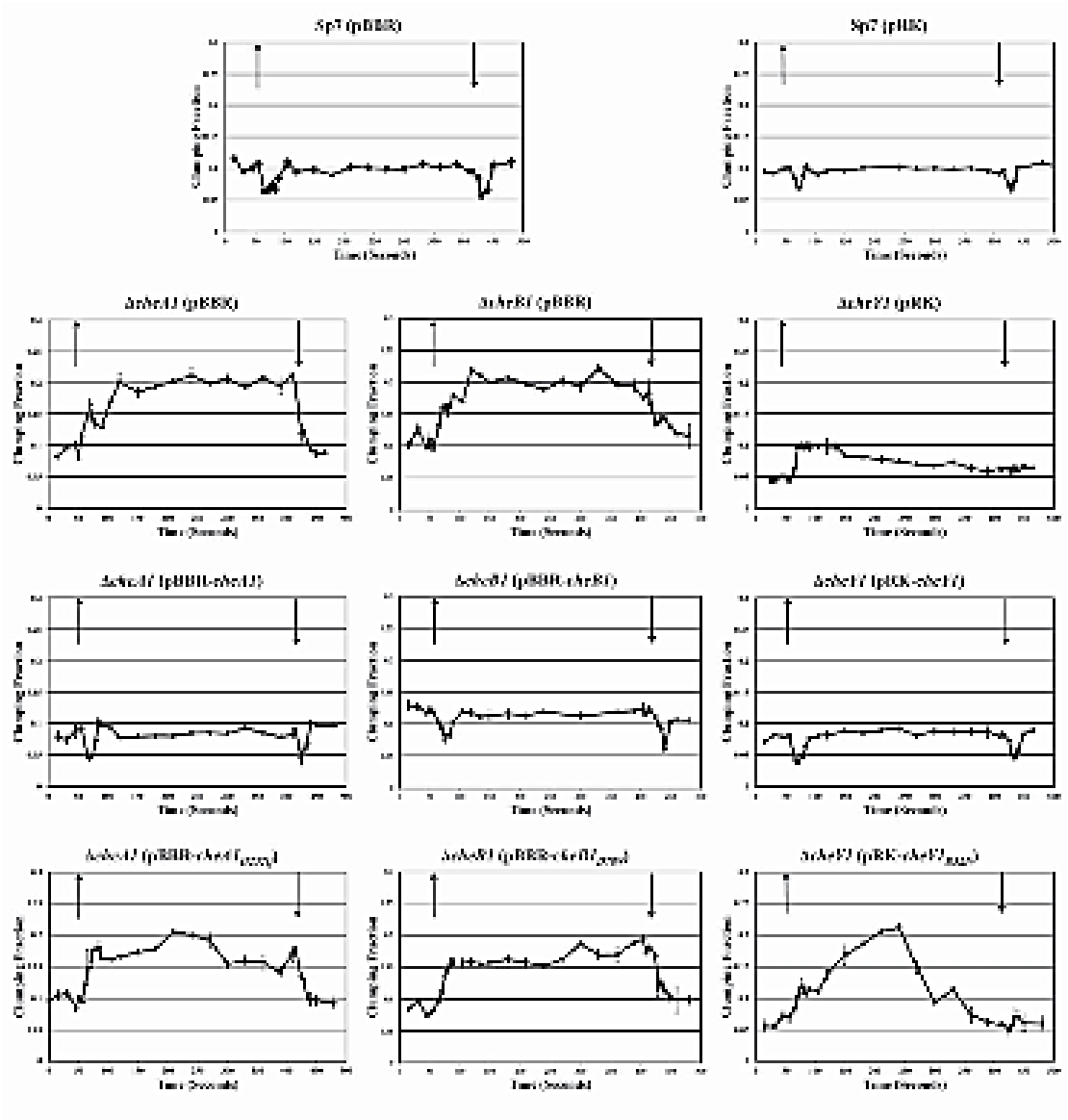

Figure 3.4: Complementation of che1 mutant phenotypes with parental (wild type) and variant alleles of CheA1, CheB1, and CheY1 proteins in the gas perfusion assay. The fraction of clumps to free-swimming cells over the time course of the assay is shown. The total experiment time is about 10 minutes. The up and down arrows indicate events of air removal and air addition from the atmosphere of the cells, respectively.

type cells decreased to pre-stimulus levels upon adaptation, the clumping fraction increased to pre-stimulus levels, as well. Similar to the wild type strain, the Δ*cheR1* mutant cells also swam faster by about 5 μm/sec in response to air removal with concomitant decrease in clumping by half. The Δ*cheB1cheR1* strain, on the other hand, did not respond to air removal by modulating clumping but it did respond by transiently swimming faster (a ~ 5 μm/sec increase in swimming velocity). Noticeably, the average swimming velocity of the Δ*cheB1cheR1* mutant strain was also the highest of all strains analyzed (ranging from 30-37 μm/sec), differing from wild type by about 4 μm/sec and from the Δ*cheA1* (the slowest of the Che1 mutants) mutant by nearly 14 μm/sec (Figure 3.3). Given that clumping decreases with increased swimming velocities in the wild type, the higher average swimming velocity of the Δ*cheB1cheR1* mutant may explain the lack of clumping observed in this strain (Figure 3.3). In contrast, the swimming velocity of the mutants lacking *cheA1*, *cheB1*, *cheY1*, or *che1* decreased by an average of 3 to 7 μm/sec upon air removal and it was concomitant with a doubling in the amount of clumping in cell suspensions of these mutants (Figure 3.3). These results thus suggest that the inability of these *che1* strains to increase swimming velocity upon air removal correlates with the increase in clumping observed under these conditions (Figure 3.3). These data further imply that changes in transient clumping upon air removal may be modulated by direct effects of Che1 on the swimming velocity.

Although changes in swimming velocity correlated with changes in clumping upon air removal in the *che1* mutant strains, we were unable to detect such a correlation upon air addition (Figure 3.3). Changes in swimming velocity detected for the wild type and the various *che1* mutant strains upon air removal were also detected and followed a similar pattern upon air removal (Figure 3.3). While the wild type cells as well as Δ*cheR1* and Δ*cheB1cheR1* mutant cells swam transiently faster by about 5 μm/sec upon air addition, the Δ*cheA1*, Δ*cheB1*, Δ*cheY1*, and Δ*che1* mutant cells swam with a reduced velocity (by 4 μm/sec on average) under these conditions.

Similar to the behavior observed upon air removal, the transient increased in the swimming velocity correlated with a decrease in clumping by half for the wild type and the Δc*heR1* mutant, while clumping was not detected for the Δ*cheB1cheR1* mutant for which the average swimming velocity remained the greatest (Figure 3.3). In contrast and despite swimming transiently slower, clumping decreased by half in suspension of the Δ*cheA1* and the Δ*cheB1* mutant strains upon air addition, while there was no change in clumping (no response) in suspension of the Δ*cheY1*, and of the Δ*che1* (Figure 3.3). These observations suggest that the effect of the decreased swimming velocity on clumping may be significant only when cells experience a decrease in aeration conditions (air removal). This suggests that transient clumping is modulated by direct effects of Che1 on the swimming behavior, as well as by other Che1-independent effects that are likely prevalent under conditions of increased aeration in the atmosphere of the cells.

Control of the swimming velocity is a signaling output of Che1.

In order to gain further insight into how signaling via Che1 regulates the swimming velocity and clumping, the behavior of mutant strains expressing wild type *che1* genes or genes carrying mutations of conserved phosphorylation residues expressed from low copy plasmids was characterized under flocculation conditions and in the gas perfusion chamber assay (Figure 3.5). Expression of CheA1, $CheA_{H252Q}$, CheY1 and $CheY1_{D52N}$ from the plasmids used for complementation was detected with antibodies to the *A. brasilense* wild type proteins and found to be comparable to the level of the wild-type

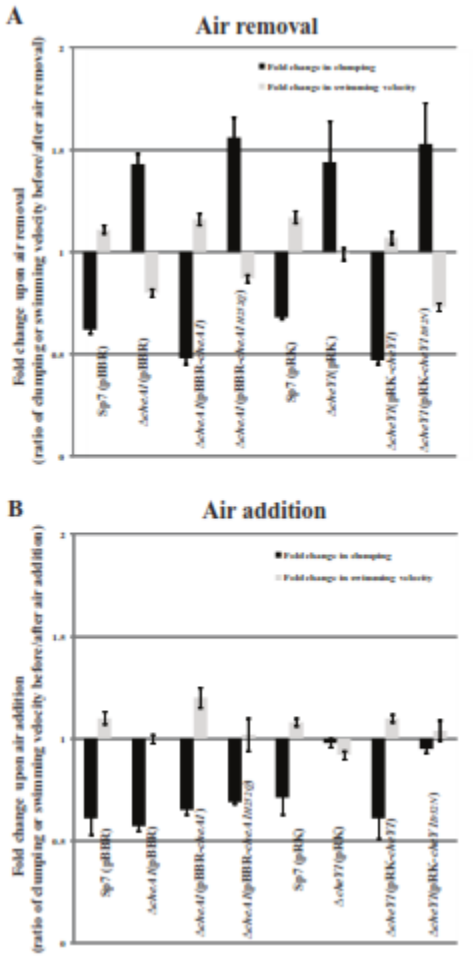

Figure 3.5: Effects of CheA1 and CheY1 on the relative fold change in swimming velocity and clumping upon air removal or air addition to the atmosphere of the cells. The strains carried either an empty vector (controls pRK or pBBR) or a vector in which a wild type *cheA1* or *cheY1* allele or mutant alleles (*cheA1*$_{H252Q}$ and c*heY1*$_{D52N}$) are expressed from low copy plasmids. Clumping represents the fraction of cells within clumps (clumping fraction) relative to the total number of cells in the video frame analyzed. The fold change in swimming velocity and in clumping upon air removal or addition is calculated relative to the swimming velocity or clumping prior to the switch in the atmosphere of the cells (air removal or addition).

proteins. Similar controls of protein expression could not be performed with CheB1 since we do not have any antibody to CheB1 and none of the antibodies against CheB of other bacterial species that we have tried cross-reacted with the CheB1 protein from *A. brasilense*. While functional complementation of Δ*cheA1* (AB101) with the wild type *cheA1* expressed from a plasmid restored wild-type clumping behavior in both the flocculation and the gas perfusion chamber assays, complementation with a plasmid expressing a mutated *cheA1* gene in which the codon for the conserved phosphorylatable histidine residue is replaced with glutamine ($CheA1_{H252Q}$) failed to restore the wild type phenotype: the pattern of changes in clumping within the suspension upon air removal or addition paralleled that of the mutant strain (Figure 3.5). An intact CheA1 is thus required for its function in clumping. Similar functional complementation of Δ*cheY1* (AB102) with the wild type CheY1, but not with a $CheY1_{D52N}$ variant, restored the wild-type clumping phenotype, indicating that functional CheY1 is also essential for its function in clumping (Figure 3.5). An intact phosphorylatable aspartate site (D78) in the receiver domain of CheB1 was found to be required to restore the wild type clumping behavior of a Δ*cheB1* mutant strain. Functional CheA1 and CheY1, but not $CheA1_{H252Q}$ or $CheY1_{D52N}$ also restored the ability of strains to transiently increase swimming velocity upon air removal and air addition in the gas perfusion chamber assay, correlating with a transient reduction in the fraction of clumped cells (Figure 3.5). Che1 thus modulates the cell's swimming velocity by a direct effect on CheY1 phosphorylation, likely via a phosphorelay between CheA1 and CheY1. The analysis of the Δ*cheA1*, Δ*cheY1* and Δ*che1* mutant phenotypes together with the effects of expressing nonfunctional $CheA1_{H252Q}$ or $CheY1_{D52N}$ on the swimming velocity of cells also indicate that Che1 signaling output causes an increase in the swimming velocity of cells.

A taxis receptor modulates Che1-dependent effects on clumping.

Mutations affecting the *A. brasilense* energy taxis receptor *aerC* were previously shown to possess small clumps under most growth conditions [23], suggesting that this receptor functions to modulate clumping. Consistent with this hypothesis, a Δ*aerC* mutant strain clumped after 1-3 hours post-inoculation (Table 3.2) and quantitatively more than the wild type strain, resulting in greater flocculation, as well (data not shown). A double mutant lacking both *aerC* and *che1* (Δ*aerC*Δ*che1*, strain AB302) behaved as the Δ*che1* mutant strain (Table 3.2) for clumping and flocculation. This is consistent with previous observations [28] and suggests that AerC functions upstream of Che1 to modulate clumping.

Next, the behavior of the Δ*aerC* (AB301) and the Δ*aerC*Δ*che1* (AB302) mutant strains were analyzed in the gas perfusion chamber assay (Figure 3.3). The swimming velocity of both the Δ*aerC* and the Δ*aerC*Δ*che1* mutant strains decreased at least 5 μm/sec immediately upon air removal. Upon air addition, the swimming velocity increased approximately 5 μm/sec in the Δ*aerC* strain, but decreased by 5 μm/sec in the Δ*aerC*Δ*che1* strain. These results are consistent with the role of Che1 in modulating changes in swimming velocity as well as with the role of AerC in mediating Che1-dependent changes in the swimming velocity, likely by sensing conditions of decreased aeration.

Compared to the wild type strain, the Δ*aerC* mutant strain doubled in clumping, but with a significant delay (of about 15 seconds compared to the wild type) relative to the time of air removal. The delayed clumping response seen in the Δ*aerC* mutant strain upon air removal was no longer observed in the Δ*aerC*Δ*che1* strain: clumping increased immediately upon air removal (Figure 3.3). Similar to Δ*cheA1* and Δ*cheB1* mutants, clumping in each of these strains remained at levels higher than pre-stimulus conditions after it initially increased upon air removal. Clumping returned to lower levels only after air addition in the Δ*aerC* mutant strain (Figure 3.3).

Under conditions of increased aeration, the Δ*aerC*Δ*che1* mutant strain responded by decreasing the fraction of clumps by more than 2-fold (Figure 3.3). In contrast to the response of the Δ*aerC* mutant, the decrease in clumping upon air addition was transient in the Δ*aerC*Δ*che1* strain (Figure 3.3). The ability of the Δ*aerC*Δ*che1* mutant to respond to air addition by transiently decreasing clumping also lends support to the hypothesis that Che1 effects on the swimming speed does not directly contribute to clumping under conditions of increased aeration. The transient decreased clumping response of the Δ*aerC*Δ*che1* mutant upon air addition is similar to the response of the wild type strain, i.e. appears to correspond to adaptation; however, steady state clumping in suspension of the wild type strain remained at lower levels. In contrast, the steady-state levels of clumping remained at significantly higher levels relative to pre-stimulus in suspension of the Δ*aerC*Δ*che1* mutant, suggesting indirect effects of AerC on the steady-state levels of clumping. Taken together, these results argue that in addition to modulating Che1-dependent effects on transient clumping via an effect on the swimming speed, AerC may also mediate indirect effects that modulate the ability of cells to maintain constant steady-state levels of clumping, after changes in aeration conditions.

Discussion

The Che1 chemotaxis-like pathway of *A. brasilense* has been implicated in the control of chemo- and aerotaxis as well as cell surface adhesive properties, clumping and flocculation. Here, we show that clumping and flocculation are distinct processes and that Che1 contributes to the control of the initial reversible and transient cell-to-cell clumping behavior. While transient clumping correlates with changes in motility of cells, transition to stable clumps depends on the

production of EPS that are produced independently of Che1. Our results demonstrate that the signaling output of Che1 is the modulation of the flagellar swimming velocity, illuminating its role in chemo- and aerotaxis.

The signaling output of Che1 is the control of the swimming velocity.

Che1 appears to directly regulate the propensity of cells to increase swimming velocity with changes in aeration conditions. A functional Che1 pathway, including a phosphorylatable CheY1 response regulator is required for this response, identifying modulation (increase) of the swimming velocity as a signaling output of the Che1 pathway. This finding implies that changes in swimming velocity contribute to aerotaxis in *A. brasilense* with receptors signaling to Che1 upon changes in aeration conditions in order to modulate this response. AerC is an energy taxis receptor [23] that is shown here and elsewhere [23] to function in a Che1-dependent manner to modulate the swimming velocity and aerotaxis. Changes in swimming velocity have not been directly implicated in the tactic behaviors of *A. brasilense*. However, the results obtained here imply that changes in the swimming speed of cells represent a mechanism by which motile *A. brasilense* cells actively navigate in gradients. This assumption is supported by the observation that wild type *A. brasilense* cells responded to temporal changes in aeration conditions by increasing the swimming speed, as well as decreasing the reversal frequency by nearly 3-fold (an attractant response). Further, the Δ*cheB1cheR1* mutant strain, in which CheA1 and CheY1 are supposed to be active, has a constantly greater swimming velocity than the wild type cells (Figure 3.3). In addition to identifying the signaling output of the Che1 pathway, these results also shed light on how the Che1 pathway could contribute to chemotaxis and aerotaxis, while not having any apparent effect on the reversal frequency of the cells [16]. Che1 signaling output could regulate swimming velocity either via direct effect(s) of phosphorylated CheY1 on the flagellar

motor or switch complex to ultimately increase flagellar swimming velocity, or through indirect effects involving additional protein(s) capable of affecting flagellar motor rotation or torque. Direct effects of CheY proteins on flagellar rotation have been recently demonstrated in *R. sphaeroides*, a species that employs multiple CheY homologs which are able to bind to the flagellar motor and switch complex that act as a "brake" to stop flagellar rotation [29]. The genome of *A. brasilense* encodes six CheY homologs that have not been characterized yet [30]. The role of CheY1 in increasing the swimming velocity and the contribution of Che1 to chemo- and aerotaxis in *A. brasilense*, albeit minor [11, 13], collectively suggest the possibility of a similar function. However, other mechanisms are possible. For example CheY1 could counteract the effect of potential flagellar velocity braking protein(s) and thus act indirectly to increase the speed at which cells swim. The observation that mutations affecting *cheA1*, *cheY1* or deletion of *che1* cause the cells to respond to changes in aeration conditions by swimming slower relative to the wild type (Figure 3.3) gives credence to this hypothesis. Several proteins from diverse bacteria have been recently shown to control the flagellar motor with typical effects observed on the cell's swimming velocity. The proteins involved and the mechanisms by which they interact with flagellar motor components appear diverse, even within a single bacterial species, making their direct identification from sequences alone challenging (for a recent review, see [31]).

Che1-dependent changes in the swimming speed modulate transient clumping.

When wild type cells were analyzed in a temporal assay for clumping, a transient decrease in the fraction of clumps was observed upon air removal and air addition from the atmosphere of the cells. Concomitant with this transient change in cell-to-cell interactions, swimming was biased toward less frequent changes in the swimming direction (reversals per second) and the swimming speed increased, immediately in response to changes in aeration conditions. Changes in clumping

paralleled changes in the swimming pattern (bias and velocity) of the cells. Results obtained here establish that changes in the swimming velocity mediated by Che1 are sufficient to promote a reduction in transient clumping upon downshifts in aeration conditions. Changes in the swimming speed could affect clumping, perhaps by increasing the likelihood of loosely adherent cells within clumps to detach and swim away and/or by decreasing the probability of initial cell-to-cell contacts, thus reducing the possibility of transient clump formation. A decrease in flagellar swimming bias and/or flagellar swimming velocity was previously shown to promote surface attachment and biofilm formation in many bacterial species [32-35]. Similarly, changes in the swimming motility of *A. brasilense* cells appear to contribute to the propensity of cells to interact within clumps. A major role for Che1-dependent changes in motility in modulating cell-to-cell interactions in transient clumps is consistent with the dynamic and short-lived nature of these associations and with the propensity of transient clumps to dissociate rapidly in response to changes in aeration conditions. While Che1 appears to control the flagellar swimming velocity under all conditions, a significant effect of the swimming speed on transient clumping was detected only upon air removal, under the conditions of the gas perfusion chamber assay. This suggests that while the swimming velocity may significantly affect transient clumping under some conditions, other behavior(s) may modulate the dynamics of transient reversible clumping under other conditions, such as an increase in aeration. Given the changes in the motility pattern of the wild type cells detected upon air removal and air addition, it is likely that the swimming reversal frequency or perhaps other transient changes in the motility behavior that were not detected here could contribute to modulate clumping upon increases in aeration conditions. Given that clumping was correlated with increased biofilm formation in *A. brasilense* (27), these results also raise the intriguing possibility that changes in the swimming pattern of cells are directly

implicated in the initiation of transient cell-to-cell and cell-to-surface interactions that precede most steps in colonization.

Cross-talk may be involved in modulating clumping.

In addition to direct effects on the swimming velocity, Che1 also appears to have indirect effects on clumping behavior. For instance, some Che1 mutants show increased steady-state levels of clumping that do not return to pre-stimulus levels in the gas perfusion chamber assay, which did not appear to directly correlate with a generally lower swimming velocity of the cells. Indirect effects also include the observation that *che1* mutations affect the timing to clumping in the flocculation assay, consistent with effects of Che1 on the sensitivity of the clumping response under the conditions of this assay. Adaptation proteins in chemotaxis signal transduction function to maintain response sensitivity over a broad range of background conditions, and allow the behavior to return to pre-stimulus bias after a rapid response to environmental stimuli [1, 6]. Loss of function in adaptation proteins is thus expected to affect the sensitivity and/or activity of chemotaxis receptors that are regulated by these proteins. The following lines of evidence support the hypothesis that indirect effects of Che1 on clumping are mediated through the activity of adaptation proteins and chemotaxis receptors. First, mutations affecting CheB1 directly or indirectly (e.g. mutations affecting CheA1 function), yielded the most dramatic clumping phenotypes. Second, increased clumping triggered in response to air removal from the atmosphere of the cells remained at high levels in strains with Δc*heA1* or Δ*cheB1* mutations or expressing nonfunctional CheA1 or CheB1 variant proteins. Persistent clumping at high levels was also detected in a mutant strain lacking a functional AerC receptor. This clumping response pattern suggested that a stimulus and an initial response must be implemented for this change in the steady-state clumping behavior to be detected, implicating defects in a response feedback

loop. In contrast, higher clumping levels decayed slowly to reach lower levels in strains carrying Δ*cheY1* (or non-functional $CheY1_{D52N}$ variant) and Δ*che1* mutations. Last, a strain carrying a Δ(*cheB1cheR1)* mutation does not clump under any growth conditions. Collectively, these results implicate both a receptor (AerC) and Che1 adaptation proteins, in particular CheB1, in mediating the indirect effects of Che1 on the sensitivity of cells that allows them to maintain clumping at constant steady-state levels. How could indirect effects of Che1 be mediated by adaptation proteins and/or receptors? One possibility is that other pathways in addition to Che1 contribute to modulating the swimming behavior and thus transient clumping. Results obtained here and in previous studies [14, 16] support this hypothesis. CheB1 and CheR1 of the Che1 pathway were previously implicated in a signaling cross-talk between Che1 and other unknown pathway(s) in regulation of aero- and chemotaxis responses in *A. brasilense*, with the most notable effects being the relative sensitivity of receptors and associated pathway(s) to changes in environmental conditions [14]. Genetic, biochemical and/or modeling data in a few other bacterial species support the hypothesis that cross-talk between different chemotaxis or Che-like operons may be mediated by the activity of CheB proteins [36-40]. The methylation status of the FrzCD receptor also depends on signaling by two Che-like pathways in *Myxococcus xanthus* [41], lending further support to this possibility. In such a scenario, if receptors are modified by adaptation proteins from independent signaling pathways, then sensory input to one pathway could modulate the activity of the adaptation protein of this pathway, which in turn will affect the sensitivity and thus the response output of other pathway(s).

Clumping and its relationship with flocculation.

While they are both formed as a result of cell-to-cell interactions, clumping cells are morphologically and behaviorally distinct from flocculated cells in that flocculated cells are non-

motile, round and encased in large aggregates of polysaccharides [18]. Consistent with this observation, FlcA, a key transcriptional regulator for flocculation [20], has no effect on clumping in *A. brasilense*. Mutant strains that lack FlcA could produce stable clumps but they fail to lose motility or to differentiate into round flocculated cells. Clumping thus precedes and appears required for flocculation. Our data are consistent with Che1 modulating transient cell-to-cell clumping in response to changes in aeration conditions. *A. brasilense* flocculates only under conditions of high aeration, as well as when the source of combined nitrogen for growth is limiting [12, 18]. This observation further supports the hypothesis that clumping and flocculation are distinct processes. The effect that Che1 has on the ability of cells to flocculate is thus indirect and is most likely the result of Che1-dependent effects on clumping. However, the identity of the kinase(s) or of the phosphorelay(s) that regulate(s) the activity of FlcA remains unknown.

Che1 modulates transient clumping behavior, which depends on changes in motility and precedes the formation of stable clumps and flocculation. Over time, stable clumps accumulate and data obtained in this study suggest that specific EPS are produced by cells in order to stabilize clumping. While our data clearly establish that the signaling output of Che1, and thus its main function, is not the regulation of clumping-specific EPS production, mutations within *che1* result in mutant strains differentially affected in their ability to transition from transient to stable clumping. These differences in timing for the transition to stable clumps suggest that Che1 may indirectly modulate clumping-specific EPS production. One possibility is if production of clumping-specific EPS depends on the activity of another chemotaxis-like pathway. Che-like pathways regulating EPS production have been identified in other bacterial species [42, 43]. The genome of *A. brasilense* encodes for four Che-like pathways, with one of them predicted to have an alternative cellular function, distinct from motility [30]. This or perhaps another pathway could ultimately function in modulating clumping-specific EPS production. Together with

evidence obtained previously [14, 16] and discussed above, cross-talk involving CheB1 and CheR1 is plausible to explain the role of Che1 in modulating indirectly the signaling output of other signaling pathway(s), including perhaps some regulatory pathway controlling clumping-specific EPS production. In support of this hypothesis, clumping-specific EPS were produced in strains where the activity of CheB1 was affected (strains carrying *cheA1* and *cheB1* deletions) while the role of CheY1 in modulating the production of EPS yielding stable clumps was opposite.

What advantage could clumping afford *A. brasilense* cells with? Our results indicate that transient clumping is inversely correlated with free-swimming behavior such as aerotaxis. Motile cells within clumps are unlikely to be able to explore their surroundings using taxis-dependent behaviors. In turn, this suggests that clumping functions to transiently prevent motility-dependent responses. Clumping is initially a transient behavior, progressing over time toward increasingly more stable clumps of motile cells. Therefore, while motility changes may mediate transient clumping behaviors, additional physiological changes are implemented to allow for the transition to more stable clumps, with the production of EPS being such a prominent change. The finding that Che1, quite likely together with other pathway(s), regulates clumping in *A. brasilense* is consistent with the observation that clumping is a behavior extremely sensitive to ambient conditions in which clumping cells are able to rapidly transition between cell-to-cell interactions and free-swimming motility. Given the dynamic changes in clumping and the fact that it precedes the production of stable clumps, we hypothesize that clumping could afford the cells with the ability to maintain a relatively static position in a gradient without having to commit to a permanently attached lifestyle by remaining motile and able to respond to changes in ambient conditions.

Acknowledgements

The authors thank Dr. Z. Xie, for constructing strain AB104 and anonymous reviewers for their insightful comments and suggestions as well as members of the Alexandre laboratory for comments on the manuscript. This work was supported by NSF (MCB-0919819) to G.A.

List of References

1. Wadhams, G.H. and J.P. Armitage, Making Sense of It All: Bacterial Chemotaxis. *Nature Reviews Molecular Cell Biology*, 2004. 5(12): p. 1024-37.
2. Sourjik, V., Receptor Clustering and Signal Processing in E Coli Chemotaxis. *Trends in Microbiology*, 2004. 12(12): p. 569-76.
3. Wuichet, K. and I.B. Zhulin, Origins and Diversification of a Complex Signal Transduction System in Prokaryotes. *Science Signaling*, 2010. 3(128): p. ra50.
4. Zhulin, I.B., The Superfamily of Chemotaxis Transducers: From Physiology to Genomics and Back. *Advances in Microbial Physiology, Vol 45*, 2001. 45: p. 157-98.
5. Szurmant, L. and G.W. Ordal, Diversity in Chemotaxis Mechanisms among the Bacteria and Archaea. *Microbiology and Molecular Biology Reviews*, 2004. 68(2): p. 301-+.
6. Kirby, J.R., Chemotaxis-Like Regulatory Systems: Unique Roles in Diverse Bacteria. *Annu Rev Microbiol*, 2009. 63: p. 45-59.
7. Zhulin, I.B., et al., Oxygen Taxis and Proton Motive Force in Azospirillum Brasilense. *J Bacteriol*, 1996. 178(17): p. 5199-204.
8. Alexandre, G., Coupling Metabolism and Chemotaxis-Dependent Behaviours by Energy Taxis Receptors. *Microbiology-Sgm*, 2010. 156: p. 2283-93.
9. Alexandre, G., S.E. Greer, and I.B. Zhulin, Energy Taxis Is the Dominant Behavior in Azospirillum Brasilense. *J Bacteriol*, 2000. 182(21): p. 6042-8.
10. Greer-Phillips, S.E., B.B. Stephens, and G. Alexandre, An Energy Taxis Transducer Promotes Root Colonization by *Azospirillum Brasilense*. *Journal of Bacteriology*, 2004. 186(19): p. 6595-604.
11. Bible, A.N., et al., Function of a Chemotaxis-Like Signal Transduction Pathway in Modulating Motility, Cell Clumping, and Cell Length in the Alphaproteobacterium Azospirillum Brasilense. *Journal of Bacteriology*, 2008. 190(19): p. 6365-75.

12. Edwards, A.N., et al., Characterization of Cell Surface and Extracellular Matrix Remodeling of Azospirillum Brasilense Chemotaxis-Like 1 Signal Transduction Pathway Mutants by Atomic Force Microscopy. *Fems Microbiology Letters*, 2011. 314(2): p. 131-9.

13. Hauwaerts, D., et al., A Major Chemotaxis Gene Cluster in Azospirillum Brasilense and Relationships between Chemotaxis Operons in Alpha-Proteobacteria. *FEMS Microbiol Lett*, 2002. 208(1): p. 61-7.

14. Stephens, B.B., S.N. Loar, and G. Alexandre, Role of Cheb and Cher in the Complex Chemotactic and Aerotactic Pathway of Azospirillum Brasilense. *J Bacteriol*, 2006. 188(13): p. 4759-68.

15. Siuti, P., et al., The Chemotaxis-Like Che1 Pathway Has an Indirect Role in Adhesive Cell Properties of Azospirillum Brasilense. *Fems Microbiology Letters*, 2011. 323(2): p. 105-12.

16. Bible, A.N., et al., Function of a Chemotaxis-Like Signal Transduction Pathway in Modulating Motility, Cell Clumping, and Cell Length in the Alphaproteobacterium Azospirillum Brasilense. *J Bacteriol*, 2008. 190(19): p. 6365-75.

17. Wisniewski-Dye, F., et al., Azospirillum Genomes Reveal Transition of Bacteria from Aquatic to Terrestrial Environments. *PLoS Genet*, 2011. 7(12): p. e1002430.

18. Sadasivan, L. and C.A. Neyra, Flocculation in Azospirillum-Brasilense and Azospirillum-Lipoferum - Exopolysaccharides and Cyst Formation. *Journal of Bacteriology*, 1985. 163(2): p. 716-23.

19. Katupitiya, S., et al., A Mutant of Azospirillum-Brasilense Sp7 Impaired in Flocculation with a Modified Colonization Pattern and Superior Nitrogen-Fixation in Association with Wheat. *Applied and Environmental Microbiology*, 1995. 61(5): p. 1987-95.

20. Pereg-Gerk, L., et al., A Transcriptional Regulator of the Luxr-Uhpa Family, Flca, Controls Flocculation and Wheat Root Surface Colonization by Azospirillum Brasilense Sp7. *Mol Plant Microbe Interact*, 1998. 11(3): p. 177-87.

21. Pereg Gerk, L., K. Gilchrist, and I.R. Kennedy, Mutants with Enhanced Nitrogenase Activity in Hydroponic Azospirillum Brasilense-Wheat Associations. *Appl Environ Microbiol*, 2000. 66(5): p. 2175-84.

22. Hauwaerts, D., et al., A Major Chemotaxis Gene Cluster in Azospirillum Brasilense and Relationships between Chemotaxis Operons in Alpha-Proteobacteria. *Fems Microbiology Letters*, 2002. 208(1): p. 61-7.

23. Xie, Z., et al., Pas Domain Containing Chemoreceptor Couples Dynamic Changes in Metabolism with Chemotaxis. *Proc Natl Acad Sci U S A*, 2010. 107(5): p. 2235-40.

24. Kovach, M.E., et al., Four New Derivatives of the Broad-Host-Range Cloning Vector Pbbr1mcs, Carrying Different Antibiotic-Resistance Cassettes. *Gene*, 1995. 166(1): p. 175-6.

25. Alexandre, G. and I.B. Zhulin, Different Evolutionary Constraints on Chemotaxis Proteins Chew and Chey Revealed by Heterologous Expression Studies and Protein Sequence Analysis. *J Bacteriol*, 2003. 185(2): p. 544-52.

26. Laszlo, D.J. and B.L. Taylor, Aerotaxis in Salmonella Typhimurium: Role of Electron Transport. *J Bacteriol*, 1981. 145(2): p. 990-1001.

27. Bradford, M.M., Rapid and Sensitive Method for Quantitation of Microgram Quantities of Protein Utilizing Principle of Protein-Dye Binding. *Analytical Biochemistry*, 1976. 72(1-2): p. 248-54.

28. Xie, Z.H., et al., Pas Domain Containing Chemoreceptor Couples Dynamic Changes in Metabolism with Chemotaxis. *Proceedings of the National Academy of Sciences of the United States of America*, 2010. 107(5): p. 2235-40.

29. Pilizota, T., et al., A Molecular Brake, Not a Clutch, Stops the Rhodobacter Sphaeroides Flagellar Motor. *Proceedings of the National Academy of Sciences of the United States of America*, 2009. 106(28): p. 11582-7.

30. Wisniewski-Dye, F., et al., Azospirillum Genomes Reveal Transition of Bacteria from Aquatic to Terrestrial Environments. *Plos Genetics*, 2011. 7(12): p. e1002430.

31. Brown, M.T., N.J. Delalez, and J.P. Armitage, Protein Dynamics and Mechanisms Controlling the Rotational Behaviour of the Bacterial Flagellar Motor. *Current Opinion in Microbiology*, 2011. 14(6): p. 734-40.

32. Fang, X. and M. Gomelsky, A Post-Translational, C-Di-Gmp-Dependent Mechanism Regulating Flagellar Motility. *Molecular Microbiology*, 2010. 76(5): p. 1295-305.

33. McClaine, J.W. and R.M. Ford, Reversal of Flagellar Rotation Is Important in Initial Attachment of Escherichia Coli to Glass in a Dynamic System with High- and Low-Ionic-Strength Buffers. *Appl Environ Microbiol*, 2002. 68(3): p. 1280-9.

34. Merritt, J.H., et al., Specific Control of Pseudomonas Aeruginosa Surface-Associated Behaviors by Two C-Di-Gmp Diguanylate Cyclases. *Mbio*, 2010. 1(4).

35. Toutain, C.M., M.E. Zegans, and G.A. O'Toole, Evidence for Two Flagellar Stators and Their Role in the Motility of Pseudomonas Aeruginosa. *J Bacteriol*, 2005. 187(2): p. 771-7.

36. Tindall, M.J., et al., Modeling Chemotaxis Reveals the Role of Reversed Phosphotransfer and a Bi-Functional Kinase-Phosphatase. *Plos Computational Biology*, 2010. 6(8).

37. Wadhams, G.H., et al., Targeting of Two Signal Transduction Pathways to Different Regions of the Bacterial Cell. *Molecular Microbiology*, 2003. 50(3): p. 763-70.

38. Porter, S.L. and J.P. Armitage, Chemotaxis in Rhodobacter Sphaeroides Requires an Atypical Histidine Protein Kinase. *Journal of Biological Chemistry*, 2004. 279(52): p. 54573-80.

39. Hamer, R., et al., Deciphering Chemotaxis Pathways Using Cross Species Comparisons. *Bmc Systems Biology*, 2010. 4.

40. Miller, L.D., et al., The Major Chemotaxis Gene Cluster of Rhizobium Leguminosarum Bv. Viciae Is Essential for Competitive Nodulation. *Molecular Microbiology*, 2007. 63(2): p. 348-62.

41. Xu, Q., et al., Independence and Interdependence of Dif and Frz Chemosensory Pathways in Myxococcus Xanthus Chemotaxis. *Molecular Microbiology*, 2008. 69(3): p. 714-23.

42. Hickman, J.W., D.F. Tifrea, and C.S. Harwood, A Chemosensory System That Regulates Biofilm Formation through Modulation of Cyclic Diguanylate Levels. *Proceedings of the National Academy of Sciences of the United States of America*, 2005. 102(40): p. 14422-7.

43. Yang, Z., et al., *Myxococcus Xanthus Dif* Genes Are Required for Biogenesis of Cell Surface Fibrils Essential for Social Gliding Motility. *J Bacteriol*, 2000. 182(20): p. 5793-8.

Chapter 4

The bacterial second messenger molecule, c-di-GMP, modulates the sensitivity of cells to navigate in oxygen gradients

This chapter is a manuscript in preparation for publication by Matthew H. Russell, Amber, N. Bible, Xin Fang, Jessica Gooding, Shawn Campagna and Mark Gomelsky and Gladys Alexandre

Author contributions

GA designed and led the experimental project. Xin Fang and Mark Gomelsky conducted experiments on c-di-GMP binding to Tlp1 and analyzed the data. I did sample collection for c-di-GMP detection by mass spectrometry as well as synthesis of internal standard. Jessica Gooding and I conducted the mass spectrometry experiments before Jessica and Shawn Campagna analyzed the raw data. Jessica and I analyzed the data and normalized c-di-GMP concentrations based on protein concentrations taken at time of sample collection by me. Construction and complementation of wild type and mutant alleles of *tlp1* were conducted by me as well as characterization and behavioral assays including aerotaxis. Amber Bible conducted molecular cloning for *chsA*::Tn5 and its complemented variant, soft agar plate assays, microscopy, and analyzed data. I conducted aerotaxis assays for *chsA*::Tn5(pRK415) and *chsA*::Tn5(pRKChsA). Gladys Alexandre and I designed the experiments, analyzed the data and Gladys wrote a majority of the paper. I wrote the remainder.

Abstract

In order to maintain a competitive advantage under various environmental conditions, all cells, must be able to coordinate changes in their metabolism with acute sensory ability. Bacterial chemotaxis signal transduction guides motile cells in gradient of attractants and repellents and is characterized by a remarkable sensitivity over a broad dynamic range that allows bacteria to quickly adapt to change in the surrounding. Cells must also remain sensitive to environmental cues that are pertinent to their metabolism and thus mechanism(s) that coordinate metabolism

with sensing are expected to exist. Here we show that c-di-GMP binding to the C-terminal domain of a receptor mediates sensory adaptation. The *Azospirillum brasilense* chemotaxis receptor, Tlp1, functions in chemotaxis and aerotaxis and it is shown here to bind c-di-GMP at its C-terminal PilZ domain, with high affinity. C-di-GMP binding to Tlp1 affected the ability of cells to navigate in oxygen gradient (aerotaxis) but it had no effect on chemotaxis. Increased aeration correlated with increased in intracellular c-di-GMP content of cells that could be detected by Tlp1. Similar to other bacteria, conditions of increased c-di-GMP concentrations trigger transition to a sessile lifestyle in *A. brasilense* but c-di-GMP binding to Tlp1 promoted motility in oxygen gradients and prevented transition to a sessile lifestyle. Aerotaxis allows *A. brasilense* to seek niches where metabolism is optimum. Therefore, sensing the intracellular pool of the second-messenger signaling molecule, c-di-GMP, by Tlp1 represents a strategy by which a chemotaxis receptor functions to integrate metabolic status with sensory sensitivity to afford cells with extended metabolic opportunities.

Introduction

Motile bacteria detect changes in environmental conditions and respond by navigating toward niches where conditions are optimal for growth by chemotaxis [1]. This behavior is widespread in various environments and it is especially significant in bacteria found in soils and sediments [2]. In chemotaxis, physico-chemical cues are detected by dedicated receptors that relay information to the flagellar motors via a conserved signal transduction cascade [3]. The model organism for chemotaxis, *Escherichia coli*, possesses five transmembrane chemoreceptors (Tar, Tsr, Tap, Trg and Aer) and the sensory specificities for each of these receptors have been determined [4]. The chemoreceptors in *E. coli*, as well as in all other bacterial species studied in this respect, are organized as higher ordered arrays of trimers of receptors dimers that form an extended lattice of interacting receptor proteins at one or both cell poles [5-7]. Most bacterial species have a greater number of chemoreceptors than *E. coli* [8]; however, the sensory specificity of most chemotaxis receptors encoded within bacterial genomes remains unknown.

Azospirillum brasilense are motile bacteria and possess a single polar flagellum. Motile *A. brasilense* cells respond tactically not only by biasing the probability of changes in the swimming direction of the polar flagellum but also by modulating swimming velocity, via at least two distinct chemotaxis pathways [9]. Aerotaxis (movement in oxygen gradients) is the strongest behavioral response in this organism [10]. In oxygen gradients, *A. brasilense* cells quickly navigate to a specific zone where the oxygen concentration is low enough (3-5 μM) to support their microaerobic lifestyle [11]. Both chemotaxis and aerotaxis serve as major mechanisms by which cells seek a position in gradients where metabolism is optimal. Most chemoeffectors are sensed indirectly in *A. brasilense* via net changes in intracellular energy levels through their metabolism [12]. Chemo- and aerotactic responses to changes in energy metabolism have been identified in several bacterial species and are collectively referred to as “energy taxis” [13-16]. An energy taxis receptor, AerC, has been previously shown to mediate the ability of motile *A.*

brasilense cells to locate niches compatible with nitrogen fixation, via an FAD cofactor present within the sensory domain of AerC [17]. A transmembrane chemoreceptor, Tlp1, has also been shown to function as an energy taxis receptor in *A. brasilense*. The sensory domain of Tlp1 is located in the periplasm and lacks a recognizable motif for redox or energy sensing, and thus the energy-related parameter sensed by Tlp1 is unknown [18]. Tlp1 has also been shown to possess a PilZ domain at its C-terminus [19]. PilZ domains are ubiquitous in bacterial genomes and they have been shown to bind the bacterial second messenger molecule, c-di-GMP [20-22]. While c-di-GMP signaling promotes transition to a sessile lifestyle [23-25], aerotaxis or chemotaxis allows motile cells to further explore the surroundings to seek niches which are optimum for growth [26, 27]. The domain arrangement of Tlp1 thus provided an opportunity to test the effect of these conflicting signals on bacterial behavior as well as to probe the mechanism by which they would be integrated.

Here, we demonstrate that c-di-GMP binds to the PilZ domain of Tlp1 to regulate its activity in aerotaxis (but not in chemotaxis) under conditions of increased aeration, which correlates with increased c-di-GMP production. C-di-GMP bound to Tlp1 promotes sensitivity to changes in oxygen gradients and affords cells the ability to navigate by aerotaxis, thereby preventing transition to a sessile lifestyle. Results presented here illustrate how motility may trump second messenger signaling by c-di-GMP, which has been thus far shown to promote attachment. Given the ubiquity of c-di-GMP signaling in bacteria and the obvious requirement to coordinate sensing with motility and attachment, these findings are directly relevant to other bacterial species.

Results

The PilZ domain of Tlp1 binds c-di-GMP

To test whether the PilZ domain of Tlp1 binds c-di-GMP, we used a C-terminal Tlp1 fragment fused to MBP (as described in the Experimental Procedures) and analyzed its ability to bind c-di-GMP using equilibrium dialysis [28]. Tlp1 bound c-di-GMP with an apparent K_d 6.9 ± 1.2 μM (Figure 4.1). Given that only a fragment of Tlp1 was tested, it is possible that the actual K_d is lower. However, the obtained value correlates well with the estimated intracellular c-di-GMP levels in the proteobacterial species, believed to be in the 1–10 μM range [29]. Therefore, Tlp1 is likely able to respond to physiologically relevant alterations in c-di-GMP levels. The binding capacity of Tlp1, B_{max}, calculated based on the equilibrium dialysis experiments, was 2.1 ± 0.1 mol c-di-GMP (mol protein)$^{-1}$. This suggests that Tlp1 binds two molecules of c-di-GMP, i.e. similar to *E. coli* YcgR [28] and *Pseudomonas putida* PP4397 [30]. Two Tlp1 variants, Tlp1^{R562A} and Tlp1^{R562AR563A}, in which conserved arginine residues thought to be involved in c-di-GMP binding were mutated to alanine, were also tested in the same manner. The Tlp1^{R562A} protein showed significantly lower capacity to bind c-di-GMP, with an apparent K_d 21.8 ± 7.1 μM (Figure 4.1). Arg562 lies close to Arg563, the residue that physically interacts with c-di-GMP, however, it is nonessential for c-di-GMP binding. The drastic drop in c-di-GMP binding observed in the Tlp1^{R562A} protein was therefore somewhat unexpected. It suggests that the residues near the c-di-GMP-binding loop can significantly influence affinity for c-di-GMP. However, it was fully expected that the Tlp1^{R562AR563A} variant that also lacks the essential residue for binding Arg563 would be incapable of binding, as was observed experimentally (Figure 4.1).

The PilZ domain of Tlp1 is dispensable for chemotaxis

Previous data have indicated that Tlp1 contributes to chemotaxis towards rapidly oxidizable substrates, such as organic acids [18], a behavior that can be readily detected in the soft agar plate assays. Compared to wild type chemotaxis, the Δ*tlp1* mutant strain showed a significant defect in

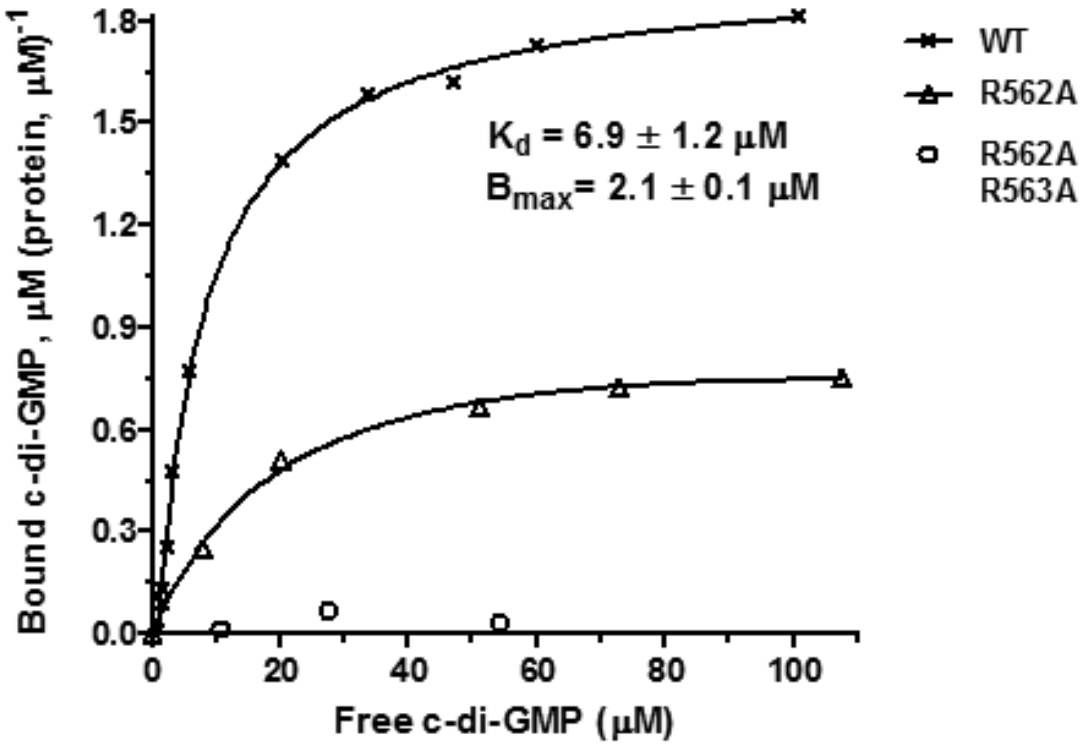

Figure 4.1: Saturation plot of equilibrium binding between Tlp1 and c-di-GMP. C-di-GMP was injected into one cell of a dialysis cassette, while MBP–Tlp1 protein was injected into the opposite cell, separated by a membrane with a 10-kDa cutoff. Concentrations of free and protein-bound c-di-GMP were measured following the establishment of an equilibrium.

chemotaxis to several organic acids that are strong attractants for *A. brasilense* (Figure 4.2). Chemotaxis was restored to wild type levels by expressing *tlp1* from a low copy plasmid in the Δ*tlp1* mutant background. A similar functional complementation of the Δ*tlp1* mutant strain chemotaxis defect was obtained by expressing a Tlp1 variant protein carrying an in-frame deletion of the PilZ domain (Δ*tlp1* (pRKTlp1$^{\Delta PilZ}$)), or expressing variants of Tlp1 in which residues implicated in c-di-GMP binding were mutated (Δ*tlp1* (pRKTlp1^{R562A}) and Δ*tlp1* (pRKTlp1^{R562AR563A})). The wild type and variant Tlp1 proteins were expressed at similar levels in all strains and these were comparable to those of the wild type protein (data not shown). These results indicate that the PilZ domain of Tlp1 is dispensable for chemotaxis.

The PilZ domain of Tlp1 affects aerotaxis responses

The strongest behavioral responses of *A. brasilense* motile cells are observed in oxygen gradients and Tlp1 was previously shown to mediate aerotaxis in this organism [18]. Aerotaxis can be detected in spatial gradients established in flat capillary tubes where the oxygen gradient is created by diffusion of oxygen from the air into the cell suspension inside the tube [18]. Under these conditions, the wild type *A. brasilense* strain form an aerotactic band within 2 minutes at some distance from the meniscus which corresponds to a position in the gradient where metabolism is optimum [11]. Cells within the band and outside the band remain motile and the aerotactic band remains stable. As expected, the Δ*tlp1* mutant was significantly affected in its ability to form an aerotactic band in that while it was capable of sensing and responding to the oxygen gradient, it formed an aerotactic band farther away from the meniscus compared to the wild type strain (Figure 4.3). Expression of the wild type Tlp1 restored wild type aerotaxis behavior to the Δ*tlp1* mutant strain. All of the Tlp1$^{\Delta PilZ}$, Tlp1^{R562A}, Tlp1^{R562AR563A} variants failed to

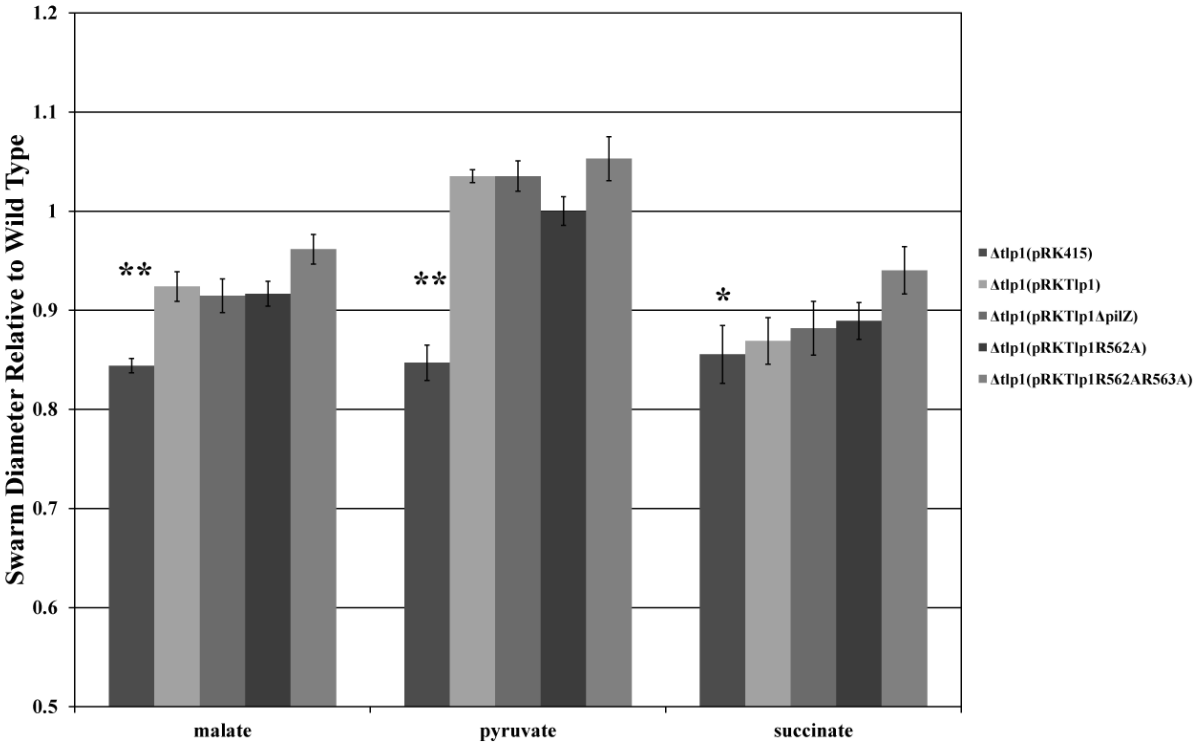

Figure 4.2: Soft agar assay for detection of chemotaxis to organic acids in *A. brasilense* Sp7, its Δ*tlp1* mutant derivatives. Chemotactic ring diameters were measure for the wild type strain expressing pRK415, *Δtlp1* expressing empty vector, wild type Tlp1, or mutant derivatives. Cells were tested for chemotaxis defects to organic acids in minimal semi-solid media supplemented with 0.1% (w/v) ammonium chloride and 10mM of carbon source tested. Plates were incubated at 28°C for 48 hours and ring diameters measured. Resulting diameters are displayed relative to wild type diameters. *Δtlp1* was significantly defective to all acids tested. However, this defect was complemented by all variations of Tlp1 suggesting the PilZ domain is not essential for chemotaxis to organic acids as measured by the soft agar assay.

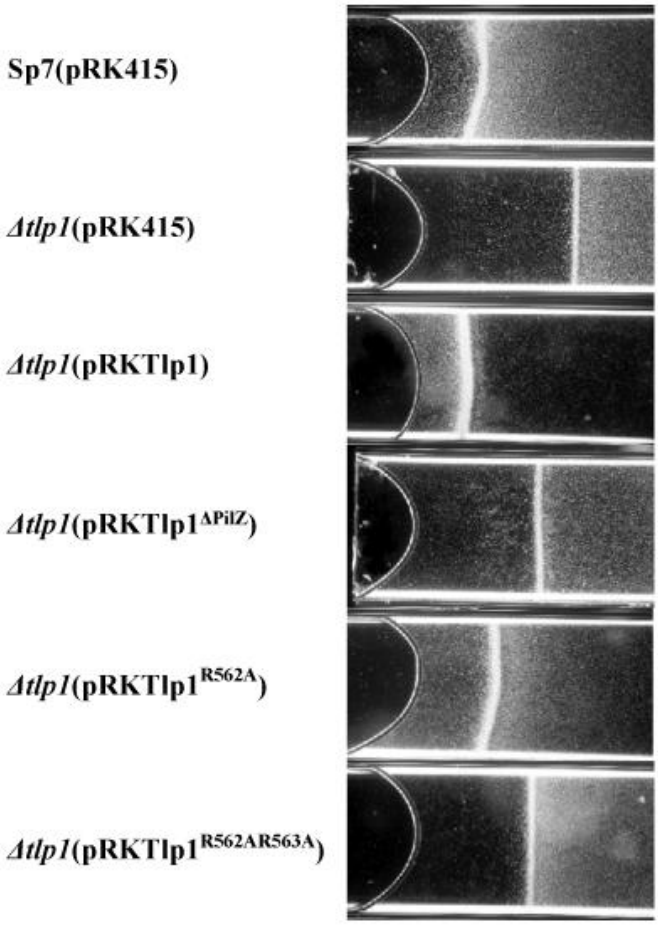

Figure 4.3: Spatial aerotaxis mediated by Tlp1, Tlp1$^{\Delta PilZ}$, Tlp1^{R562A} and Tlp1^{R562AR563A}. Motile cells grown to exponential phase (O.D.$_{600nm}$ ~0.7-0.8) were washed and resuspended in a flat glass capillary (see Experimental Procedures). The cells were of equivalent cell density (O.D.$_{600nm}$ of 1.0). Within 2 minutes, the wild type *A. brasilense* Sp7(pRK415) forms an aerotactic band at a certain distance from the meniscus (air/liquid interface) where the dissolved oxygen concentration is optimum for intracellular energy production [11]. The *Δtlp1*(pRK415) mutant forms an aerotactic band farther away from the meniscus. Expressing Tlp1 in the *Δtlp1* as pRKTlp1 restored wild type aerotaxis and aerotactic band position in the gradient. Expression of Tlp1$^{\Delta PilZ}$, Tlp1^{R562A} or Tlp1^{R562AR563A} as *Δtlp1*(pRKTlp1$^{\Delta PilZ}$), *Δtlp1*(pRKTlp1^{R562A}), or Δtlp1(Tlp1^{R562AR563A}) failed to rescue the mutant phenotype.

fully rescue the Δ*tlp1* mutant aerotaxis phenotype; however, the Tlp1^{R562A} appeared to partially complement the aerotaxis defect of the mutant while both Tlp1$^{\Delta PilZ}$ and Tlp1^{R562AR563A} behaved similar to the Δ*tlp1* mutant, carrying an empty vector. These results suggest that the PilZ domain of Tlp1 and its ability to bind c-di-GMP modulate the function of Tlp1 in aerotaxis.

C-di-GMP binding to Tlp1 affects the ability of cells to increase swimming velocity in oxygen gradients

Next, we analyzed the response of strains expressing Tlp1 or its variants in the temporal gradient assay for aerotaxis. In this assay, motility parameters that characterized the aerotaxis response to an increase (air addition) or a decrease (air removal) in aeration conditions in the atmosphere of the cells can be simultaneously determined. In this assay, wild type *A. brasilense* cells respond immediately to air removal and air addition by both transiently increasing the swimming velocity as well as decreasing the probability of changes in the swimming direction (i.e., motility bias is "smoother"), before adapting to the imposed aeration conditions [9].

As expected, wild type *A. brasilense* cells expressing an empty vector responded to air removal and air addition in the atmosphere by transiently increasing the swimming speed before adapting to these conditions (Figure 4.4). Similar to the aerotaxis response of the wild type strain, the *Δtlp1* mutant strain also responded by increasing swimming speed upon both air removal and addition; however, the response time of the Δ*tlp1* mutant to such changes in aeration conditions was shorter compared to wild type, and most notably upon air addition (~3 sec.). Expressing wild type Tlp1 in the Δ*tlp1* mutant background restored the swimming velocity response time to values comparable to that of the wild type strain, upon both air removal (~30 sec.) and air addition (~30 sec.). In contrast, when the *Δtlp1* mutant strain was complemented with Tlp1 variants defective (Tlp1$^{\Delta PilZ}$, Tlp1^{R562AR563A}) or severely impaired (Tlp1^{R562A}) in c-di-GMP binding, there was no

Figure 4.4: Temporal Changes in swimming velocity of *A. brasilense* wild type and its *tlp1* variant derivatives in the gas perfusion chamber assay. A cell suspension was analyzed for temporal changes in swimming speed upon air removal (up arrow) and air addition (down arrow) by motion tracking analysis software from video segments recorded during assays. Cells were equilibrated 6 minutes prior to air removal and air addition. A, Average swimming speed of all motile Sp7(pRK415) cells in frame over 20 second intervals around time of air removal and air addition determined by Prism non-linear regression. B, Average swimming speed of all motile *Δtlp1*(pRK415) cells in frame over 20 second intervals around time of air removal and air addition determined by Prism non-linear regression. C, Average swimming speed of all motile *Δtlp1*(pRKTlp1) cells in frame over 20 second intervals around time of air removal and air addition determined by Prism non-linear regression. D, Average swimming speed of all motile *Δtlp1*(pRKTlp1$^{\Delta PilZ}$) cells in frame over 20 second intervals around time of air removal and air addition determined by Prism non-linear regression. E, Average swimming speed of all motile *Δtlp1*(pRKTlp1^{R562A}) cells in frame over 20 second intervals around time of air removal and air addition determined by Prism non-linear regression. F, Average swimming speed of all motile *Δtlp1*(pRKTlp1^{R562AR563A}) cells in frame over 20 second intervals around time of air removal and air addition determined by Prism non-linear regression.

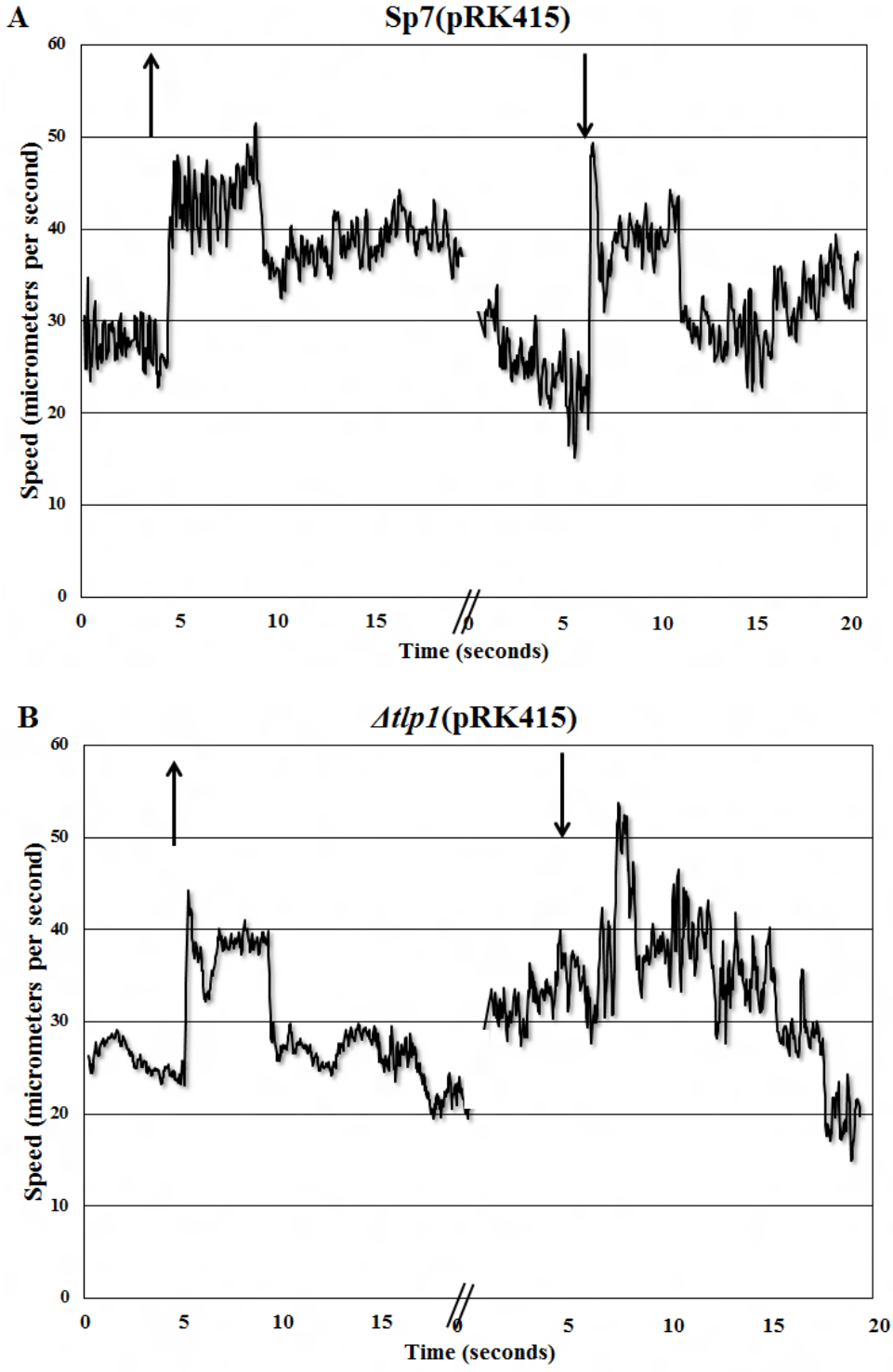
A
Sp7(pRK415)
Speed (micrometers per second)
Time (seconds)
B
Δtlp1(pRK415)
Speed (micrometers per second)
Time (seconds)

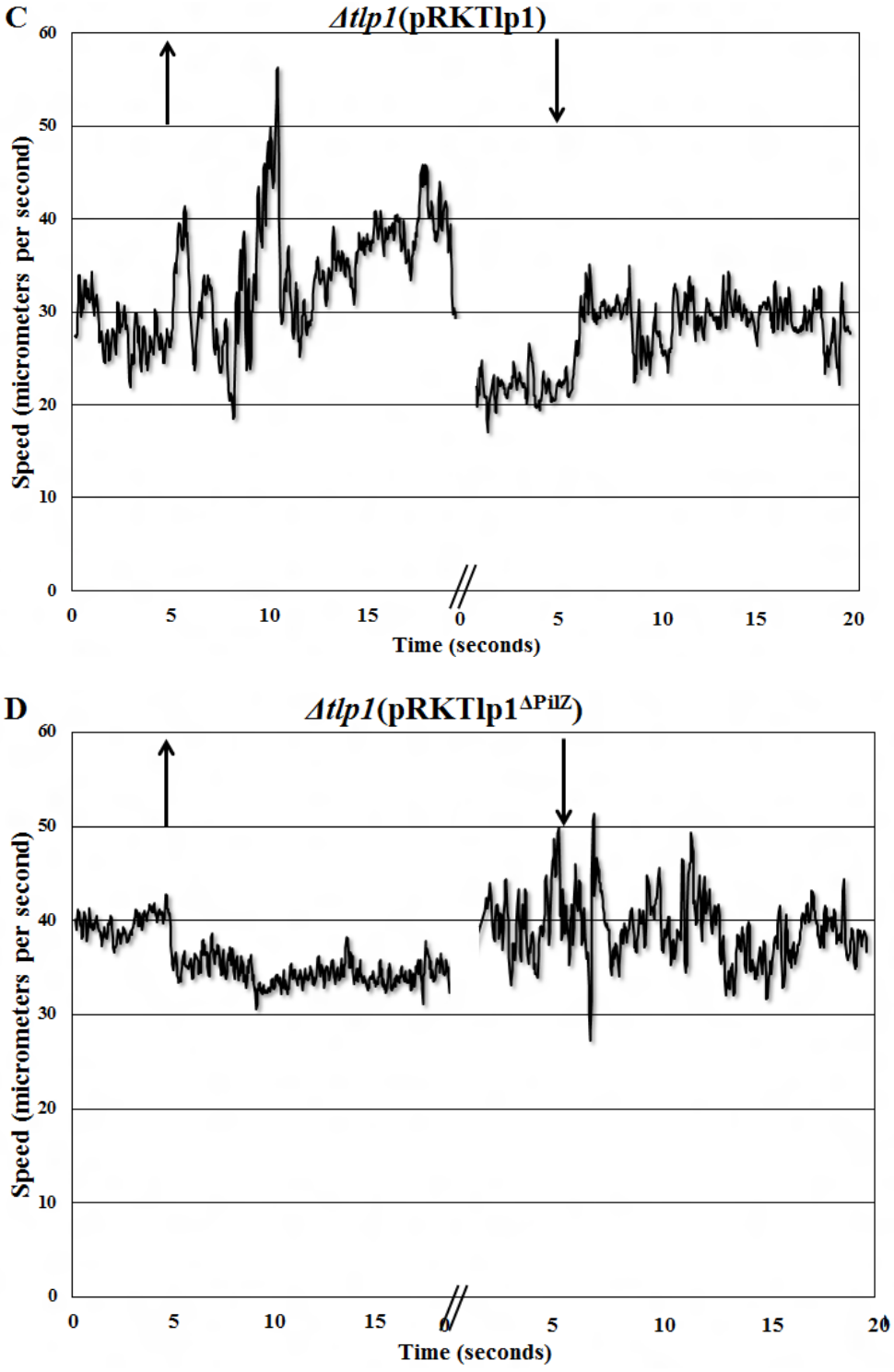

Figure 4.5, continued

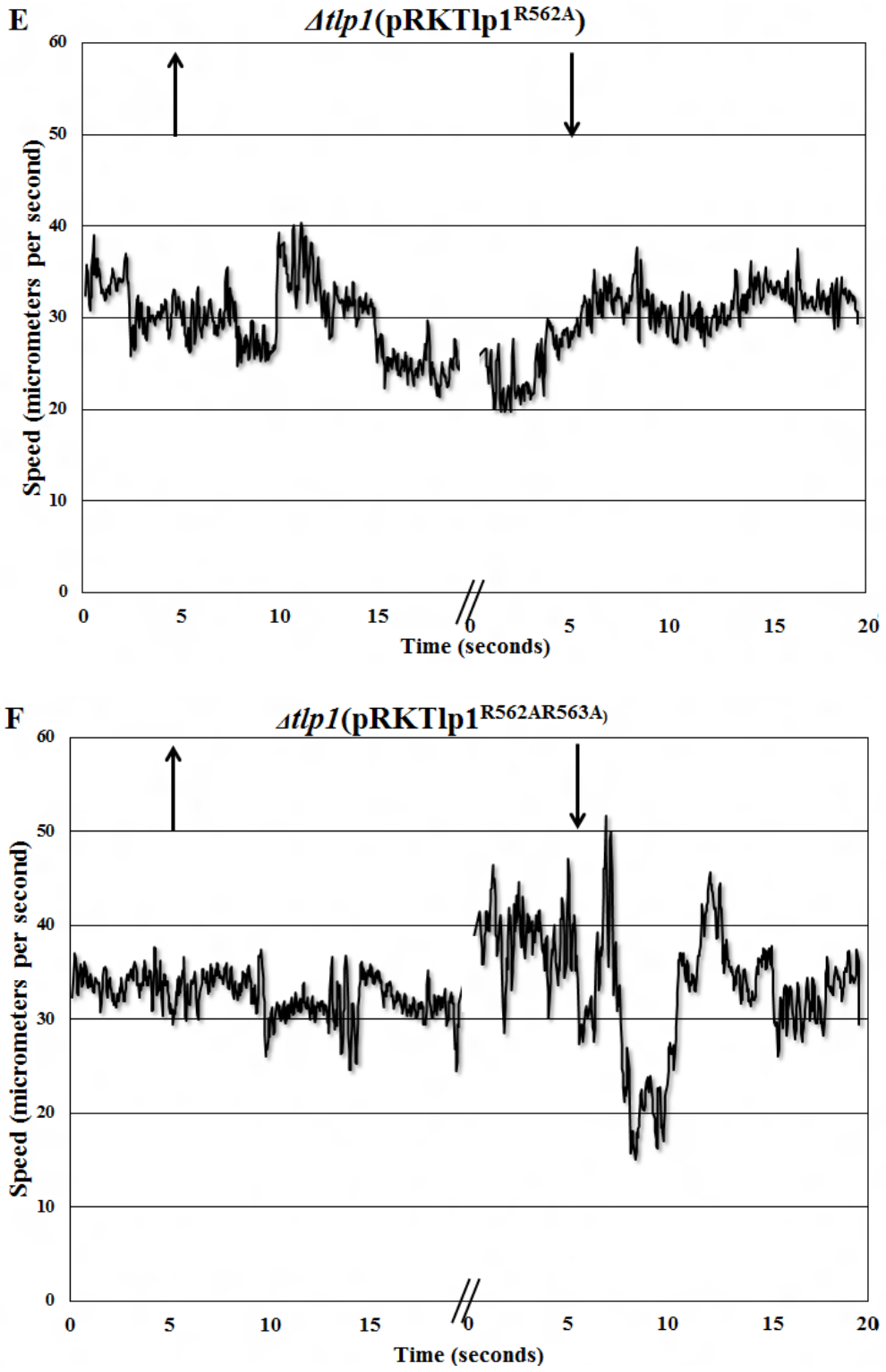

Figure 4.5, continued

functional complementation and the cells were unable to increase swimming speed upon either air removal or air addition (Figure 4.4D-F). These results suggest that cells expressing Tlp1 variants affected in c-di-GMP binding are no longer sensitive to changes in aeration conditions. These data also imply that expressing Tlp1 variants affected in c-di-GMP binding has a dominant–negative effect on the ability of the cells to respond to changes in aeration conditions via changes in swimming velocity. $Tlp1^{\Delta pilZ}$, $Tlp1^{R562A}$, or $Tlp1^{R562AR563A}$ are thus probably able to interact with the cellular machinery that controls changes in the swimming velocity, but lack of c-di-GMP binding appears to affect Tlp1 function in coupling sensing (aeration) and response (swimming velocity).

C-di-GMP binding to Tlp1 regulates the ability of cells to modulate changes in the swimming reversal frequency in oxygen gradients

Upon decreased (air removal) or increased (air addition) aeration in the atmosphere of the cells, the wild type not only swim faster but also with a reduced reversal frequency, before adapting to these conditions [18]. The Δ*tlp1* mutant strain responded to air removal by reducing the probability of changes in the swimming direction, with a pattern that was not significantly different ($p<0.05$) from the response of the wild type, suggesting that Tlp1 play only a minor role in sensing changes in aeration under these conditions (Figure 4.5A). Expressing the wild type Tlp1 in the Δ*tlp1* mutant background did not affect the response which remained similar to that of the wild type (Figure 4.5A). Surprisingly, expressing $Tlp1^{\Delta PilZ}$, $Tlp1^{R562A}$ or $Tlp1^{R562AR563A}$ caused the Δ*tlp1* mutant strain to respond to air removal by increasing its probability of changes in the swimming direction briefly (about 10 sec), before adapting to the aeration conditions (Figure 4.5B). This unexpected response was the opposite of wild type or the Δ*tlp1*mutant strain regardless of expression of *tlp1* in this background (Figure 4.5A). These results suggest that the

Figure 4.5: Temporal changes in swimming reversal frequency of wild type *A. brasilense* and its *tlp1* derivatives in the gas perfusion chamber assay. The swimming reversal frequency is determined as the average change in the swimming direction per second and per cell. The values were obtained from video recorded during the assay by manual analysis of 30 frame segments (taken as 1 second) using ImageJ software. The arrows pointing up indicate event of air removal from the atmosphere of the cells. The arrow pointing down indicates event of air addition to the atmosphere of the cells. The cells were equilibrated for 5 minutes in air prior to air removal or in N2 prior to air addition. A, Swimming reversal frequency of Sp7(pRK415), *Δtlp1*(pRK415), and *Δtlp1*(pRKTlp1) before and after air removal. B, Swimming reversal frequency of *Δtlp1*(pRKTlp1$^{\Delta PilZ}$), *Δtlp1*(pRKTlp1^{R562A}), and *Δtlp1*(pRKTlp1^{R562AR563A}) before and after air removal. C, Swimming reversal frequency of Sp7(pRK415), *Δtlp1*(pRK415), and *Δtlp1*(pRKTlp1) before and after air addition. D, Swimming reversal frequency of *Δtlp1*(pRKTlp1$^{\Delta PilZ}$), *Δtlp1*(pRKTlp1^{R562A}), and *Δtlp1*(pRKTlp1^{R562AR563A}) before and after air addition.

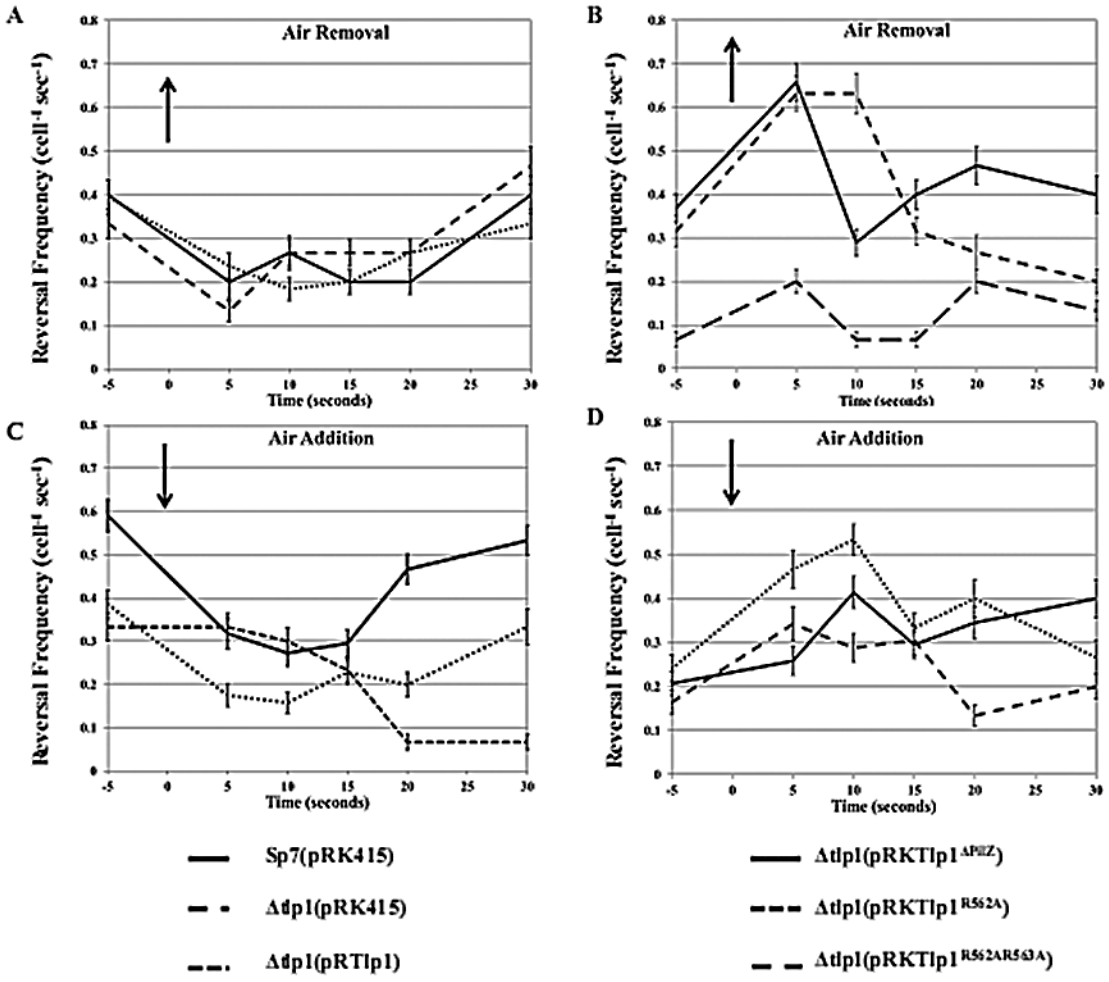
A
Air Removal
Reversal Frequency (cell-1 sec-1)
Time (seconds)
B
Air Removal
Reversal Frequency (cell-1 sec-1)
Time (seconds)
C
Air Addition
Reversal Frequency (cell-1 sec-1)
Time (seconds)
D
Air Addition
Reversal Frequency (cell-1 sec-1)
Time (seconds)
Sp7(pRK415)
Δtlp1(pRK415)
Δtlp1(pRTlp1)
Δtlp1(pRKTlp1ΔPilZ)
Δtlp1(pRKTlp1R562A)
Δtlp1(pRKTlp1R562AR563A)

ability of Tlp1 to bind c-di-GMP affects how the signal (aeration) is processed by the cellular machinery that controls the probability of changes in swimming direction. In addition, expressing Tlp1^{R562AR563A}, which cannot bind c-di-GMP, but possesses an otherwise intact PilZ domain, but not Tlp1$^{\Delta PilZ}$ or Tlp1^{R562A}, also caused the cells to have a decreased steady state swimming bias (0.07 reversals sec^{-1}), relative to the wild type cells (0.4 reversals sec^{-1}) (Figure 4.5B). This further supports the notion that c-di-GMP binding to Tlp1 modulates the sensitivity of Tlp1 to changes in aeration and signal processing from receptor to the flagellar motor where changes in the swimming direction can be controlled. Noticeably, inability of Tlp1 to bind c-di-GMP causes the receptor to transduce an inverted signal.

Upon air addition, the wild type strain immediately decreased the probability of changes in the swimming direction for several seconds (~30 sec.) before adapting to the ambient conditions and returning to a steady state swimming behavior (0.6 reversals sec^{-1}) (Figure 4.5C). In contrast, the *Δtlp1* mutant did not respond to air addition and there was no change in the swimming motility bias of these cells immediately upon air addition; instead, the swimming reversal frequency decreased gradually (Figure 4.5C). Expressing Tlp1 in the *Δtlp1* mutant restored the wild type response to air addition (Figure 4.5C). These observations indicate that Tlp1 contributes most to aerotaxis upon increased aeration (air addition), further suggesting that the defect in aerotaxis observed in a spatial gradient assay in a strain lacking Tlp1 results primarily, if not exclusively, from a failure to sense increased aeration. The variants Tlp1$^{\Delta PilZ}$, Tlp1^{R562A} or Tlp1^{R562AR563A} caused the cells to respond to air addition by increasing the probability of changes in swimming direction, i.e. to display a repellent response to air addition (Figure 4.5D). This response was opposite to the attractant response (decrease in reversal frequency) of the wild type strain under similar conditions and further confirms that c-di-GMP binding to Tlp1 affects how the signal

regarding aeration conditions is processed by the molecular machinery that controls the probability of changes in the swimming direction.

c-di-GMP binding to Tlp1 modulates aerotaxis controlled by Che1 as well as other pathway(s)

The results above suggested that c-di-GMP binding to Tlp1 regulates all the locomotor responses that contribute to aerotaxis in *A. brasilense*, with Tlp1 contribution to these responses being more pronounced when cells experienced increased aeration.

In *A. brasilense*, the signal output of the Che1 pathway controls the ability of cells to increase the swimming velocity upon temporal changes in aeration conditions [9], prompting us to test if c-di-GMP binding to Tlp1 mediates its effect on the locomotor behavior of cells via Che1. First, we compared the aerotaxis responses of a Δ*che1* mutant as well as a double mutant lacking both Tlp1 and Che1 (Δ*tlp1*Δ*che1*) in the gas perfusion chamber assay (Figure 4.7). Consistent with previous results [9] and in contrast to the wild type strain, a Δ*che1* mutant was incapable of responding to air removal or air addition by increasing swimming velocity and a double Δ*che1*Δ*tlp1*mutant strain behaved as the Δ*che1* mutant strain (Figure 4.6). Expressing the wild type Tlp1 or any of the Tlp1 variants ($Tlp1^{\Delta PilZ}$, $Tlp1^{R562A}$ or $Tlp1^{R562AR563A}$) did not have any effect on the swimming velocity upon air removal or addition. These results indicate that Tlp1 effects on changes in swimming velocity upon changes in aeration are Che1-dependent. Che1 was shown to affect the swimming reversal frequency by an indirect, yet unknown mechanism [9, 31, 32]. However, a Δ*che1* mutant strain swam with a very low probability of changes in the swimming direction compared to the wild type strain and in contrast to the wild type, the swimming bias of this

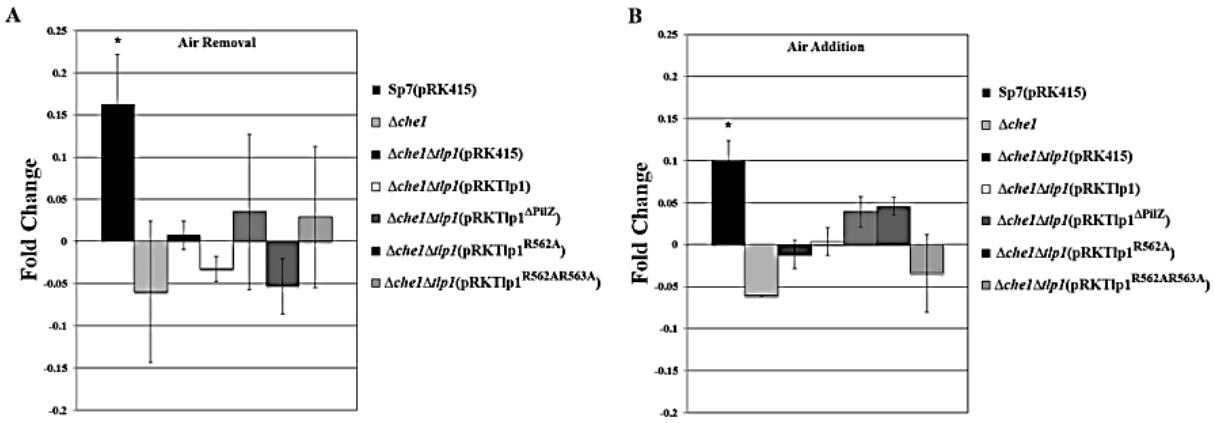

Figure 4.6: Fold change in swimming velocity upon air removal and air addition for *Δche1Δtlp1* double mutants. Fold change swimming velocity (μm/sec) was determined from the average change in the swimming direction per cell compared to before air removal or air addition. The swimming velocity values were obtained by motion tracking analysis of video segments recorded during the assay. Speed of cells was calculated for each strain before and after change in aeration. A, Fold change in swimming velocity upon air removal. B, Fold change in swimming velocity upon air addition. Asterisk denotes significant fold change (p-value < 0.05).

mutant strain did not change upon air removal or air addition, suggesting that this strain is not sensitive to the changes in aeration conditions. Deleting both *che1* and *tlp1* caused the cells to swim with a greater steady state reversal frequency (0.26 ± 0.03 sec^{-1}) relative to the effect of the Δ*che1* mutation. The increased reversal frequency was intermediate between that of the Δ*che1* (0.07 ± 0.02 sec^{-1}) and of the Δ*tlp1* (0.33 ± 0.03 sec^{-1}) strains (Table 4.1). As expected from the behavior of the Δ*che1* mutant, a double Δ*che1Δtlp1* mutant strain failed to decrease its reversal frequency upon air removal or air addition (Table 4.1). These results suggest that Tlp1 may function in a Che1-dependent manner to transduce sensory signals (aeration) to the molecular machinery controlling changes in the swimming direction. If this hypothesis is correct, then expressing the wild type Tlp1 in the Δ*che1*Δ*tlp1* mutant background should have no effect on the ability of cells to modulate the swimming direction upon changes in aeration conditions. However, this is not what we observed. Upon air removal, the Δ*che1*Δ*tlp1* mutant expressing Tlp1 increased the reversal frequency and thus displayed an inverted response relative to the wild type (Table 4.1). These results suggest that Che1 contributes to how the information is processed from Tlp1 since the Δ*che1*Δ*tlp1*(pRKTlp1) cells responded to changes in aeration but the response was inverted relative to the wild type. Expressing $Tlp1^{\Delta PilZ}$, $Tlp1^{R562A}$ or $Tlp1^{R562AR563A}$ variants, which are affected in c-di-GMP binding in the Δ*che1*Δ*tlp1* mutant strain, was sufficient to restore a wild type response (Table 4.1). These results provide further support to the hypothesis that the ability of Tlp1 to bind c-di-GMP affects signal transduction leading to changes in the swimming reversal frequency, and further suggest that c-di-GMP binding to Tlp1 affects Che1 contribution to this response. The Δ*che1*Δ*tlp1*(pRKTlp1) responded to air addition similar to the wild type strain, i.e., with an immediate decrease in the reversal frequency (wild type: 0.43 ± 0.05 to 0.29 ± 0.04 sec^{-1} and *Δche1Δtlp1*(pRKTlp1): 0.4 ± 0.04 to 0.07 ± 0.02 sec^{-1}).

Table 4.1: Swimming reversal frequency of *A. brasilense* Sp7, *Δche1*, and *Δche1Δtlp1* double mutant derivatives upon temporal changes in aeration.

Gas atmosphere [a]	**Air**	**N_2**	**N_2**	**N_2**	**N_2**	**Air**	**Air**	**Air**
Time[b]	**55 sec**	**65 sec**	**70 sec**	**75 sec**	**415 sec**	**425 sec**	**430 sec**	**435 sec**
Sp7(pRK415)	0.4 ± 0.03	0.20 ± 0.04[c]	0.27 ± 0.04[c]	0.20 ± 0.03[c]	0.43 ± 0.05	0.29 ± 0.04[c]	0.29 ± 0.03[c]	0.21 ± 0.03[c]
Δche1	0.13 ± 0.03	0.07 ± 0.02	0.07 ± 0.02	0.13 ± 0.02	0.07 ± 0.02	0.07 ± 0.02	0	0
***Δche1Δtlp1*(pRK415)**	0.27 ± 0.03	0.27 ± 0.03	0.20 ± 0.03	0.20 ± 0.03	0.27 ± 0.03	0.20 ± 0.03	0.13 ± 0.02	0.20 ± 0.03
***Δche1Δtlp1*(pRKTlp1)**	0.21 ± 0.03	0.59 ± 0.03[c]	0.5 ± 0.03[c]	0.27 ± 0.03	0.40 ± 0.04	0.07 ± 0.02[c]	0.13 ± 0.02	0.13 ± 0.02
***Δche1Δtlp1*(pRKTlp1$^{\Delta PilZ}$)**	0.37 ± 0.04	0.23 ± 0.02	0.14 ± 0.02[c]	0.13 ± 0.02[c]	0.13 ± 0.02	0.13 ± 0.02	0.13 ± 0.02	0.13 ± 0.02
***Δche1Δtlp1*(pRKTlp1^{R562A})**	0.43 ± 0.03	0.20 ± 0.03[c]	0.40 ± 0.03	0.33 ± 0.03	0	0.07 ± 0.02	0	0.20± 0.03
***Δche1Δtlp1*(pRKTlp1^{R562AR563A})**	0.33 ± 0.03	0.07 ± 0.02[c]	0.53 ± 0.03	0.27 ± 0.03	0.48 ± 0.04	0.22 ± 0.03[c]	0.33 ± 0.03	0.47 ± 0.03

[a] the atmosphere composition is determined by the nature of the gas flowing above the cell suspension within the gas perfusion chamber at the time cell reversal events were calculated; either compressed air (Air, 21% oxygen) or pure nitrogen (100% N_2) were used.

[b] Time elapsed from beginning of temporal assay (but not including a 5 minutes equilibration under air atmosphere at the beginning of the assay) with air removal (switch from air to N_2) occurring at 60 seconds and air addition (switch from N_2 to air) occurring at 420 seconds

[c] denotes p-value < 0.05 compared to reversal frequency prior to removal or addition

These results indicate that Che1 is dispensable and imply that Tlp1 relay sensory information to regulate the swimming reversal frequency independently of Che1, under these conditions. Consistent with this hypothesis, when a full-length Tlp1 variant unable to bind c-di-GMP ($Tlp1^{R562AR563A}$) was expressed in the Δ*che1*Δ*tlp1* mutant, air removal evoked a transient decrease in the reversal frequency that was similar to the wild type response, albeit with a somewhat shorter response time. Expressing $Tlp1^{\Delta PilZ}$ or $Tlp1^{R562A}$ under these conditions caused the cells to display a very low steady state swimming reversal frequency (0.13 $cell^{-1}$ sec^{-1} for Δ*che1*Δ*tlp1*($Tlp1^{\Delta PilZ}$) or 0 $cell^{-1}$ sec^{-1} for Δ*che1*Δ*tlp1*($Tlp1^{R562A}$)) (Table 4.1) and these cells were also no longer able to respond to air addition, similar to the Δ*che1* or the Δ*che1*Δ*tlp1* (pRK415) mutants. Together with the major function of Tlp1 under increased aeration conditions, these results indicate that the Tlp1 variants lacking the PilZ domain ($Tlp1^{\Delta PilZ}$) or possessing a partially functional c-di-GMP binding site ($Tlp1^{R562A}$) are non-functional variants for signal transduction under these conditions. This hypothesis further implies that binding of c-di-GMP may be essential to maintain Tlp1 function during aerotaxis, with c-di-GMP binding promoting Tlp1 activity under conditions of increased aeration for controlling Che1-independent changes in the reversal frequency. Taken together, the results obtained indicate that Tlp1 sensory input modulates Che1 effects on the swimming velocity as well as the indirect effect(s) of this pathway on the swimming reversal frequency but it also appears to regulate the swimming reversal frequency in a Che1-independent manner, i.e., via another pathway.

C-di-GMP production varies in oxygen gradients

Previous results indicated that intracellular c-di-GMP may be sensed by Tlp1. Recently, a putative diguanylate phosphodiesterase (EAL) enzyme, ChsA, was suggested to function in chemotaxis in *A. brasilense* [33]. Sequence analysis indicated that ChsA possesses a N-terminal

PAS domain (amino acids 33 to 110) with conserved residues for a heme-binding pocket [34], suggesting a possible function in oxygen sensing. Thus, we first analyzed the chemotaxis and aerotaxis behaviors of a mutant strain lacking *chsA* (*chsA*::Tn5; [33]) and found severe defects in both behaviors (Figure 4.7). The *chsA*::Tn5 mutant did not form an aerotactic band and the limited complementation obtained in chemotaxis was not sufficient to restore aerotaxis in this strain. Temporal assays also confirmed that *chsA*::Tn5 did not respond to air removal or air addition by changes in swimming reversal frequency (Table 4.2) velocity (Table 4.3). Consistent with its predicted function, a strain lacking functional ChsA contained a greater concentration of c-di-GMP (6.6 $\pm$ 0.7 nmol c-di-GMP/mg protein) than the wild type or the Δ*tlp1* mutant strain, which each produced comparable amounts of c-di-GMP (wild type: 3.3 $\pm$ 0.4 nmol/mg protein; Δ*tlp1*: 3.9 $\pm$ 0.7 nmol/mg protein; not statistically significant at $p<0.05$) as determined by mass spectrometry. Together, these data suggest that increased intracellular c-di-GMP impede both chemo- and aerotaxis. In order to test if intracellular c-di-GMP content varies when cells experienced temporal changes in aeration conditions, we compared the intracellular concentration of c-di-GMP of the wild type and the *chsA*::Tn5 mutant strains in the gas perfusion chamber assay. Regardless of the aeration conditions, the intracellular levels of c-di-GMP were elevated in the *chsA*::Tn5 mutant strain relative to the wild type (Figure 4.8A). Variations in the amount of c-di-GMP detected in each strain over time followed a similar pattern (Figure 4.8A). The most significant increase in the c-di-GMP content of cells was detectable 40 seconds after air addition: the c-di-GMP levels in the wild type strain were half the amount measured prior to air addition but they were 1.5 times greater in the *chsA*::Tn5 mutant strain (Figure 4.8A). These results suggest that intracellular c-di-GMP content increases significantly under conditions of increased aeration, with a role for ChsA under these conditions as well.

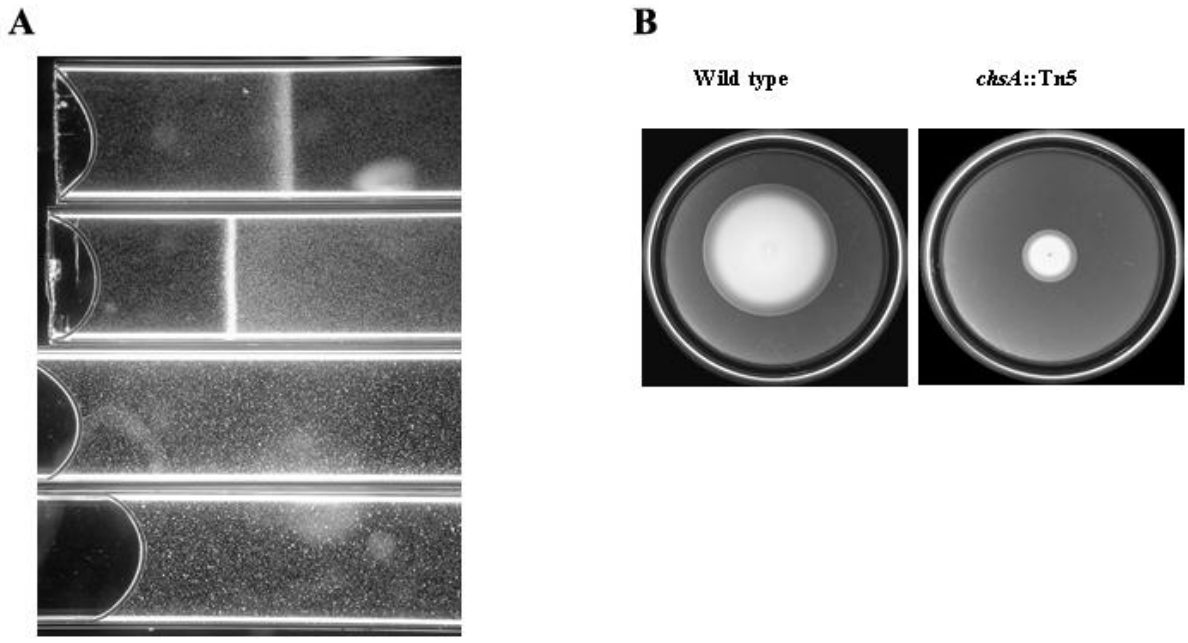

Figure 4.7: Chemotaxis and aerotaxis in strain lacking a functional diguanylate phosphodiesterase (ChsA) in *A. brasilense*. Sp7 and *chsA*::Tn5 were incubated 48 hours in semi-solid minimal media supplied with 0.1% (w/v) ammonium chloride and 0.5% (w/v) malate. Aerotaxis was with strains grown to late exponential growth and washed with che buffer. The cells were e-suspended to equivalent OD_{600nm} of 1.0. A, Spatial aerotaxis responses of (from top to bottom) Sp7(pRK415), Sp7(pRKChsA), *chsA*::Tn5(pRK415), and *chsA*::Tn5(pRKChsA). B, Representative image showing *chsA*::Tn5 is unable to effectively navigate in gradients of nutrients as observed using the soft agar assay.

Table 4.2: Swimming reversal frequency of the *chsA*::Tn5 mutant derivative of *A. brasilense* upon temporal changes in aeration conditions.

Air	**N_2**	**N_2**	**N_2**	**N_2**	**Air**	**Air**	**Air**
55 sec	**65 sec**	**70 sec**	**75 sec**	**415 sec**	**425 sec**	**430 sec**	**435 sec**
0.1 ± 0.02	0.05 ± 0.01	0.1 ± 0.02	0.05 ± 0.01	0.3 ± 0.02	0.3 ± 0.02	0.25 ± 0.02	0.25 ± 0.02

Table 4.3: Swimming velocity of a free-swimming population of *chsA*::Tn5 mutant derivatives of *A. brasilense* in the gas perfusion chamber assay.

	Air Removal Speed ($\mu m\ sec^{-1}$)		**Air Addition Speed ($\mu m\ sec^{-1}$)**
Before	26.6 ± 0.2*	**Before**	25.5 ± 0.1
After	26.9 ± 0.2*	**After**	22.9 ± 0.1

*The mean swimming velocity of cells, 20 seconds before air removal or addition (Before) or 20 seconds after air removal or addition (After) is represented.

Figure 4.8: Changes in C-di-GMP concentration with aeration and the effect on the transition from free-swimming to sessile clumps in *A. brasilense*. A, Temporal changes in intracellular c-di-GMP concentrations in response to changes in aeration for *A. brasilense* Sp7 and *chsA*::Tn5 in the gas perfusion chamber assay. Air was bubbled in a cell culture for 5 minutes to equilibrate cells. Aliquots were taken at times listed in graph. Up and down arrows indicate air removal and air addition, respectively. Slash bars indicate a time interval of approximately 5 minutes (see Supplemental Material and Methods). B, Representative images showing amount of clumping in *chsA*::Tn5 (right panel) compared to wild type (left panel) in late exponential phase growth in minimal medium supplement with ammonium and pyruvate as the nitrogen and carbon sources, respectively. C, Aerotactic bands formed by *Δtlp1* strain expressing Tlp1 variants unable or affected in c-di-GMP binding are not stable over time. Time lapse images of Sp7(pRK415) and *Δtlp1* mutant derivatives 5 minutes (left) after re-suspension in flat glass capillaries and 15 minutes (right) after re-suspension. By 15 minutes, c-di-GMP binding mutants of Tlp1 are no longer sensitive to the oxygen gradient. However, clumped cells just in front of aerotactic band at 5 minutes (arrows) are still present at 15 minutes. D. Surface attachment of Sp7 and *Δtlp1* mutant derivatives to an abiotic surface**.** The deletion mutant of *tlp1* and its derivatives expressing Tlp1 unable to bind c-di-GMP attached significantly (p-value < 0.005) more than wild type or *Δtlp1* expressing wild type Tlp1 to an abiotic (polystyrene) surface incubated 3 days in minimal medium absent a combined nitrogen source.

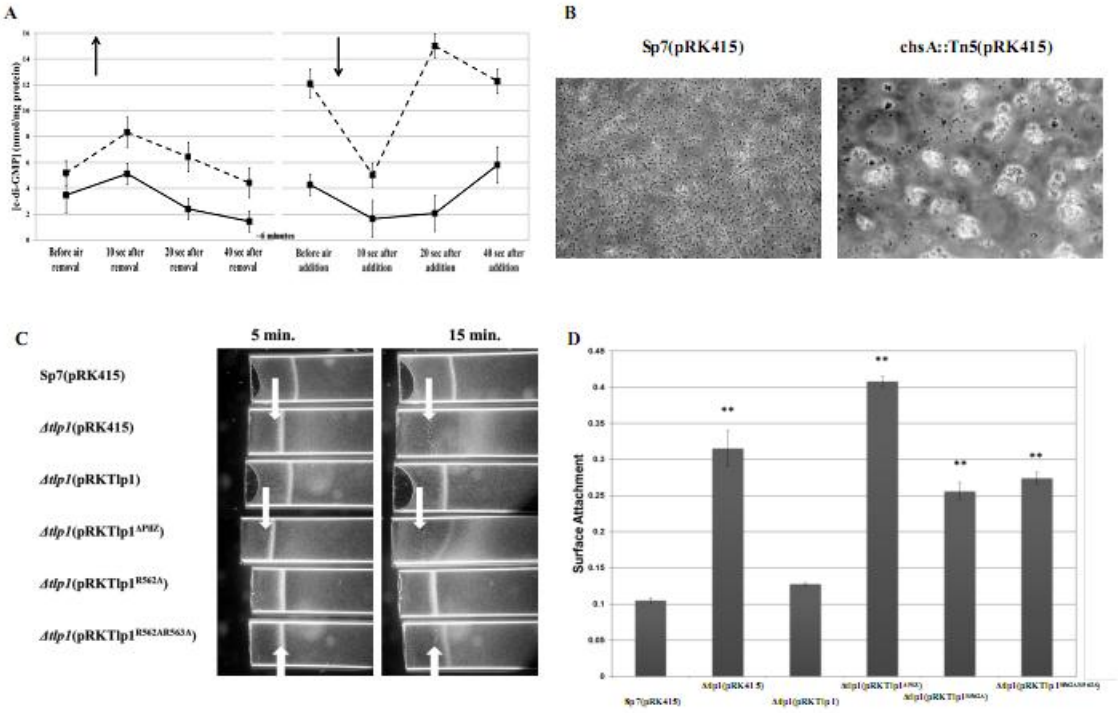
A
[c-di-GMP] (nmol/mg protein)
Before air removal
10 sec after removal
20 sec after removal
40 sec after removal
Before air addition
10 sec after addition
20 sec after addition
40 sec after addition
B
Sp7(pRK415)
chsA::Tn5(pRK415)
C
5 min.
15 min.
Sp7(pRK415)
Δtlp1(pRK415)
Δtlp1(pRKTlp1)
Δtlp1(pRKTlp1ΔPilZ)
Δtlp1(pRKTlp1R562A)
Δtlp1(pRKTlp1R562AR563A)
D
Surface Attachment

Subcellular localization of Tlp1 does not depend on c-di-GMP sensing

A C-terminal translational fusion of yellow fluorescent protein (YFP) with Tlp1, expressed under the control of its native promoter from a broad host range low-copy plasmid, was used to determine the subcellular localization of this chemoreceptor (Figure 4.9). When expressed in the Δ*tlp1* mutant background, the plasmid could restore chemotaxis and aerotaxis to wild type levels (Figure 4.9A). *Bright* fluorescent foci were detected at either one or both cell poles in more than 90% of the cells examined (Figure 4.9B). The subcellular localization of $Tlp1^{\Delta PilZ}$-YFP, $Tlp1^{R562A}$-YFP and $Tlp1^{R562AR563A}$-YFP, expressed at comparable levels in all strains (Figure 4.10B), and it was also higher than that observed in the wild type strain background. Localization of the Tlp1-YFP fusion in polar foci was also detected when Tlp1-YFP was expressed in a *Δche1* strain [32] (Figure 4.9C). A C-terminal translational fusion of ChsA to YFP (ChsA-YFP) was also expressed in the *chsA*::Tn5, the Δ*tlp1* and the Δ*che1* mutant strains. The expression levels detected were sufficient for the expressed ChsA-YFP to restore chemotaxis to the Δ*chsA*::Tn5 suggesting it is functional (data not shown). The expressed ChsA-YFP was found to be mostly diffuse in all the strains analyzed with some occasional weak foci observed at various positions around the cells (Figure 4.9E). These results indicate that ChsA and Tlp1 do not co-localize, and that c-di-GMP binding to Tlp1 does not affect its localization. These observations imply that ChsA-dependent modulation of c-di-GMP content is likely to affect the overall cell physiology.

c-di-GMP controls the transition of cells from free-swimming to sessile clumps

The inability to complement *chsA*::Tn5 by expressing wild type ChsA to functionally restore aerotaxis to the mutant and to have limited effect on chemotaxis suggested to us that mutation within *chsA* may cause additional defects on cell physiology that would prevent functional

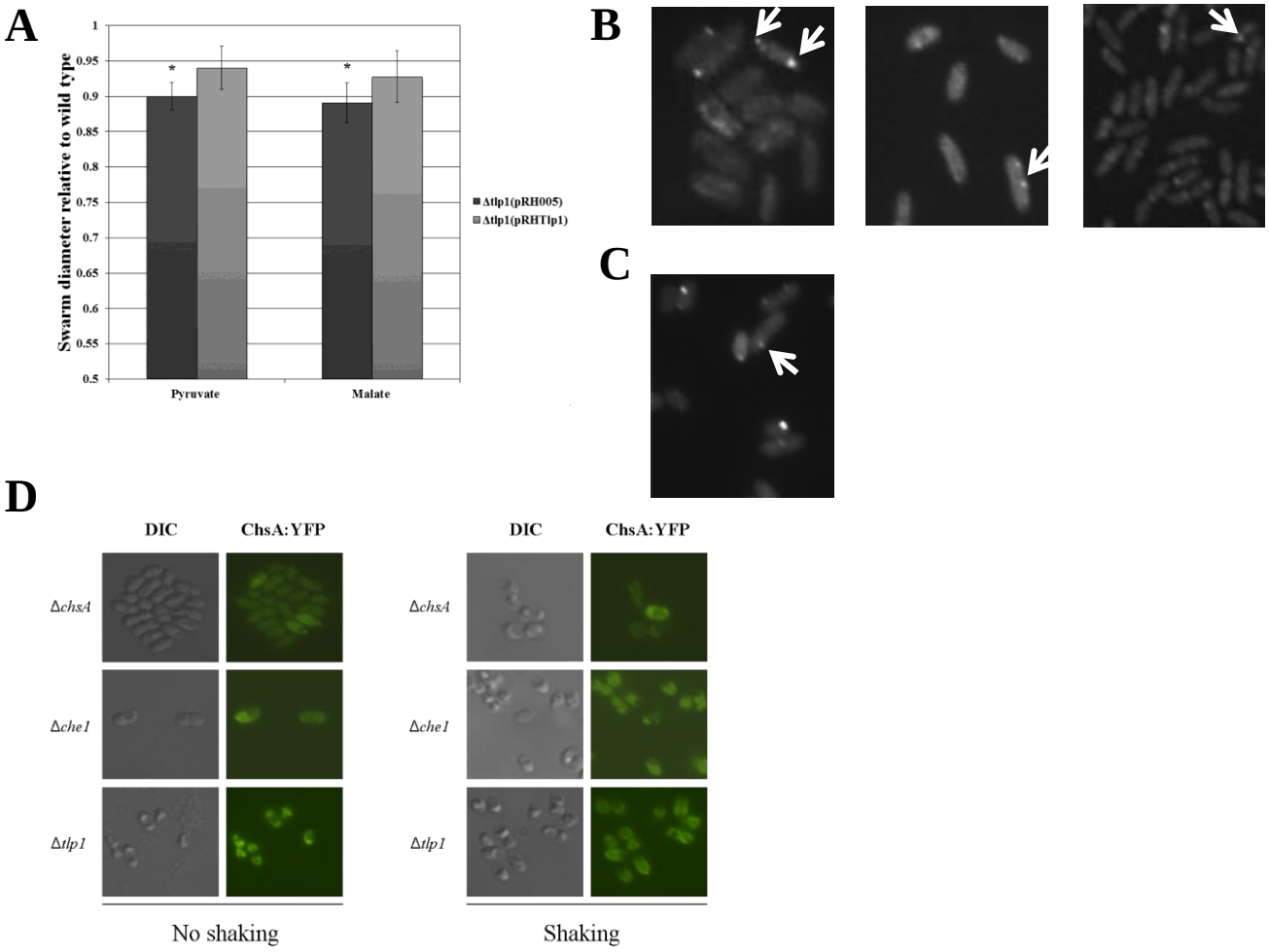

Figure 4.9: Cellular localization of Tlp1 wild type and mutant variants and ChsA. A, functional complementation by Tlp1-YFP in the *Δtlp1* mutant background as determined by soft agar plate assays to oxidizable substrates; asterisks indicate p-value < 0.05 compared to wild type. B, (left to right) localization of wild type Tlp1-YFP, Tlp1$^{\Delta PilZ}$-YFP, and Tlp1^{R562AR563A}-YFP in the *Δtlp1* mutant background. C, Tlp1-YFP localization in the *Δche1* mutant background. D, localization of ChsA-YFP incubated with or without shaking in chsA::Tn5, *Δche1*, and *Δtlp1* backgrounds.

complementation. Indeed, cultures of the Δ*chsA*::Tn5 mutant strain possessed a high density of stable cell-to-cell clumps, regardless of the growth conditions (Figure 4.9B). In *A. brasilense*, clumps are formed under conditions of high aeration by transient cell-to-cell interactions that usually become more stable as the increased aeration conditions persist, which are detrimental to *A. brasilense* microaerophilic metabolism [9, 32]. Expressing the wild type ChsA from a low copy plasmid only partially restored the ability of cells to swim freely (1.2 times more free-swimming cells). These results lend further support to the notion that the significant increase in c-di-GMP content of the *chsA*::Tn5 mutant cells has effects on physiology that may not be exclusively related to aerotaxis or chemotaxis, including effects promoting the formation of stable clumps.

When compared for the ability to clump under conditions of growth with high aeration, the Δ*tlp1* mutant expressing $Tlp1^{\Delta PilZ}$, $Tlp1^{R562A}$ or $Tlp1^{R562AR563A}$ variants formed significantly more clumps while the fraction of clumps in suspension of wild type cells or the Δ*tlp1* mutant carrying an empty vector as control or wild type Tlp1 were similar and produced significantly less clumps (Table 4.4). Similarly, the Δ*tlp1* mutant strain expressing Tlp1 variants that are impaired in the ability to bind c-di-GMP formed more clumps that remained at the position of the aerotactic band when it moved further away from the meniscus in the capillary over time through an observed loss of sensitivity to the oxygen gradient (Figure 4.9C). $Tlp1^{\Delta PilZ}$, $Tlp1^{R562A}$ or $Tlp1^{R562AR563A}$

Table 4.4: Clump fractions of *A. brasilense* Sp7 and *Δtlp1* mutant derivatives under conditions of growth with high aeration.

	Clump Fraction	**p-value**
Sp7(pRK415)	0.09 ± 0.002	-
Δtlp1(pRK415)	0.08 ± 0.002	0.07
Δtlp1(pRKTlp1)	0.06 ± 0.002	0.0005
Δtlp1(pRKTlp1$^{\Delta PilZ}$)	0.18 ± 0.001	0.0003
Δtlp1(pRKTlp1^{R562A})	0.19 ± 0.01	0.0005
Δtlp1(pRKTlp1^{R562AR563A})	0.16 ± 0.01	0.0006

variant proteins expressed in the Δ*tlp1* mutant background also increased the ability of the cells to form biofilms on abiotic surfaces, compared to the wild type or the Δ*tlp1* mutant strains in which Tlp1 is expressed, which both formed less biofilms than a Δ*tlp1* mutant strain carrying an empty vector, indicative of a direct role for Tlp1 sensing in this behavior (Figure 4.8D).

Discussion

As motile bacterial cells navigate the environment by chemo-or aerotaxis, they constantly adjust chemosensory sensibility to remain responsive to changing parameters in the surroundings. Little is known regarding how motile cells integrate metabolism with receptor sensitivity. Here, we demonstrate how a chemotaxis receptor functions to integrate metabolic status and adjust chemosensory sensitivity accordingly, by sensing the intracellular pool of the second-messenger signaling molecule, c-di-GMP. While a PilZ domain was predicted at the extreme C-terminus of this protein [19], its function has not been analyzed. Here we show that the PilZ domain of Tlp1 binds c-di-GMP with high affinity and that c-di-GMP binding to Tlp1 affects the ability of cells to navigate in oxygen gradient (aerotaxis) but not chemotaxis. Our data also show that intracellular c-di-GMP content increases with increased aeration. Some of the proteins implicated in c-di-GMP metabolism in *A. brasilense*, such as ChsA, are most active upon increases in aeration conditions. These observations are consistent with c-di-GMP being produced under conditions of metabolism imbalance since higher aeration conditions are detrimental to the microaerophilic metabolism of this organism [11, 17]. Evidence from X-ray crystal structures of c-di-GMP-bound and unbound-PilZ domains suggests that c-di-GMP binding induces a large conformational change [35, 36]. The packing of chemotaxis receptors within arrays, together with the activity of adaptation proteins, have been shown in experiments and via mathematical modeling to affect the sensitivity of the taxis response [37-39]. Upon binding c-di-GMP, a

significant conformational change within the C-terminal domain of Tlp1 could be induced that could modulate Tlp1 ability to function in signal transduction by affecting interaction with other receptors and/or with components of the cytoplasmic signaling complex [40, 41]. C-di-GMP binding to Tlp1 had major effects on sensitivity of the cells to the oxygen gradient with c-di-GMP binding to Tlp1 affecting how the aerotactic signal is processed, an effect especially apparent in the inverted responses. The direction of the taxis response (attractant or repellent) as well as the sensitivity of cells to chemoeffectors depends on the activity of adaptation proteins that sets the methylation status of the receptors in *E. coli* [42, 43] as well as for some but not all responses in *A. brasilense* [31]. There is no evidence that Tlp1 is modified by differential methylation and temporal responses to oxygen do not appear to involve adaptation by differential methylation in *A. brasilense* [31]. Therefore, c-di-GMP binding to Tlp1 could conceivably function to mediate sensory adaptation under conditions of elevated intracellular c-di-GMP content. This hypothesis is consistent with our observations that c-di-GMP binding to Tlp1 had significant effect on the ability of Tlp1 to transduce signals to mediate aerotaxis. Methylation-independent adaption has been suggested for other chemotaxis receptors [44-46], especially those involved in energy taxis, which includes aerotaxis, suggesting that binding of intracellular signaling molecules such as c-di-GMP by receptors may represent an alternative adaptation mechanism that could function in these systems as well.

Evidence from the literature [23, 47, 48] are consistent with the data obtained here that clearly indicate that elevated c-di-GMP in *A. brasilense* correlates with additional effects on cell physiology that include cell-to-cell clumping and biofilm formation. Thus, another, possibility is that conditions of elevated c-di-GMP concentrations cause changes in the organization of receptors or receptor-associated proteins within chemotaxis signaling complexes that can be counteracted by a significant conformational change in the signaling domain of Tlp1, that would

be induced by c-di-GMP binding. Given that most effectors for c-di-GMP have not been identified and the established functional link between motility, chemotaxis, and c-di-GMP signaling [23, 49-51], such effect is possible. Results presented here also support this hypothesis. We show that Tlp1 signals to at least two different chemotaxis pathways to mediate changes in the swimming velocity (Che1-dependent) as well as the swimming reversal frequency (other pathway(s)) to mediate aerotaxis. While there is no evidence that Tlp1 physically interacts with two different pathways, the *A. brasilense* Che1 pathway was shown to mediate signaling cross-talk during chemo- and aerotaxis perhaps via receptors, by a mechanism that is yet to be determined [9, 31, 32]. Such unknown mechanism could be regulated and/or significantly affected by changes in intracellular c-di-GMP content of the cells.

C-di-GMP signaling negatively regulates motility but also positively regulates the production of exopolysaccharides as well as the expression of other traits associated with a sessile lifestyle [20], it has been proposed and demonstrated [52-55] that c-di-GMP inhibitory effect on motility may be an early precursor for commitment to a sedentary lifestyle in biofilms, or as shown here, in formation of stable clumps. By binding to Tlp1, c-di-GMP thus stimulates motility in the oxygen gradient. Aerotaxis would thus allow cells to seek preferred oxygen concentrations for metabolism, an assumption supported by previous experimental evidence [10, 11, 17]. This behavior would afford the cells with the ability to prolong oxidative metabolism. The data obtained here thus indicate that aerotaxis can trump c-di-GMP second messenger signaling to license cells extended metabolic opportunities.

Experimental Procedures

Bacteria strains, Medium, Growth conditions

Azospirillum brasilense strains Sp7 (wild type) and SG323, a Sp7 derivative with *tlp1* deleted [18], were grown in TY rich medium (10g tryptone $^{-l}$, 5g yeast extract $^{-l}$) with appropriate antibiotics or MMAB, minimal media for *A. brasilense* [56], at 28°C shaking. For nitrogen fixation conditions, cells were incubated in MMAB without shaking at 28°C. *E. coli* Top10, S17.1, BL21 Star (DE3), were grown in LB at 37°C with appropriate antibiotics.

Complementation of SG323 and site-directed mutagenesis

For complementation, *tlp1* plus 737 bp upstream of the start codon were PCR amplified from genomic DNA with primers Tlp1HindIII-F and Tlp1XbaI-R1. The PCR product was gel extracted (Qiagen) and ligated into pUC19 after restriction enzyme digestion yielding pUCTlp1. After DNA sequence verification, this plasmid was used to construct $tlp1^{\Delta pilZ}$ by PCR amplification with primers Tlp1HindIII-F and Tlp1XbaI-R2 which was gel extracted, digested with HindIII and XbaI and ligated into pRK415 [57] digested with the same enzymes yielding pRKpilZ. The *Hind*III/*Xba*I fragment of pUCTlp1 was also ligated into pRK415 resulting in pRKTlp1. Both constructs were sequenced and introduced into *A. brasilense* SG323 by triparental mating using pRK2013 as a helper [58]. For site-directed mutagenesis, codons were replaced using the QuikChange II kit (Stratagene) using the manufacturer's protocol. The codon for Arg562 (CGC) was replaced with the codon for alanine (GCC) using pUCTlp1 as template DNA. Positive clones were sequenced for nucleotide mutation. A correct clone was harboring the new vector (pUCSDM1) was used as the template for mutagenesis of Arg563 (CGC) to alanine (GCC). A sequenced-positive clone was used as pUCSDM2. The site-directed *tlp1* genes were cloned into plasmid pRK415 described for wild type *tlp1*.

Tlp1 and ChsA protein localization and fluorescence microscopy

C-terminal translational fusions of Tlp1, Tlp1$^{\Delta PilZ}$, Tlp1^{R562A}, Tlp1^{R562AR563A} and ChsA with YFP were generated essentially as described [59].

The coding region of *tlp1* including the putative promoter was fused to yellow fluorescent protein (YFP) using Gateway® technology (Invitrogen). A 2732 bp fragment of tlp1 including the promoter was amplified by PCR and recombined into pDONR 221 (Invitrogen) using BP Clonase® II (Invitrogen) per manufacturer's protocol yielding pDONR-Tlp1. For Tlp1$^{\Delta PilZ}$, a 2420 bp fragment of *tlp1* with promoter was PCR amplified using an internal reverse primer and recombined into pDONR 221 per manufacturer's protocol resulting in pDONR-Tlp1$^{\Delta PilZ}$. For ChsA, a 1758 bp fragment was PCR amplified and recombined into pDONR 221. Positive clones verified by DNA sequencing for pDONR-Tlp1, pDONR-Tlp1$^{\Delta PilZ}$, and pDONR-ChsA before recombination into pRH005 [38] using LR Clonase® II (Invitrogen). Clones were selected for on LB medium with chloramphenicol 34µg/ml and kanamycin 50µg/ml, verified by sequencing, and named pRHTlp1 and pRHTlp1$^{\Delta PilZ}$, respectively. The constructs were transformed into *E. coli* S17.1 [60]. pRHTlp1 and pRHTlp1$^{\Delta PilZ}$ were introduced into *A. brasilense* by biparental mating [61] and selection on MMAB with no nitrogen containing chloramphenicol and Kanamycin.

For fluorescence microscopy, 30µL of cell culture was embedded on a 100µL 1% agarose pad on microscope slides, and covered with a cover slip. Differential interference contrast (DIC) and fluorescence images were acquired using a Nikon 80i microscope. At least three independent experiments were performed, and at least five different fields of view from each experiment were analyzed.

Soft agar assay and other behavioral assays

The soft agar assay was performed by incubating liquid cultures in MMAB shaking overnight at 28°C. The optical density of the cultures was standardized and 5µl was inoculated into 0.3% MMAB with varying carbon sources as indicated. Plates were incubated 48 hours at 28°C. Assay of chemotaxis was measured by ring diameters relative to wild type.

Spatial aerotaxis assays was performed in a perfused chamber as previously described (Alexandre et al., 2000). For the aerotaxis assay, actively growing cultures (early Log phase) are washed with 0.8% (w/v) sterile potassium chloride three times and resuspended in Chemotaxis buffer (10mM potassium phosphate, pH 7.0, and 0.1mM EDTA) supplemented with 10mM malate (as the electron donor) to an $O.D._{600}$ of 1.0. Over 95% of cells are motile within the cell suspension prepared. Typical aerotactic band formation occurs within 2 minutes in the wild type strain.

Temporal aerotaxis assay

A 10µl drop of motile cells suspended in MMAB supplied with 10 mM pyruvate as a carbon source is placed in a chamber in which the humidified gas flowing above the drop can be controlled as previously described [62]. First, compressed air (21% oxygen) is allowed to flow over the cell suspension until cells are equilibrated (usually 5 minutes). Then, a valve is switched to provide pure nitrogen to the cell suspension in a fraction of a second (air to nitrogen stimulus). After a period of 6 minutes, the nitrogen gas flowing into the chamber is switched back to air (nitrogen to air stimulus). Then entire assay is recorded with use of a CCD camera for video and motion tracking analysis. Analysis of swimming velocity was performed using CellTrak v1.5 (Motion Analysis Corp., Santa Rosa, CA). One to three second segments of video were optimized to subtract background using ImageJ (http://rsb.info.nih.gov/ij/). For determination of reversal

frequencies of cell suspensions, 30 frame-segments (30 frames taken as 1 second) of video are analyzed using ImageJ. Individual cells visible in all frames are analyzed for changes in swimming direction. Each cell analyzed is marked (Cell Counter plugin) to ensure no duplications and the resulting number of direction changes is recorded in Excel (Microsoft Corp., Redmond, WA). At least 100 cells are analyzed for each time point. The average reversal frequency is calculated in Excel with a standard error.

Flocculation assay

Cells are grown overnight at 28°C shaking in TY medium to an $O.D._{600}$ 1.1-1.3. The O.D. is standardized to 1.0 and 200µl is inoculated into 5ml MMAB supplied with 0.5mM sodium nitrate and 8mM fructose as the nitrogen and carbon sources, respectively. The cultures are incubated 48 hours at 28°C with shaking. After 48 hours, cultures are placed on benchtop for 30 min to settle flocculated cells. The $O.D._{600}$ of free-living cells was taken on an Eppendorf BioPhotometer (Hamburg, Germany). The cells are placed back in culture and homogenized with a tissue homogenizer to disrupt flocculated cells. Another $O.D._{600}$ reading is taken to determine turbidity of entire culture. The fraction of flocculation is calculated by the following equation:

$$\frac{O.D._{600\,final} - O.D._{600\,initial}}{O.D._{600\,final}}$$

Protein Overexpression and Purification

The DNA fragments corresponding to aa 344-660 of the wild-type Tlp1 and two Tlp1 mutants, $Tlp1^{R562A}$ and $Tlp1^{R562AR563A}$, were amplified and cloned into pMAL-c2x to construct maltose-binding protein (MBP) translational fusions. The MBP–Tlp1 fusion proteins were overexpressed

and purified, essentially as previously reported [63]. Briefly, isopropyl-ß-D-thiogalactopyranoside, IPTG, (final concentration, 0.5 mM) was added to exponentially growing E. coli XL-Blue (A_{600} 0.5-0.6) containing the appropriate expression plasmids. After 5 h of induction, cells were collected by centrifugation. Cell pellets were resuspended in a buffer containing 200 mM NaCl, 0.5 mM EDTA, 5 mM MgCl2, 20 mM Tris-HCl (pH 7.4), 5% glycerol and protease inhibitors (phenylmethylsulfonyl fluoride and P8465) at the concentrations recommended by the manufacturer (Sigma-Aldridge) at the concentrations specified by the manufacturer. Cell suspensions were passed through a French pressure minicell (Spectronic Instruments), followed by brief sonification (Sonifier 250; Branson). Crude cell extracts were centrifuged at 35,000 x g for 25 min. Soluble protein fractions were collected and mixed with the pre-equilibrated amylose resin (New England Biolabs) for 1 h at 4°C. The MBP-protein fusions were eluted with maltose and dialyzed against the equilibrium dialysis buffer (300 mm NaCl, 0.5 mm EDTA, 10% glycerol, 50 mm sodium phosphate, pH 7.4) in Slide-A-Lyzer dialysis cassettes (Pierce) according to the instructions of the manufacturer. Protein purity was assessed by SDS-PAGE (sodium dodecyl sulfate-polyacrylamide gel electrophoresis). Protein concentrations were measured with the Bradford protein assay kit (Biorad).

Equilibrium Dialysis

Protein-nucleotide binding was examined by equilibrium dialysis in Dispo-Biodialyzer cassettes (The Nest Group, Southborough, MA) as previously reported [28]. Briefly, 0.5-100 μm c-di-GMP were injected into one cell of a cassette, while the analyzed proteins, 10 ± 2 μm, were injected into the opposite cell, separated by a dialysis membrane with a 10-kDa molecular weight cut off. The cassettes were maintained for 29 h at room temperature under moderate agitation. The samples (70 μl) from both cassette cells were withdrawn, boiled for 10 min (to denature the

protein, where present), and centrifuged, and supernatants were filtrated through a 0.22-μm microfilter. The nucleotide concentrations were quantified by measuring peak areas of the eluted nucleotides from the HPLC column as described earlier [63]. Binding constants were calculated by the GraphPad Prism software, version 5.03 (GraphPad Software, San Diego, CA) using nonlinear regression model.

Antibody production and affinity purification

A C-terminal fragment of Tlp1 (aa 299-664) was PCR amplified from pUCTlp1 with the native stop codon and recombined into pDONR221 using BP Clonase II (Invitrogen) using manufacturer's protocol and sequence verified to yield pDONR*tlp*^{Cterm}. Tlp1^{Cterm} was introduced into pET-59-DEST (Novagen) using LR clonase II (Invitrogen) yielding pET-Tlp1C and sequence verified. A correct clone was transformed into *E. coli* BL21 (DE3) for recombinant protein expression. An aliquot of overnight culture was re-inoculated in fresh LB and incubated at 37°C until O.D.$_{600nm}$ of 0.5 and induced by 1mM IPTG and incubated overnight at 25°C shaking. Cells were collected and lysed by French Press. Tlp1^{Cterm} was purified over a Ni-NTA agarose column (Qiagen). Affinity tags were cleaved from Tlp1^{Cterm} by thrombin (Novagen) per manufacturer's protocol, and Tlp1^{Cterm} was purified as the eluate from an additional Ni-NTA agarose column. Protein purity was verified by SDS-PAGE, concentrated, and sent for antibody production in rabbit (Thermo Scientific). Resulting antisera was affinity purified using whole cell extracts conjugated to NHS-Sepharose 4B (Sigma).

Western blots

Proteins from SDS-PAGE were transferred to nitrocellulose (Whatman) using a Trans-Blot® SD Semi-Dry Transfer Cell (BioRad) set at 15 volts for 20-40 minutes dependent upon the size and

cell location of the protein probed. Nitrocellulose membranes were blocked for 1 hour with 5% dry milk (Carnation) in TTBS (Tris Buffered Saline, pH 7.5 and Tween-20 0.05% (v/v)) and washed twice with TTBS. Proteins were probed with HRP conjugated Mouse Anti-6xHis (BD Pharmingen) at a 1:4000 dilution from 1 hour to overnight and detected by SuperSignal® West Dura Extended Duration Substrate (Pierce). For Tlp1-YFP, $Tlp1^{\Delta PilZ}$-YFP, $Tlp1^{R562A}$-YFP, and $Tlp1^{R562AR563A}$-YFP proteins were probed with rabbit anti-GFP sera (gift from R. Goodchild) at a 1:2000 dilution overnight. Membranes were then washed extensively and probed with a secondary ImmunoPure® goat anti-rabbit antibody conjugated to HRP (Thermo Scientific) and detected by SuperSignal® West Dura Extended Duration Substrate. Exposed X-ray film (Phenix) was developed with a Konica SRX-101 X-ray Processor (Konica Minolta).

Preparation of [U-^{13}C]-c-di-GMP

Due to incorporation of endogenous *E. coli* unlabeled cyclic-di-GMP, *E. coli* BL21 cells containing PleD* (constitutively active) from *Caulobacter crescentus* [29] expressed from the plasmid pRP87 were grown and induced in M9 medium supplemented with ^{13}C-glucose as the carbon source. Briefly, cells were inoculated into M9 medium from an overnight culture and grown until $O.D._{600}$ reached 0.5. IPTG was added to a final concentration of 0.4mM and cells continued to incubate at 22°C overnight. Cells were collected and resuspended in lysis buffer (25mM Tris-HCl, pH 8.0, 500mM NaCl, 10mM imidazole) and lysed by several passages through a French Press. Cell debris was removed by centrifugation at 17,000 rpm for 45 minutes. The resulting supernatant was incubated with equilibrated Ni-agarose resin by batch binding at 4°C for 30 minutes and loaded onto a gravity column, washed thoroughly with wash buffer (lysis buffer with 30mM imidazole) and eluted with 250mM imidazole. The eluate was concentrated by ultrafiltration and dialyzed to remove imidazole prior to c-di-GMP synthesis.

Cyclic-di-GMP was synthesized using ^{13}C labeled GTP (25μM) and aliquots of purified PleD* (30μM) in synthesis buffer (75 mM Tris-HCl, pH 8, 250 mM NaCl, 25 mM KCl, and 10mM $MgCl_2$) overnight at 25°C. Due to c-di-GMP inhibition of PleD activity, the enzyme was concentrated by ultrafiltration with analysis of the flow through ($^{13}C_{20}$)c-di-GMP purity. The enzyme fraction was diluted in fresh synthesis buffer with an additional 25μM ($^{13}C_{10}$)GTP for additional synthesis. After overnight incubation, samples were boiled 10 minutes, centrifuged, and supernatant collected for ($^{13}C_{20}$)c-di-GMP analysis.

Solutions were tested for the presence of any GDP, GTP or c-di-GMP. Those that contained only ($^{13}C_{20}$)-c-di-GMP were pooled and lyophilized. The powder was then resuspended and the final concentration was measured by a UV-Vis spectrometer at 254 nm with an extinction coefficient of 26,100 M^{-1} cm^{-1} [64]. This stock solution (190 μM) was stored at room temperature.

Temporal aerotaxis c-di-GMP extraction

Cultures of *A. brasilense* to be studied were grown overnight in MMAB supplemented with pyruvate 5% (w/v) instead of malate. Cultures are transferred to sterile media bottles allowing gas infusion into the media. Cultures are infused with air for several minutes to equilibrate cells. An initial 40ml sample of cells are extracted and quickly frozen in conical tubes with liquid nitrogen as a time 0. The gas is switched to nitrogen and three additional 40ml samples are extracted and frozen 10, 20, and 40 seconds after gas switch. After 5.5 minutes of nitrogen infusion, a 40ml sample is extracted and frozen. At 6 minutes after initial gas switch, air replaces nitrogen for infusion and three additional samples are taken 10, 20, and 40 seconds after the switch and frozen. Samples are centrifuged at 6,000 rpm until all media has thawed and aspirated. Cell pellets are quickly resuspended with extraction buffer (acetonitrile:methanol:water 40:40:20 with 0.1M formic acid) supplemented with benzoic acid (17 μM) and ($^{13}C_{20}$)c-di-GMP (0.76 μM) and

incubated on ice for 30 minutes. Cell extract is centrifuged at 14,000 rpm for 15 minutes. 300µl of supernatant is quickly transferred to an autosampler vial with 26µl 15% ammonium carbonate.

Mass Spectrometry and Quantification of c-di-GMP

For separation of metabolites, a C18 stationary phase column with a proprietary imbedded polar group was used (Synergi Hydro-RP, Phenomenex, Torrance CA) packed with 80 Å particles with 4 µm pores and maintained at 25 ^{o}C. The mobile phases consisted of solvent A, 11 mM tributylamine and 15 mM acetic acid in 97% HPLC grade water and 3% HPLC grade methanol, and solvent B, HPLC grade methanol. These solvents were used to create a 50 min gradient of the following profile: t) 0 min, 100% solvent A, 0% solvent B; t) 5 min, 100% solvent A, 0% solvent B; t) 10 min, 80% solvent A, 20% solvent B; t) 15, 80% solvent A, 20% solvent B; t) 30, 35% solvent A, 65% solvent B; t) 33, 5% solvent A, 95% solvent B t) 37, 5% solvent A, 95% solvent B; t) 38, 100% solvent A, 0% solvent B; t) 50, 100% solvent A, 0% solvent B. The flow rate was 200 µL/min. The eluent was introduced directly into a Finnigan TSQ Quantum Discovery Max triple quadrupole mass spectrometer. Ions were detected using multiple reaction monitoring mode. Peaks were integrated manually in Xcalibur QualBrowser and the concentration of c-di-GMP was calculated using the following equation:

$$\frac{cdiGMP\ signal}{(^{13}C_{20})cdiGMP\ signal} * known\ (^{13}C_{20})cdiGMP * \frac{1}{[protein]} * \frac{1}{volume\ sampled} * volume\ extraction\ solvent = \frac{[cdiGMP]}{Protein}$$

Acknowledgements

The authors thank R. Goodchild (Univ. of Tennessee) for the gift of the anti-GFP antibody.

This work was supported by NSF (MCB-0919819) to G.A.

List of References

1. Wadhams, G.H. and J.P. Armitage, *Making sense of it all: Bacterial chemotaxis.* Nature Reviews Molecular Cell Biology, 2004. **5**(12): p. 1024-1037.
2. Buchan, A., B. Crombie, and G.M. Alexandre, *Temporal dynamics and genetic diversity of chemotactic-competent microbial populations in the rhizosphere.* Environ Microbiol, 2010. **12**(12): p. 3171-84.
3. Alexander, R.P. and I.B. Zhulin, *Evolutionary genomics reveals conserved structural determinants of signaling and adaptation in microbial chemoreceptors.* Proceedings of the National Academy of Sciences of the United States of America, 2007. **104**(8): p. 2885-2890.
4. Hazelbauer, G.L., J.J. Falke, and J.S. Parkinson, *Bacterial chemoreceptors: high-performance signaling in networked arrays.* Trends in Biochemical Sciences, 2008. **33**(1): p. 9-19.
5. Ames, P., et al., *Collaborative signaling by mixed chemoreceptor teams in Escherichia coli.* Proceedings of the National Academy of Sciences of the United States of America, 2002. **99**(10): p. 7060-7065.
6. Briegel, A., et al., *Bacterial chemoreceptor arrays are hexagonally packed trimers of receptor dimers networked by rings of kinase and coupling proteins.* Proc Natl Acad Sci U S A, 2012. **109**(10): p. 3766-71.
7. Briegel, A., et al., *Universal architecture of bacterial chemoreceptor arrays.* Proc Natl Acad Sci U S A, 2009. **106**(40): p. 17181-6.
8. Alexandre, G., S. Greer-Phillips, and I.B. Zhulin, *Ecological role of energy taxis in microorganisms.* Fems Microbiology Reviews, 2004. **28**(1): p. 113-126.

9. Bible, A., M.H. Russell, and G. Alexandre, *The Azospirillum brasilense Che1 chemotaxis pathway controls the swimming velocity which affects transient cell-to-cell clumping.* J Bacteriol, 2012.

10. Alexandre, G., S.E. Greer, and I.B. Zhulin, *Energy taxis is the dominant behavior in Azospirillum brasilense.* J Bacteriol, 2000. **182**(21): p. 6042-8.

11. Zhulin, I.B., et al., *Oxygen taxis and proton motive force in Azospirillum brasilense.* J Bacteriol, 1996. **178**(17): p. 5199-204.

12. Alexandre, G., *Coupling metabolism and chemotaxis-dependent behaviours by energy taxis receptors.* Microbiology, 2010. **156**(Pt 8): p. 2283-93.

13. Taylor, B.L., I.B. Zhulin, and M.S. Johnson, *Aerotaxis and other energy-sensing behavior in bacteria.* Annual Review of Microbiology, 1999. **53**: p. 103-128.

14. Vegge, C.S., et al., *Energy Taxis Drives Campylobacter jejuni toward the Most Favorable Conditions for Growth.* Applied and Environmental Microbiology, 2009. **75**(16): p. 5308-5314.

15. Sarand, I., et al., *Metabolism-dependent taxis towards (methyl)phenols is coupled through the most abundant of three polar localized Aer-like proteins of Pseudomonas putida.* Environmental Microbiology, 2008. **10**(5): p. 1320-1334.

16. Nichols, N.N. and C.S. Harwood, *An aerotaxis transducer gene from Pseudomonas putida.* Fems Microbiology Letters, 2000. **182**(1): p. 177-183.

17. Xie, Z.H., et al., *PAS domain containing chemoreceptor couples dynamic changes in metabolism with chemotaxis.* Proceedings of the National Academy of Sciences of the United States of America, 2010. **107**(5): p. 2235-2240.

18. Greer-Phillips, S.E., B.B. Stephens, and G. Alexandre, *An energy taxis transducer promotes root colonization by Azospirillum brasilense.* Journal of Bacteriology, 2004. **186**(19): p. 6595-6604.

19. Amikam, D. and M.Y. Galperin, *PilZ domain is part of the bacterial c-di-GMP binding protein.* Bioinformatics, 2006. **22**(1): p. 3-6.

20. Merighi, M., et al., *The second messenger bis-(3 '-5 ')-cyclic-GMP and its PilZ domain-containing receptor Alg44 are required for alginate biosynthesis in Pseudomonas aeruginosa.* Molecular Microbiology, 2007. **65**(4): p. 876-895.

21. Benach, J., et al., *The structural basis of cyclic diguanylate signal transduction by PilZ domains.* Embo Journal, 2007. **26**(24): p. 5153-66.

22. Pratt, J.T., et al., *PilZ domain proteins bind cyclic diguanylate and regulate diverse processes in Vibrio cholerae.* Journal of Biological Chemistry, 2007. **282**(17): p. 12860-12870.

23. Krasteva, P.V., et al., *Vibrio cholerae VpsT regulates matrix production and motility by directly sensing cyclic di-GMP.* Science, 2010. **327**(5967): p. 866-8.

24. Navarro, M.V., et al., *Structural basis for c-di-GMP-mediated inside-out signaling controlling periplasmic proteolysis.* Plos Biology, 2011. **9**(2): p. e1000588.

25. Kuchma, S.L., et al., *Cyclic-di-GMP-mediated repression of swarming motility by Pseudomonas aeruginosa: the pilY1 gene and its impact on surface-associated behaviors.* J Bacteriol, 2010. **192**(12): p. 2950-64.

26. Schweinitzer, T. and C. Josenhans, *Bacterial energy taxis: a global strategy?* Archives of Microbiology, 2010. **192**(7): p. 507-520.

27. Taylor, B.L., K.J. Watts, and M.S. Johnson, *Oxygen and redox sensing by two-component systems that regulate behavioral responses: Behavioral assays and structural studies of*

aer using in vivo disulfide cross-linking. Two-Component Signaling Systems, Pt A, 2007. **422**: p. 190-232.

28. Ryjenkov, D.A., et al., *The PilZ domain is a receptor for the second messenger c-di-GMP - The PilZ domain protein YcgR controls motility in enterobacteria.* Journal of Biological Chemistry, 2006. **281**(41): p. 30310-30314.

29. Paul, R., et al., *Cell cycle-dependent dynamic localization of a bacterial response regulator with a novel di-guanylate cyclase output domain.* Genes Dev, 2004. **18**(6): p. 715-27.

30. Ko, J., et al., *Structure of PP4397 Reveals the Molecular Basis for Different c-di-GMP Binding Modes by Pilz Domain Proteins.* Journal of Molecular Biology, 2010. **398**(1): p. 97-110.

31. Stephens, B.B., S.N. Loar, and G. Alexandre, *Role of CheB and CheR in the complex chemotactic and aerotactic pathway of Azospirillum brasilense.* J Bacteriol, 2006. **188**(13): p. 4759-68.

32. Bible, A.N., et al., *Function of a chemotaxis-like signal transduction pathway in modulating motility, cell clumping, and cell length in the alphaproteobacterium Azospirillum brasilense.* J Bacteriol, 2008. **190**(19): p. 6365-75.

33. Carreno-Lopez, R., et al., *Characterization of chsA, a new gene controlling the chemotactic response in Azospirillum brasilense Sp7.* Arch Microbiol, 2009. **191**(6): p. 501-7.

34. Pellequer, J.L., R. Brudler, and E.D. Getzoff, *Biological sensors: More than one way to sense oxygen.* Current Biology, 1999. **9**(11): p. R416-8.

35. Benach, J., et al., *The structural basis of cyclic diguanylate signal transduction by PilZ domains.* Embo Journal, 2007. **26**(24): p. 5153-5166.

36. Shin, J.S., et al., *Structural characterization reveals that a PilZ domain protein undergoes substantial conformational change upon binding to cyclic dimeric guanosine monophosphate.* Protein Science, 2011. **20**(2): p. 270-277.

37. Sourjik, V. and H.C. Berg, *Functional interactions between receptors in bacterial chemotaxis.* Nature, 2004. **428**(6981): p. 437-441.

38. Kim, S.H., W.R. Wang, and K.K. Kim, *Dynamic and clustering model of bacterial chemotaxis receptors: Structural basis for signaling and high sensitivity.* Proceedings of the National Academy of Sciences of the United States of America, 2002. **99**(18): p. 11611-11615.

39. Duke, T. and I. Graham, *Equilibrium mechanisms of receptor clustering.* Progress in Biophysics & Molecular Biology, 2009. **100**(1-3): p. 18-24.

40. Massazza, D.A., J.S. Parkinson, and C.A. Studdert, *Cross-linking evidence for motional constraints within chemoreceptor trimers of dimers.* Biochemistry, 2011. **50**(5): p. 820-7.

41. Hu, W., *A possible degree of motional freedom in bacterial chemoreceptor cytoplasmic domains and its potential role in signal transduction.* Int J Biochem Mol Biol, 2011. **2**(2): p. 99-110.

42. Dang, C.V., et al., *Inversion of aerotactic response in Escherichia coli deficient in cheB protein methylesterase.* J Bacteriol, 1986. **166**(1): p. 275-80.

43. Bespalov, V.A., I.B. Zhulin, and B.L. Taylor, *Behavioral responses of Escherichia coli to changes in redox potential.* Proceedings of the National Academy of Sciences of the United States of America, 1996. **93**(19): p. 10084-10089.

44. Bibikov, S.I., et al., *Methylation-independent aerotaxis mediated by the Escherichia coli aer protein.* Journal of Bacteriology, 2004. **186**(12): p. 3730-3737.

45. Zhulin, I.B. and J.P. Armitage, *Motility, chemokinesis, and methylation-independent chemotaxis in Azospirillum brasilense.* J Bacteriol, 1993. **175**(4): p. 952-8.

46. Zimmer, M.A., et al., *The role of heterologous receptors in McpB-mediated signalling in Bacillus subtilis chemotaxis.* Molecular Microbiology, 2002. **45**(2): p. 555-568.

47. Wilksch, J.J., et al., *MrkH, a Novel c-di-GMP-Dependent Transcriptional Activator, Controls Klebsiella pneumoniae Biofilm Formation by Regulating Type 3 Fimbriae Expression.* Plos Pathogens, 2011. **7**(8).

48. Jonas, K., O. Melefors, and U. Romling, *Regulation of c-di-GMP metabolism in biofilms.* Future Microbiology, 2009. **4**(3): p. 341-358.

49. Paul, K., et al., *The c-di-GMP binding protein YcgR controls flagellar motor direction and speed to affect chemotaxis by a "backstop brake" mechanism.* Mol Cell, 2010. **38**(1): p. 128-39.

50. Kuchma, S. and G.A. O'Toole, *C-Di-Gmp-Mediated Repression of Swarming Motility by Pseudomonas Aeruginosa: The Pily1 Locus & Its Impact on Surface-Associated Behaviors.* Pediatric Pulmonology, 2010: p. 339-339.

51. Fang, X. and M. Gomelsky, *A post-translational, c-di-GMP-dependent mechanism regulating flagellar motility.* Molecular Microbiology, 2010. **76**(5): p. 1295-305.

52. Caiazza, N.C., et al., *Inverse regulation of biofilm formation and swarming motility by Pseudomonas aeruginosa PA14.* J Bacteriol, 2007. **189**(9): p. 3603-12.

53. Ferreira, R.B., et al., *Output targets and transcriptional regulation by a cyclic dimeric GMP-responsive circuit in the Vibrio parahaemolyticus Scr network.* J Bacteriol, 2012. **194**(5): p. 914-24.

54. Moscoso, J.A., et al., *The Pseudomonas aeruginosa sensor RetS switches Type III and Type VI secretion via c-di-GMP signalling.* Environmental Microbiology, 2011. **13**(12): p. 3128-3138.

55. Ueda, A. and T.K. Wood, *Connecting Quorum Sensing, c-di-GMP, Pel Polysaccharide, and Biofilm Formation in Pseudomonas aeruginosa through Tyrosine Phosphatase TpbA (PA3885).* Plos Pathogens, 2009. **5**(6).

56. Vanstockem, M., et al., *TRANSPOSON MUTAGENESIS OF AZOSPIRILLUM-BRASILENSE AND AZOSPIRILLUM-LIPOFERUM - PHYSICAL ANALYSIS OF TN5 AND TN5-MOB INSERTION MUTANTS.* Applied and Environmental Microbiology, 1987. **53**(2): p. 410-415.

57. Keen, N.T., et al., *Improved Broad-Host-Range Plasmids for DNA Cloning in Gram-Negative Bacteria.* Gene, 1988. **70**(1): p. 191-197.

58. Figurski, D.H. and D.R. Helinski, *Replication of an origin-containing derivative of plasmid RK2 dependent on a plasmid function provided in trans.* Proc Natl Acad Sci U S A, 1979. **76**(4): p. 1648-52.

59. Hallez, R., et al., *Gateway-based destination vectors for functional analyses of bacterial ORFeomes: Application to the min system in Brucella abortus.* Applied and Environmental Microbiology, 2007. **73**(4): p. 1375-1379.

60. Simon, L.D., et al., *Stabilization of proteins by a bacteriophage T4 gene cloned in Escherichia coli.* Proc Natl Acad Sci U S A, 1983. **80**(7): p. 2059-62.

61. Vanstockem, M., et al., *Transposon Mutagenesis of Azospirillum brasilense and Azospirillum lipoferum: Physical Analysis of Tn5 and Tn5-Mob Insertion Mutants.* Appl Environ Microbiol, 1987. **53**(2): p. 410-5.

62. Laszlo, D.J. and B.L. Taylor, *Aerotaxis in Salmonella typhimurium: role of electron transport.* J Bacteriol, 1981. **145**(2): p. 990-1001.

63. Ryjenkov, D.A., et al., *Cyclic diguanylate is a ubiquitous signaling molecule in bacteria: Insights into biochemistry of the GGDEF protein domain.* Journal of Bacteriology, 2005. **187**(5): p. 1792-1798.

64. Zhang, Z., B.L. Gaffney, and R.A. Jones, *c-di-GMP displays a monovalent metal ion-dependent polymorphism.* J Am Chem Soc, 2004. **126**(51): p. 16700-1.

Chapter 5

Conclusions and directions for future research

During my residency in this program unraveling the chemosensory strategies of *A. brasilense*, I was able to determine the specificity of a novel chemoreceptor, Tlp2 (Chapter 2), help expand the understanding of the cellular role of Che1 in regards to clumping (Chapter 3), and determine a role of the PilZ domain of Tlp1 in the *A. brasilense* aerotaxis behavior (Chapter 4). In this chapter, I briefly discuss unpublished work that has led me to build a hypothesis that could form the basis for future directions for this research.

C-di-GMP signaling in *A. brasilense*

The majority of c-di-GMP research is within model organisms; *Caulobacter crescentus* [1-3], *Vibrio spp.* [4-9], *Pseudomonas spp.* [1, 10-12], and *E. coli* [13-18]. However, the second messenger is ubiquitous across Eubacteria [19]. The signaling molecule is known to have a role in the control of flagellar motility. For example, in enteric bacteria, YcgR was shown to bind c-di-GMP via a C-terminal PilZ domain [14]. The N-terminal domain (YcgRN) binds flagellar switch proteins FliG and FliM strongly in the presence of c-di-GMP presumably reducing their interactions with the torque generating stator complex proteins MotA and MotB [17]. Unfortunately, the mechanism by which c-di-GMP directly (or indirectly) suppresses motility in nonenteric bacteria is less clear because there is no known YcgR homolog (discussed below). The only other mechanism identified to date involves the PilZ-domain proteins DgrA and DgrB of *C. crescentus* [20]. It is hypothesized when bound to c-di-GMP, DgrA inhibits motility by an unknown mechanism lowering cellular levels of FliL, a flagellar motor protein not encoded within flagellar operons but necessary for *C. crescentus* motility [20, 21]. The DgrA/c-di-GMP effect on motility is an all-or-nothing effect involving gene transcription/translation, therefore, it is not suitable for transient control of motility.

The *A. brasilense* genome encodes 30 annotated GGDEF enzymes and 25 c-di-GMP degrading enzymes (15 EALs and 10 HD-GYPs) [22]. Analysis of GGDEFs and EALs reveals the presence

of several sensing/regulation domains with PAS domains being found in the majority of these proteins (Figure 5.1). This suggests the turnover of c-di-GMP is dynamic and regulated by a number of intracellular and extracellular signals. The genome also contains 5 PilZ domains, all of which are fused to the C-terminus of chemoreceptors suggesting the second messenger could play a role in modulating the output of the chemotaxis-like pathways. This observation leads to several questions, three of which I will address in this chapter. First, what GGDEF(s) are responsible for the synthesis of c-di-GMP which binds to these receptors? Second, what signal(s) lead to this synthesis? Third, what other potential binding proteins could be encoded within the *A. brasilense* genome?

Possible GGDEFs that synthesize c-di-GMP which binds to PilZ-containing receptors in *A. brasilense*

One possible candidate for this function is a homolog of the characterized PleD protein from *C. crescentus* [23, 24]. In *C. crescentus*, PleD consists of a prototypical phosphorylatable receiver domain followed by another CheY-like receiver domain with the conserved aspartate replaced, and finally a GGDEF domain with cyclase activity [23]. PleD is dynamically localized to the poles of dividing cells upon phosphorylation by two histidine kinases, DivJ and PleC [23]. Homologs of PleD (AZOBRv2_p130136), DivJ

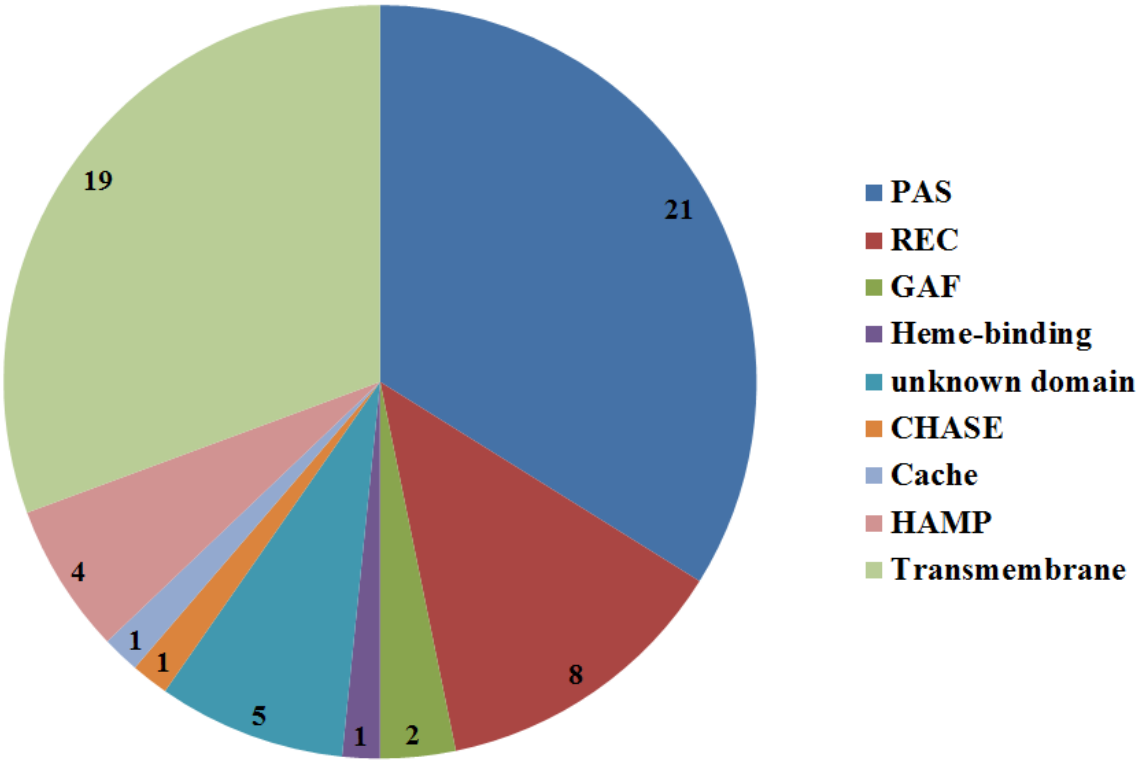

Figure 5.1: Diagram of domains associated with c-di-GMP synthesizing and degrading enzymes within the *A. brasilense* genome. Chart depicts the number of each annotated domain associated with GGDEFs and EALs as compared to the total number of domains. Proteins containing more than one of a particular domain (ex. 2 PAS domains) have each domain represented. Some GGDEFs and EALs are single domain proteins and are not represented in this figure.

(AZOBRv2_200168) and PleC (AZOBRv2_p130138) are found within the *A. brasilense* genome. If *A. brasilense* PleD (AbPleD) does localize to the cell pole, this would be in close proximity to chemoreceptor clusters in *A. brasilense* as observed by YFP fusions to multiple chemoreceptor proteins. It has also been suggested [24] and demonstrated [1] that c-di-GMP concentrations within the cell are asymmetrically distributed and c-di-GMP-binding proteins respond to local pools of second messenger. One hypothesis for protein localization in bacteria is the presence of transmembrane regions that can sequester proteins to microdomains by a diffusion and capture mechanism in which membrane proteins freely diffuse throughout the membrane until captured by interacting partners [25, 26]. Membrane-bound GGDEFs are also candidates for involvement in c-di-GMP synthesis for PilZ containing chemoreceptors. 9 of 30 GGDEF-containing proteins within the *A. brasilense* genome are predicted to have 1 or more transmembrane domains.

Possible signals for c-di-GMP synthesis and degradation in *A. brasilense*

The domain architecture of GGDEFs and EALs can help predict what signals or cues are important for regulation of enzyme activity. Most (10 of 15) EAL-containing proteins in *A. brasilense* are fused to GGDEF domains (active or degenerate) suggesting c-di-GMP degradation is coupled to or regulated by the domain which is responsible for its synthesis. Almost half (14 of 30) GGDEFs contain at least one PAS domain. This suggests c-di-GMP synthesis could be regulated by monitoring the energy status of the cell through binding of cofactors (FAD, Heme, FMN, etc.) as discussed in Chapter 1. In *A. brasilense*, energy taxis is a dominant behavior [27]. *A. brasilense* cells display a strong taxis response to oxygen, the preferred terminal electron acceptor. Further, we show in Chapter 4 that intracellular c-di-GMP levels increased when *A. brasilense* cells experience an increase in the oxygen availability, suggesting that a net increase in the intracellular c-di-GMP content of cells is modulated by oxygen itself and/or oxygen-

metabolism dependent cues (such as changes in intracellular energy). However, this bacterium was not shown to release volatile methanol, a consequence of chemotaxis adaptation to persistent stimuli, upon oxygen addition or removal [28]. This suggests CheA activity (or pathway output), which is ultimately responsible for the activity of proteins functioning in chemotaxis adaptation, is not coupled to the direct sensing of oxygen and/or that responsible chemoreceptors adapt to persistent cues via a methylation-independent mechanism. One hypothesis is that cells could monitor oxygen availability and regulate c-di-GMP levels via PAS-containing GGDEFs, with c-di-GMP levels in turn modulating chemotaxis or aerotaxis behaviors of the cell, rather than oxygen itself. This would also provide a mechanism explaining how *A. brasilense* could monitor the intracellular metabolism during aerotaxis while not sensing oxygen itself. One recent observation supports this hypothesis. Wild type *A. brasilense* cells overexpressing ChsA, a PAS-containing EAL protein (predicted to degrade c-di-GMP), on a low copy number plasmid were unable to maintain an aerotactic band a certain distance from the meniscus (Figure 5.2), predicted to be the preferred oxygen concentration for cell growth [27, submitted]. Also, supporting this hypothesis, the *chsA::Tn5* mutant derivative of *A. brasilense* was unable to form an aerotactic band at all and did not respond to air removal or addition in a temporal aerotaxis assay [submitted].

Potential c-di-GMP binding proteins encoded within the *A. brasilense* genome

To date, the PilZ domain is the only recognized dedicated-c-di-GMP binding protein domain [29, submitted, 30, 31]. However, proteins containing no annotated PilZ domain are shown to bind c-di-GMP as well. One of the best characterized examples is the *C. crescentus* GGDEF protein PleD that binds c-di-GMP, the enzymatic product, allosterically within the I-site (inhibitory site) [32]. Essential residues for binding to the I-site are found in the second receiver domain (Arg148 and Arg178) and the GGDEF (Arg313, Asp362, and Arg390) domain [32]. FleQ, a transcription

factor from *P. aeruginosa*, also was shown to bind c-di-GMP [10]. FleQ consists of a receiver domain, a sigma-54 interacting domain, and a HTH DNA-binding domain [33]. Other examples of c-di-GMP binding proteins are transcription factors VpsT and CpsQ of *Vibrio spp*. [7, 9]. The structure of VpsT was solved by X-ray crystallography showing binding of c-di-GMP occurs in an interface between two response regulator (i.e. REC or CheY-like) domains upon dimerization [7]. This suggests response regulator domains alone could potentially be downstream effectors of c-di-GMP. As discussed for PilZ-c-di-GMP interactions modulating chemotaxis output, response regulator-c-di-GMP interactions could broaden the second messenger's effect by modulating output of many pathways including transcription and chemotaxis (via CheY). The presence of all PilZ domains on chemotaxis receptors and the demonstrated role of the Tlp1 PilZ domain in modulating taxis behaviors (Chapter 4; submitted) in *A. brasilense* together support the hypothesis that c-di-GMP signaling is intimately linked to the chemotactic output of this organism. As mentioned above, no YcgR homolog is detectable within alphaproteobacterial genomes. YcgR is a protein linking c-di-GMP signaling and flagellar motility through the C-terminal PilZ domain and the flagellar switch complex binding N-terminal domain. One hypothesis for not detecting YcgR homologs within many bacterial genomes is sequence variability, and proteins very distantly related to YcgR are actually present. A PSI-BLAST query of the *A. brasilense* Sp245 genome with the N-terminal domain of YcgR (domain of unknown function found exclusively fused to the N-terminus of the YcgR PilZ domain) provides evidence for the hypothesis. PSI-BLAST is a bioinformatics tool that aligns sequences, builds a profile to determine important residues that best aligned the queried sequences, and then, searches the database again to find new protein sequences that match this profile [34]. A PSI-BLAST thus refines the sequence profile or pattern after each iteration depending on the sequences retrieved (34).

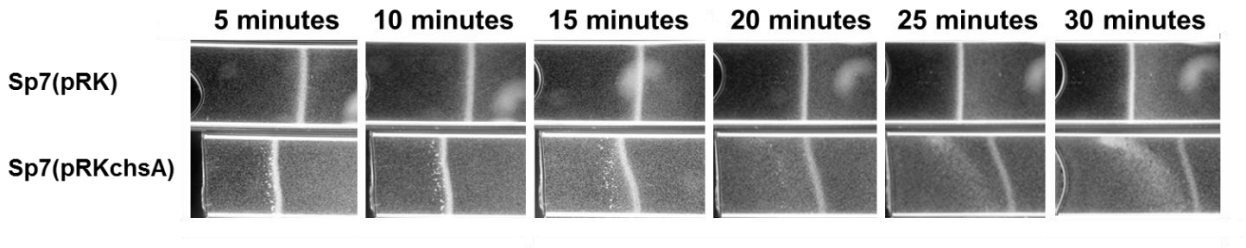

Figure 5.2: Effect on spatial aerotaxis by putative overexpression of c-di-GMP degrading enzyme ChsA in the wild type background. Wild type Sp7 with empty vector (top panels) is able to maintain an aerotactic band over the time period shown. Sp7 expressing ChsA from a low copy vector in addition to chromosomal ChsA (bottom panels) clumps in front of aerotactic band and is unable to maintain an aerotactic band at a certain distance from meniscus: the aerotactic band is seen moving away from the meniscus when ChsA is overexpressed, a phenotype not observed with the wild type strain where the aerotactic band position remains unchanged during the time of the experiment.

Indeed, I found that using the YcgRN domain as a query for PSI-BLAST search of the Sp245 genome and identified numerous hits with confident e-values (e-value: expected number of chance matches) that are significant after several iterations (Table 5.1). Moreover, one protein contained an expect e-value below threshold after the first search (i.e. without iteration; e-value4e-4): a CheY homolog (locus AZOBRv2_180191), suggesting this is a closely related domain to that of the YcgRN. In fact, the same query repeated in PSI-BLAST search against all alphaproteobacteria genomes identifies AZOBRv2_180191 as the top protein, after the first iteration (e-value of 1e-26). In PSI-BLAST, all the returned sequences from the first iteration are used to produce a "pattern" used in the second iteration to identify additional protein candidates that would share this pattern. After a second iteration, 12 of 16 protein sequences retrieved that scored above threshold possessed response regulator domains. After three iterations, a majority of returned protein sequences (82 or 88) are known or putative response regulators (Table 5.1), including *A. brasilense* CheY4 (amino acids 8-110) within the chemotaxis operon homologous to the F7 chemotaxis operon of model organism *E. coli* [35], CheY1, and transcriptional regulators. While the N-terminal of YcgR has no known sequence similarity with response regulators, this suggests that the N-terminal domain of YcgR may either be related to response regulator domains, perhaps with a very low sequence similarity and/or that a motif within YcgRN may be similar to a particular motif within response regulators. Given that most of these response regulators are CheY homologs, it is possible that YcgRN may share homology with flagellar switch complex binding proteins or present a putative nucleotide binding motif. This also suggests the N-terminal domain of YcgR, which was found to bind FliG and FliM (switch complex) in presence of c-di-GMP could potentially predict proteins which are likely to interact with the flagellar switch complex in other bacterial genomes, a proposition that would be especially valuable in species with multiple CheY homologs for which such prediction has not

Table 5.1 PSI-BLAST hits using the N-terminal domain of *E. coli* YcgR as the query sequence within the genome of *A. brasilense* and related bacteria *C. crescentus* and *R. centenum*. An abbreviated list of returned proteins are shown.

	YcgRN	
Bacterium	**Gene Product**	**Notes**
A. brasilense	AZOBRv2_180191	Response regulator similar to *E. coli* CheY
	AZOBRv2_90006	Response regulator similar to *P. aeruginosa* CheY
	AZOBRv2_p350063	Response regulator similar to *E. coli* CheY
	CheB4	
	FlcA	Orphan response regulator necessary for flocculation
	CheY4	
	AZOBRv2_200195	Response regulator upstream of *che4*
	AZOBRv2_200216	Response regulator downstream of *che4*
	CheY1	
C. crescentus	CtrA	Response regulator for cell cycle progression
	CheYIII	
	CheYIV	
	CheYII	
	DivK	Response regulator in polar development
	McpE	
	PhoB	
	PleD	
R. centenum	CheA3	
	CheW3b	
	FtsK	Cell division chromosome partition protein
	DivJ	Polar histidine kinase regulating PleD phosphorylation

been made. Such hypothesis could be tested by demonstrating that the proteins retrieved in the search all bind flagellar motor proteins. After 7 iterations, the PSI-BLAST search converged, indicating that all homologs that share the motif identified had been retrieved from the genome. The result of these PSI-BLAST iterations did not identify any specific amino acid motif suggesting the similarity could be ambiguous and rely on other characteristics like secondary structure. Since most of the sequences retrieved are single domain proteins or possess a receiver/CheY-like domain, it is likely that YcgRN is homologous to CheY-like receiver domain proteins and may have diverged from an ancient CheY-like domain.

Also included in the returned sequences was orphan response regulator and transcription factor FlcA (amino acids 1-104), a protein necessary for flocculation in *A. brasilense* [36, Bible, Russell, and Alexandre in press]. FlcA consists of a helix-turn-helix DNA binding-terminal domain and a receiver/CheY-like domain at the N-terminus. The PSI-BLAST query indicated a hit with the CheY-like domain of FlcA. The hypothesis that FlcA could act upon the flagellar switch complex (to promote cell aggregation) can easily be tested by a number of biochemical techniques including co-immunoprecipitation and affinity chromatography. One transcription factor, H-NS, is already known to bind the switch complex protein FliG in *E. coli* [37-40]. To further test this approach of predicting proteins which interact with the flagellar switch complex, YcgRN was queried within other closely related bacterial genomes including *C. crescentus* and *R. centenum* (Table 5.1) to predict proteins which interact with the flagellar switch complex in these species. Among the returned protein sequences in *C. crescentus* were 3 CheY proteins (II, III, and IV) and 2 response regulators. In *R. centenum*, however, no CheY proteins were identified. Interestingly, CheA3 (phospho transfer region) and CheW3b (low complexity region C-terminal of CheW domain) of the cyst regulation *che* operon [41] and the polar-localized histidine kinase DivJ were among the top hits. These results suggest not all bacteria could have evolved similar

strategies for switch complex binding. Interestingly, the 3 chemotaxis-like operons of *R. centenum* are homologous to Che1, Che2, and Che3 of *A. brasilense*. However, as stated in Chapter 1, *A. brasilense* has acquired a fourth chemotaxis operon through horizontal gene transfer that regulates flagellar motility.

To further test this approach, the PilZ domain of YcgR was used as the query within selected genomes for identification of possible c-di-GMP interacting proteins (Table 5.2). Among the returned sequences in *A. brasilense* were 4 chemoreceptors containing a PilZ domain as well as 2 GGDEF domain proteins and an adenylate cyclase. Surprisingly, RpoH also was identified and the uridylyltransferase GlnD involved in nitrogen metabolism [42]. These proteins are all able to bind nucleotydyl or nucleotides, suggesting that the PSI-BLAST query was capable of identifying a subset of nucleotydyl or nucleotide binding proteins. Given that PilZ binds c-di-GMP and thus is a divergent nucleotide-binding domain, homology to these proteins is not absolutely unexpected. Also, proteins identified in the query using YcgRN were identified using the PilZ domain including FlcA (amino acids 3-118), CheY4 (amino acids 9-123), and many proteins proximal to Che4 (within 10 open reading frames up or downstream) including a CheY homolog that was likely transferred to *Azospirilla* with Che4, based upon synteny. The identification of FlcA and CheY4 with both YcgRN and the PilZ domain of YcgR aligning over essentially the same amino acids suggest both domains of YcgR are similar to response regulators within *A. brasilense* and possibly homologous to each other through duplication. A PSI-BLAST query within the *E. coli* K12 genome with both YcgRN and YcgR-PilZ identified response regulator-containing proteins but did not identify the sequence of the other YcgR domain.

The query within *R. centenum* identified the PilZ containing chemoreceptor Aer, polar histidine kinase PleC, and two chemotaxis proteins CheB2 and CheAY (*A. brasilense* CheA1 homolog) (Table 5.2). Using annotated PilZ domains to query within the same genome (example: Tlp1 PilZ

domain against the *A. brasilense* genome) gave similar results as YcgR-PilZ and has shed light on putative c-di-GMP binding proteins.

A recent investigation in *P. aeruginosa* using a proteomic approach with an immobilized c-di-GMP identified interacting proteins by mass spectrometry [43]. A majority of the identified proteins using the proteomic approach contained no recognized c-di-GMP binding domain, however, the proteomic data gave me a blueprint to test the accuracy of the PSI-BLAST approach. To increase accuracy, I queried the *P. aeruginosa* PAO1 genome with the PilZ domain of Alg44 experimentally shown to bind c-di-GMP in *P. aeruginosa* [44] (Table 5.3). Some advantages to a bioinformatics approach are 1) the identification of integral membrane proteins are not easily assayed *in vitro* and 2) the investigator is not limited to proteins expressed only at the stage in growth at time of disruption of the cells. For example, the work utilizing the proteomic approach only used cell grown to stationary phase. It must be noted the PSI-BLAST query does not return the same proteins regardless of the genome used. For example, a query of *B. subtilis*, *V. cholera*, and *Rhodobacter sphaeroides* using YcgRN identifies predominantly ABC transporter proteins, not response regulators as in *A. brasilense*. This suggests bacteria have evolved numerous strategies/proteins to modulate flagellar motility that may not rely on YcgR-like proteins but instead acquired or duplicated CheY proteins, for example, and cannot be detected using this approach. The YcgR PilZ query was successful in identifying some known proteins to bind c-di-GMP in *V. cholera* and *B. subtilis* as well as ATP binding domain of some ABC transporters. This suggests this approach may identify a broader nucleotide binding motif rather than one specific for c-di-GMP. This is logical if c-di-GMP signaling is ubiquitous among all bacteria and PilZ domains evolved in an early common ancestor. However, I cannot confidently assert all c-di-GMP binding proteins were identified.

Table 5.2: Relevant PSI-BLAST hits using the PilZ domain of *E. coli* YcgR as the query sequence within the genome of *A. brasilense* and *Rhodospirillum centenum*.

		YcgR-PilZ
A. brasilense	Tlp1	PilZ domain
	AZOBRv2_70073	MCP with Hemerythrin domain
	AZOBRv2_p150051	GGDEF domain
	AZOBRv2_200121	GGDEF/EAL protein with I-site
	AZOBRv2_p220106	MCP with PilZ domain
	AZOBRv2_40341	MCP with PilZ domain
	AZOBRv2_p220070	Adenylate cyclase
	AZOBRv2_140119	DNA polIII epsilon subunit
	AZOBRv2_10198	RpoH (sigma 32)
	AZOBRv2_10466	GlnD (PII protein)
	AZOBRv2_40395	SfsA sugar fermentation stimulation protein
	AZOBRv2_p210130	Transcription regulator
	AZOBRv2_p1130080	Transcriptional regulator just downstream of Che1
	AZOBRv2_p160004	FlbA homolog flagellum biogenesis
	AZOBRv2_200216	RsbU downstream of Che4
	FlcA	
	AZOBRv2_200200	CheY4
	AZOBRv2_200195	CheY homolog just upstream of Che4
R. centenum	RpoD	Sigma 70
	PleC	Polar histidine kinase phosphorylates PleD
	PpdK	Pyruvate phosphate dikinase
	CorA	Magnesium transport protein
	CheB2	In flagella biosynthesis che2 operon
	CheAY	Homolog of CheA1 from *A. brasilense*
	CsgA	Major curli protein
	Aer	PilZ domain

Table 5.3: Relevant PSI-BLAST hits using the PilZ domain of *P. aeruginosa* Alg44 as the query sequence within the genome of *P. aeruginosa* PAO1. Proteins listed in the left column are proteins identified by PSI-BLAST using Alg44 PilZ domain. "**x**" indicates protein also identified using the chemical proteomic approach in [43].

Identified *P. aeruginosa* protein	**Identified in [43]?**
FtsE	
CcmA	**x**
PelF	
CheB	
FlhA flagellar biosynthesis protein	
LadS Lost adherence sensor	
PilH CheY homolog	
ZipA cell division protein	**x**
ChpA CheA homolog	**x**
RhlB	**x**
PilG, CheY homolog	
ZnuA Adhesin	
WspF CheB homolog	
PqsH monooxygenase	**x**
MotC Flagellar motor protein	
MCP	
PA4781 Response regulator/HD-GYP	**x**
YraM putative lipoprotein	**x**
NarL	
GlnQ polar amino acid transporter	**x**

The PSI-BLAST approach to identify putative c-di-GMP binding proteins was able to provide a list of *A. brasilense* candidate proteins using the known PilZ domain of YcgR. Unexpectedly, a query with the switch complex interacting YcgRN sequence provided support for the hypothesis that CheY is not the only protein able to bind and interact with the flagellar switch complex in multiple genomes. However, this *in silico* hypothesis must be verified in experiments before a more systematic conclusion can be reached regarding the homology between these domains. Most surprising, perhaps, was the redundancy in *A. brasilense* proteins identified in both queries again suggesting the intimate link between c-di-GMP signaling and chemotaxis in this bacterium. This also suggests YcgR itself may be redundant by some perceivable duplication event.

Summary of PSI-BLAST Approach

The use of a bioinformatics approach cannot replace experimental data, especially when trying to discover potential binding partners of compounds like c-di-GMP. However, it can potentially predict the likelihood of experimental outcomes or lead experimenters into a guided exploration rather than a "fishing expedition". The use of PSI-BLAST as a first step has led to additional steps to verify its discoveries including structure superimpositions and multiple sequence analyses. For example, a PSI-BLAST search against the PDB structure database using YcgRN as the query returns response regulator domains almost exclusively. To investigate similarity further, a multiple sequence alignment was generated with the MAFFT program [45, 46] using all annotated YcgRN domains (~ 1000 protein sequences) and the response regulator proteins from *A. brasilense* returned in the original PSI-BLAST search (~ 100 sequences, only single domain proteins or transcriptional regulators containing a CheY-like response regulator domain). The resulting alignment was used to generate a Logo to illustrate sequence similarity visually (Figure 5.3). Interestingly, the conserved aspartate phosphorylation site in the response regulator domain

(by the cognate histidine kinase) was the only strictly conserved residue in the alignment (Figure 5.3). The study by Benach et al. concluded, although sequence similarity between the two domains of the YcgR homolog of *V. cholera* is low (5%), the domain structures superimpose with an RMSD of 2.7Å [47]. They suggested YcgR homologs evolved from an ancestor protein containing two PilZ domains; a domain organization still present in some bacterial genomes. In conclusion, using the N-terminal domain of YcgR in a PSI-BLAST query could potentially identify possible switch complex interacting proteins in genomes which do not contain an obvious YcgR homolog.

Possible future research to validate PSI-BLAST technique

The next logical step in this research would involve studies to test interactions between putative proteins and either c-di-GMP or possibly components of the flagellar switch complex, FliM or FliG. The orphan response regulator FlcA from *A. brasilense* was identified by sequence similarity using both YcgRN and YcgR-PilZ domains and would be a candidate for further studies. To test possible binding interactions between FlcA and c-di-GMP, the former could be recombinantly expressed and purified. C-di-GMP is easily synthesized *in vitro* by *C. crescentus* PleD recombinantly expressed in *E. coli* [23, Chapter 4]. Binding of c-di-GMP to FlcA could be investigated by several techniques already shown to positively identify interactions in other bacteria [7, 10, 14, 31, 48]. Also, FlcA interactions with flagellar switch proteins could follow the protocol established in studies with YcgR [17]. Other possible candidate proteins from *A. brasilense* to test for interactions with c-di-GMP include CheY1 and CheY4. CheY4 was also identified by both N-terminal and C-terminal YcgR queries within the *A. brasilense* genome. These proteins could be used as putative positive controls for flagellar switch protein interactions due to their involvement in chemotaxis-like pathways.

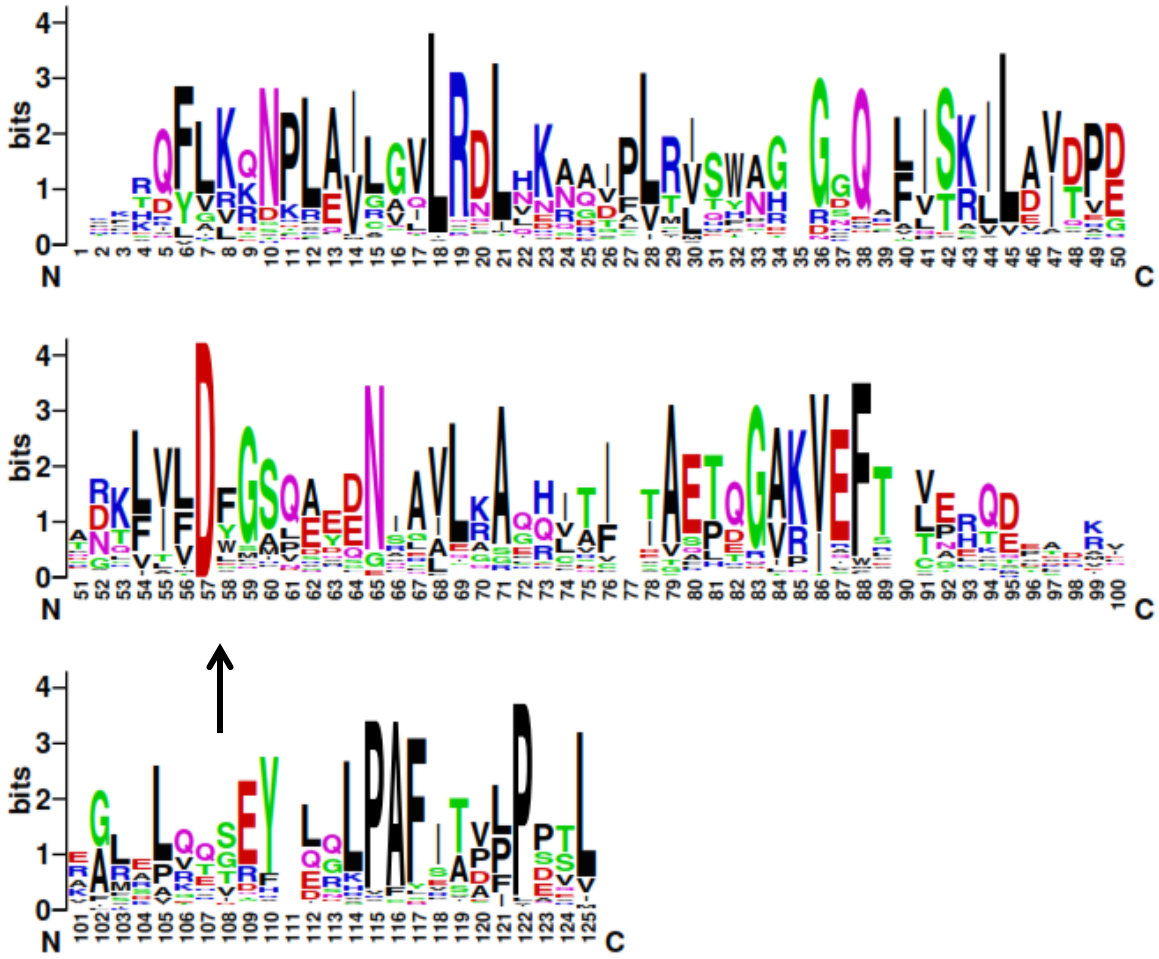

Figure 5.3: WebLogo output generated from the multiple sequence alignment of YcgRN and *A. brasilense* response regulator domains. The logo was generated using [49, 50] with all YcgRN sequences from Pfam [51] as well as response regulator domains from *A. brasilense* returned in a genome PSI-BLAST query with YcgRN sequence from *E. coli* as query. The phosphorylation site of response regulators remains strictly conserved in the multiple sequence alignment with YcgRN (arrow).

A working model of c-di-GMP effects on the taxis behavior of *A. brasilense*

The study of the PilZ function of Tlp1 has shifted the known model of c-di-GMP effects on motility that higher levels of the intracellular c-di-GMP signal lead to sessility. In the case of *A. brasilense* during increased aeration, cells able to sense c-di-GMP via the Tlp1 PilZ domain remain aerotactic, but cells containing a variant Tlp1 unable to bind c-di-GMP have increased cell-cell aggregation. In this case, cells remain motile and tactic in presence of c-di-GMP as long as cells have the ability to sense its presence through the PilZ domain of Tlp1. However, a model for explaining this observation mechanistically

was not presented in manuscript presented in Chapter 4. According to the Pfam database of domain architectures, very few of the over 20,000 annotated chemotaxis receptors also contain an additional domain fused to the C-terminus, most of which are hemerythrin and PilZ domains [51]. This suggests perturbations to the signaling domain confirmation of receptors within the receptor cluster caused by such domain fusions could be detrimental to their ability to effectively modulate CheA activity. Therefore, the incorporation of these additional domains is not random.

There are two solved structures of c-di-GMP binding PilZ domains which occur fused to another protein domain, the YcgR homolog VCA0042 from *V. cholera* (PBD ID 1YLN; R Zhang, M Zhou, S Moy, F Collart, and A Joachimiak and [47]). The N-terminus of the PilZ domain, known as the c-di-GMP switch, is a flexible coil in the apo state [47]. This suggests the PilZ domain of Tlp1 could potentially be found in many confirmations relative to the MCP homodimers given the conservation of this switch. This flexibility could affect signaling in several ways including modulating the helical bundle confirmation of the Tlp1 homodimer or allow interactions with other proteins or other domains within receptors. To gain further insight, homology models were constructed using Phyre2 software [52] for the conserved signaling domain of Tlp1 and PilZ domain separately because no structural templates are available to model the entire cytoplasmic

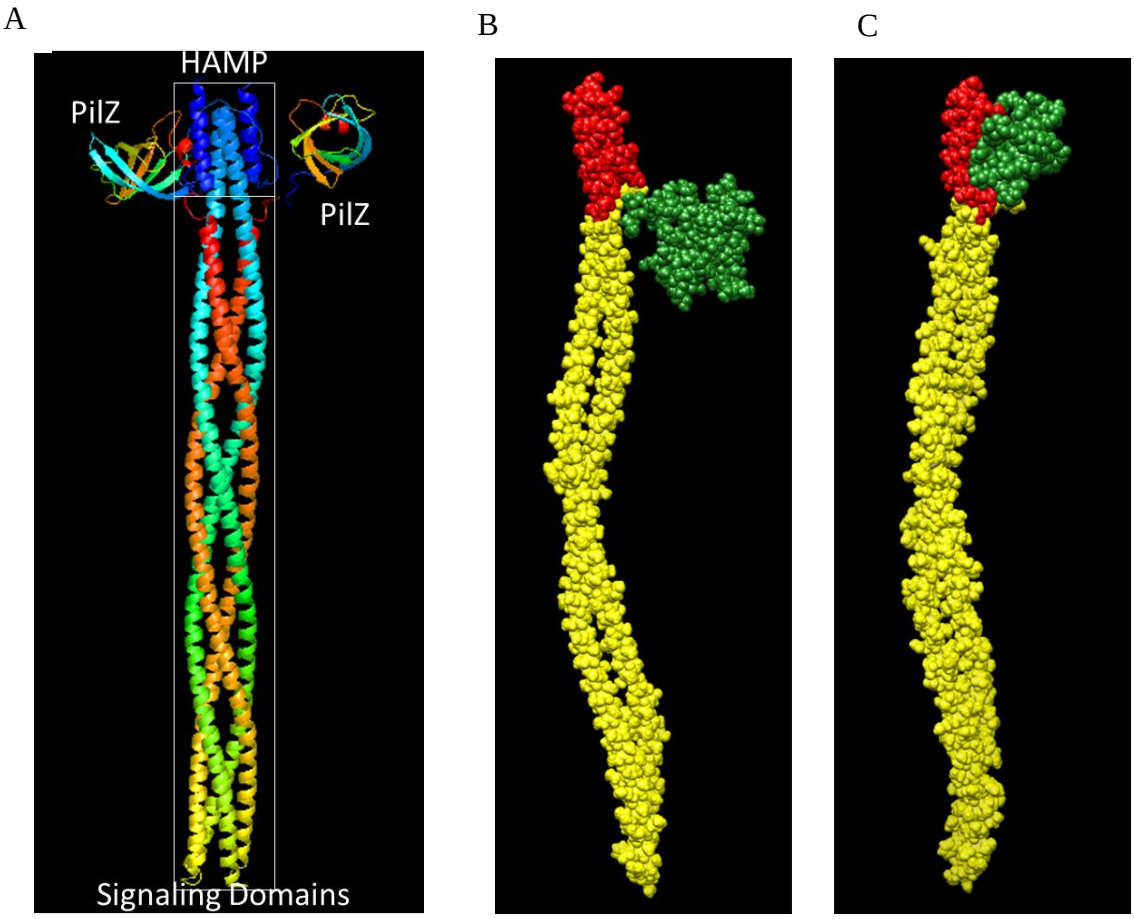

Figure 5.4: Homology modeling results for Tlp1 cytoplasmic domains with the PilZ domain in multiple confirmations. A, Homodimer ribbon diagram of the cytoplasmic domains of Tlp1 produced from homology modeling using known structures of Tsr from *E. coli* and PilZ protein PA4608 of *P. aeruginosa*. HAMP and signaling domains are boxed. B, Spacefill representation of a monomer from A with PilZ domain in a hypothesized c-di-GMP bound state. C, Spacefill representation of monomer with apo PilZ domain extended with possible interactions with HAMP domain.

portion of Tlp1. The two models were combined by incorporation of a new bond between the C-terminus of the MA domain and N-terminus of PilZ using Sirius [53] (Figure 5.4). Rotation of the backbone bonds in the c-di-GMP switch illustrated possible interactions between PilZ and HAMP domains (Figure 5.4C). The HAMP domain is responsible for conversion of the extracellular signal into the intracellular signal regulating CheA activity [54]. Therefore, any protein-protein interactions between the HAMP and PilZ domains could change CheA activity and thus chemotaxis output. Evidence for this hypothesis is presented in Chapter 4. For example, a *Δtlp1* strain expressing $Tlp1^{\Delta PilZ}$ does not respond to increases or decreases in aeration by increasing swimming velocity, however, wild type *A. brasilense* does (Figure 4.4). Also, *Δtlp1*(pRK$Tlp1^{\Delta PilZ}$) has an inverted response relative to wild type in swimming reversal frequency upon both increases and decreases in aeration. An inverted response (repellant response) to oxygen was observed in *E. coli* cells expressing a mutant variant of Aer with a single residue mutation in the HAMP domain (V264M) [55]. This suggests changes to HAMP confirmation or function can cause an inverted response similar to $Tlp1^{\Delta PilZ}$. A model of Tlp1-c-di-GMP function is proposed (Figure 5.5).

Chemotaxis pathway crosstalk in *A. brasilense*

The laboratory of Jeff Stock first observed cross-talk between the chemotaxis and nitrogen assimilation pathways in 1988 [56]. Phosphorylated CheA was able to transfer the phosphoryl group *in vitro* to NtrC (NR_I), the response regulator for nitrogen assimilation gene transcription in enteric bacteria [57, 58]. NtrB, the cognate histidine kinase for NtrC and nitrogen assimilation regulator, could also phosphorylate CheY *in vitro* [56]. Evidence for suggested crosstalk in *A. brasilense* was obtained in the Alexandre laboratory while characterizing Δ*cheB1* and Δ*cheB1cheR1* deletion mutants

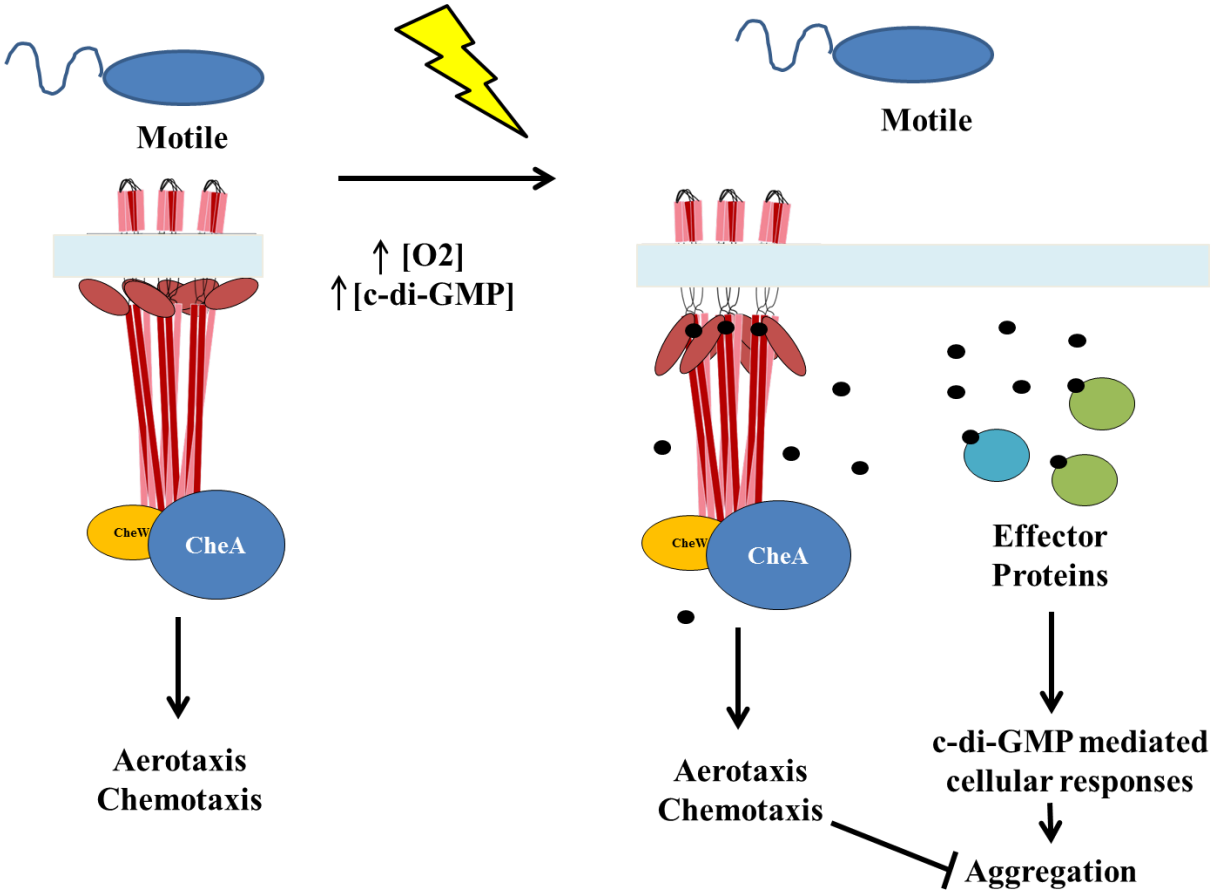

Figure 5.5: Working model of the integration of c-di-GMP signaling and the chemotaxis pathway(s) of *A. brasilense* through Tlp1. *A. brasilense* cells are aerotactic and chemotactic with random motility. Upon an increase in aeration and subsequent increase in c-di-GMP concentrations, which signal for a transition to a sessile lifestyle, the PilZ domain of Tlp1 is able to bind c-di-GMP allowing cells to remain aero- and chemotactic to navigate to an environment better suited for energy production. Thus, aerotaxis is able to block the persistent aggregation signal sensed by other unknown c-di-GMP effector proteins.

using a temporal methanol release assay used to detect the by-product of CheB1-dependent demethylation of receptors during adaptation [28]. Specially, no net methanol release was detected for wild type Sp7 or Δ*cheB1* in response to succinate addition or removal. However, methanol release was observed for both succinate addition and removal in a Δ*cheB1cheR1* strain [28]. This suggests that i) methylation/demethylation of receptors that respond to succinate was masked in the wild type and became apparent only when both CheB1 and CheR1 were deleted and that ii) the sensitivity of the responsible receptors to succinate was modified by the absence of CheB1 and CheR1. Methanol release in response to galactose is another example. In Sp7, methanol release was detected upon galactose removal. In the Δ*cheB1* mutant, no methanol release occurred upon addition or removal suggesting CheB1 could be responsible for adaptation to galactose removal. However, methanol release occurred upon addition of galactose in the Δ*cheB1cheR1* mutant but not removal [28].

This suggested crosstalk involves adaptation of chemoreceptors in response to a single stimulus by CheB1 and CheR1. Sensitivity and adaptation to persistent stimuli is mediated at the chemoreceptor-level by methylation/demethylation. In *A. brasilense*, changing the adaptation protein repertoire uncovers multiple layers of possible adaptation that relies upon competition from various proteins (from various pathways) that can only be observed when the better competitors are absent. However, the Δ*cheB1cheR1* mutant often displays opposite phenotypes to those displayed by strains carrying single deletions of CheA1, CheY1, or Che1 [59]. One example is the clumping phenotype. A majority of Che1 mutants have a greater propensity to clump, a transient form of cell-to-cell contacts [59, Bible, Russell, and Alexandre]. Cells with a deletion of CheA1 or CheB1 clump more under conditions of high aeration compared to wild type while a deletion of CheY1 or Che1 has an intermediate effect on clumping [59, Bible,

Russell, and Alexandre]. The Δ*cheB1cheR1* mutant hardly clumps at all or under any tested conditions [59, Bible, Russell, and Alexandre].

My observations during characterization of the clumping behavior of *A. brasilense* could further support the occurrence of crosstalk between chemotaxis pathways. As my work has shown (Chapter 3), motile *A. brasilense* cells can transiently modulate the amount of clumping in response to air removal and addition [Bible, Russell, and Alexandre]. Wild type cells transiently decrease clumping upon both air addition and removal before returning to the prestimulus level of clumping (Figure 5.6). However, the *Δche1* mutant increases clumping upon air removal. Clumping returns to the prestimulus level over a period of several minutes and no response in clumping is observed upon air addition. A recently constructed *Δche4* mutant (Z. Xie, unpublished) slightly decreases clumping upon air removal prior to an increase similar to the *Δche1* response; in fact the increase in clumping is delayed relative to that seen in the Δ*che1* mutant (Figure 5.6). In contrast to *Δche1*, clumping in the *Δche4* mutant continues to increase over time while in a pure nitrogen atmosphere. Upon air addition, clumping transiently decreases in the *Δche4* mutant, a response reminiscent of the wild type, before returning to a high clumping behavior similar to that observed before addition. The *Δche1Δche4* double mutant increases clumping upon air removal (similar to *Δche1*). The amount of clumping remains high and relatively constant while under a nitrogen atmosphere before a transient decrease in clumping upon air addition (similar to wild type and *Δche4*). However, instead of returning to the high prestimulus amount of clumping, clumping reaches a lower steady state level in the *Δche1Δche4* mutant. These data suggest that 1) Che1 is necessary for the transient decrease in clumping upon air removal and addition with a contribution from one or more Che4 proteins, and 2) the steady state clumping after air removal requires both functional Che1 and Che4

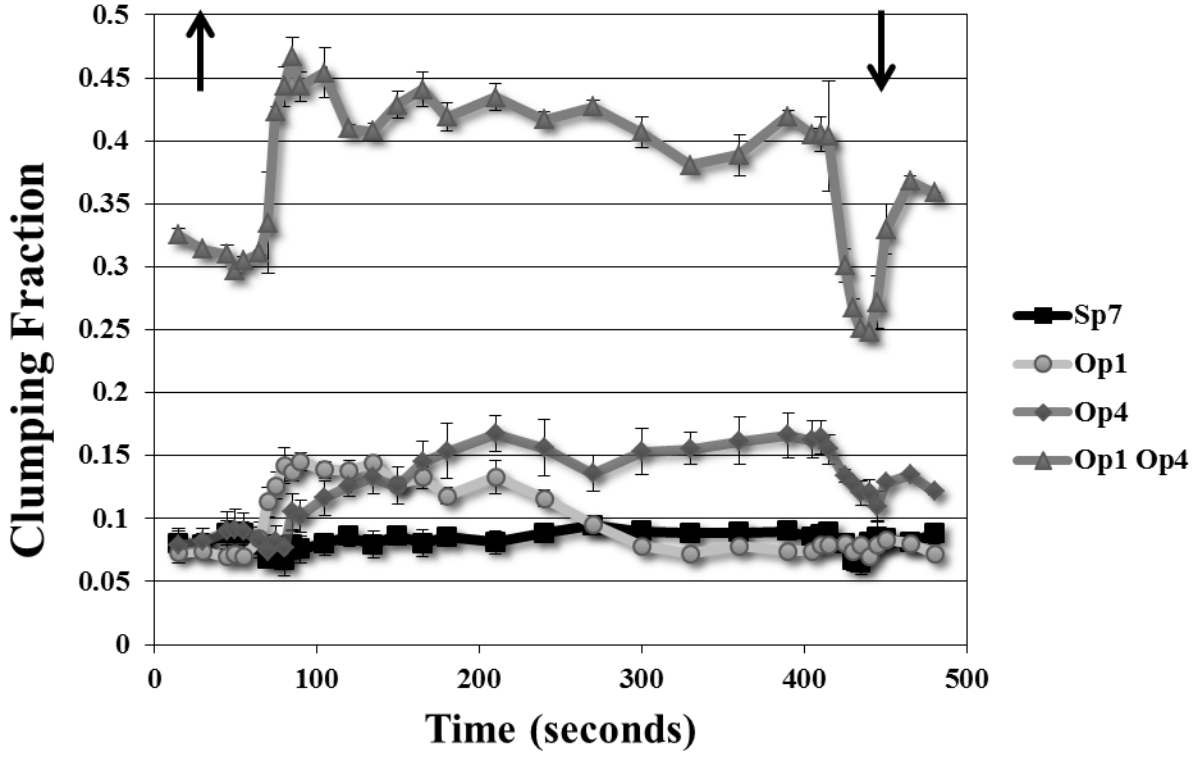

Figure 5.6: Clumping of Sp7 and mutant derivatives in the temporal gas perfusion assay. Sp7 has a relatively low clump fraction that transiently decreases upon air removal (up arrow) and air addition (down arrow). Op1 increases clumping at air removal and gradually decreases over several minutes with no response to air addition. Op4 slightly decreases clumping upon air removal before increasing the clump fraction relative to prestimulus. Clumping decreases upon air addition for Op4. The Op1Op4 mutant clumps significantly more than wild type under steady state conditions. However, Op1Op4 increases clumping upon air removal after a slight time delay and remains high until air addition causes a transient decrease in clumping before returning to a higher clump fraction.

pathways. The single mutants displayed opposite clumping phenotypes in regards to steady state clumping fraction after air removal; *Δche1* decreased clumping until reaching the prestimulus

steady state and *Δche4* increased clumping until subjected to a new stimulus (air addition) suggesting the pathways may have opposite effects on steady state clumping.

The duration between air removal and addition in the assay was 6 minutes upon which time *Δche1* was no longer sensitive to addition. Next, I tested the hypothesis that the changes in the steady state level of clumping seen after the initial air removal and air addition may reflect changes in the ability of the cells to adapt to the new aeration conditions and thus to adjust their sensitivity, a behavior that is dependent on the ability of receptors to be reset by differential methylation. First, I tested if the *Δche1* mutant could be sensitive to air addition if the time duration between air removal and air addition was shortened. The assay was modified to test clumping i) with 3 minutes (*Δche1* returned to prestimulus clumping) or ii) 1 minute between temporal changes in aeration conditions (air removal followed by air addition). In both cases, wild type cells displayed a similar clumping behavior to previous assays, transient decreases in clumping upon air removal and addition, indicating a robust response (Figure 5.7A). The *Δche1* mutant strain displayed a similar increase in clumping upon air removal followed by a gradual decrease of clumping back to prestimulus levels. However, when stimulated by air addition after 3 minutes, *Δche1* responded with an increase in clumping similar to air removal but no gradual decrease in clumping for the remainder of the assay (2 minutes). Interestingly, when stimulated by air addition 1 minute after removal, *Δche1* transiently decreased clumping before increased clumping compared to before addition (Figure 5.7B). A gradual decrease in clumping was observed until cells reached the clump fraction at time of air addition. Therefore, *Δche1* clumping sensitivity to air addition is dynamic and seems to depend on the time the cells remained under particular aeration conditions. The ability of the Δ*che1* cells to respond to air addition when the time was shortened suggests that this pathway functions directly in resetting the sensitivity of cells and thus contribute to their ability to respond to further changes in aeration. This was

A

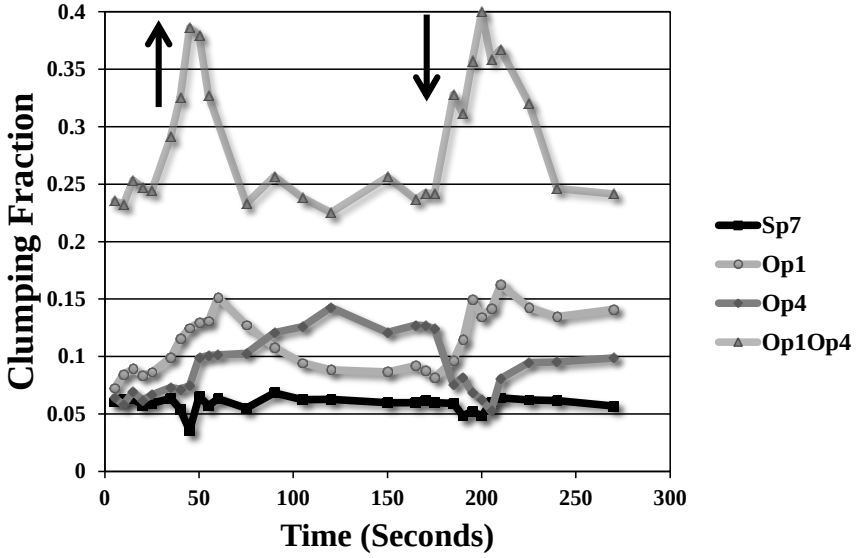

Figure 5.7: Clumping of Sp7 and mutant derivatives in the temporal gas perfusion assay with different durations between air removal and air addition. (A) Gas perfusion assay with 3 minutes between air removal and addition. Sp7 transiently decreases clumping in response to both stimuli. Op1 increases clumping after each stimulus except does not decrease clumping after air addition. Op4 responds similarly to the 6 minute duration described in Figure 5.2. Op1Op4 has an inverted response relative to wild type. (B) Gas perfusion assay with 1 minute between air removal and addition. Sp7 transiently decreases clumping upon air removal and addition. Op1 transiently decreases clumping upon air addition before increasing clumping relative to before air addition. Op4 does not respond to air addition while Op1Op4 responds similar to Figure 5.2.

B

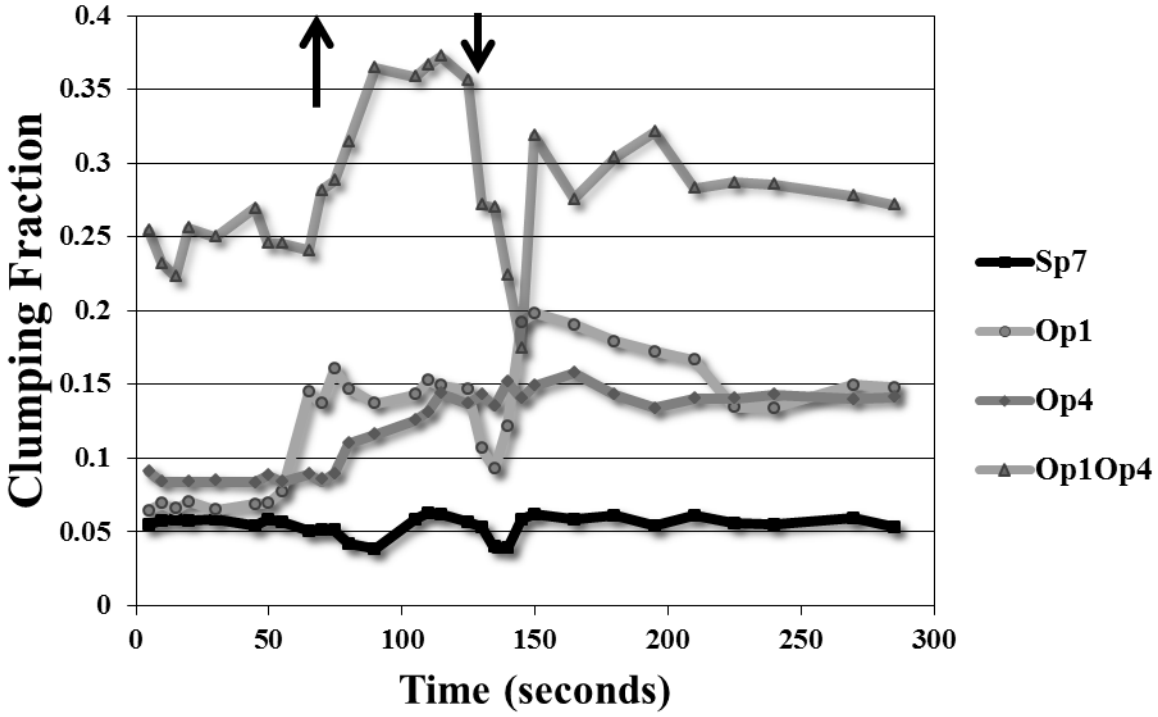

Figure 5.7 continued.

unexpected if the only adaptation mechanism that functions in *A. brasilense* is dependent upon differential methylation of receptors because these are active in matter of seconds and would be required only upon additional stimuli received, not over several minutes as shown here. Results for *Δche4* also indicated a similar dynamic sensitivity to temporal changes in aeration conditions. When stimulated by air addition 3 minutes after removal, *Δche4* cells transiently decreased clumping (Figure 5.7A). No clumping response was observed for this mutant with air addition 1 minute after removal (Figure 5.7B). These results suggest that the Che4 pathway is essential for the ability of cells to remain sensitive to changes in aeration conditions immediately after chemostimulation (thus at short time scales) which supports a role for a chemotaxis adaptation system; however, Che4 appears dispensable under persistent aeration conditions, at longer time scales. Thus *A. brasilense* is able to adapt and remain sensitive to changes in aeration conditions by using chemotaxis-dependent systems (short timescale) as well as additional systems that appear to be novel in that they function at longer time scales. Previous results indicate no net release of methanol upon oxygen addition or removal for wild type, *ΔcheB1*, or Δ*cheB1ΔcheR1* [28]. This suggests sensitivity or adaptation to changes in aeration could be methylation-independent (i.e., independent of CheB activity) and could involve a different mode of adaptation, perhaps one relying on the activity of the CheD deamidase which also resets receptors by increasing the total number of CheR methylation sites (and thus antagonizes CheR, similar to CheB). In this case, it would be a function dependent on Che4, as my results suggest. The presence of a CheD homolog within Che4 is consistent with such a hypothesis, For longer time scales, sensitivity of cells to changes in aeration conditions is dependent on Che1 but not likely via an effect of a methylation/demethylation adaption system which are expected to function at shorter time scales. The observation that the PilZ-containing Tlp1 chemoreceptor is necessary for aerotaxis [60] and that the ability to sense c-di-GMP by Tlp1 is required for Tlp1 function

[submitted] in maintaining cell sensitivity to aeration conditions provides evidence that PilZ/c-di-GMP interactions modulate response sensitivity in aerotaxis in this organism and thus, provides a possible methylation-independent mechanism for maintaining sensory sensitivity over a broad range of background effector concentrations. The activity of CheR/CheB on chemoreceptors was shown to change chemoreceptor packing within the receptor cluster by changing charge coupling, in model organisms [61, 62]. The PilZ domain is shown to undergo a large conformational change upon c-di-GMP binding [47]. One could hypothesize that c-di-GMP binding to Tlp1 may modulate the ability of the chemoreceptors within signaling clusters to process sensory input: c-di-GMP binding to the PilZ domain of Tlp1 could conceivably cause a very large conformational change within the receptor that would perhaps affect the ability of the chemoreceptor cluster to modulate CheA activity in the same fashion regardless of prototypical sensing via the periplasmic sensing domain. In this case, intracellular sensing of c-di-GMP would trump extracellular sensing. The inhibitory effect of c-di-GMP binding on chemosensing would persist as long as the local c-di-GMP concentrations are high, suggesting another mechanism by which the cells would maintain an intimate coupling between sensing and metabolism.

List of References

1. Christen, M., et al., *Asymmetrical Distribution of the Second Messenger c-di-GMP upon Bacterial Cell Division.* Science, 2010. **328**(5983): p. 1295-1297.

2. Paul, R., et al., *Activation of the diguanylate cyclase PleD by phosphorylation-mediated dimerization.* Journal of Biological Chemistry, 2007. **282**(40): p. 29170-7.

3. Schirmer, T. and U. Jenal, *Structural and mechanistic determinants of c-di-GMP signalling.* Nature Reviews Microbiology, 2009. **7**(10): p. 724-735.

4. Pratt, J.T., et al., *PilZ domain proteins bind cyclic diguanylate and regulate diverse processes in Vibrio cholerae.* Journal of Biological Chemistry, 2007. **282**(17): p. 12860-12870.

5. Martinez-Wilson, H.F., et al., *The Vibrio cholerae hybrid sensor kinase VieS contributes to motility and biofilm regulation by altering the cyclic diguanylate level.* Journal of Bacteriology, 2008. **190**(19): p. 6439-6447.

6. Guo, Y.Z. and D.A. Rowe-Magnus, *Identification of a c-di-GMP-Regulated Polysaccharide Locus Governing Stress Resistance and Biofilm and Rugose Colony Formation in Vibrio vulnificus.* Infection and Immunity, 2010. **78**(3): p. 1390-1402.

7. Krasteva, P.V., et al., *Vibrio cholerae VpsT regulates matrix production and motility by directly sensing cyclic di-GMP.* Science, 2010. **327**(5967): p. 866-8.

8. Wang, H.X., et al., *Interplay among Cyclic Diguanylate, HapR, and the General Stress Response Regulator (RpoS) in the Regulation of Vibrio cholerae Hemagglutinin/Protease.* Journal of Bacteriology, 2011. **193**(23): p. 6529-6538.

9. Ferreira, R.B., et al., *Output targets and transcriptional regulation by a cyclic dimeric GMP-responsive circuit in the Vibrio parahaemolyticus Scr network.* J Bacteriol, 2012. **194**(5): p. 914-24.

10. Hickman, J.W. and C.S. Harwood, *Identification of FleQ from Pseudomonas aeruginosa as a c-di-GMP-responsive transcription factor.* Molecular Microbiology, 2008. **69**(2): p. 376-389.

11. Monds, R.D., et al., *Phosphate-dependent modulation of c-di-GMP levels regulates Pseudomonas fluorescens Pf0-1 biofilm formation by controlling secretion of the adhesin LapA.* Molecular Microbiology, 2007. **63**(3): p. 656-679.

12. Matilla, M.A., et al., *Cyclic diguanylate turnover mediated by the sole GGDEF/EAL response regulator in Pseudomonas putida: its role in the rhizosphere and an analysis of its target processes.* Environmental Microbiology, 2011. **13**(7): p. 1745-1766.

13. Fang, X. and M. Gomelsky, *A post-translational, c-di-GMP-dependent mechanism regulating flagellar motility.* Molecular Microbiology, 2010. **76**(5): p. 1295-1305.

14. Ryjenkov, D.A., et al., *The PilZ domain is a receptor for the second messenger c-di-GMP - The PilZ domain protein YcgR controls motility in enterobacteria.* Journal of Biological Chemistry, 2006. **281**(41): p. 30310-30314.

15. Zahringer, F., C. Massa, and T. Schirmer, *Efficient Enzymatic Production of the Bacterial Second Messenger c-di-GMP by the Diguanylate Cyclase YdeH from E. coli.* Applied Biochemistry and Biotechnology, 2011. **163**(1): p. 71-79.

16. Zhu, M.J., et al., *C-di-GMP signaling pathways are critical for acid resistance of E. coli O157:H7.* Journal of Dairy Science, 2010. **93**: p. 854-854.

17. Paul, K., et al., *The c-di-GMP Binding Protein YcgR Controls Flagellar Motor Direction and Speed to Affect Chemotaxis by a "Backstop Brake" Mechanism.* Mol Cell, 2010. **38**(1): p. 128-139.

18. Tuckerman, J.R., et al., *An Oxygen-Sensing Diguanylate Cyclase and Phosphodiesterase Couple for c-di-GMP Control.* Biochemistry, 2009. **48**(41): p. 9764-9774.

19. Ryjenkov, D.A., et al., *Cyclic diguanylate is a ubiquitous signaling molecule in bacteria: Insights into biochemistry of the GGDEF protein domain.* Journal of Bacteriology, 2005. **187**(5): p. 1792-1798.

20. Christen, M., et al., *DgrA is a member of a new family of cyclic diguanosine monophosphate receptors and controls flagellar motor function in Caulobacter crescentus.* Proc Natl Acad Sci U S A, 2007. **104**(10): p. 4112-7.

21. Jenal, U., J. White, and L. Shapiro, *Caulobacter flagellar function, but not assembly, requires FliL, a non-polarly localized membrane protein present in all cell types.* Journal of Molecular Biology, 1994. **243**(2): p. 227-44.

22. Wisniewski-Dye, F., et al., *Azospirillum genomes reveal transition of bacteria from aquatic to terrestrial environments.* PLoS Genet, 2011. **7**(12): p. e1002430.

23. Paul, R., et al., *Cell cycle-dependent dynamic localization of a bacterial response regulator with a novel di-guanylate cyclase output domain.* Genes Dev, 2004. **18**(6): p. 715-27.

24. Aldridge, P., et al., *Role of the GGDEF regulator PleD in polar development of Caulobacter crescentus.* Mol Microbiol, 2003. **47**(6): p. 1695-708.

25. Deich, J., et al., *Visualization of the movement of single histidine kinase molecules in live Caulobacter cells.* Proc Natl Acad Sci U S A, 2004. **101**(45): p. 15921-6.

26. Margolin, W., *FtsZ and the division of prokaryotic cells and organelles.* Nat Rev Mol Cell Biol, 2005. **6**(11): p. 862-71.

27. Alexandre, G., S.E. Greer, and I.B. Zhulin, *Energy taxis is the dominant behavior in Azospirillum brasilense.* J Bacteriol, 2000. **182**(21): p. 6042-8.

28. Stephens, B.B., S.N. Loar, and G. Alexandre, *Role of CheB and CheR in the complex chemotactic and aerotactic pathway of Azospirillum brasilense.* J Bacteriol, 2006. **188**(13): p. 4759-68.

29. Ko, J., et al., *Structure of PP4397 Reveals the Molecular Basis for Different c-di-GMP Binding Modes by Pilz Domain Proteins.* Journal of Molecular Biology, 2010. **398**(1): p. 97-110.

30. Ramelot, T.A., et al., *NMR structure and binding studies confirm that PA4608 from Pseudomonas aeruginosa is a PilZ domain and a c-di-GMP binding protein.* Proteins-Structure Function and Bioinformatics, 2007. **66**(2): p. 266-271.

31. Merighi, M., et al., *The second messenger bis-(3 '-5 ')-cyclic-GMP and its PilZ domain-containing receptor Alg44 are required for alginate biosynthesis in Pseudomonas aeruginosa.* Molecular Microbiology, 2007. **65**(4): p. 876-895.

32. Wassmann, P., et al., *Structure of BeF3- -modified response regulator PleD: implications for diguanylate cyclase activation, catalysis, and feedback inhibition.* Structure, 2007. **15**(8): p. 915-27.

33. Arora, S.K., et al., *A transcriptional activator, FleQ, regulates mucin adhesion and flagellar gene expression in Pseudomonas aeruginosa in a cascade manner.* J Bacteriol, 1997. **179**(17): p. 5574-81.

34. Altschul, S.F., et al., *Basic local alignment search tool.* J Mol Biol, 1990. **215**(3): p. 403-10.

35. Wuichet, K. and I.B. Zhulin, *Origins and diversification of a complex signal transduction system in prokaryotes.* Science Signaling, 2010. **3**(128): p. ra50.

36. Pereg-Gerk, L., et al., *A transcriptional regulator of the LuxR-UhpA family, FlcA, controls flocculation and wheat root surface colonization by Azospirillum brasilense Sp7.* Mol Plant Microbe Interact, 1998. **11**(3): p. 177-87.

37. Ko, M. and C. Park, *Two novel flagellar components and H-NS are involved in the motor function of Escherichia coli.* Journal of Molecular Biology, 2000. **303**(3): p. 371-82.

38. Donato, G.M. and T.H. Kawula, *Enhanced binding of altered H-NS protein to flagellar rotor protein FliG causes increased flagellar rotational speed and hypermotility in Escherichia coli.* Journal of Biological Chemistry, 1998. **273**(37): p. 24030-6.

39. Marykwas, D.L., S.A. Schmidt, and H.C. Berg, *Interacting components of the flagellar motor of Escherichia coli revealed by the two-hybrid system in yeast.* Journal of Molecular Biology, 1996. **256**(3): p. 564-76.

40. Paul, K., W.C. Carlquist, and D.F. Blair, *Adjusting the spokes of the flagellar motor with the DNA-binding protein H-NS.* J Bacteriol, 2011. **193**(21): p. 5914-22.

41. Berleman, J.E. and C.E. Bauer, *Involvement of a Che-like signal transduction cascade in regulating cyst cell development in Rhodospirillum centenum.* Molecular Microbiology, 2005. **56**(6): p. 1457-66.

42. Van Dommelen, A., et al., *Cloning and characterisation of the Azospirillum brasilense glnD gene and analysis of a glnD mutant.* Molecular Genetics and Genomics, 2002. **266**(5): p. 813-20.

43. Duvel, J., et al., *A chemical proteomics approach to identify c-di-GMP binding proteins in Pseudomonas aeruginosa.* J Microbiol Methods, 2012. **88**(2): p. 229-36.

44. Merighi, M., et al., *The second messenger bis-(3'-5')-cyclic-GMP and its PilZ domain-containing receptor Alg44 are required for alginate biosynthesis in Pseudomonas aeruginosa.* Mol Microbiol, 2007. **65**(4): p. 876-95.

45. Katoh, K., et al., *Improvement in the accuracy of multiple sequence alignment program MAFFT.* Genome Inform, 2005. **16**(1): p. 22-33.

46. Katoh, K., et al., *MAFFT: a novel method for rapid multiple sequence alignment based on fast Fourier transform.* Nucleic Acids Research, 2002. **30**(14): p. 3059-66.

47. Benach, J., et al., *The structural basis of cyclic diguanylate signal transduction by PilZ domains.* Embo Journal, 2007. **26**(24): p. 5153-66.

48. Benach, J., et al., *The structural basis of cyclic diguanylate signal transduction by PilZ domains.* Embo Journal, 2007. **26**(24): p. 5153-5166.

49. Crooks, G.E., et al., *WebLogo: a sequence logo generator.* Genome Research, 2004. **14**(6): p. 1188-90.

50. Schneider, T.D. and R.M. Stephens, *Sequence logos: a new way to display consensus sequences.* Nucleic Acids Research, 1990. **18**(20): p. 6097-100.

51. Punta, M., et al., *The Pfam protein families database.* Nucleic Acids Research, 2012. **40**(D1): p. D290-D301.

52. Kelley, L.A. and M.J. Sternberg, *Protein structure prediction on the Web: a case study using the Phyre server.* Nat Protoc, 2009. **4**(3): p. 363-71.

53. Singh, J. and J.M. Thornton, *SIRIUS - AN AUTOMATED-METHOD FOR THE ANALYSIS OF THE PREFERRED PACKING ARRANGEMENTS BETWEEN PROTEIN GROUPS.* Journal of Molecular Biology, 1990. **211**(3): p. 595-615.

54. Manson, M.D., *A mutational wrench in the HAMP gearbox.* Molecular Microbiology, 2009. **73**(5): p. 742-6.

55. Ma, Q.H., M.S. Johnson, and B.L. Taylor, *Genetic analysis of the HAMP domain of the Aer aerotaxis sensor localizes flavin adenine dinucleotide-binding determinants to the AS-2 helix.* Journal of Bacteriology, 2005. **187**(1): p. 193-201.

56. Ninfa, A.J., et al., *Crosstalk between bacterial chemotaxis signal transduction proteins and regulators of transcription of the Ntr regulon: evidence that nitrogen assimilation and chemotaxis are controlled by a common phosphotransfer mechanism.* Proc Natl Acad Sci U S A, 1988. **85**(15): p. 5492-6.

57. McFarland, N., et al., *Nitrogen regulatory locus "glnR" of enteric bacteria is composed of cistrons ntrB and ntrC: identification of their protein products.* Proc Natl Acad Sci U S A, 1981. **78**(4): p. 2135-9.

58. Hirschman, J., et al., *Products of nitrogen regulatory genes ntrA and ntrC of enteric bacteria activate glnA transcription in vitro: evidence that the ntrA product is a sigma factor.* Proc Natl Acad Sci U S A, 1985. **82**(22): p. 7525-9.

59. Bible, A.N., et al., *Function of a chemotaxis-like signal transduction pathway in modulating motility, cell clumping, and cell length in the alphaproteobacterium Azospirillum brasilense.* J Bacteriol, 2008. **190**(19): p. 6365-75.

60. Greer-Phillips, S.E., B.B. Stephens, and G. Alexandre, *An energy taxis transducer promotes root colonization by Azospirillum brasilense.* Journal of Bacteriology, 2004. **186**(19): p. 6595-6604.

61. Starrett, D.J. and J.J. Falke, *Adaptation mechanism of the aspartate receptor: electrostatics of the adaptation subdomain play a key role in modulating kinase activity.* Biochemistry, 2005. **44**(5): p. 1550-60.

62. Trammell, M.A. and J.J. Falke, *Identification of a site critical for kinase regulation on the central processing unit (CPU) helix of the aspartate receptor.* Biochemistry, 1999. **38**(1): p. 329-36.

Appendix

Diversity in Bacterial Chemotactic Responses and Niche Adaptation

From: Lance D. Miller, Matthew H. Russell and Gladys Alexandre,
Diversity in
Bacterial Chemotactic Responses and Niche
Adaptation.
In Allen I. Laskin, Sima Sariaslani, and Geoffrey M. Gadd, editors:
Advances in Applied Microbiology, Vol 66, Burlington: Academic
Press, 2009, pp. 53-75. ISBN: 978-0-12-374788-4

Contents

Abstract

The ability of microbes to rapidly sense and adapt to environmental changes plays a major role in structuring microbial communities, in affecting microbial activities, as well as in influencing various microbial interactions with the surroundings. The bacterial chemotaxis signal transduction system is the sensory perception system that allows motile cells to respond optimally to changes in environmental conditions by allowing cells to navigate in gradients of diverse physicochemical parameters that can affect their metabolism. The analysis of complete genome sequences from microorganisms that occupy diverse ecological niches reveal the presence of multiple chemotaxis pathways and a great diversity of chemoreceptors with novel sensory specificities. Owing to its role in mediating rapid responses of bacteria to changes in the surroundings, bacterial chemotaxis is a behavior of interest in applied microbiology as it offers a unique opportunity for understanding the environmental cues that contribute to the survival of bacteria. This chapter explores the diversity of bacterial chemotaxis and suggests how gaining further insights into such diversity may potentially impact future drug and pesticides development and could inform bioremediation strategies.

I. INTRODUCTION

The ability of unicellular organisms to survive, to grow, and to compete with other microorganisms in changing environments is dependent on sensing and adapting to changes by modifying their cellular physiology. Bacteria are capable of detecting a wide range of environmental stimuli, including osmolarity, pH, temperature, and chemical ligands of diverse physicochemical properties (Wadhams and Armitage, 2004). Bacteria have evolved several ways of responding to their environment and thereby maintaining optimum physiological states for growth. Sensing and adapting to changes is thus anticipated to play a major role in structuring microbial communities, in affecting dynamic changes in microbial activities, as well as in influencing various microbial interactions with the surroundings. At the cellular level, two-component signal transduction systems mediate specific changes in cellular physiology in response to environmental stimuli. At the molecular level, two-component signal transduction systems typically consist of a sensor histidine kinase that detects specific cues and a cognate response regulator that mediates the response (Lukat and Stock, 1993). One major way bacteria respond to environmental stimuli is by regulating gene expression—either increasing or decreasing expression of a gene or set of genes. Chemotaxis is another way motile bacteria respond to their environment. In fact, most understanding on signal transduction in prokaryotes comes from studying the two-component regulatory system that controls chemotaxis in motile bacteria, such as *Escherichia coli* and *Salmonella typhymurium* (Hazelbauer et al., 2008). Motile bacteria will first detect a cue and then navigate in its direction, if the cue perceived corresponds to an attractant signal or away from it if the cue corresponds to a repellent signal. The bacterial chemotaxis signal transduction system is the sensory perception system that allows motile cells to respond optimally to changes in environmental conditions by facilitating motion towards small-

molecule chemoattractants and away from repellents (Wadhams and Armitage, 2004). Thus, chemotaxis provides motile bacteria with an effective means to navigate their environment and to localize in niches that support optimum growth. Such an advantage provided by chemo-taxis was observed very early on by Engelmann in the late nineteenth century. Engelmann noticed that bacteria observed under the microscope were actively swimming toward and accumulating near sources of oxygen (algae or air bubbles), but when a harmful chemical was added, the cells slowed down and were no longer capable of actively locating in these niches (Engelmann, 1881). Owing to its role in mediating rapid responses of bacteria to changes in the surroundings, bacterial chemotaxis is a behavior of interest in applied microbiology and it has been previously used to isolate microorganisms with desirable metabolic abilities, especially in bioremediation. This chapter will explore the diversity in bacterial chemotaxis and how such diversity could possibly be used in bioremediation, agriculture, or biosensor applications.

II. MOLECULAR MECHANISMS OF BACTERIAL CHEMOTAXIS

A. Chemotaxis: Control of the motility pattern

1. Biasing the random walk

The ability to swim and navigate the surrounding environment by chemotaxis confers motile bacteria with a competitive advantage in that it allows the cells to maintain and occupy niches that are optimum for growth and survival. In chemotaxis, motile bacteria constantly sample their environment and will detect and process only certain signals as cues. If the cue perceived corresponds to an attractant signal, the cells will move in the direction of the cue, but if the cue provides a repellent signal they will move away from it. The bacterial chemotaxis signal transduction system is the sensory perception system that allows motile cells to respond optimally to changes in environmental conditions by facilitating motion towards small-molecule

chemoattractants and away from repellents (Adler and Tso, 1974). Bacteria swim by rotating their flagella and navigate in the environment with a swimming pattern that resemble three-dimensional walk (Berg, 2000). In a homogeneous chemical environment, cells move along their long axis in relatively straight paths (runs) that are punctuated by brief reorientation events (reversals) where forward motion stops. Reversals are followed by runs in a new and randomly determined direction. In an increasing concentration of a chemical attractant, the cells tend to suppress the reversals and swim longer in the direction of the attractant. Conversely, in an increasing gradient of a repellent, the cells tend to reverse more frequently when swimming towards the repellent and run longer when swimming away from it. Therefore, motile bacteria bias their swimming pattern by modulating the probability of reversals. Such behavior allows motile bacteria to respond efficiently to what are perceived as temporal changes in their environmental conditions. Whether or not a change in a concentration of a stimulus will result in change in swimming pattern is controlled at the level of sensory perception. The fundamental principles of sensory or signal perception and transduction have mostly been studied in model organisms such as *E. coli*. The general principles of signal perception and transduction are conserved in bacteria and archaea despite the diversity of flagellation patterns and mechanisms of flagellar rotation and directional changes (Wadhams and Armitage, 2004).

2. Spatial and temporal sensing

It is often said that bacteria are too small to sense chemical gradients spatially. This may not be true in either theory or experience. The theoretical size limit for spatial sensing has been proposed to be <1 mm (Dusenbery, 1998), and evidence has been found suggesting that a Gram-negative vibriod performs aerotaxis via spatial sensing of steep oxygen gradients (Thar and Kuhl, 2003). Moreover, some cyanobacteria exhibit phototaxis in response to spatial gradients along the length of the cell (Hader, 1987). However, temporal sensing may be more efficient for bacteria, despite

the estimated 10% loss in velocity towards increasing attractant gradients due to the biased random walk. Bacteria tend to inhabit chemically heterogeneous environments. What is important for the bacterium may not be to always move up the gradient of the strongest chemoattractant. For instance, a gradient of attractant could coincide with a repellant gradient. In this situation, it would be disadvantageous to merely follow the attractant gradient. Instead, it may be more advantageous for a bacterium to seek a niche with a balance of different chemoattractants optimized for its individual physiology. This is particularly true provided that energy taxis is the dominant behavior of some organisms (Alexandre and Zhulin, 2001; Alexandre et al., 2000, 2004). Instead of sensing chemical gradients spatially, bacteria use a temporal sensing mechanism that compares the instantaneous concentration of an attractant or repellent to that of a few seconds prior. Based on this comparison, a ‘‘decision’’ is made which results in adjusting the probability of random changes in the swimming direction (reversals). Controlling the frequency at which these instances of reorientation occur, cells are able to bias their movement towards environments most suitable for growth and division.

B. Molecular mechanisms of chemotaxis: The *E. coli* paradigm

1. The chemotaxis signal transduction excitation and adaptation pathways

At the center of the protein regulatory network that controls chemotaxis lies a two-component system (TCS). TCS are typically comprised of a membrane bound sensor histidine kinase coupled with a cytoplasmic cognate response regulator (Stock and Da Re, 2000; Zapf et al., 1998). TCS can sense a wide range of environmental stimuli and usually result in a change in gene expression although they can regulate other cellular processes. Until recently, TCS were thought to be the dominant mechanism for prokaryotic signal transduction. However, a recent study has found that so-called one-component systems consisting of a single protein with both input and output

domains are more numerous and likely represent the evolutionary precursors to TCS (Ulrich and Zhulin, 2005). In *E. coli*, the TCS at the core of the chemotactic system consists of CheA, the sensor histidine kinase, and CheY, the response regulator (Fig. A.1). Environmental stimuli are sensed by chemosensory proteins (or chemoreceptors), so-called methyl-accepting chemotaxis proteins or MCPs that are embedded in the cytoplasmic membrane. An N-terminal sensory domain protrudes into the periplasm and receives signals that are then transmitted to the C-terminal signaling domain localized in the cytoplasm. CheW is a linker protein that connects the histidine kinase CheA to the MCPs. When CheA is activated, it autophosphorylates at a conserved histidine residue and in turn phosphorylates its cognate response regulator CheY. Phosphorylated CheY, CheY-P, then freely diffuses through the cytoplasm and binds FliM, the switch protein of the flagellar motor thus effecting a change in the direction of rotation. The signal is terminated by dephosphorylation of CheY-P by CheZ, a phosphatase. The system allowing for the temporal comparison of attractant or repellent concentrations is comprised of CheB and CheR, a methylesterase and methyltransferase, respectively. CheR is constitutively active, constantly adding methyl groups from S-adenosylmethionine to the conserved methylation sites on the chemoreceptors. Increasing methylation of MCPs results in a suppression of signaling. CheB becomes active after it is phosphorylated by CheA. Once activated, CheB removes methyl groups from MCPs thus restoring their ability to signal (Fig. A.1). CheB and CheR act in concert to allow the cell to adapt to its present level of stimulation. This adaptation system allows a cell to navigate gradients of either attractants or repellents over a wide range of concentrations over several orders of magnitude ranging from the nanomolar to millimolar.

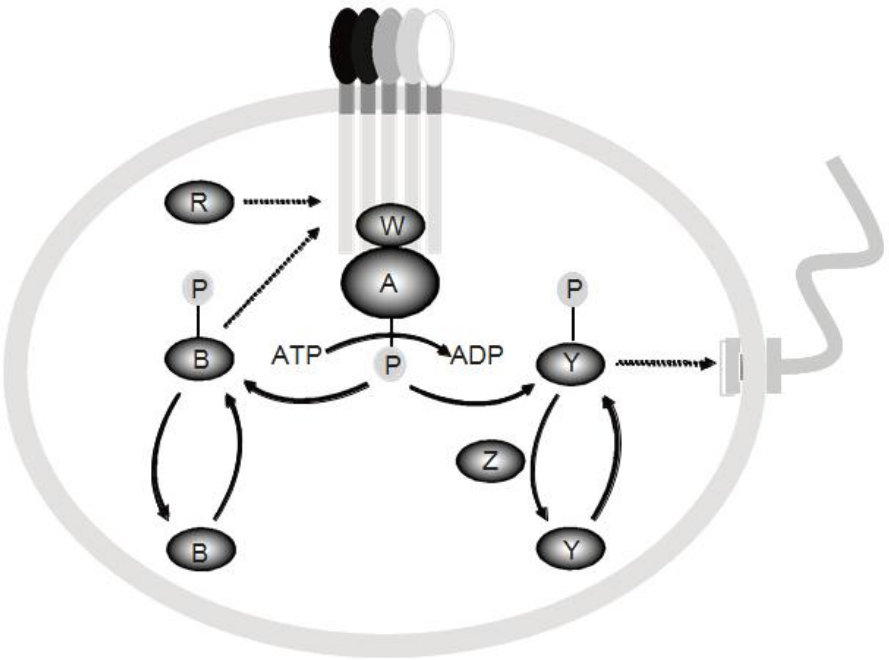

FIGURE A.1 Schematic diagram of the *E. coli* chemotactic signal transduction pathway. Methyl-accepting chemotaxis proteins, MCPs, transduce signals from chemoeffectors in the periplasmic space thereby modulating the activity of the histidine kinase, CheA, which is linked to the MCPs by CheW. CheA phosphorylates the response regulators CheB and CheY whose phosphorylated forms interact with the MCPs and the flagellar motor, respectively. CheR also interacts with the MCPs whereas the dephosphatase CheZ dephosphorylates CheY.

2. Sensing the environment and the chemoreceptors repertoire

The first step in adaptation to the environment is sensing its changes. In motile bacteria, environmental cues are sensed in the extracellular environment by transmembrane receptors (chemoreceptors) that transmit the signal to a cytoplasmic two-component signal transduction pathway controlling the direction of flagellar rotation and chemotaxis (Hazelbauer et al., 2008). Signal perception and transduction are mediated by a series of conformational changes that are transmitted from the N-terminal sensory domain of the chemoreceptor to the C-terminal signaling domain that interacts with CheW and CheA (Ottemann et al., 1998, 1999). In *E. coli*, trimers of dimers of chemoreceptors are clustered at the cell poles in a large lattice that interacts with the cytoplasmic CheA and CheW proteins to form a large array that can be observed under specific conditions by electron microscopy (Zhang et al., 2007). The organization of chemoreceptors into an array and the association of the clustered chemoreceptors' signaling tips with CheA and CheW allow sensory information from multiple chemoreceptors of various sensing capabilities (inputs) to be collected into a single output and trigger coordinated changes in rotational direction of the flagellar motors (Cluzel et al., 2000; Gestwicki and Kiessling, 2002; Jasuja et al., 1999).

The chemoreceptor repertoire is responsible for the specificity of the signal sensed and appears to be quite different in bacteria that occupy different ecological niches. The model organism for chemotaxis, *E. coli* inhabits the mammalian digestive tracts, including human, and it responds chemotactically mainly to amino acids via a metabolism-independent mechanism, where the response is triggered by the amino acid binding to specific transmembrane receptors. *E. coli* possesses four membrane-spanning chemoreceptors (Tsr, Tar, Trg, and Tap) that mea-sure the concentrations of specific chemicals, such as amino acids (serine, leucine, and aspartate), sugars

(ribose, galactose, mannose), dipeptides, and also heavy metals, such as cobalt and nickel. It also possesses a fifth chemoreceptor, Aer, that monitors changes in the redox state of the electron transport system and is thus an energy transducer that detects changes in intracellular energy levels (Bespalov et al., 1996; Bibikov et al., 2000; Greer-Philips et al., 2003; Rebbapragada et al., 1997; Repik et al., 2000). Chemotaxis receptors are extremely sensitive and detect chemicals over a wide range of concentrations. For example, the Tar receptor responds to aspartate in a concentration range from 0.1 mM to 100 mM. Many other bacterial species possess a large number of different chemoreceptors (typically 10–20).

C. *Bacillus subtilis*, another model for chemotaxis signal transduction

Similar to *E. coli*, *Bacillus subtilis* possesses a single chemotaxis operon, but it possesses additional accessory proteins that participate in chemotaxis, CheC, CheD, and CheV. CheC functions in adaptation and signal termination. CheD is a deamidase that functions in receptor maturation by deamidating specific glutamine residues of MCPs. This function is carried out by CheB in *E. coli* (Fig. A.2A). CheV also has a role in adaptation and in coupling CheA to the chemotaxis transducers (Szurmant and Ordal, 2004).

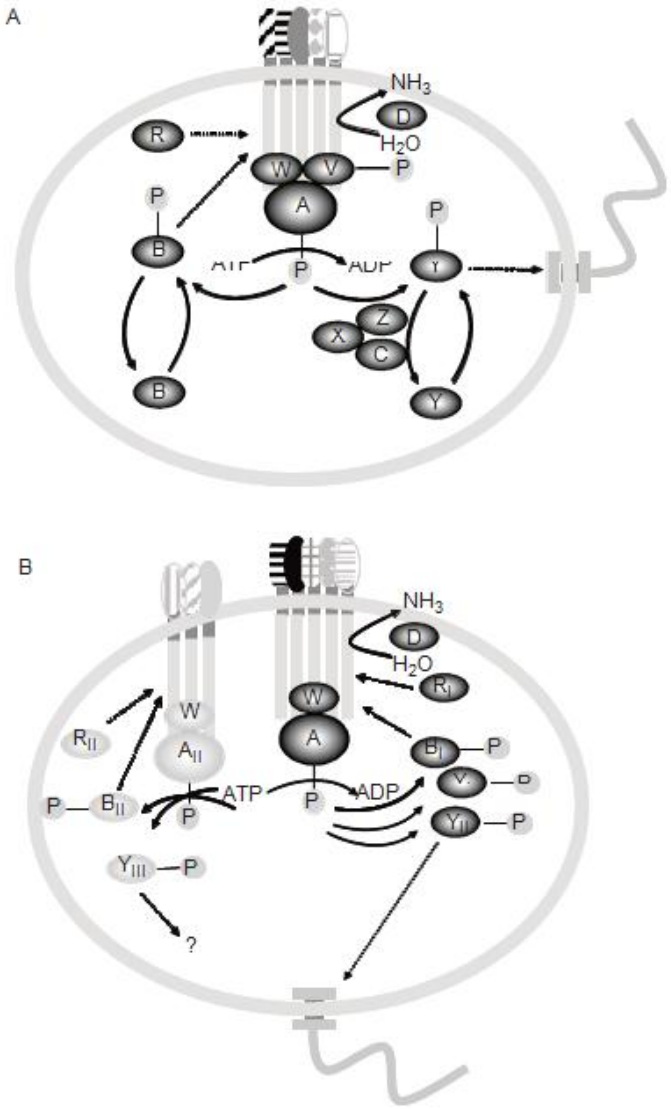

FIGURE A.2 Examples of diversity in chemotactic signal transduction pathways. (A) Schematic representation of the chemotactic signal transduction pathways in B. subtilis and (B) in *R. leguminosarum bv. viciae*. The number of chemotaxis-like pathways, the number and diversity of chemoreceptors vary in different bacterial species. Note that the putative sensory domains of

chemoreceptors are different the two examples shown to illustrate the diversity in chemosensory systems.

III. DIVERSITY IN CHEMOTAXIS

A. Complete genome sequencing projects and the diversity in chemotaxis

1. Diversity in the number of chemotaxis signal transduction pathways

The majority of bacteria whose genomes have been completely sequenced are motile and possess complex chemotaxis sensory machinery that differ from the model microorganisms studied so far. In addition, these chemo-taxis pathways possess additional chemotaxis genes that are not present in the genomes of either *E. coli* or *B. subtilis* and whose functions remain to be determined (Park et al., 2004; Rajagopala et al., 2007) (Fig. 3.2). However, many studies have demonstrated that the principles of signal transduction and perception are conserved among diverse bacteria, although there are some variations on this theme (Szurmant and Ordal, 2004; Wadhams and Armitage, 2004) (Figs. 3.2A and B). The conserved set of CheAWYBRZ proteins and five MCPs comprising the chemotaxis protein network of *E. coli* is a streamlined version resulting from the evolutionary loss of chemotaxis proteins still present in the chemotaxis systems of other organisms (Zhulin, personal communication). The analysis of completely sequenced genomes also revealed that most bacteria possess more than one chemotaxis-like signal transduction pathway (Table 3.1). However, the function of redundant signal transduction pathways cannot be predicted from sequence analysis alone. The chemotaxis operons in these organisms can regulate flagellar and pili-mediated motility as well as perform other cellular functions such as regulation

of gene expression and cellular differentiation (Berleman and Bauer, 2005a,b; Bible et al., 2008; Kirby and Zusman, 2003; Vlamakis et al., 2004).

2. Chemoreceptors diversity

Variations in the sensory specificity of the N-terminal domains of the chemoreceptors tailor them to a particular sensory function (Galperin et al., 2001) and the diversity in the sequence of the N-terminal sensory domains reflects the diversity of cues a microorganism can detect and respond to. Therefore, it is not surprising that the greatest diversity in the chemotaxis system is seen in the set of chemoreceptors (Alexandre and Zhulin, 2001). Chemotaxis receptors are extremely sensitive naturally occurring biosensors that allow bacteria to monitor their environments and to detect chemicals over wide concentration ranges. The number of chemoreceptors per microbial genome correlates with the genome size and the metabolic versatility of the bacteria (Alexandre et al., 2004) (Table A.1).

TABLE A.1 Number of chemotaxis-like operons and chemoreceptors (MCPs) in completely sequenced genome of selected organisms[a]

Organisms	Number of chemotaxis-like operons	Number of chemoreceptors
Escherichia coli	1	5
Bacillus subtilis	1	10
Helicobacter pylori	1	4
Borrelia burgdorferi	2	5
Shewanella oneidensis	3	27
Rhodobacter sphaeroides	3	11
Rhizobium leguminosarum bv. viciae	2	27
Sinorhizobium meliloti	2	10
Ralstonia eutropha JMP134 (pJP4)	3	22
Desulfovibrio vulgaris Hildenborough	3	28
Geobacter metallireducens GS-15	5	17
Dechloromonas aromatica	4	25
Vibrio cholera	3	45
Magnetospirillum magnetotacticum	3	61

[a] The chemotaxis-like operons and chemoreceptors homologs were identified using the MiST database at http://genomics.oml.gov/mist/ (Ulrich and Zhulin, 2007).

Interestingly, the substrate specificity of bacterial chemoreceptors is known for only a few of them, mainly from enteric bacteria. However, microbial genome sequencing projects reveal the presence of hundreds of different chemoreceptors: some are restricted to few bacteria, whereas others are widespread. The diversity in their sensory abilities is yet to be discovered. Because of their role in bacterial adaptation, establishing the substrate specificity for chemotaxis receptors will lead to the identification of the signals important for the survival of bacteria in different environments and will potentially impact future drug and pesticides development and could inform bioremediation strategies. However, to date, there are few experimental tools available to systematically analyze the sensory specificity of chemoreceptors and methods that usually work well in model organisms may not work well or not at all in other bacteria.

3. Predicting chemotaxis behavior from completely sequenced genomes

The observation that orthologous chemotaxis operons perform different functions in different organisms further complicates the prediction of their role in the biology of the organisms based on sequence comparisons alone. For example, the dominant chemotaxis operon in the rhizobial species *Agrobacterium tumefaciens* and *Sinorhizobium meliloti* controls chemotaxis and motility, but it does not appear to be a major regulator of chemotaxis under laboratory conditions in *Rhodobacter sphaeroides* (Armitage and Schmitt, 1997; Wright et al., 1998).

In addition, various experimental data indicate that multiple chemotaxis pathways may modulate the motility swimming pattern of organ-isms that possess several chemotaxis-like operons encoded in their genome. In *R. sphaeroides*, *Rhizobium leguminosarum bv. viciae*, and *Azospirillum brasilense*, chemosensory components from at least two operons are required for chemotaxis (Bible et al., 2008; Ferrandez et al., 2002; Miller et al., 2007; Porter and Armitage, 2002, 2004; Stephens et al., 2006).

B. Chemotaxis in bacterial species colonizing diverse niches

1. Ecological advantage provided by chemotaxis

The widespread presence of chemotaxis operons in the complete genomes of bacteria and archaea is evidence of the evolutionary and biological benefits of chemotaxis. Since bacteria inhabit almost every conceivable environmental niche in the biosphere and are capable of undergoing complex cellular differentiation processes in order to live, grow, and divide in different environments, the ecological role of chemotaxis has long been of interest. Studies are beginning to address the question of what role chemotaxis plays in structuring microbial communities and under which environmental conditions chemotaxis provides a competitive advantage (Alexandre et al., 2004). The obvious advantage that chemotaxis provide the cells with is the ability to simultaneously monitor multiple cues and rapidly navigate in the environment. The chemotaxis two-component signal transduction systems are unique compared to other TCSs in that they function with a ‘‘molecular memory’’ provided by the adaptation system which endows cells with the ability to make temporal comparisons about the chemical composition of the environment by modulating sensory sensitivity of the chemoreceptors (Kentner and Sourjik, 2006). As a result of the activity of the adaptation system, cells are able to respond to changes over a wide range of background conditions and they may initiate changes in behavior when thresholds are reached instead of responding to the presence of a dedicated cue as in other TCSs. This level of control is analogous to a lamp controlled by a rheostat compared to a simple on/off switch. The advantage provided by the ability to temporally sample the environment has been recognized by several authors as the main advantages provided by chemotaxis-like signal transduction pathways (Bible et al., 2008; Kirby and Zusman, 2003; Wadhams and Armitage, 2004).

2. Bacterial chemotaxis enhances competitiveness and facilitates adaptation

The ability to sense and navigate towards niches that are optimal for growth is a likely prerequisite for motile bacteria in order to colonize new environments. Therefore, motility and chemotaxis, by allowing the cells to navigate along gradients so that they can localize in optimum environments, have long been proposed to play a major role in the ability to compete for resources (Alexandre et al., 2004). Consistent with this hypothesis, bacterial chemotaxis has repeatedly been shown to be essential for the competitive ability of beneficial, as well as pathogenic, bacteria to colonize their eukaryotic host. For example, chemotaxis was shown to be essential for the beneficial association of *A. brasilense* with wheat (Greer-Phillips et al., 2004), for the symbiotic association of *R. leguminosarum bv. viciae* with the common pea plant (Miller et al., 2007), and for the persistent association of *Helicobacter pylori* within a narrow zone of the stomach (Foynes et al., 2000; McGee et al., 2005; Schweinitzer et al., 2008). In contrast, the human pathogen *Vibrio cholera* appears to require motility but not chemotaxis to establish infection (Butler and Camilli, 2004; Gardel and Mekalanos, 1994) and chemotaxis genes are downregulated in stool isolates from infected humans providing further evidence that motility but not chemotaxis is required for infection by *V. cholera* (Butler et al., 2006; Merrell et al., 2002). Such a negative effect of chemotaxis in host colonization has not been identified in any other system studied to date.

Chemotaxis allows bacteria to navigate towards ecological niches that support their metabolism. Chemotaxis could thus be used to ‘‘enrich’’ certain environments with bacteria that possess desirable properties in bioremediation. In fact, such a principle has been applied previously to chemotactically attract certain motile bacteria to environmental pollutants that they can degrade (Harms and Wick, 2006; Lanfranconi et al., 2003; Pandey and Jain, 2002). In a few cases,

dedicated chemoreceptors specific to certain pollutants have been identified (Iwaki et al., 2007; Kim et al., 2006).

IV. CHARACTERIZING THE CHEMOTAXIS RESPONSE: QUALITATIVE AND QUANTITATIVE ASSAYS

Insight into chemotaxis diversity and the potential application of this behavior to bioremediation, agriculture, or health-related fields is dependent on the ability to accurately describe the behavior and the development of quantitative methods that enable the determination of parameters that best describe the characteristics of bacterial motion. Characterization of the motility behavioral responses in nonmodel bacteria requires the development of sensitive qualitative and quantitative methods to measure the chemotaxis response. This was recognized very early on in the study of bacterial chemotaxis since Pfeffer (Pfeffer, 1884) who first used glass capillaries filled with attractant solutions to demonstrate that bacteria accumulated first outside then inside the capillary. Since then, numerous qualitative and quantitative methods have been developed for chemotaxis and several computerized motion-analysis systems are commercially available (HobsonTracking, Inc., UK; CellTrack, Santa Rosa, CA, etc.) to assist in the characterization and the statistical analysis of bacterial motion parameters.

There are two general types of behavioral assays used to measure bacterial chemotaxis, namely, temporal or spatial gradient assays. In a temporal assay, usually an attractant or repellant is abruptly added to a bacterial suspension to measure the chemotactic response of the motile bacteria. The same compound is then abruptly removed after a given time to measure the bacterial response, usually by examining reversal frequency of cells. However, in spatial chemotaxis assays, cells have to respond to much more shallow gradients, and in the case of the soft-agar

plate assay, cells are responding to gradients which they created by metabolizing provided chemicals around the inoculation point (usually a nitrogen or carbon source, or both).

A. Temporal gradient assays

The most common temporal assay measures the probability of changes in the swimming direction (also called cell reversal frequency or reorientation frequency) of free-swimming bacteria when a potential attractant or repellant is added to the suspension. This is the most direct way to assay chemotaxis since one must directly observe the effect of a chemical on the swimming behavior of individual cells. A change in the number of directional changes per second (changes in the reversal frequency) relative to steady-state conditions indicates a chemotactic response to the stimulus. A decrease in reversal frequency (i.e., cells change their swimming direction less frequently) indicates the stimulus is an attractant while an increase in reversal frequency (i.e., cells tend to change swimming directions more frequently) is indicative of a repellant response (Berg and Brown, 1972; Segall et al., 1986). The addition and removal of a stimulus is hardly physiological and would not typically be observed within a bacterium's normal environment but it is a good approach to directly screen the effect of a chemical stimulus on swimming behavior. This assay requires that the bacteria can be tracked and that their mode of changing swimming direction be easily identified, usually with the help of a computerized motion-tracking system. These restrictions limit the use of these assays to only a few bacterial species.

B. Spatial gradient assays

1. Soft agar plate assay

Several spatial behavioral assays are used to screen chemotaxis in motile bacteria (Table A.2). These assays test for chemotactic responses to supplied chemical stimuli, predominantly nitrogen

or carbon to help deter-mine their sensing specificity (Hartmann and Zimmer, 1994). One such assay is the swarm, or soft-agar, plate assay (Fig. A.3). In this assay, a culture inoculum is placed in the center of a semisolid agar plate, usually 0.2–0.3% agar (w/v), in which the cells can swim (Adler, 1966a; Alexandre et al., 2000). As the cells grow and deplete the agar of the supplied nitrogen and carbon source, they generate a gradient, and if they are motile and chemotactic, they will form typical chemotactic rings at some distance from the inoculation point, indicative of a positive chemotactic response. As the cells continue to metabolize the provided nutrients, the migration outward from the inoculation point continues and the ‘‘chemotactic’’ ring expands with time. Therefore, chemotactic rings are observed in this assay if the cells are able to sense and navigate in the chemical gradient formed as a result of metabolism. In this assay, mutants affected in metabolism, motility, or chemotaxis will fail to form a chemotactic ring. Figure A.3 shows some examples of typical results and their interpretation. In Fig.A.3A, the bacteria inoculated were able to metabolize the nutrients provided in the plates and grow within the agar and thus they formed a typical sharp chemotactic ring as indicated by the arrow. In contrast, as shown in Fig. A.3B, the bacteria inoculated were able to grow but did not move outward from the inoculation point. This result indicates that the bacteria are unable to respond chemotactically.

2. Chemical-in-plug assay

The chemical-in-plug assay also utilizes semisolid agar, but unlike the swarm plate assay, cell metabolism is not required to generate a chemical gradient and cells are judged solely on their ability to sense spatial gradients of attractants or repellents (chemotaxis per se). In this assay, a solid (1.5%, w/v) agar plug containing a specific concentration of chemical attractant or repellant in buffer is placed in a semi-soft buffered medium containing a high concentration of motile cells

to be tested. A gradient is formed by diffusion of the chemical from the hard agar plug to the surrounding semi-soft agar medium where cells are present. If the cells' sense and respond positively to the chemical stimulus, a ring

TABLE A.2 Spatial chemotaxis assays and their applications in diverse microorganisms

Methods	Organisms	References
Capillary assay		
	E. coli	Adler (1966a, 1966b, 1973)
	B. subtilis	Ordal and Gibson (1977), Ordal and Goldman (1975)
	Pseudomonas aeruginosa	Kato et al. (1992)
	Pseudomonas fluorescens	Singh and Arora (2001)
	B. burgdorferi	Shi et al. (1998)
	Ralstonia sp. SJ98	Pandey et al. (2002)
	Bradyrhizobium japonicum	Chuiko et al. (2002), Kurdish et al. (2001)
	Acidithiobacillus ferrooxidans	Meyer et al. (2002)
	D. Vulgaris	Meyer et al. (2002)
Modified capillary assay[a]		
	Pseudomonas putida G7 and *Pseudomonas sp.* NCIB 9816–4	Grimm and Harwood (1997)
Soft agar (Swarm) plate		
	E. coli	Adler (1966a), Hazelbauer et al. (1969)
	R. sphaeroides	Hamblin et al. (1997), Porter et al. (2002)
	R. leguminosarum bv. viciae	Miller et al. (2007)
	R. eutropha JMP134 (pJP4)	Hawkins and Harwood (2002)
	Vibrio fischeri	DeLoney-Marino et al. (2003)
Chemical-in-plug assay		
	E. coli	Tso and Adler (1974)
	B. burgdorferi	Shi et al. (1998)
	Halobacterium salinarum	Hyung and Yu (1997)
Drop assay		
	E. coli	Fahrner et al. (1994)
	P. putida G7 and *Pseudomonas sp.* NCIB 9816–4	Grimm and Harwood (1997)

[a] Assay used for chemicals poorly soluble in chemotaxis buffer. These chemicals include petroleum-based products and polyaromatic hydrocarbons such as toluene and naphthalene.

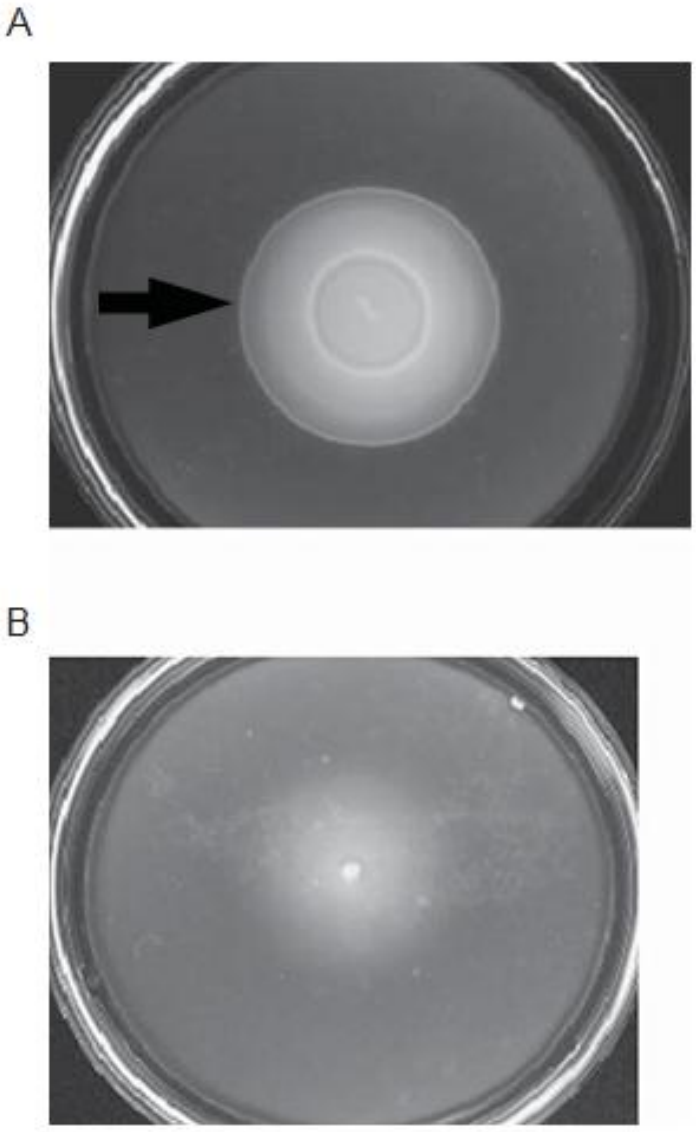

FIGURE A.3 Examples of typical results obtained using the soft agar plate and chemical-in-plug assays. (A) Soft agar plate result with bacteria positive for chemotaxis under the conditions provided. Arrow indicates location of outer chemotactic ring, true ring specific for the provided

nutrients in the plate. (B) Soft agar plate showing growth but no chemotaxis under conditions provided.

will form around the plug within a few hours (Tso and Adler, 1974). If the chemical is a repellant, a zone of clearing, where no bacteria are present, will form around the chemical plugs. Controls should also be used with this assay including a hard plug containing only buffer as a negative control as well as any nonchemotactic or nonmotile strains which may be available for the organism being tested.

3. Capillary assay

The capillary assay as described by Julius Adler (Adler, 1973) is the most widely used method to quantitatively measure chemotaxis in bacteria. Several modifications have been made to Adler's original assay, but it remains the primary assay to measure directed motility in a wide variety of microorganisms (Fig. A.4). In this method, chemotaxis towards a potential attractant is measured by comparing the number of bacteria from a suspension in buffer that enter a glass capillary tube filled with the potential chemical attractant with the number entering a capillary tube filled with buffer alone. Quantitation is obtained by emptying the bacteria

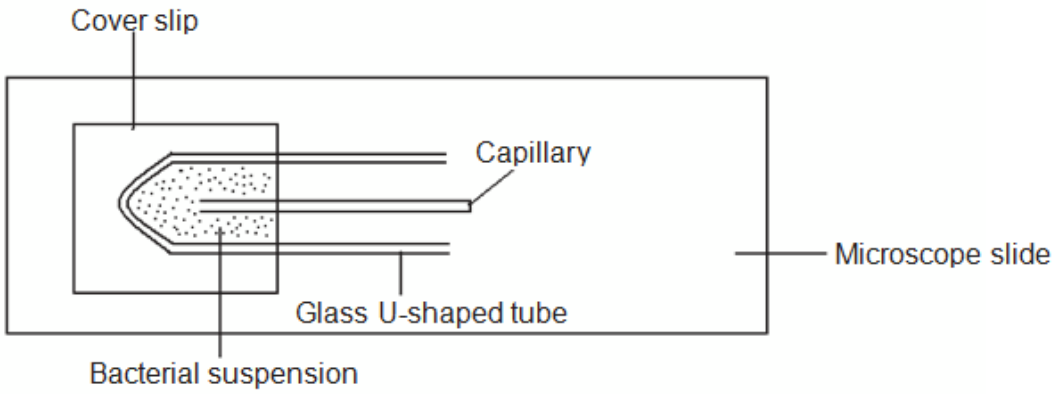

FIGURE A.4 Setup of Adler's capillary assay. Diagram showing the setup of the capillary assay described by Adler (1973). The bacterial suspension is in the space between cover slip and microscope slide. The glass U-shaped tube is used to keep the suspension within the reservoir created. Prepared solutions of the chemical being tested are loaded within the capillary and place within the bacterial suspension and placed on the microscope for viewing.

that accumulated in the capillary and plating serial dilutions to determine the number of cells that entered the tube. This assay is also valuable for determining the sensitivity of bacteria towards an attractant by finding the threshold concentration required for a chemotactic response. The primary limitation of the capillary assay is the requirement for the test compound to be soluble in an aqueous solution. A modification of this method by Harwood and colleagues allows for a qualitative observation of chemotaxis in bacteria to poorly soluble compounds, including poly-aromatic hydrocarbons (PAHs) like toluene or naphthalene (Grimm and Harwood, 1997). In this modified assay, a buffer solution is taken up into a glass capillary followed by pressing the open end of the capillary into a mound of finely granulated crystals of the PAH prior to placing the capillary in the bacterial suspension reservoir. The chemotactic response is judged positive if a visible cloud or mass of cells accumulates near the opening of the capillary. Another useful method for poorly soluble substrates is the drop assay in which a crystal of the compound is added to the center of a viscous cell suspension and chemotaxis is observed as an accumulation of cells encircling the crystal (Fahrner et al., 1994; Grimm and Harwood, 1997).

The capillary aerotaxis assay is useful in testing the cell's ability to sense a spatial oxygen gradient. A flat capillary tube is filled with a suspension of motile cells to be tested. A dense band of cells forms a certain distance from the air–water interface (meniscus) where the cells are essentially trapped. For example, *A. brasilense* is a microaerophilic soil bacterium and seeks an environment with a low optimum oxygen concentration which is suitable for maximum energy production (Zhulin et al., 1996). For *A. brasilense*, oxygen is both an attractant and repellant, resulting in a dense aerotactic band of cells at the distance corresponding to its preferred oxygen concentration. Any perturbation in sensing oxygen, by a chemo-taxis mutant for instance, results in a change in the distance between the meniscus and the dense cell band (Alexandre et al., 2000).

C. Use of chemotaxis assays to characterize new microbial functions

Chemotaxis assays are not only used to screen for the range of chemicals to which motile bacteria respond. These assays are also useful in deter-mining the sensory specificity of individual chemoreceptors, providing that isogenic mutants are available for the bacterial strain and the chemo-receptor(s) under study. These assays can also be modified to isolate motile bacteria with metabolic abilities desirable for bioremediation or agriculture. For example, the soft agar assay has previously been used to isolate microaerophilic nitrogen-fixing bacteria from the rhizosphere of cereals (Chowdhury et al., 2007; Doroshenko et al., 2007; Tarrand et al., 1978) or to isolate bacteria capable of degrading specific organic contaminants found in a gas oil-contaminated soil (Lanfranconi et al., 2003; Marx and Aitken, 2000a; Parales, 2004). Bacterial chemotaxis is also being considered as a microbially-driven strategy to increase the bioavailability of certain contaminants (Marx and Aitken, 2000b; Pandey and Jain, 2002).

V. CONCLUSIONS AND FUTURE PROSPECTS

Bacterial chemotaxis provides an obvious ecological advantage to motile bacteria since it allows motile cells to rapidly navigate in chemical gradients that may affect their survival and growth. The ecological advantages that chemotaxis provides to motile bacteria is reflected in the observation that the great majority of motile bacteria are chemotactic and that the most metabolically versatile bacterial species that also have the largest genomes possess multiple chemotaxis-like operons (Alexandre et al., 2004; Szurmant and Ordal, 2004; Wadhams and Armitage, 2004). There are few examples where motile flagellated bacteria lack complete chemotaxis signal transduction pathways. However, in these few cases, the gene loss seems to be limited to certain strains within the species. It is possible that motility per se may be required for dispersion while the ability to actively direct the movement (chemotaxis) may not endow the cells

with a particular competitive advantage, thereby favoring the loss of this function (Badger et al., 2006; Deckert et al., 1998; Glockner et al., 2003; Moran et al., 2004). Bacterial chemotaxis signal transduction is arguably one of the few biological systems known in great detail and thus it offers a unique opportunity for understanding the environmental cues that con-tribute to the shaping of bacterial communities. However, several challenges must be overcome, including the characterization of the function of multiple chemotaxis systems in phylogenetically diverse microbial species that have different swimming strategies and inhabit distinct ecological niches. Such analysis would greatly enhance our understanding of the evolution of this signal transduction pathway and it would also facilitate the development of algorithms for the prediction of the function of these pathways in completely sequenced genomes of bacterial species that may not be easily amenable to classical microbial physiology experiments. A particularly intriguing question is what ecological advantage(s) do multiple chemotaxis systems provide the cells with? In addition, the sensory specificity of chemoreceptors is a potential treasure's trove for novel biosensors and for understanding how bacteria couple sensing environmental cues with cellular adaptation. Characterizing the sensory specificity of diverse chemoreceptors remains challenging but it is an attainable objective in the near future owing to the development of sensitive high throughput biochemical methods.

ACKNOWLEDGMENTS

The authors thank NSF (CAREER, MCB-0622777) for support and the University of Tennessee, Knoxville for generous start-up funds.

List of REFERENCES

Adler, J. (1966a). Chemotaxis in bacteria. Science 153, 708–711.

Adler, J. (1966b). Effect of amino acids and oxygen on chemotaxis in *Escherichia coli*. J. Bacteriol. 92, 121–128.

Adler, J. (1973). Method for measuring chemotaxis and use of method to determine optimum conditions for chemotaxis by *Escherichia coli*. J. Gen. Microbiol. 74, 77–91.

Adler, J., and Tso, W. W. (1974). ‘‘Decision’’-making in bacteria: Chemotactic response of *Escherichia coli* to conflicting stimuli. Science. 184, 1292–1294.

Alexandre, G., and Zhulin, I. B. (2001). More than one way to sense chemicals. J. Bacteriol. 183, 4681–4686.

Alexandre, G., Greer, S. E., and Zhulin, I. B. (2000). Energy taxis is the dominant behavior in *Azospirillum brasilense*. J. Bacteriol. 182, 6042–6048.

Alexandre, G., Greer-Phillips, S., and Zhulin, I. B. (2004). Ecological role of energy taxis in microorganisms. FEMS Microbiol. Rev. 28, 113–126.

Armitage, J. P., and Schmitt, R. (1997). Bacterial chemotaxis: *Rhodobacter sphaeroides* and *Sinorhizobium meliloti*—variations on a theme? Microbiology 143, 3671–3682.

Badger, J. H., Hoover, T. R., Brun, Y. V., Weiner, R. M., Laub, M. T., Alexandre, G., Mrazek, J., Ren, Q., Paulsen, I. T., Nelson, K. E., Khouri, H. M., Radune, D., et al. (2006). Comparative genomic evidence for a close relationship between the dimorphic prosthecate bacteria *Hyphomonas neptunium* and *Caulobacter crescentus*. J. Bacteriol. 188, 6841–6850. Berg, H. C. (2000). Motile behavior of bacteria. Phys. Today 53, 24–29.

Berg, H. C., and Brown, D. A. (1972). Chemotaxis in *Escherichia coli* analyzed by 3-dimensional tracking. Nature 239, 500–504.

Berleman, J. E., and Bauer, C. E. (2005a). A che-like signal transduction cascade involved in controlling flagella biosynthesis in *Rhodospirillum centenum*. Mol. Microbiol. 55, 1390–1402.

Berleman, J. E., and Bauer, C. E. (2005b). Involvement of a Che-like signal transduction cascade in regulating cyst cell development in *Rhodospirillum centenum*. Mol. Microbiol. 56, 1457–1466.

Bespalov, V. A., Zhulin, I. B., and Taylor, B. L. (1996). Behavioral responses of *Escherichia coli* to changes in redox potential. Proc. Natl. Acad. Sci. USA 93, 10084–10089.

Bibikov, S. I., Barnes, L. A., Gitin, Y., and Parkinson, J. S. (2000). Domain organization and flavin adenine dinucleotide-binding determinants in the aerotaxis signal transducer Aer of *Escherichia coli*. Proc. Natl. Acad. Sci. USA 97, 5830–5835.

Bible, A. N., Stephens, B. B., Ortega, D. R., Xie, Z., and Alexandre, G. (2008). Function of a chemotaxis-like signal transduction pathway in modulating motility, cell clumping and cell length in the alpha-proteobacterium *Azospirillum brasilense*. J. Bacteriol. 190, 6365–6375.

Butler, S. M., and Camilli, A. (2004). Both chemotaxis and net motility greatly influence the infectivity of *Vibrio cholerae*. Proc. Natl. Acad. of Sci. USA 101, 5018–5023.

Butler, S. M., Nelson, E. J., Chowdhury, N., Faruque, S. M., Calderwood, S. B., and Camilli, A. (2006). Cholera stool bacteria repress chemotaxis to increase infectivity. Mol. Microbiol. 60, 417–426.

Chowdhury, S. P., Schmid, M., Hartmann, A., and Tripathi, A. K. (2007). Identification of diazotrophs in the culturable bacterial community associated with roots of *Lasiurus sindicus*, a perennial grass of thar desert, India. Microb. Ecol. 54, 82–90.

Chuiko, N. V., Antonyuk, T. S., and Kurdish, I. K. (2002). The chemotactic response of Bradyrhizobium japonicum to various organic compounds. Microbiology 71, 391–396. Cluzel, P., Surette, M., and Leibler, S. (2000). An ultrasensitive bacterial motor revealed by monitoring signaling proteins in single cells. Science 287, 1652–1655.

Deckert, G., Warren, P. V., Gaasterland, T., Young, W. G., Lenox, A. L., Graham, D. E., Overbeek, R., Snead, M. A., Keller, M., Aujay, M., Huber, R., Feldman, R. A., et al. (1998). The complete genome of the hyperthermophilic bacterium *Aquifex aeolicus*. Nature 392, 353–358.

DeLoney-Marino, C. R., Wolfe, A. J., and Visick, K. L. (2003). Chemoattraction of *Vibrio fischeri* to serine, nucleosides, and N-acetylneuraminic acid, a component of squid light-organ mucus. Appl. Environ. Microbiol. 69, 7527–7530.

Doroshenko, E. V., Boulygina, E. S., Spiridonova, E. M., Tourova, T. P., and Kravchenko, I. K. (2007). Isolation and characterization of nitrogen-fixing bacteria of the genus *Azospirillum* from the soil of a Sphagnum peat bog. Microbiology 76, 93–101.

Dusenbery, D. B. (1998). Spatial sensing of stimulus gradients can be superior to temporal sensing for free-swimming bacteria. Biophys. J. 74, 2272–2277.

Engelmann, T. W. (1881). *Bacterium photometricum*: An article on the comparative physiology of the sense for light and colour. Arch. Ges. Physiol. Bonn. 30, 95–124.

Fahrner, K. A., Block, S. M., Krishnaswamy, S., Parkinson, J. S., and Berg, H. C. (1994). A mutant hook-associated protein (HAP3) facilitates torsionally induced transformations of the flagellar filament of *Escherichia col*i. J. Mol. Biol. 238, 173–186.

Ferrandez, A., Hawkins, A. C., Summerfield, D. T., and Harwood, C. S. (2002). Cluster II *che* genes from *Pseudomonas aeruginosa* are required for an optimal chemotactic response. J. Bacteriol. 184, 4374–4383.

Foynes, S., Dorrell, N., Ward, S. J., Stabler, R. A., McColm, A. A., Rycroft, A. N., and Wren, B. W. (2000*). Helicobacter pylori* possesses two CheY response regulators and a histidine kinase sensor, CheA, which are essential for chemotaxis and colonization of the gastric mucosa. Infect. Immun. 68, 2016–2023.

Galperin, M. Y., Nikolskaya, A. N., and Koonin, E. V. (2001). Novel domains of the prokary-otic two-component signal transduction systems. FEMS Microbiol. Lett. 203, 11–21.

Gardel, C. L., and Mekalanos, J. J. (1994). Modus operandi of *Vibrio cholerae*-swim to arrive-stop to kill-the relationship among chemotaxis, motility and virulence. J. Cell. Biochem. 56, 65.

Gestwicki, J. E., and Kiessling, L. L. (2002). Inter-receptor communication through arrays of bacterial chemoreceptors. Nature 415, 81–84.

Glockner, F. O., Kube, M., Bauer, M., Teeling, H., Lombardot, T., Ludwig, W., Gade, D., Beck, A., Borzym, K., Heitmann, K., Rabus, R., Schlesner, H., et al. (2003). Complete genome sequence of the marine planctomycete *Pirellula sp*. strain 1. Proc. Natl. Acad. Sci. USA 100, 8298–8303.

Greer-Phillips, S. E., Alexandre, G., Taylor, B. L., and Zhulin, I. B. (2003). Aer and Tsr guide *Escherichia coli* in spatial gradients of oxidizable substrates. Microbiology 149, 2661–2667.

Greer-Phillips, S. E., Stephens, B. B., and Alexandre, G. (2004). An energy taxis transducer promotes root colonization by *Azospirillum brasilense*. J. Bacteriol. 186, 6595–6604.

Grimm, A. C., and Harwood, C. S. (1997). Chemotaxis of *Pseudomonas spp*. to the polyaromatic hydrocarbon naphthalene. Appl. Environ. Microbiol. 63, 4111–4115.

Hader, D. P. (1987). Photosensory behavior in prokaryotes. Microbiol. Rev. 51, 1–21.

Hamblin, P. A., Maguire, B. A., Grishanin, R. N., and Armitage, J. P. (1997). Evidence for two chemosensory pathways in *Rhodobacter sphaeroides*. Mol. Microbiol. 26, 1083–1096.

Harms, H., and Wick, L. Y. (2006). Dispersing pollutant-degrading bacteria in contaminated soil without touching it. Eng. Life Sci. 6, 252–260.

Hartmann, A., and Zimmer, W. (1994). Physiology of *Azospirillum*. In ‘‘*Azospirillum*/Plant Associations’’ (Y. Okon, ed.), pp. 15–41. CRC Press, Boca Raton, FL.

Hawkins, A. C., and Harwood, C. S. (2002). Chemotaxis of *Ralstonia eutropha* JMP134(pJP4) to the Herbicide 2,4-Dichlorophenoxyacetate. Appl. Environ. Microbiol. 68, 968–972.

Hazelbauer, G. L., Falke, J. J., and Parkinson, J. S. (2008). Bacterial chemoreceptors: High-performance signaling in networked arrays. Trends Biochem. Sci. 33, 9–19.

Hyung, S., and Yu, M. A. (1997). An agarose-in-plug bridge method to study chemotaxis in the Archaeon *Halobacterium salinarum*. FEMS Microbiol. Lett. 156, 265–269.

Iwaki, H., Muraki, T., Ishihara, S., Hasegawa, Y., Rankin, K. N., Sulea, T., Boyd, J., and Lau, P. C. K. (2007). Characterization of a pseudomonad 2-nitrobenzoate nitroreductase and its catabolic pathway-associated 2-hydroxylaminobenzoate mutase and a chemore-ceptor involved in 2-nitrobenzoate chemotaxis. J. Bacteriol. 189, 3502–3514.

Jasuja, R., Yu, L., Trentham, D. R., and Khan, S. (1999). Response tuning in bacterial chemotaxis. Proc. Natl. Acad. Sci. USA 96, 11346–11351.

Kato, J., Ito, A., Nikata, T., and Ohtake, H. (1992). Phosphate taxis in *Pseudomonas aeruginosa*. J. Bacteriol. 174, 5149–5151.

Kentner, D., and Sourjik, V. (2006). Spatial organization of the bacterial chemotaxis system. Curr. Opin. Microbiol. 9, 619–624.

Kim, H.-E., Shitashiro, M., Kuroda, A., Takiguchi, N., Ohtake, H., and Kato, J. (2006). Identification and characterization of the chemotactic transducer in *Pseudomonas aeruginosa* PAO1 for positive chemotaxis to trichloroethylene. J. Bacteriol. 188, 6700–6702.

Kirby, J. R., and Zusman, D. R. (2003). Chemosensory regulation of developmental gene expression in *Myxococcus xanthus*. Proc. Natl. Acad. Sci. USA 100, 2008–2013.

Kurdish, I. K., Antonyuk, T. S., and Chuiko, N. V. (2001). Influence of environmental factors on the chemotaxis of *Bradyrhizobium japonicum*. Microbiology 70, 91–95.

Lanfranconi, M. P., Alvarez, H. M., and Studdert, C. A. (2003). A strain isolated from gas oil-contaminated soil displays chemotaxis towards gas oil and hexadecane. Environ. Micro-biol. 5, 1002–1008.

Lukat, G. S., and Stock, J. B. (1993). Response regulation in bacterial chemotaxis. J. Cell. Biochem. 51, 41–46.

Marx, R. B., and Aitken, M. D. (2000a). A material-balance approach for modeling bacterial chemotaxis to a consumable substrate in the capillary assay. Biotechnol. Bioeng. 68, 308–315.

Marx, R. B., and Aitken, M. D. (2000b). Bacterial chemotaxis enhances naphthalene degradation in a heterogeneous aqueous system. Environ. Sci. Technol. 34, 3379–3383.

McGee, D. J., Langford, M. L., Watson, E. L., Carter, J. E., Chen, Y. T., and Ottemann, K. M. (2005). Colonization and inflammation deficiencies in Mongolian gerbils infected by *Helicobacter pylori* chemotaxis mutants. Infect. Immun. 73, 1820–1827.

Merrell, D. S., Butler, S. M., Qadri, F., Dolganov, N. A., Alam, A., Cohen, M. B., Calderwood, S. B., Schoolnik, G. K., and Camilli, A. (2002). Host-induced epidemic spread of the *cholera* bacterium. Nature 417, 642–645.

Meyer, G., Schneider-Merck, T., Bohme, S., and Sand, W. (2002). A simple method for investigations on the chemotaxis of *Acidithiobacillus ferrooxidans* and *Desulfovibrio vulgaris*. Acta Biotechnol. 22, 391–399.

Miller, L. D., Yost, C. K., Hynes, M. F., and Alexandre, G. (2007). The major chemotaxis gene cluster of *Rhizobium leguminosarum bv. viciae* is essential for competitive nodulation. Mol. Microbiol. 63, 348–362.

Moran, M. A., Buchan, A., Gonzalez, J. M., Heidelberg, J. F., Whitman, W. B., Kiene, R. P., Henriksen, J. R., King, G. M., Belas, R., Fuqua, C., Brinkac, L., Lewis, M., et al. (2004). Genome sequence of *Silicibacter pomeroyi* reveals adaptations to the marine environment. Nature 432, 910–913.

Ordal, G. W., and Gibson, K. G. (1977). Chemotaxis toward amino-acids by *Bacillus subtilis*. J. Bacteriol. 129, 151–155.

Ordal, G. W., and Goldman, D. J. (1975). Chemotaxis away from uncouplers of oxidative-phosphorylation in *Bacillus subtilis*. Science 189, 802–805.

Ottemann, K. M., Thorgeirsson, T. E., Kolodziej, A. F., Shin, Y. K., and Koshland, D. E. (1998). Direct measurement of small ligand-induced conformational changes in the aspartate chemoreceptor using EPR. Biochemistry 37, 7062–7069.

Ottemann, K. M., Xiao, W. Z., Shin, Y. K., and Koshland, D. E. (1999). A piston model for transmembrane signaling of the aspartate receptor. Science 285, 1751–1754.

Pandey, G., and Jain, R. K. (2002). Bacterial chemotaxis toward environmental pollutants: Role in bioremediation. Appl. Environ. Microbiol. 68, 5789–5795.

Pandey, G., Chauhan, A., Samanta, S. K., and Jain, R. K. (2002). Chemotaxis of a *Ralstonia sp*. SJ98 toward co-metabolizable nitroaromatic compounds. Biochem. Biophys. Res. Comm. 299, 404–409.

Parales, R. E. (2004). Nitrobenzoates and aminobenzoates are chemoattractants for Pseudomonas strains. Appl. Environ. Microbiol. 70, 285–292.

Park, S. Y., Chao, X. J., Gonzalez-Bonet, G., Beel, B. D., Bilwes, A. M., and Crane, B. R. (2004). Structure and function of an unusual family of protein phosphatases: The bacterial chemotaxis proteins CheC and CheX. Mol. Cell 16, 563–574.

Pfeffer, W. (1884). Locomotorische Richtungsbewegungen durch chemische Reize. Unters Bot Inst Tu¨bingen 1, 363.

Porter, S. L., and Armitage, J. P. (2002). Phosphotransfer in *Rhodobacter sphaeroides* chemotaxis. J. Mol. Biol. 324, 35–45.

Porter, S. L., and Armitage, J. P. (2004). Chemotaxis in *Rhodobacter sphaeroides* requires an atypical histidine protein kinase. J. Biol. Chem. 279, 54573–54580.

Rajagopala, S. V., Titz, B., Goll, J., Parrish, J. R., Wohlbold, K., McKevitt, M. T., Palzkill, T., Mori, H., Finley, R. L., and Uetz, P. (2007). The protein network of bacterial motility. Mol. Syst. Biol. 3, 1–13.

Rebbapragada, A., Johnson, M. S., Harding, G. P., Zuccarelli, A. J., Fletcher, H. M., Zhulin, I. B., and Taylor, B. L. (1997). The Aer protein and the serine chemoreceptor Tsr independently sense intracellular energy levels and transducer oxygen, redox, and energy signals for *Escherichia coli* behavior. Proc. Natl. Acad. Sci. USA 94, 10541–10546.

Repik, A., Rebbapragada, A., Johnson, M. S., Haznedar, J. O., Zhulin, I. B., and Taylor, B. L. (2000). PAS domain residues involved in signal transduction by the Aer redox sensor of *Escherichia coli*. Mol. Microbiol. 36, 806–816.

Schweinitzer, T., Mizote, T., Ishikawa, N., Dudnik, A., Inatsu, S., Schreiber, S., Suerbaum, S., Aizawa, S. I., and Josenhans, C. (2008). Functional characterization and mutagenesis of the proposed behavioral sensor TlpD of *Helicobacter pylori*. J. Bacteriol. 190, 3244–3255.

Segall, J. E., Block, S. M., and Berg, H. C. (1986). Temporal comparisons in bacterial chemotaxis. Proc. Natl. Acad. Sci. USA 83, 8987–8991.

Shi, W. Y., Yang, Z. M., Geng, Y. Z., Wolinsky, L. E., and Lovett, M. A. (1998). Chemotaxis in *Borrelia burgdorferi*. J. Bacteriol. 180, 231–235.

Singh, T., and Arora, D. K. (2001). Motility and chemotactic response of *Pseudomonas fluorescens* toward chemoattractants present in the exudate *of Macrophomina phaseolina*. Microbiol. Res. 156, 343–351.

Stephens, B. B., Loar, S. N., and Alexandre, G. (2006). The role of CheB and CheR in a complex chemotaxis and aerotaxis pathway in *Azospirillum brasilense*. J. Bacteriol. 188, 4759–4768.

Stock, J., and Da Re, S. (2000). Signal transduction: Response regulators on and off. Curr. Biol. 10, R420–R424.

Szurmant, L., and Ordal, G. W. (2004). Diversity in chemotaxis mechanisms among the bacteria and archaea. Microbiol. Mol. Biol. Rev. 68, 301–319.

Tarrand, J. J., Krieg, N. R., and Dobereiner, J. (1978). Taxonomic study of *Spirillum lipoferum* group, with descriptions of a new genus, *Azospirillum* gen-NOV and 2 species, *Azospirillum lipoferum* (Beijerinck) comb Nov and *Azospirillum brasilense* sp-NOV. Can. J. Micro-biol. 24, 967–980.

Thar, R., and Kuhl, M. (2003). Bacteria are not too small for spatial sensing of chemical gradients: An experimental evidence. Proc. Natl. Acad. Sci. USA 100, 5748–5753.

Tso, W. W., and Adler, J. (1974). Negative chemotaxis in *Escherichia coli*. J. Bacteriol. 118, 560–576.

Ulrich, L. E., and Zhulin, I. B. (2005). Four-helix bundle: a ubiquitous sensory module in prokaryotic signal transduction. Bioinformatics 21, 45–48.

Ulrich, L. E., and Zhulin, I. B. (2007). MiST: A microbial signal transduction database. Nucleic Acids Res. 35, D386–D390.

Vlamakis, H. C., Kirby, J. R., and Zusman, D. R. (2004). The Che4 pathway of *Myxococcus xanthus* regulates type IV pilus-mediated motility. Mol. Microbiol. 52, 1799–1811.

Wadhams, G. H., and Armitage, J. P. (2004). Making sense of it all: Bacterial chemotaxis. Nat. Rev. Mol. Cell Biol. 5, 1024–1037.

Wright, E. L., Deakin, W. J., and Shaw, C. H. (1998). A chemotaxis cluster from *Agrobacterium tumefaciens*. Gene 220, 83–89.

Zapf, J., Madhusudan, C. E., Grimshaw, C. E., Hoch, J. A., Varughese, K. I., and Whiteley, J. M. (1998). Source of response regulator autophosphatase activity: The critical role of a residue adjacent to the SpoOF autophosphorylation active site. Biochemistry 37, 7725–7732.

Zhang, P. J., Weis, R. M., Peters, P. J., and Subramaniam, S. (2007). Electron tomography of bacterial chemotaxis receptor assemblies. In ‘‘Methods in Cell Biology’’ (J. R. McIntosh, ed.), Vol. 79, pp. 373–384. Academic Press, San Diego.

Zhulin, I. B., Bespalov, V. A., Johnson, M. S., and Taylor, B. L. (1996). Oxygen taxis and proton motive force in *Azospirillum brasilense*. J. Bacteriol. 178, 5199–5204.

Vita

Matthew Russell was born in Knoxville, Tennessee on December 18, 1978 to the parents of Gene and Wilma Russell and brother Mark. He attended Sunnyview Elementary School before moving on to Carter Middle and High School. After graduation in 1997, he attended Walters State Community College as a Pre-Medicine major until 2000. He then transferred to the University of Tennessee, Knoxville studying Biochemistry, Cellular and Molecular Biology. After graduation with a Bachelors of Science in December 2005, he began the graduate program in preparation for the Ph.D. track in Biochemistry, Cellular and Molecular Biology. Matthew graduated with a Doctor of Philosophy degree August 2012.